Brackish Groundwater in the Hill Country Trinity Aquifer and Trinity Group Formations, Texas

Mark C. Robinson, P.G., Alysa K. Suydam, P.G., Evan D. Strickland, P.G., Azzah AlKurdi

Report 388
September 2022

Texas Water Development Board
www.twdb.texas.gov

Texas Water Development Board

Report 388

Brackish Groundwater in the Hill Country Trinity aquifer and Trinity Group formations, Texas

By

Mark C. Robinson, P.G.

Alysa K. Suydam, P.G.

Evan D. Strickland, P.G.

Azzah AlKurdi

September 2022

Texas Water Development Board

Geoscientist Seal

The contents of this report (including figures and tables) document the work of the following licensed Texas geoscientists:

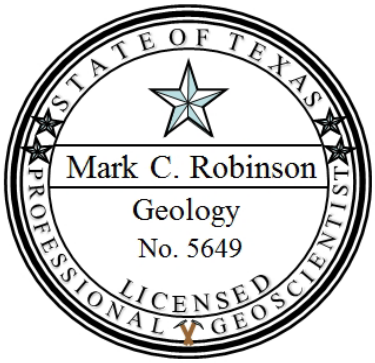

Mark C. Robinson, P.G. No. 5649

Mr. Robinson was responsible for working on all aspects of the project and preparing the report. The seal appearing on this document was authorized on September 15, 2022, by

Mark C. Robinson

Evan D. Strickland, P.G. No. 12849

Mr. Strickland was responsible for working on groundwater geochemistry aspects of the project and preparing the report. The seal appearing on this document was authorized on September 15, 2022, by

Evan D. Strickland

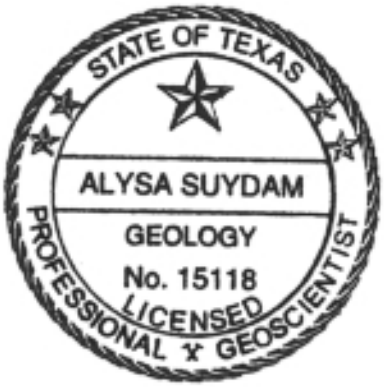

Alysa K. Suydam, P.G. No. 15118

Ms. Suydam was responsible for working on groundwater geochemistry aspects of the project and preparing the report. The seal appearing on this document was authorized on September 15, 2022, by

Alysa K. Suydam

Cover photo courtesy of James Golab

"Glen Rose Formation outcrop, Canyon Lake Spillway, Comal County, Texas"

Texas Water Development Board

Leading the state's efforts in ensuring a secure water future for Texas and its citizens.

Published and distributed by the
Texas Water Development Board
P.O. Box 13231, Capitol Station
Austin, Texas 78711-3231

(Printed on recycled paper)

This page is intentionally blank.

Table of Contents

List of Figures viii
List of Tables xiii
1 Executive summary 1
2 Introduction 7
3 Study area 14
4 Regional water planning area strategies 21
4.1 Region J 21
4.2 Region K 21
4.3 Region L 22
5 Previous groundwater investigations 23
6 Data collection and analysis 25
7 Hydrogeology 28
7.1 Stratigraphic framework 28
7.2 Structural features 31
7.3 Hydrologic impact of relay ramp faults 32
7.4 Surface creation process 33
7.5 Hydrostratigraphic units 37
7.5.1 Pre-Cretaceous formations 38
7.5.2 Hosston sandstone 38
7.5.3 Sligo limestone 39
7.5.4 Hammett shale 39
7.5.5 Cow Creek limestone 39
7.5.6 Hensell sandstone 40
7.5.7 Lower Glen Rose limestone 40
7.5.8 Upper Glen Rose limestone 41
7.6 Stratigraphic type logs 67
7.7 Study area cross sections 82
8 Aquifer determination 89
8.1 Assignment of top depths 89
8.2 Assignment of bottom depths 89
8.3 Aquifer code assignment 90
9 Aquifer hydraulic properties 92
9.1 Hydraulic property definitions 92
9.2 Data sources and collection process 93
9.2.1 Analysis criteria 93
9.2.2 Data sources 95
9.3 Results and analysis 95
10 Water quality data 111
10.1 Sources of measured water quality 111
10.2 Total dissolved solids 112
10.2.1 Contributing factors of dissolved solids in the study area 112
10.2.2 Total dissolved solids quality control 113
10.2.3 Analysis of major chemical constituents 115

10.2.4 Spatial trends of major constituents 129
10.3 Parameters of concern for desalination 135
10.3.1 Arsenic 135
10.3.2 Iron 135
10.3.3 Barium 135
10.3.4 Radionuclides 135
10.4 Relationship of total dissolved solids to specific conductance 138
10.4.1 Erroneous specific conductance measurements 139
10.4.2 Final total dissolved solids versus specific conductance relationships 141
11 Salinity calculations from geophysical well logs 146
11.1 Geophysical well log tools 149
11.2 Calculation method literature review 151
11.2.1 Alger-Harrison method 152
11.2.2 Data availability 154
11.3 Application of the Alger-Harrison method 155
11.3.1 Well pairs 155
11.3.2 Mud filtrate resistivity (R_{mf}) parameter 156
11.3.3 Well log curve input methods 160
11.3.4 Comparison of tested variations of the Alger-Harrison method 161
11.3.5 Selecting appropriate depths 165
11.3.6 Alger-Harrison method procedure 170
11.3.7 QA/QC procedures 174
11.4 Salinity calculations discussion 178
12 Salinity class determination 180
12.1 Salinity maps discussion 181
13 Groundwater volumes 189
13.1 Static water levels and saturated thickness 189
13.2 Groundwater volume calculation 195
13.2.1 Mechanics of calculating groundwater volumes in the Trinity Aquifer 195
13.2.2 Confined and unconfined aquifer 195
13.2.3 Specific yield and storativity values used 197
13.2.4 Process for calculating groundwater volumes 198
13.3 Calculated groundwater volumes 198
14 Desalination concentrate disposal 216
15 Future improvements 218
16 Conclusions 219
17 Acknowledgements 220
18 References 221
19 Appendices 232
19.1 Python scripts 232
19.1.1 Convert spreadsheet data to shapefiles in GAM projection 232
19.1.2 Use TopoToRaster to interpolate surfaces 233
19.1.3 Clip surfaces at onlaps and ground surface 237
19.1.4 Make isopach maps for each hydrostratigraphic unit 245
19.1.5 Volume calculations 252
19.2 Modeled ion concentrations 255

19.3 BRACS Database....257
19.3.1 Table relationships....257
19.4 Geographic information system datasets....261

List of Figures

Figure 1-1 Hill Country Trinity BRACS study area. 2
Figure 1-2 Hill Country Trinity Group simplified geologic setting. 3
Figure 1-3 Stratigraphic and hydrostratigraphic column 4
Figure 1-4 Hill Country Trinity BRACS salinity maps 5
Figure 2-1 Completed studies of the BRACS program. 12
Figure 2-2 Ongoing studies of the BRACS program. 13
Figure 3-1 Study area boundary 15
Figure 3-2 Regional water planning areas 16
Figure 3-3 Groundwater Management Areas 17
Figure 3-4 Groundwater conservation districts and agencies 18
Figure 3-5 City and public water supply system boundaries 19
Figure 6-1 Well control 26
Figure 7-1 Surface geology 29
Figure 7-2 Stratigraphic column of geological units 30
Figure 7-3 Major structural features 32
Figure 7-4 Schematic block diagram of a relay ramp. 33
Figure 7-5 Correlation section showing stratigraphic picks for the upper Trinity (Upper Glen Rose formation) and middle Trinity (Lower Glen Rose, Hensell and Cow Creek formations) 35
Figure 7-6 Correlation section showing stratigraphic picks for the lower Trinity (Sligo and Hosston formations) 36
Figure 7-7 Base of Cretaceous structure map 43
Figure 7-8 Base of Cretaceous depth surface map 44
Figure 7-9 Hosston sandstone structure map 45
Figure 7-10 Hosston sandstone depth surface map 46
Figure 7-11 Hosston sandstone thickness map 47
Figure 7-12 Sligo limestone structure map 48
Figure 7-13 Sligo limestone depth surface map 49
Figure 7-14 Sligo limestone thickness map 50
Figure 7-15 Hammett shale structure map 51
Figure 7-16 Hammett shale depth surface map 52
Figure 7-17 Hammett shale thickness map 53
Figure 7-18 Cow Creek limestone structure map 54
Figure 7-19 Cow Creek limestone depth surface map 55
Figure 7-20 Cow Creek limestone thickness map 56
Figure 7-21 Hensell sandstone structure map 57
Figure 7-22 Hensell sandstone depth surface map 58
Figure 7-23 Hensell sandstone thickness map 59
Figure 7-24 Lower Glen Rose limestone structure map 60
Figure 7-25 Lower Glen Rose limestone depth surface map 61
Figure 7-26 Lower Glen Rose limestone thickness map 62
Figure 7-27 Upper Glen Rose limestone structure map 63
Figure 7-28 Upper Glen Rose limestone depth surface map 64
Figure 7-29 Upper Glen Rose limestone thickness map 65

Figure 7-30 Bexar County lower Trinity correlations for the Sligo limestone and Hosston sandstone 68
Figure 7-31 Bexar County upper and middle Trinity correlations for the Upper Glen Rose limestone, Lower Glen Rose limestone, Hensell sandstone, and Cow Creek limestone units 69
Figure 7-32 Guadalupe County lower Trinity correlations for the Sligo limestone and Hosston sandstone 70
Figure 7-33 Guadalupe County upper and middle Trinity correlations for the Upper Glen Rose limestone, Lower Glen Rose limestone, Hensell sandstone, and Cow Creek limestone 71
Figure 7-34 Caldwell County lower Trinity correlations for the Sligo limestone and Hosston sandstone 72
Figure 7-35 Caldwell County upper and middle Trinity correlations for the Upper Glen Rose limestone, Lower Glen Rose limestone, Hensell sandstone, and Cow Creek limestone 73
Figure 7-36 Bastrop County lower Trinity correlations for the Sligo limestone and Hosston sandstone 74
Figure 7-37 Bastrop County upper and middle Trinity correlations for the Upper Glen Rose limestone, Lower Glen Rose limestone, Hensell sandstone, and Cow Creek limestone 75
Figure 7-38 Hays County lower Trinity correlations for the Sligo limestone and Hosston sandstone 76
Figure 7-39 Hays County upper and middle Trinity correlations for the Upper Glen Rose limestone, Lower Glen Rose limestone, Hensell sandstone, and Cow Creek limestone 77
Figure 7-40 Medina County lower Trinity correlations for the Sligo limestone and Hosston sandstone 78
Figure 7-41 Medina County upper and middle Trinity correlations for the Upper Glen Rose limestone, Lower Glen Rose limestone, Hensell sandstone, and Cow Creek limestone 79
Figure 7-42 Uvalde and Zavala Counties lower Trinity correlations for the Sligo limestone and Hosston sandstone 80
Figure 7-43 Uvalde and Zavala Counties upper and middle Trinity correlations for the Upper Glen Rose limestone, Lower Glen Rose limestone, Hensell sandstone, and Cow Creek limestone 81
Figure 7-44 Location of cross section lines and type-log wells 82
Figure 7-45 Cross section A-A' 85
Figure 7-46 Cross section B-B' 86
Figure 7-47 Cross section C-C' 87
Figure 7-48 Cross section D-D' 88
Figure 9-1 Transmissivity ranges and distribution for wells in the upper Trinity 99
Figure 9-2 Transmissivity ranges and distribution for wells in the middle Trinity 100
Figure 9-3 Transmissivity ranges and distribution for wells in the lower Trinity 101

Figure 9-4 Well yield ranges and distribution for wells in the upper Trinity 102
Figure 9-5 Well yield ranges and distribution for wells in the middle Trinity..... 103
Figure 9-6 Well yield ranges and distribution for wells in the lower Trinity..... 104
Figure 9-7 Hydraulic conductivity ranges and distribution for wells in the upper Trinity..... 105
Figure 9-8 Hydraulic conductivity ranges and distribution for wells in the middle Trinity..... 106
Figure 9-9 Hydraulic conductivity ranges and distribution for wells in the lower Trinity 107
Figure 9-10 Specific capacity ranges and distribution for wells in the upper Trinity..... 108
Figure 9-11 Specific capacity ranges and distribution for wells in the middle Trinity..... 109
Figure 9-12 Specific capacity ranges and distribution for wells in the lower Trinity..... 110
Figure 10-1 Major anion concentration versus total dissolved solids for the Upper Glen Rose limestone and Lower Glen Rose limestone 116
Figure 10-2 Major cation concentration versus total dissolved solids for the Upper Glen Rose limestone and Lower Glen Rose limestone 116
Figure 10-3 Major anion concentration versus total dissolved solids for the Hensell sandstone and Cow Creek limestone..... 117
Figure 10-4 Major cation concentration versus total dissolved solids for the Hensell sandstone and Cow Creek limestone..... 117
Figure 10-5 Major anion concentration versus total dissolved solids for the Sligo limestone and Hosston sandstone..... 118
Figure 10-6 Major cation concentration versus total dissolved solids for the Sligo limestone and Hosston sandstone..... 118
Figure 10-7 Piper plots of the Upper Glen Rose limestone and Lower Glen Rose limestone..... 119
Figure 10-8 Piper plots of the Upper Glen Rose limestone..... 120
Figure 10-9 Piper plots of the Lower Glen Rose limestone..... 121
Figure 10-10 Piper plots of the Lower Glen Rose limestone, Hensell sandstone, and Cow Creek limestone..... 122
Figure 10-11 Piper plots of the Hensell sandstone and Cow Creek limestone..... 123
Figure 10-12 Piper plots of the Hensell sandstone 124
Figure 10-13 Piper plots of the Cow Creek limestone..... 125
Figure 10-14 Piper plots of the Sligo limestone and Hosston sandstone 126
Figure 10-15 Piper plots of the Sligo limestone 127
Figure 10-16 Piper plots of the Hosston sandstone..... 128
Figure 10-17 Sample depth versus total dissolved solids 130
Figure 10-18 Map of water quality samples for the Upper Glen Rose limestone..... 131
Figure 10-19 Map of water quality samples for the Lower Glen Rose limestone..... 132
Figure 10-20 Map of water quality samples for the Hensell sandstone and Cow Creek limestone 133
Figure 10-21 Map of water quality samples for the Sligo limestone and Hosston sandstone 134

Figure 10-22 Map of well locations with water quality samples exceeding arsenic (two wells) or radium-228 plus radium-226 (six wells) maximum contamination levels 137
Figure 10-23 Map of well locations with water quality samples exceeding iron secondary maximum contamination levels 138
Figure 10-24 Graph of total dissolved solids versus specific conductance for all water quality analyses of the Hill Country Trinity aquifer 140
Figure 10-25 Graph of total dissolved solids versus specific conductance for all water quality analyses of the Hill Country Trinity aquifer, symbolized by whether the analysis was conducted by the Texas Department of Health 140
Figure 10-26 Graph of the ratio of dissolved solids to conductance versus the sample year of all water quality samples for the Hill Country Trinity aquifer 141
Figure 10-27 Plot of total dissolved solids versus specific conductance for the Upper Glen Rose limestone and Lower Glen Rose limestone 142
Figure 10-28 Plot of total dissolved solids versus specific conductance for the Upper Glen Rose limestone and Lower Glen Rose limestone 143
Figure 10-29 Plot of total dissolved solids versus specific conductance for the Hensell sandstone and Cow Creek limestone 144
Figure 10-30 Plot of total dissolved solids versus specific conductance for the Sligo limestone and Hosston sandstone 145
Figure 10-31 Plot of total dissolved solids versus specific conductance for the Sligo limestone and Hosston sandstone 145
Figure 11-1 Locations of measured water quality (left) and combined locations of measured water quality and calculated water quality (right) for the Upper Glen Rose limestone (top) and Lower Glen Rose limestone (bottom) 147
Figure 11-2 Locations of measured water quality (left) and combined locations of measured water quality and calculated water quality (right) for the Hensell sandstone (top) and Cow Creek limestone (bottom). 148
Figure 11-3 Locations of measured water quality (left) and combined locations of measured water quality and calculated water quality (right) for the Sligo limestone (top) and Hosston sandstone (bottom). 149
Figure 11-4 Distribution of logs used to calculate estimated groundwater salinity 157
Figure 11-5 R_{m75} and R_{mf75} from 260 well logs in the study area. 158
Figure 11-6 R_{m75} and R_{mf75} from 256 well logs in the study area 159
Figure 11-7 Average of the calculated total dissolved solids minus the measured total dissolved solids by calculation variation for the straight-average approach 162
Figure 11-8 Average of the calculated total dissolved solids minus the measured total dissolved solids by calculation variation for the weighted-average approach 163
Figure 11-9 Summary statistics (minimum, average, and maximum) for the various tested salinity calculation methods 165

Figure 11-10 Two examples of depths used in salinity calculations for the Upper Glen Rose limestone highlighted in yellow from BRACS ID 68507 167
Figure 11-11 One example of depths used in salinity calculations for the Lower Glen Rose limestone highlighted in yellow from BRACS ID 67791 167
Figure 11-12 One example of depths used in salinity calculations for the Hensell sandstone highlighted in yellow from BRACS ID 37777 168
Figure 11-13 Two examples of depths used in salinity calculations for the Cow Creek limestone highlighted in yellow from BRACS ID 67791 168
Figure 11-14 One example of depths used in salinity calculations for the Sligo limestone highlighted in yellow from BRACS ID 68507 169
Figure 11-15 One example of depths used in salinity calculations for the Hosston sandstone highlighted in yellow from BRACS ID 67791 169
Figure 11-16 Depths selected (yellow highlights) to assign a salinity classification for the Lower Glen Rose limestone for example BRACS ID 68507 173
Figure 11-17 Depth of formation (D_f) in feet and the calculated total dissolved solids (TDS) in milligrams per liter for the Upper Glen Rose limestone. 175
Figure 11-18 Depth of formation (D_f) in feet and the calculated total dissolved solids (TDS) in milligrams per liter for the Lower Glen Rose limestone. 175
Figure 11-19 Depth of formation (D_f) in feet and the calculated total dissolved solids (TDS) in milligrams per liter for the Hensell sandstone. 176
Figure 11-20 Depth of formation (D_f) in feet and the calculated total dissolved solids (TDS) in milligrams per liter for the Cow Creek limestone. 176
Figure 11-21 Depth of formation (D_f) in feet and the calculated total dissolved solids (TDS) in milligrams per liter for the Sligo limestone. 177
Figure 11-22 Depth of formation (Df) in feet and the calculated total dissolved solids (TDS) in milligrams per liter for the Hosston sandstone 177
Figure 12-1 Salinity classes and well control in the Upper Glen Rose limestone. 183
Figure 12-2 Salinity classes and well control in the Lower Glen Rose limestone 184
Figure 12-3 Salinity classes and well control in the Hensell sandstone. 185
Figure 12-4 Salinity classes and well control in the Cow Creek limestone. 186
Figure 12-5 Salinity classes and well control in the Sligo limestone. 187
Figure 12-6 Salinity classes and well control in the Hosston sandstone. 188
Figure 13-1 Upper Trinity (Upper Glen Rose limestone) static water level elevation 191
Figure 13-2 Middle Trinity (Lower Glen Rose limestone, Hensell sandstone, and Cow Creek limestone) static water level elevation 192
Figure 13-3 Lower Trinity (Sligo limestone and Hosston sandstone) static water level elevation 193
Figure 13-4 Schematic graph showing the difference between unconfined and confined aquifers 195
Figure 19-1 Table relationships in the BRACS Database 258

List of Tables

Table 1-1 Calculated total aquifer storage volumes of brackish groundwater by hydrostratigraphic unit 5
Table 1-2 Average minimum and maximum depths by salinity class 6
Table 2-1 TWDB-funded projects of the BRACS program. 8
Table 2-2 Groundwater salinity classification used in the study 11
Table 3-1 Counties in study area. 14
Table 3-2 Groundwater Conservation Districts shown in Figure 3-4 18
Table 3-3 Public water system (PWS) cross-reference table 20
Table 6-1 Sources listed for BRACS database well control data 26
Table 9-1 Hill Country Trinity aquifer formations groups. 94
Table 9-2 Wells with aquifer properties per county 95
Table 9-3 Wells with aquifer properties per hydrologic unit. 95
Table 9-4 Aquifer property results for Hill Country Trinity hydrologic units 96
Table 11-1 Well pairs assessed for the study. 156
Table 11-2 Minimum, median, mean, maximum, and standard deviation of R_{m75}, R_{mf75}, and R_{m75}/R_{mf75} for study area wells. 158
Table 11-3 Summary of calculation inputs and intermediate values for example BRACS ID 68507 174
Table 12-1 Average and maximum depths of salinity zones 181
Table 13-1 Specific yield and storativity values used for volume calculations 198
Table 13-2 The volumes of fresh, slightly saline, moderately saline, very saline, and total groundwater volumes in the Hill Country Trinity aquifer 200
Table 13-3 The volumes of fresh, slightly saline, moderately saline, very saline, and total groundwater volumes in the Hill Country Trinity aquifer by county 200
Table 13-4 The volumes of fresh, slightly saline, moderately saline, very saline, and total groundwater volumes in the Hill Country Trinity aquifer by regional water planning area. 206
Table 13-5 The volumes of fresh, slightly saline, moderately saline, very saline, and total groundwater volumes in the Hill Country Trinity aquifer by groundwater management area. 208
Table 13-6 The volumes of fresh, slightly saline, moderately saline, very saline, and total groundwater volumes in the Hill Country Trinity aquifer by groundwater conservation district 210
Table 19-1 GIS file naming codes 263
Table 19-2 Project support GIS files 264
Table 19-3 Geological formation GIS files 265
Table 19-4 Salinity class polygon files 266

This page is intentionally blank.

1 Executive summary

Both Texas industry and public water supply planners are looking at brackish groundwater to supplement stressed freshwater resources. Brackish groundwater is a significant resource in Texas and an important supply component that can be used to meet future water demands. In 2003, the Texas Water Development Board (TWDB) funded a study that estimated more than 2.5 billion acre-feet of brackish groundwater (with a total dissolved solids concentration of 1,000 to 10,000 milligrams per liter) exists within the state (LBG-Guyton Associates, 2003). However, the study was designed to be broad in scope and narrow in its assessment of groundwater quality. In order to improve on the 2003 study, the TWDB requested and received funding from the 81st Texas Legislature in 2009 to implement the Brackish Resources Aquifer Characterization System (BRACS) program to thoroughly characterize the brackish portions of Texas aquifers.

Program description

The goals of the BRACS program are to (1) map and characterize the brackish parts of the major and minor aquifers of the state in greater detail using existing water well reports, geophysical well logs, and available aquifer data and (2) build datasets that can be used for groundwater exploration and replicable numerical groundwater flow models to estimate aquifer productivity. Since the program's inception, the TWDB has completed 14 brackish groundwater aquifer studies of which 8 were internal studies (including the present study). There are two brackish groundwater studies currently in progress, the Edwards-Trinity (Plateau) aquifer and the East Sparta aquifer.

In 2017, the TWDB contracted a BRACS study of the entire Trinity Aquifer. The results of that study indicated that the TWDB should separate the BRACS effort into two separate studies, one for the Northern portion of the Trinity Aquifer and one for the Hill Country portion of the Trinity Aquifer. The Northern Trinity BRACS study was completed (Robinson and others, 2019) and provided the technical support for the designation of brackish groundwater production zones. The current report details the BRACS study of the Hill Country portion of the Trinity Aquifer and associated downdip portions of the Trinity Group. To simplify terminology for this report, we hereafter refer to these collectively as the Hill Country Trinity aquifer. We note that this study area differs from the Hill Country portion of the TWDB-designated Trinity Aquifer (Figure 1-1). The Trinity Aquifer as a whole has been designated as one of the nine major aquifers of Texas because of its importance as a significant source of groundwater.

Study area

The Hill Country Trinity aquifer occurs across a large portion of central Texas. The study area covered in this report is approximately 15,500 square miles in size and encompasses all or part of Atascosa, Bandera, Bastrop, Bexar, Blanco, Burnet, Caldwell, Comal, Frio, Gillespie, Gonzales, Guadalupe, Hays, Kendall, Kerr, Kinney, Llano, Maverick, Medina, Real, Travis, Uvalde, Wilson, and Zavala counties. The study area is primarily located in the South Central Texas (L) regional water planning area, but also includes

portions of the Plateau (J), Lower Colorado (K), and Rio Grande (M) Regional Water Planning Areas. Groundwater management areas 7, 8, 9, 10, 12, and 13 all coincide to a greater or lesser extent with the study area. There are 22 groundwater conservation districts intersecting the study area including the Barton Springs/Edwards Aquifer Conservation District and the Edwards Aquifer Authority.

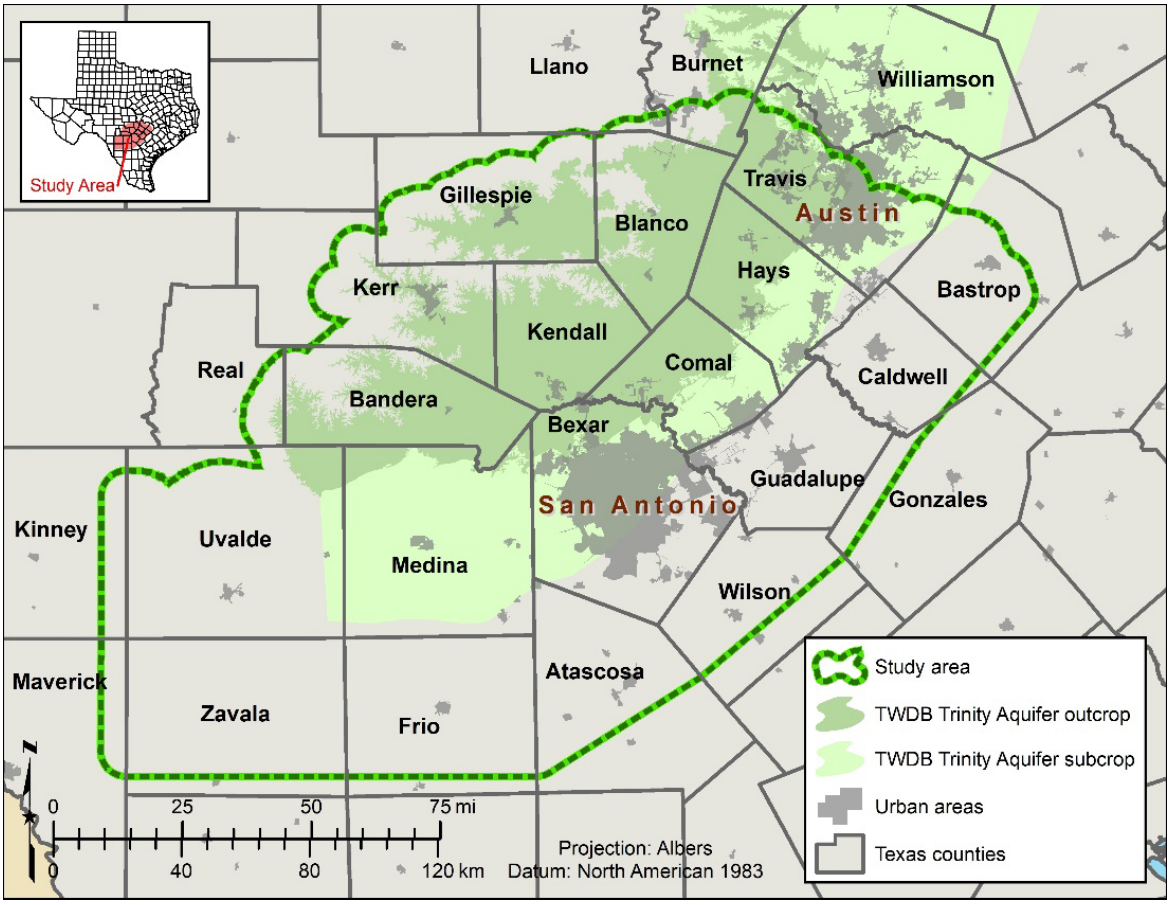

Figure 1-1 Hill Country Trinity BRACS study area.

Regional water planning groups in their 2021 plans have presented multiple water management strategies that are dependent upon the Trinity Aquifer for both fresh and brackish groundwater. Both the Plateau (J) and the Lower Colorado (K) regions have future strategies that anticipate the desalination of up to 3,000 acre-feet per year of Trinity Aquifer groundwater. Regional water planning groups J, K, and L plan for a continued dependency on producing fresh groundwater from the Trinity Aquifer.

Hydrogeologic features

The Hill Country Trinity aquifer is a thick sedimentary wedge of calcareous sandstone, shale, limestone, dolomite, and evaporites belonging to the Cretaceous Trinity Group that was deposited upon an eroded shelf of Paleozoic rocks. This wedge thickens from zero to 5,000 feet in a northwest to southeast direction. The Trinity Group is heavily faulted in the study area by the Balcones Fault Zone and the Luling Fault Zone. These fault zones tend to restrict the downdip flow of groundwater through water bearing units. In some

portions of the study area faults may form a boundary between relatively fresh or slightly saline groundwater in relatively shallow, updip portions of the Trinity Aquifer and the more moderate to very saline groundwater in deeper downdip portions of the Hill Country Trinity aquifer (Figure 1-2).

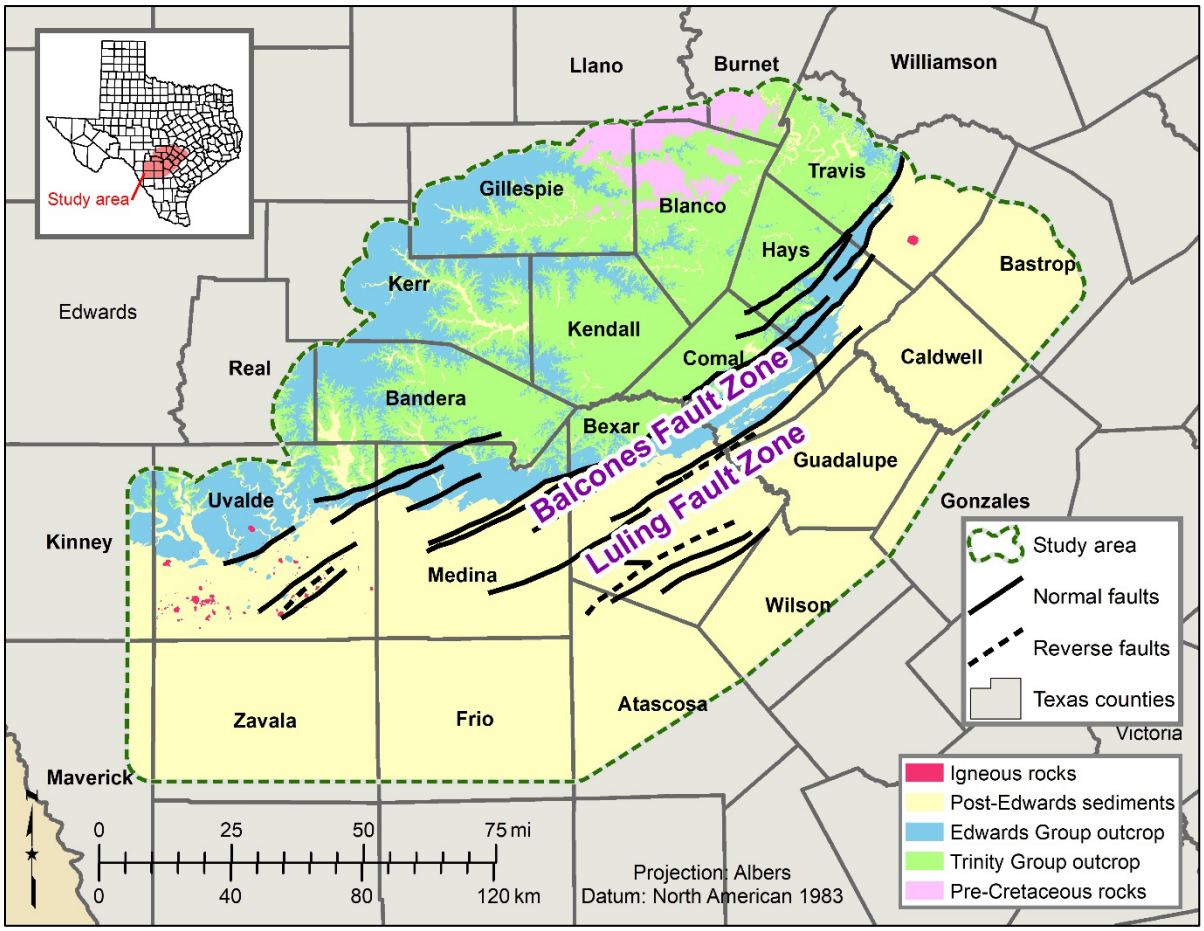

Figure 1-2 Hill Country Trinity Group simplified geologic setting.

Groundwater within the Trinity Group is present in porous and permeable sandstones and conglomerates as well as in carbonate rock units that have granular, fracture, and solution porosity. Some of the carbonate units are grainstones that may exhibit high intergranular porosity. Seven hydrostratigraphic units were defined and mapped for this study (1) Upper Glen Rose limestone, (2) Lower Glen Rose limestone, (3) Hensell sandstone, (4) Cow Creek limestone, (5) Hammett shale, (6) Sligo limestone, and (7) Hosston sandstone (Figure 1-3). The Hammett shale is considered a non-water bearing unit because of its lithologic composition.

More than 65,000 wells have been drilled for water and hydrocarbons over the last 70 years within the study area. Of these, about 24,000 have penetrated the Trinity Group formations. These well records have been invaluable in mapping the Trinity Group in the subsurface. However, we found that there are very few public records on the water quality and aquifer hydraulic properties of the generally deeper brackish groundwater intervals. Accordingly, our estimates of the magnitude and distribution of total dissolved

solids in groundwater were generally based upon sample chemistry data from water wells in the northwest (updip) portions of the study area. In contrast, the southeast (downdip) area for which there are few deep water wells, required water quality estimates to be based primarily on the interpretation of geophysical logs. Future efforts to obtain this information from wells drilled into or through the brackish groundwater formations would be extremely useful in efforts to accurately quantify this resource.

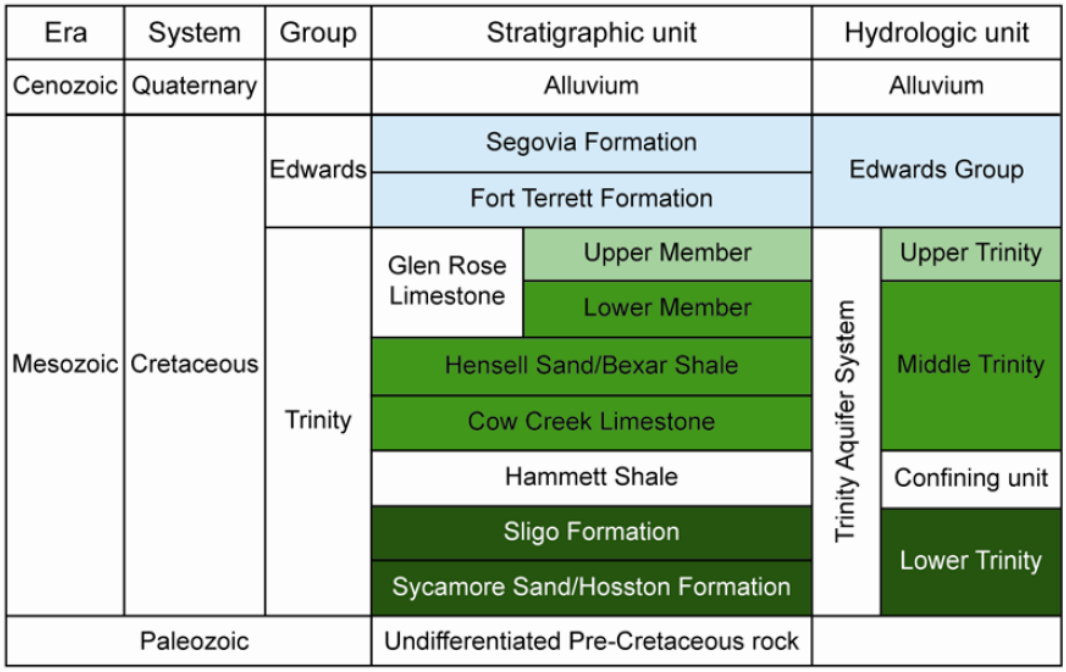

Figure 1-3 Stratigraphic and hydrostratigraphic column. (Jones and others, 2011)

Study findings

We calculated total aquifer storage volumes of both fresh and brackish groundwater for each of the water bearing hydrostratigraphic units according to salinity class. We used the following salinity classes, which are defined by the total dissolved solids content measured in milligrams-per-liter: 1) fresh 0 to 1,000, 2) slightly saline 1,000 to 3,000, 3) moderately saline 3,000 to 10,000, 4) very saline 10,000 to 35,000, and 5) brine more than 35,000. Maps of the salinity distributions by hydrostratigraphic unit are shown in Figure 1-4.

The volumes calculated in this study are estimates to be used to provide an insight into the magnitude and distribution of this important resource. We recommend that site-specific studies be conducted to support projects and efforts that will incorporate brackish groundwater resources into water resources planning. It is also important to note that these estimates are not the same as the TWDB calculated total estimated recoverable storage (TERS) volumes for the defined major and minor aquifers of Texas, which are confined to the aquifer boundaries used by the TWDB GAM models. Furthermore, this study utilized specific yield values that were determined by a recent core study (Standen, 2021) and they are significantly different than those used in previous TERS reports (Jones and Bradley, 2013; Jones and others, 2013).

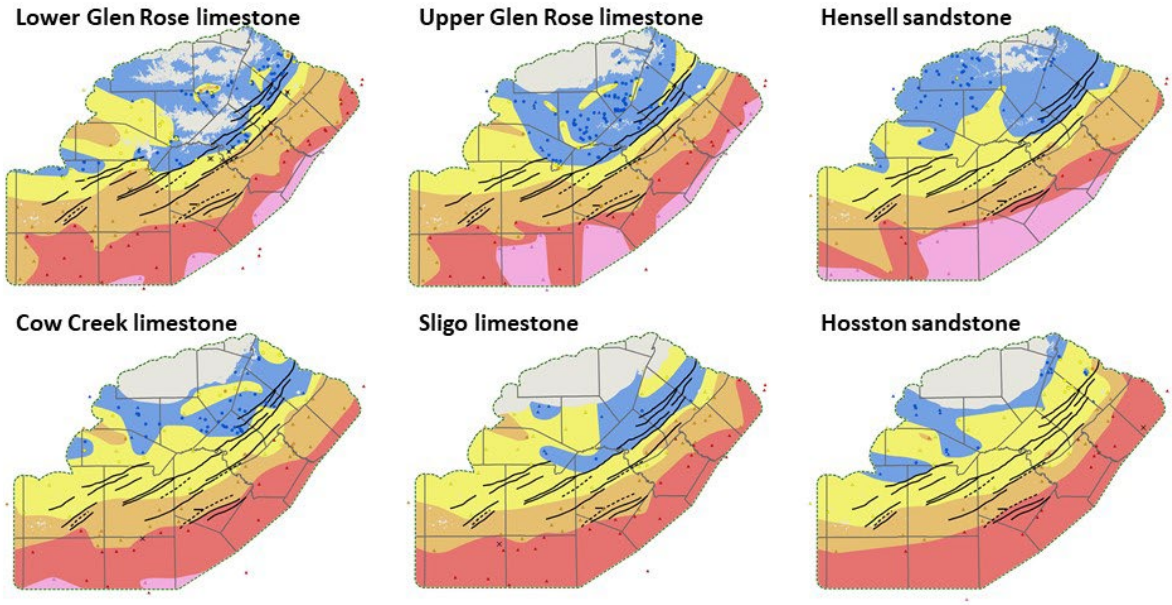

Figure 1-4 **Hill Country Trinity BRACS salinity maps. (Blue=freshwater, Yellow=slightly saline, Orange=moderately saline, Red=very saline, Pink=brine)**

Our calculations of total aquifer storage volumes of brackish groundwater for the Hill Country Trinity aquifer within the study area are shown in Table 1-1. Not all brackish groundwater can be produced or economically developed. These volumes do not consider the effects of land surface subsidence, degradation of water quality, or any changes to surface water-groundwater interaction that may result from extracting groundwater from the aquifer. These volumes should not be used for joint groundwater planning or evaluation of achieving adopted desired future conditions in the same way total estimated recoverable storage and modeled available groundwater are used according to the joint planning process described in Texas Water Code § 36.108.

Table 1-1 **Calculated total aquifer storage volumes of brackish groundwater by hydrostratigraphic unit.**

Hydrostratigraphic unit	Total aquifer storage volume (1,000,000 acre-feet)				
	Fresh	Slightly saline	Moderately saline	Very saline	Total
Upper Glen Rose limestone	9.5	22.3	53.2	49.4	134.4
Lower Glen Rose limestone	34.6	35.6	61.7	67.3	199.2
Hensell sandstone	9.3	12.9	23.3	15.8	61.3
Cow Creek limestone	24.1	12.9	10.3	18.6	65.9
Sligo limestone	4.9	30.8	17.0	74.6	127.3
Hosston sandstone	8.8	87.0	77.6	217.0	390.4
Total	**91.2**	**201.5**	**243.1**	**442.7**	**978.5**

In general, fresh and slightly saline groundwater is present in the shallower updip northern portions of the study area, with the average depths to fresh water in the Trinity Aquifer shown in Table 1-2. We observed that the downdip extent of fresh and slightly saline groundwater in the eastern half of the study area does not extend beyond the Balcones Fault Zone for all of the Trinity Group water bearing units.

Table 1-2 Average minimum and maximum depths by salinity class.

Salinity class	Minimum average depth in the Upper Glen Rose limestone (feet below ground surface)	Maximum average depth in the Hosston sandstone (feet below ground surface)
Fresh	45	708
Slightly saline	297	1,419
Moderately saline	2,257	3,897
Very saline	5,732	7,643

Study deliverables include a report, ESRI ARCMAP™ geographic information system map files, BRACS database and data dictionary, and water well and geophysical well log files. All data used for the study is readily available to the public and downloadable from the TWDB website.

2 Introduction

In 1956, the United States Geological Survey published a study that first mapped the brackish groundwater resources of Texas (Winslow and Kister, 1956). This was a high-level study designed to outline the occurrence, quantity, and quality of saline waters throughout the state. The study was part of a national effort to identify new sources of groundwater in water-scarce areas. In 1970, the TWDB funded a more detailed study to make a reconnaissance and inventory of the principal saline aquifers in Texas that discussed the salinity, the productivity, and the geology of the aquifers (Core Laboratories, 1972). In 2003, the TWDB funded a study to map the brackish aquifers and calculate the volume of brackish (slightly to moderately saline) groundwater available in these aquifers (LBG-Guyton Associates, 2003). The 2003 study was done to support the regional water planning process and help identify alternative sources to meet future water demands. The study estimated that there are approximately 2.5 billion acre-feet of brackish groundwater in place for the aquifers of Texas, demonstrating that brackish groundwater is an important resource and highlighting the need for more detailed aquifer studies.

In 2009, the 81st Texas Legislature provided funding to the TWDB to establish the Brackish Resources Aquifer Characterization System (BRACS). The goal of the program is to map and characterize the brackish portions of the aquifers in Texas. The resulting studies should be sufficiently detailed to provide basic data and information necessary for regional water planning groups and other entities interested in using brackish groundwater as a water supply. More detailed studies will be required for site specific projects. The TWDB completed the first pilot study on the Pecos Valley Aquifer in West Texas (Meyer and others, 2012) to establish the methods of data analysis for future studies.

In 2010, with legislative funding, the TWDB funded three research projects totaling $449,500 to support the BRACS program (Table 2-1). The first project identified geophysical well logs that could be used to map the geologic structure of aquifers and estimate the salinity of groundwater across Texas. The logs were then scanned into digital images and entered into a database. The BRACS Database now has more than 104,000 logs available (TWDB, 2021). The second project compiled a bibliography of more than 7,500 reports, articles, and graduate research papers with an emphasis on Texas geologic formations containing brackish groundwater into a relational database. This database serves as a source of references for evaluating existing geologic information for a project area. The third project assessed computer software capable of modeling different densities of groundwater found in brackish aquifers. A project report and a modeling code selection tool were developed to help users select the appropriate software.

In 2015, the 84th Texas Legislature passed House Bill 30, directing the TWDB to conduct studies to identify and designate brackish groundwater production zones in the state. The legislation directed the TWDB to make designations in four aquifers, 1) the Carrizo-Wilcox Aquifer located between the Colorado River and the Rio Grande, 2) the Gulf Coast

Aquifer and sediments bordering that aquifer, 3) the Blaine Aquifer, and 4) the Rustler Aquifer, and to report the designations to the legislature by December 1, 2016. The TWDB selected three additional brackish aquifers (the Trinity, Blossom, and Nacatoch aquifers) to study. The state legislature further required the TWDB to identify and designate brackish groundwater production zones in the remaining aquifers in the state before December 1, 2022. With the passing of House Bill 30, the TWDB funded seven aquifer projects totaling $1.7 million (Table 2-1).

Table 2-1 TWDB-funded projects of the BRACS program.

Report title	Short description	Contractor	Study type	Year funded	Funding
Geophysical Well Log Data Collection Project	Geophysical well logs from brackish aquifers in the state were collected from multiple sources, scanned, and entered into a database.	Bureau of Economic Geology	Research	2010	$300,000
Brackish Groundwater Bibliography Project	The project developed a comprehensive bibliography of Texas brackish aquifers.	INTERA, Inc.	Research	2010	$99,500
An Assessment of Modeling Approaches to Brackish Aquifers in Texas	The study assessed groundwater modeling approaches for brackish aquifers.	INTERA, Inc.	Research	2010	$50,000
Identification of Potential Brackish Groundwater Production Areas – Carrizo Aquifer	The project mapped and characterized the aquifer and evaluated the aquifer for potential production areas.	Bureau of Economic Geology	Research	2016	$181,446
Identification of Potential Brackish Groundwater Production Areas – Gulf Coast Aquifer	The project mapped and characterized the aquifer and evaluated the aquifer for potential production areas.	INTERA, Inc.	Research	2016	$500,000
Brackish Groundwater in the Blaine Aquifer System, North Central Texas	The project mapped and characterized the aquifer and evaluated the aquifer for potential production areas.	Daniel B. Stephens & Associates, Inc.	Research	2016	$200,000
Identification of Potential Brackish Groundwater Production Areas – Rustler Aquifer	The project mapped and characterized the aquifer and evaluated the aquifer for potential production areas.	INTERA, Inc.	Research	2016	$200,000
Identification of Potential Brackish Groundwater Production Areas – Blossom Aquifer	The project mapped and characterized the aquifer and evaluated the aquifer for potential production areas.	LBG-Guyton	Research	2016	$50,000

Report title	Short description	Contractor	Study type	Year funded	Funding
Identification of Potential Brackish Groundwater Production Areas – Nacatoch Aquifer	The project mapped and characterized the aquifer and evaluated the aquifer for potential production areas.	LBG-Guyton	Research	2016	$150,000
Identification of Potential Brackish Groundwater Production Areas – Trinity Aquifer	The project mapped and characterized the aquifer and evaluate the aquifer for potential production areas.	Southwest Research Institute	Research	2016	$400,000
Brackish Groundwater Comingling	The objective is to assess brackish groundwater comingling issues statewide and then focus on the Gulf Coast Aquifer, Eagle Ford Shale Region, and Trans-Pecos Area.	INTERA, Inc.	Research	2020	$137,700
Seismic Interpretation	The objective is to explore the application of seismic data for mapping brackish aquifers.	INTERA, Inc.	Research	2020	$150,000
Data Entry for Upper Coastal Plain East Aquifers	The objective is to enter data into the BRACS Database and use the data to map these four aquifers, characterize the brackish resources, and provide datasets that can be used for further exploration.	Allan R. Standen LLC	Research	2020	$226,000
Core Testing for Hill Country Trinity Aquifer	The objective is to conduct core testing for direct measurement of aquifer rock properties.	Allan R. Standen LLC	Research	2020	$219,710
Drilling and Logging Ideal Well	The objective is to prepare a resource document that will focus on how to drill and log the ideal exploratory brackish groundwater well.	Daniel B. Stephens & Assoc., Inc.	Research	2020	$135,000
Develop Procedures and Tools to Delineate Areas Designated or Used for Class II Well Wastewater Injectate	The objective is to develop technically defensible mapping procedures and tools to improve and refine the existing default 15-mile buffer distance applied to Class II injections wells.	WSP USA	Research	2020	$500,000
Sampling of Higher Salinity Groundwater	The objective is to obtain water quality samples for higher salinity groundwater from specific aquifers of interest.	USGS	Research	2020	$222,300

Report title	Short description	Contractor	Study type	Year funded	Funding
Core Testing and Numerical Well Simulations for Edwards-Trinity (Plateau) Aquifer	The objective is to locate, describe, and test core to determine rock properties and numerically simulate well logs for the Edwards-Trinity (Plateau) aquifers.	University of Texas	Research	2020	$90,726

In 2019, the 86th Texas Legislature restored funding for the BRACS Program with the passage of Rider 24 in House Bill 1, which appropriated $2 million to the TWDB for contract and administrative costs to support designation of brackish groundwater production zones in aquifers of the state, excluding portions of the Dockum Aquifer. The 86th Texas Legislature also passed Senate Bill 1041 that extended the deadline to complete zone designations from December 1, 2022, to December 1, 2032, and House Bill 722 that established a permitting framework for developing water supplies from TWDB-designated brackish groundwater productions zones.

The TWDB has completed eight internal studies (Figure 2-1) and presently has two ongoing studies (Figure 2-2). The eight completed studies include 1) Pecos Valley Aquifer in West Texas (Meyer and others, 2012), 2) Queen City and Sparta aquifers in Atascosa and McMullen counties (Wise, 2014), 3) Gulf Coast Aquifer in the Corpus Christi area (Meyer, 2012), 4) Lower Rio Grande Valley (Meyer and others, 2014), 5) Lipan Aquifer (Robinson and others, 2018), 6) Northern Trinity Aquifer (Robinson and others, 2019), 7) Wilcox, Carrizo, Queen City, Sparta, and Yegua aquifers in Central Texas (Meyer and others, 2020), and 8) Hill Country Trinity aquifer (Robinson and others, 2022, this report). The two ongoing studies are for the Edwards-Trinity (Plateau) Aquifer and the Sparta Aquifer, East which began the initial phase of data collection in the fall of 2020.

For each BRACS study, the TWDB staff collects as much geological, geochemical, geophysical, and well data as is available in the public domain and uses the information to map and characterize both the vertical and horizontal extent of the aquifers. Groundwater is classified into five salinity classes (Table 2-2), 1) fresh, 2) slightly saline, 3) moderately saline, 4) very saline, 5) and brine (Winslow and Kister, 1956). The volume of groundwater in each salinity class is then estimated based upon the three-dimensional mapping of the salinity zones. All project information is entered into the BRACS Database which was developed by the TWDB to store and analyze the information. The BRACS Database is a Microsoft Access database that has been carefully documented in the BRACS Database Data Dictionary (TWDB, 2021). Both the BRACS Database and the database dictionary are available for download from the TWDB website (**www.twdb.texas.gov/gw/bracs/database.asp**).

Table 2-2 **Groundwater salinity classification used in the study (Winslow and Kister, 1956). Colors used in this table for each salinity classification are consistent throughout the report and GIS datasets.**

Groundwater salinity classification	Total dissolved solids concentration (units: milligrams per liter)
Fresh	0 to 999
Slightly saline	1,000 to 2,999
Moderately saline	3,000 to 9,999
Very saline	10,000 to 34,999
Brine	Greater than 35,000

The project deliverables, both the report and data, are available to the public on the TWDB website. The data includes raw data in numerous digital formats and processed data in the form of GIS datasets. Digital geophysical well logs used for the studies are available upon request or downloadable from the TWDB Water Data Interactive website (www2.twdb.texas.gov/apps/waterdatainteractive/groundwaterdataviewer).

Information produced from these studies is not intended to serve as a substitute for site-specific evaluations of local aquifer characteristics and groundwater conditions for desalination projects. During design and development of a well field, an entity will need to determine the productivity of the brackish aquifer using monitoring and production wells and groundwater modeling. It is important to note that existing TWDB groundwater models are designed for regional assessment and are not applicable to well field analysis. These models are not constructed to analyze the effect of salinity on groundwater flow and in general should not be used for estimating withdrawal of saline water. Other significant factors an entity should evaluate before developing brackish groundwater are groundwater quantity and quality changes and potential subsidence.

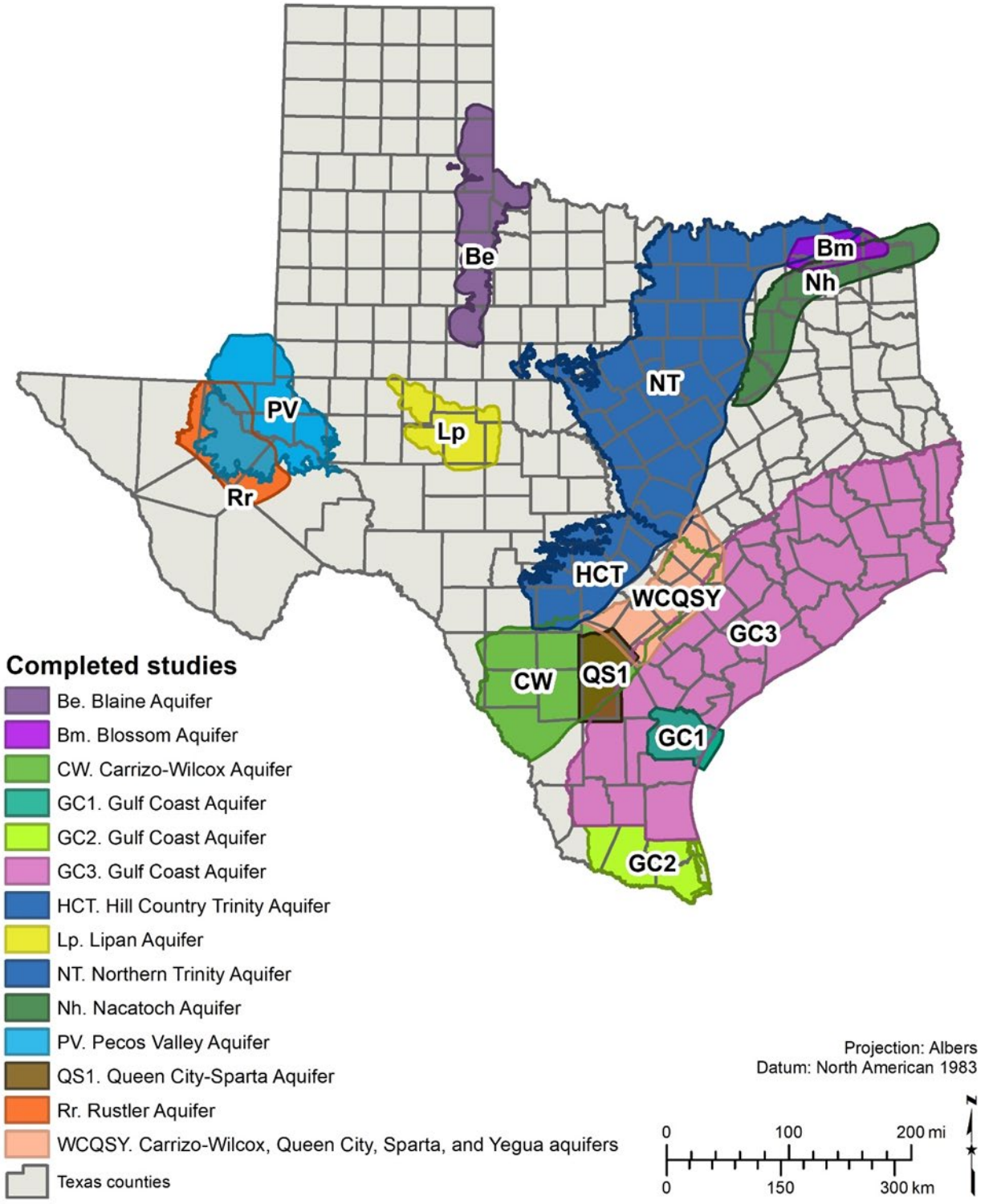

Figure 2-1 Completed studies of the BRACS program.

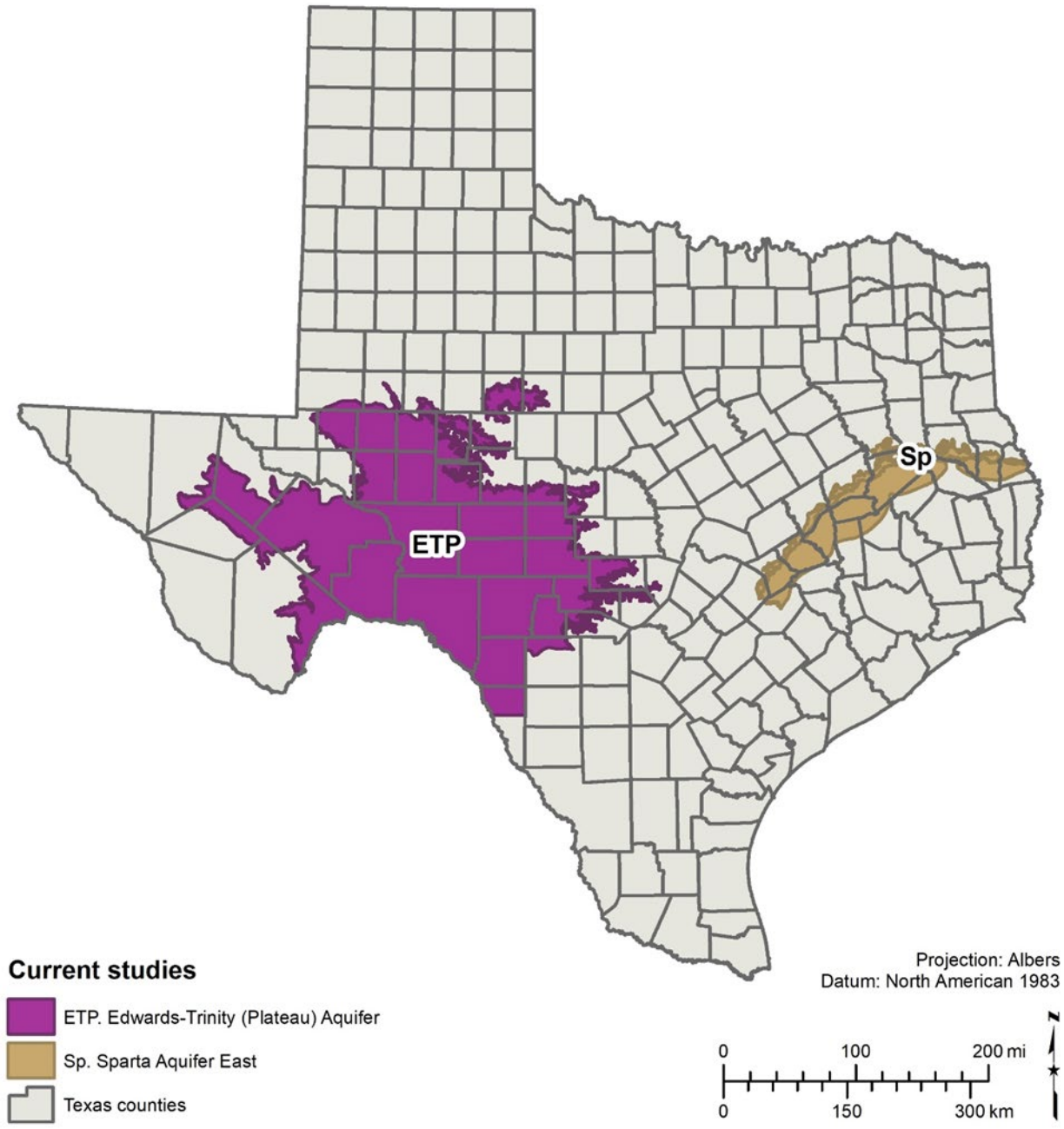

Figure 2-2 Ongoing studies of the BRACS program.

3 Study area

The Hill Country Trinity study area (Figure 3-1) is located in south-central Texas and includes all or part of 24 counties (Table 3-1). Total surface area of the project is 15,562 square miles which includes all of the TWDB-defined Trinity Aquifer outcrop and subcrop areas in the Texas Hill Country region. The study area extends beyond the limits of the recently completed conceptual model for the Hill Country Trinity GAM (Toll and others, 2018). Additional area was included to minimize edge effects and map the deeper downdip portions of the Trinity Group strata. Portions of other aquifers that overlie the Trinity in the study area are the Carrizo, Edwards, and Edwards-Trinity (Plateau) aquifers. The Ellenberger-San Saba and the Hickory aquifers are overlain in part by the Trinity Aquifer, primarily in the northwestern part of the study area.

Table 3-1 Counties in study area.

Atascosa	Frio	Llano
Bandera	Gillespie	Maverick
Bastrop	Gonzales	Medina
Bexar	Guadalupe	Real
Blanco	Hays	Travis
Burnet	Kendall	Uvalde
Caldwell	Kerr	Wilson
Comal	Kinney	Zavala

The ground surface elevation ranges from 278 to 2,342 feet above mean sea level across the study area. Half of the study area, located northwest of the Balcones Fault zone, has significant topographic changes of several hundred feet from hilltops to canyon floors. However, southeast of the Balcones Fault Zone is the beginning of the coastal plain with fewer dramatic elevation changes and an average elevation change of about 50 feet every 10 miles.

The Trinity Aquifer is one of the nine major aquifers in Texas, so designated because it is an important source of fresh water to millions of people across a large part of Central Texas. The Hill Country portion represents the southern extension of the Trinity Aquifer and is divided from the northern portion along the Colorado River. This division is based primarily upon geographic concerns but also represents possible hydrogeologic and geologic changes within the Trinity Aquifer (Brune and Duffin, 1983).

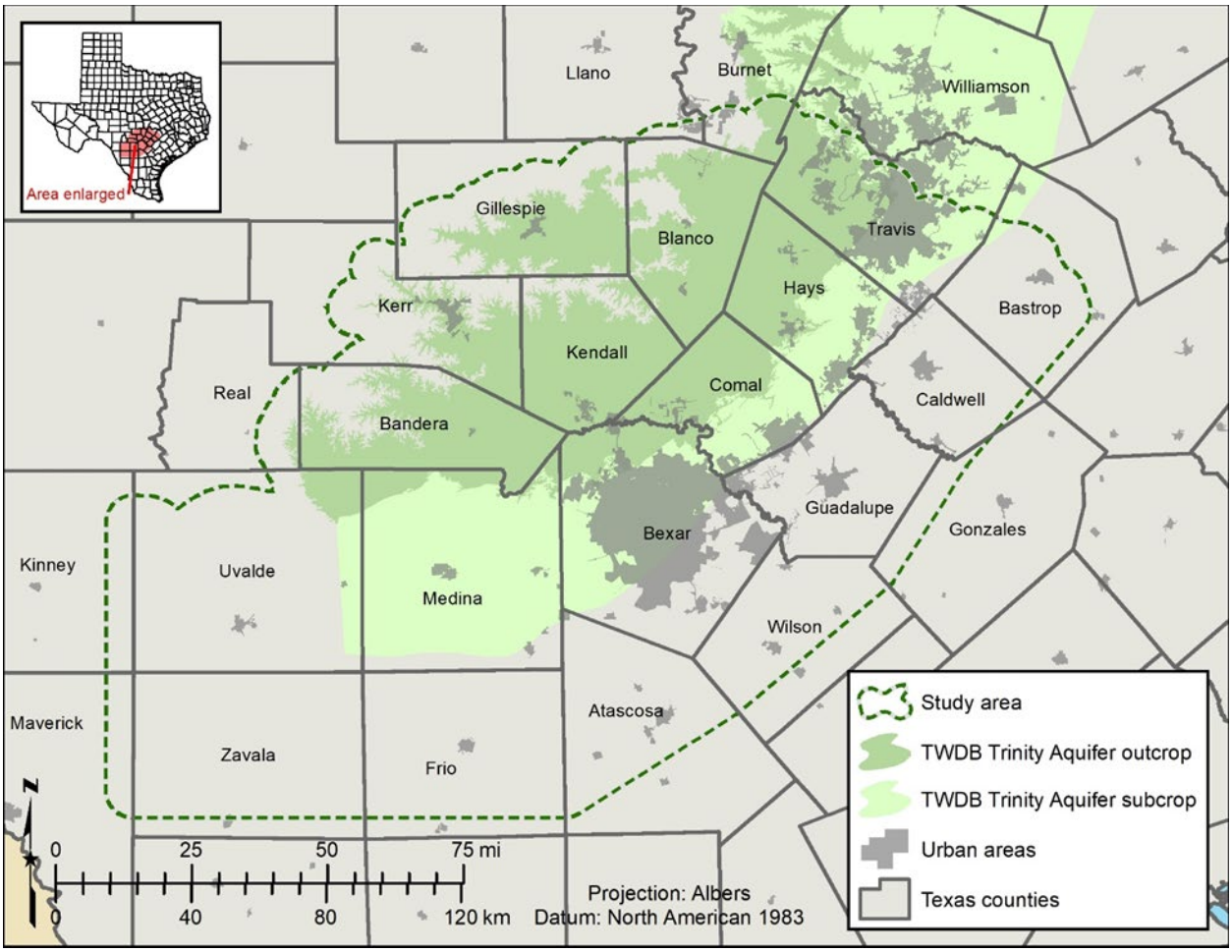

Figure 3-1 Study area boundary includes the Hill Country portion of the Trinity Aquifer as well as Trinity Group formations outside the defined aquifer.

There are four regional water planning areas intersecting the study area (Figure 3-2). Regions J, K, and L have significant overlap while Region M has only a slight area of overlap in the far western edge of the study area. The portions of Regions J and the northern portion of Region K are in a part of the study area where there is extensive use of the Hill Country Trinity aquifer for both domestic and agricultural use. The Trinity Aquifer is also an important source of groundwater for Region L. The downdip area of the Hill Country Trinity aquifer is covered by the southern portions of Region L and Region K where few if any Trinity Aquifer water wells have been drilled because of the depth and potential salinity of any groundwater.

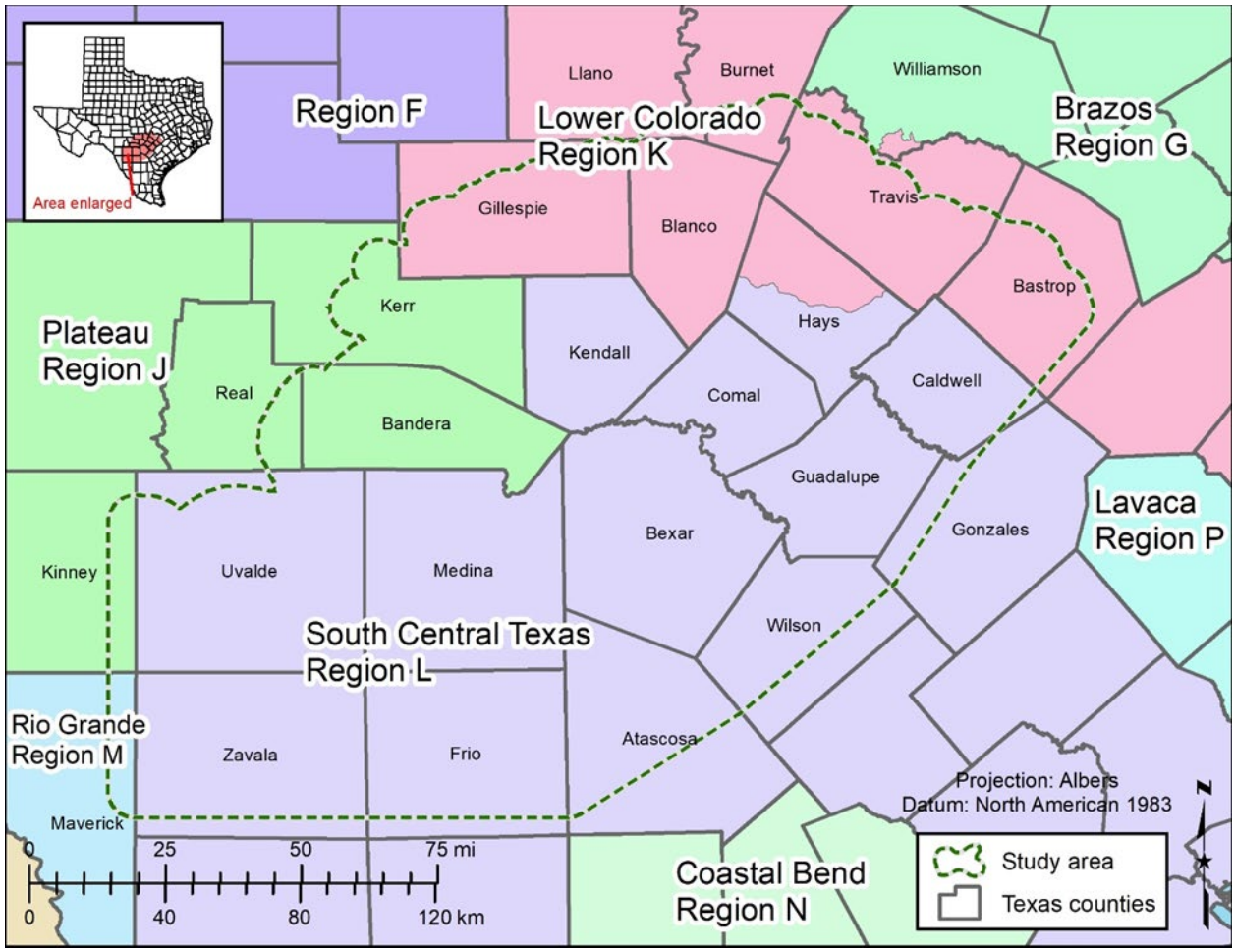

Figure 3-2 Regional water planning areas within the Hill Country Trinity aquifer study area.

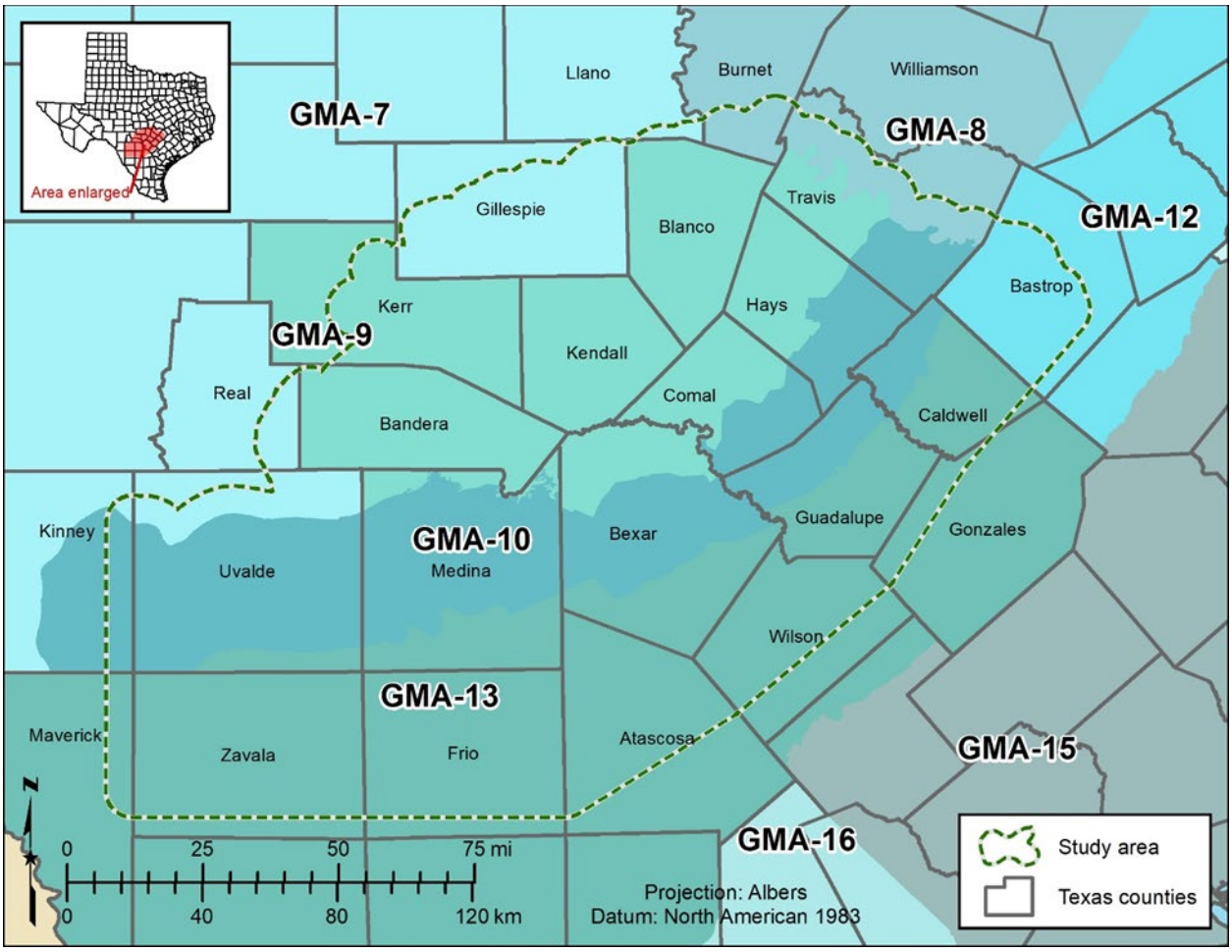

Figure 3-3 Groundwater Management Areas within the Hill Country Trinity study area.

There are six Groundwater Management Areas (GMA) intersecting the study area (Figure 3-3). Small portions of GMA-7 intersect the northwestern portions of the study area, particularly Gillespie County. Northern portions of the study area intersect GMA-8, and GMA-12 in Travis and Bastrop Counties respectively. Significant portions of GMA-9, GMA-10, and GMA-13 are overlain by the study area.

The 22 groundwater conservation districts that overlie the Hill Country Trinity aquifer in the study area are shown in Figure 3-4. Many of these districts have provided invaluable data and information used for this report. The Edwards Aquifer Authority has no direct responsibilities with regards to the Trinity Aquifer but has studied whether groundwater flows between the Edwards Aquifer and the Trinity Aquifer.

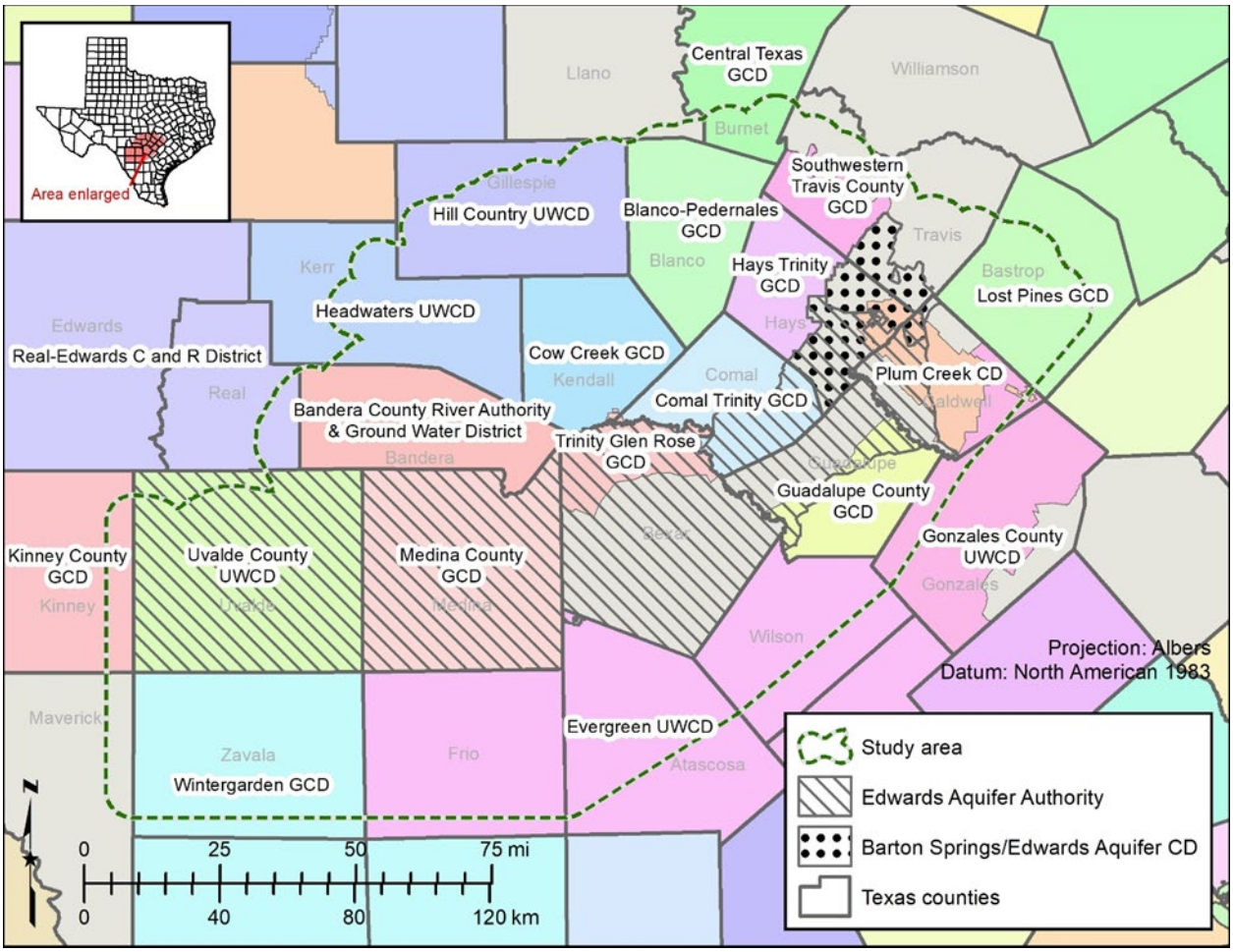

Figure 3-4 **Groundwater conservation districts and agencies within the Hill Country Trinity aquifer study area. GCD = groundwater conservation district; UWCD = underground water conservation district; CD = conservation district**

Table 3-2 **Groundwater Conservation Districts shown in Figure 3-4 that intersect the Hill Country Trinity study area.**

Bandera County River Authority & Ground Water District	Headwaters UWCD
Barton Springs/Edward Aquifer CD	Hill Country UWCD
Blanco-Pedernales GCD	Kinney County GCD
Central Texas GCD	Lost Pines GCD
Comal Trinity GCD	Medina County GCD
Cow Creek GCD	Plum Creek CD
Edwards Aquifer Authority	Real-Edwards C and R District
Evergreen UWCD	Southwestern Travis County GCD
Gonzales County UWCD	Trinity Glen Rose GCD
Guadalupe County GCD	Uvalde County UWCD
Hays Trinity GCD	Wintergarden GCD

There are 400 public water supply systems in the study area, of which 90 of them have over 1,000 connections each. Figure 3-5 displays 41 public water supply systems with 2010 census populations of more than 10,000 people within their geographic extent. The largest of these are the cities of San Antonio and Austin with a combined 2010 population of more than 2 million people.

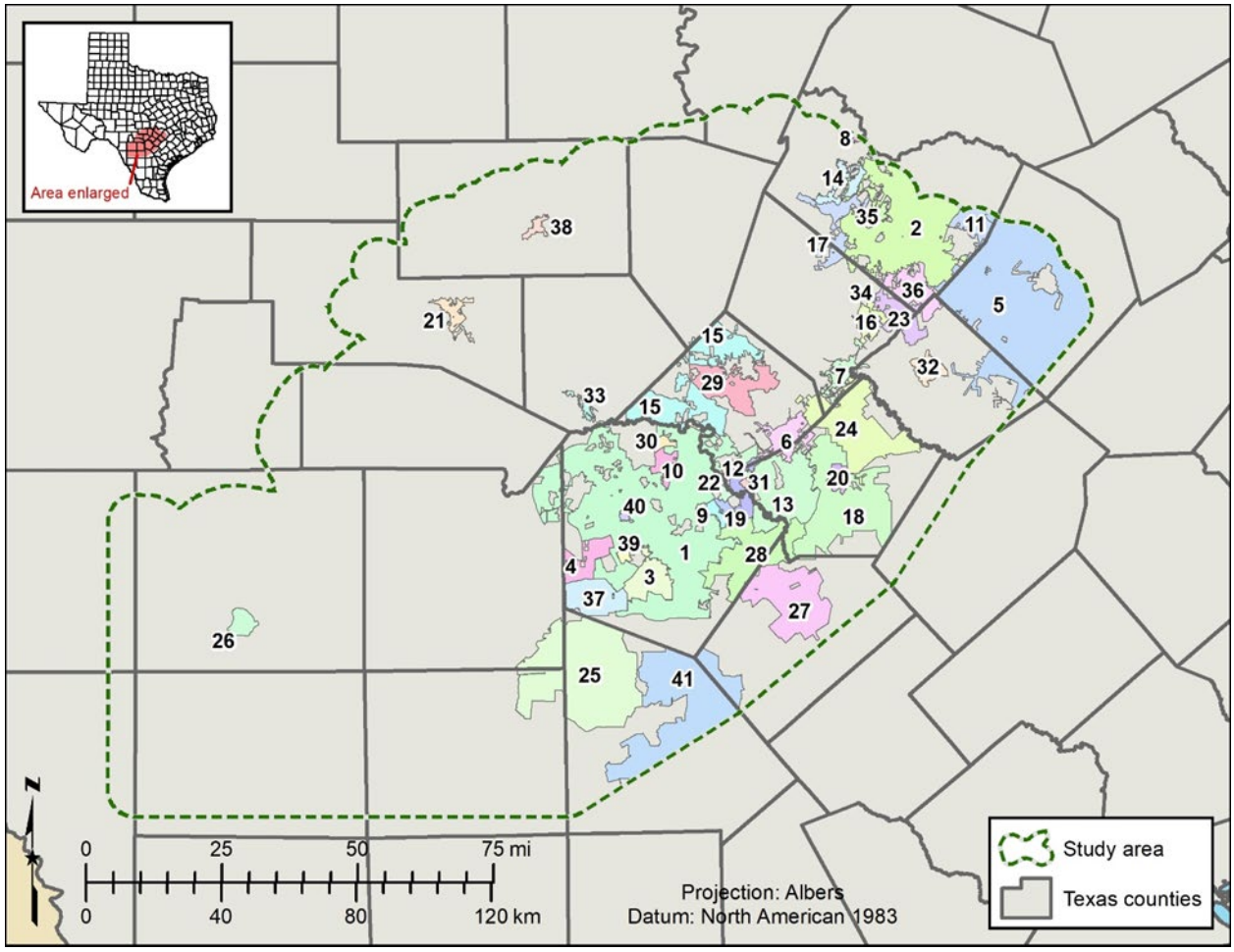

Figure 3-5 **City and public water supply system boundaries within the Hill Country Trinity aquifer study area labeled with map ID used in Table 3-3. Table 3-3 is a cross-reference of public water system map ID and system name. City boundaries from Texas Natural Resources Information System geographic information system file. Public water system boundaries are from HDR (2011). ID = identification number.**

Table 3-3 **Public water system (PWS) cross-reference table that relates the map ID number from figure 3-5 to the public water supply system name and identification number (PWS ID). The Texas Commission on Environmental Quality official public water supply system names and assigned ID numbers are used in this table.**

Map ID	PWS ID	System name	2010 Census
1	0150018	SAN ANTONIO WATER SYSTEM	1,321,419
2	2270001	CITY OF AUSTIN WATER & WASTEWATER	856,670
3	0150249	BMWD SOUTHSIDE	106,791
4	0150171	BMWD NORTH WEST	72,926
5	0110013	AQUA WSC	67,477
6	0460001	CITY OF NEW BRAUNFELS UTILITIES	60,911
7	1050001	CITY OF SAN MARCOS	53,428
8	2460009	CITY OF CEDAR PARK	51,678
9	0150084	BMWD NORTHEAST	50,768
10	0150054	BMWD HILL COUNTRY	48,432
11	2270033	MANVILLE WSC	40,851
12	0940003	CITY OF SCHERTZ	36,965
13	0940020	GREEN VALLEY SUD	28,905
14	2270027	TRAVIS COUNTY WCID 17	28,554
15	0460019	SJWTX CANYON LAKE SHORES	28,317
16	1050002	CITY OF KYLE	25,597
17	2270235	WEST TRAVIS COUNTY PUBLIC UTILITY AGENCY	25,337
18	0940022	SPRINGS HILL WSC	24,998
19	0150047	CITY OF CONVERSE	24,769
20	0940002	CITY OF SEGUIN	22,816
21	1330001	CITY OF KERRVILLE	22,778
22	0150009	CITY OF UNIVERSAL CITY	20,418
23	1050019	GOFORTH SUD	19,355
24	0940015	CRYSTAL CLEAR WSC	18,900
25	1630034	BENTON CITY WSC	18,615
26	2320002	CITY OF UVALDE	18,183
27	2470015	S S WSC	17,981
28	0150138	EAST CENTRAL SUD	17,404
29	0460172	SJWTX TRIPLE PEAK PLANT	16,898
30	0150270	BMWD TIMBERWOOD PARK	16,238
31	0940018	CITY OF CIBOLO	15,816
32	0280001	CITY OF LOCKHART	13,489
33	1300001	CITY OF BOERNE	13,070
34	1050028	PLUM CREEK	13,051
35	2270182	TRAVIS COUNTY WCID 10	12,992
36	2270008	CREEDMOOR-MAHA WSC	12,650
37	0150040	ATASCOSA RURAL WSC	12,079
38	0860001	CITY OF FREDERICKSBURG	11,446
39	0150114	LACKLAND AIR FORCE BASE	11,384
40	0150178	CITY OF LEON VALLEY	10,151
41	0070023	MCCOY WSC	10,068

Notes: WCID = Water Control and Improvement District; ID = identification number; SUD = Special Utility District; WSC = Water Supply Corporation.

4 Regional water planning area strategies

Regional water planning areas J, K, and L have significant overlap with the Hill Country Trinity aquifer study area (Figure 3-2) and groundwater from the Trinity Aquifer is an important component of the water supply for these areas. In the 2021 Regional Water Plans, the Trinity Aquifer was listed as a source in multiple recommended water management strategies for these three regions. This section provides a brief description of relevant projects.

After identifying water surpluses and potential water shortages, regional water planning groups identify, evaluate, and recommend water management strategies to avoid potential water shortages during a repeat of the drought of record over the next 50 years. A water management strategy is a plan to meet a water need (potential shortage) of a water user group. Water management strategies allocate water to specific water user groups, often through an intermediate regional or wholesale water provider. Recommended water management strategy water volumes are associated directly with water user groups. Strategies may or may not require new water infrastructure to be developed.

4.1 Region J

Water user groups in Bandera and Kerr counties, including the City of Bandera, the County of Bandera, the City of Kerrville, and Kerr County in Region J recommended a list of water management strategies for the Trinity Aquifer that include new well fields, additional wells in existing fields, and two aquifer storage and recovery projects in the City of Kerrville and in Kerr County. The supply rates for these water management strategies range from 860 acre-feet per year to 3,360 acre-feet per year. All strategies are listed to be online by 2030 (WSP and Carollo Engineers, 2021).

4.2 Region K

In Region K, the recommended water management strategies for the Trinity Aquifer are new well fields, additional wells in existing fields, and aquifer storage and recovery projects. The new well fields and additional wells in existing fields strategies are in Hays and Travis counties. Most of these strategies will be implemented by 2030 with supply rates of more than 1,100 acre-feet per year. Travis County also has a supply development strategy for Sunset Valley water user group to be implemented by 2040 with a supply rate of 300 acre-feet per year. Barton Springs/Edwards Aquifer Conservation District recommended the middle Trinity as suitable for aquifer storage and recovery and the project will serve the City of Buda and rural users in Hays County (Lower Colorado Regional Water Planning group and others, 2015). The City of Austin is looking at a water management strategy to be implemented by 2070 that would provide 2,300 acre-feet per year by desalinating brackish groundwater from the Trinity Aquifer (AECOM and others, 2020).

4.3 Region L

In Region L the City of New Braunfels (NBU) recommended adding new Trinity Aquifer wells to supplement their water supply which would supply an additional 3,360 acre-feet per year. Mining water user groups in Comal County have listed over 9,000 acre-feet per year for their Trinity Aquifer water management strategy by 2060 (Black & Veatch and others, 2020). Maxwell WSC has recommended a strategy that involves production and desalinization of 230 acre-feet per year of brackish Trinity Aquifer groundwater by year 2040. County Line SUD has recommended a strategy to produce an additional 740 acre-feet per year of Trinity Aquifer groundwater with a salinity of 1,000 milligrams per liter of total dissolved solids.

5 Previous groundwater investigations

The importance of the Trinity Aquifer in the Hill Country study area is partly evidenced by the large number of hydrologic studies that have been performed over the last 120 years. It is beyond the scope of this study to provide a comprehensive review of the vast body of work that has been published on the Hill Country Trinity aquifer and so the following citations merely provide a small sampling for those that wish to further study this aquifer. Perhaps the earliest is the work by Hill (1901) where he discussed in detail the geology of the Trinity Group and the occurrence of artesian groundwater in the Black and Grand Prairies of Central Texas. In this work, Hill also provided the foundation for the formation names used for the Lower Cretaceous rocks in the study area.

County and location specific studies began to be published by the Texas Board of Water Engineers (the precursor to the Texas Water Development Board) in conjunction with the United States Geological Survey in the mid-1900's. Two examples of these studies are George and Hastings (1947) and Lang (1954). They were important in that they compiled a large collection of water well data and groundwater chemistry data that could be referenced by subsequent work. The Trinity Aquifer however was overshadowed as a source for public water supply by the prolific water-producing capacity of the Edwards Aquifer throughout most of the study area.

Ashworth (1983) published a regional report that specifically addressed groundwater availability in the Trinity Group formations located in the Hill Country of Texas. His study utilized existing data to describe the hydrologic characteristics and groundwater quality and quantity for the Trinity Group. Additionally, the study looked at aquifer recharge, discharge, and hydrologic connections between geologic formations. It was in this report that the Trinity Group was divided into upper, middle, and lower Trinity hydrologic units as a generalized method to combine stratigraphic formations that appear to be in hydrologic communication.

The first published groundwater availability model for the Hill Country Trinity (Mace, Chowdhury and others, 2000) utilized three layers: 1) Edwards, 2) upper Trinity, and 3) middle Trinity. In Jones and others (2011) this model was updated to include the lower Trinity hydrologic unit and to conform to TWDB groundwater availability modeling standards that had been developed after the earlier model. The TWDB contracted an expanded and updated conceptual model for the Hill Country Trinity Aquifer (Toll and others, 2018) in preparation for a new revision to the groundwater availability model that addresses both additional updip and downdip water bearing formations of the Trinity Group.

Recent Trinity Aquifer studies have also been completed by groundwater conservation districts, such as the Edwards Aquifer Authority, Barton Springs/Edwards Aquifer Conservation District, Hays Trinity Groundwater Conservation District, and the Blanco-Pedernales Groundwater Conservation District to name a few (Camp and others, 2020; Hunt and others, 2019; Hunt and others, 2020; Smith and others, 2018; Wierman and

others, 2010). These studies use data and knowledge of local water wells in order to build more complete understanding of the aquifers that the districts must manage.

Another recent advance in our knowledge of the Trinity Aquifer has come from several multiport monitoring wells installed and maintained by BSEACD. These multiport wells have been completed with the capability of measuring static water levels, performing aquifer tests, and obtaining groundwater samples from dozens of isolated intervals through the Edwards and Trinity Groups. The data collected and the resulting studies have added significantly to our understanding of the connectivity of water bearing formations within the Trinity Group and with the overlying Edwards Group (Smith and Hunt, 2009; Tian and others, 2020). Tracer studies have also provided unique insights into the relationship between surface water and groundwater and the direction and speed with which groundwater moves in the updip portions of the Trinity Aquifer (Zappitello and others, 2019).

6 Data collection and analysis

Data collection efforts represented a considerable portion of the time and resources invested in this study. Historical records of wells drilled into or through the Trinity Aquifer needed to be researched, validated, and when appropriate entered in the BRACS database. Many of the well records are in the form of scanned documents that required careful review and analysis. Digital records in existing public databases were often incomplete with locations that needed to be accurately replotted. Each well that was added to the BRACS database shows the source of the information and all available well identification numbers.

Primary public databases utilized for well data in this report were:

- BRACS database maintained by the TWDB.
- Groundwater Database (GWDB) maintained by the TWDB.
- Submitted Drillers Report (SDR) database which is maintained cooperatively by the Texas Department of Licensing and Regulation (TDLR) and the TWDB.
- Oil and gas well database maintained by the Texas Railroad Commission (RRC).
- Public Water Supply (PWS) and Water Well Report (WWR) databases maintained by the Texas Commission on Environmental Quality (TCEQ).

Other sources of information included data and reports from the Edwards Aquifer Authority, Barton Springs/Edwards Aquifer Conservation District, Hill Country Underground Water Conservation District, Blanco-Pedernales Groundwater Conservation District, Hays Trinity Groundwater Conservation District, and the United States Geological Survey.

One objective of this study is to make the information and datasets gathered readily available to the public. This requirement necessitated that all data and information collected and used be non-confidential. The information collected includes raw data such as water well reports and digital geophysical well logs in numerous digital formats, and processed data such as lithology, simplified lithologic descriptions, stratigraphic picks, water chemistry, and interpreted results in the form of GIS datasets.

There are 23,991 wells within the study area that we determined to have penetrated the Trinity Group (Figure 6-1), of which 369 are oil and gas wells. Only 2,130 of the study wells, roughly nine percent, came from the BRACS database (Table 6.1). Additionally, there were 4,670 well records that came from the TWDB Groundwater database, 17,763 wells were sourced from the Texas Department of Licensing and Regulation Submitted Drillers Report database, and 1,073 were sourced from the Texas Commission on Environmental Quality Public Water Well database. We determined that 1,052 of the 2,130 BRACS database wells also exist in one or more of the other databases.

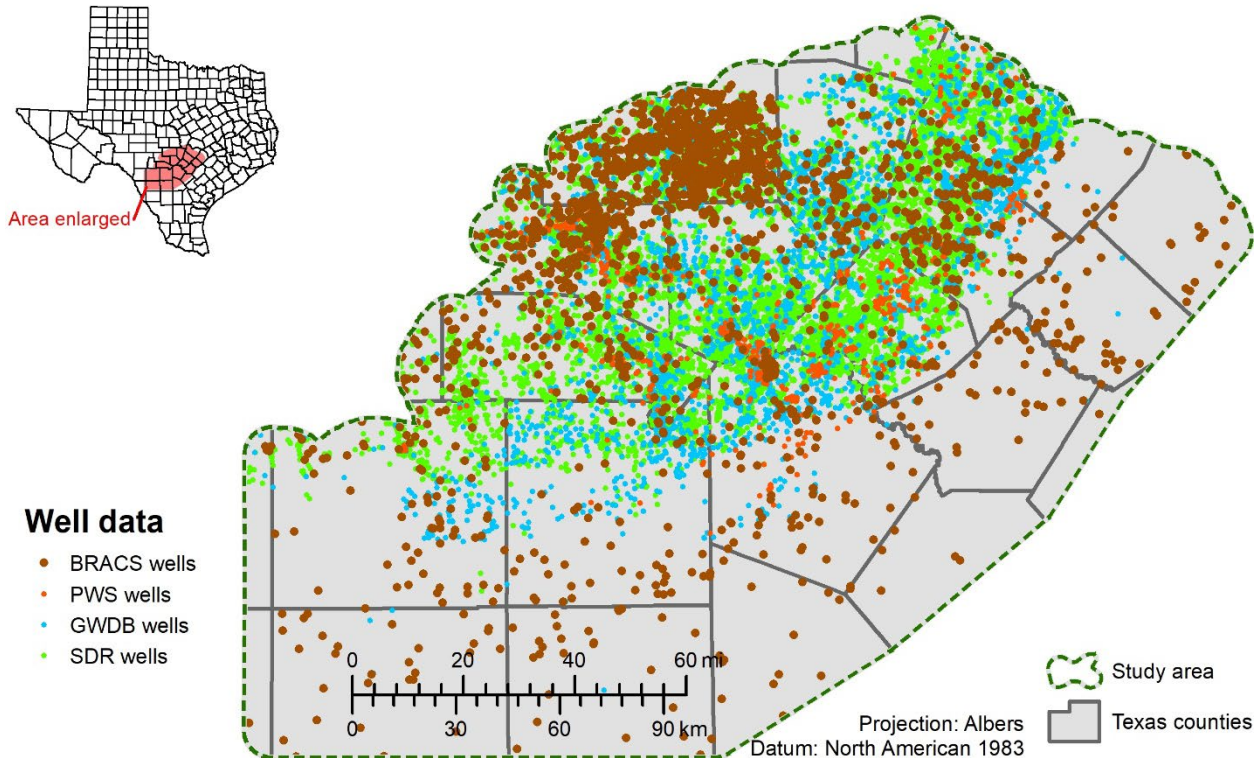

Figure 6-1 **Well control in the Hill Country Trinity aquifer study area. The well control consists of 23,991 wells: 2,130 have been assigned a well identification number in the TWDB BRACS Database, 4,670 wells have been assigned a state well number in the TWDB Groundwater Database, 17,763 have been assigned a tracking number in the TWDB Submitted Drillers Report Database, and 1,073 have been assigned well identifiers in the TCEQ Public Water Supply Database. Many of the wells exist in two or more of the sourced databases.**

Table 6-1 **Sources listed for BRACS database well control data.**

Source	Wells
Bureau of Economic Geology	63
Daniel B. Stephens and Associates. Llano Aquifers Study	527
Hays Trinity Groundwater Conservation District	159
INTERA Inc.	4
Texas Railroad Commission	67
San Antonio Water System	1
Subsurface Library	1
Texas Commission on Environmental Quality	37
Texas Department of Licensing and Regulation	609
Texas Water Development Board	601
Unknown	59
USGS	2

Although, we made a significant effort to identify all relevant and available well information for inclusion in this study, there exist a number of water wells and oil and gas wells that have not been included because information about these wells was either unavailable, incomplete, limited in scope, of poor quality, confidential, or did not meet the requirements of the study. Researchers looking for information that we may not have used in this study can review the following public sources for additional well data:

- Water Well Report Viewer of the Texas Commission on Environmental Quality for well reports older than 2001
- Railroad Commission of Texas for digital geophysical well logs
- Bureau of Economic Geology for paper and digital geophysical well logs and miscellaneous records
- Groundwater Conservation Districts for well records

We did not verify the location of every well that was obtained from other agency datasets unless there appeared to be a problem, such as a mismatch in the geology. When locations had to be verified or digital locations were not available, the digital files of the Original Texas Land Survey and linen maps from the Groundwater Advisory Unit of the Railroad Commission of Texas were used as base maps. The location legal description noted on the geophysical well log header or noted in the well record was used to plot the location of the well using a geographic information system to determine the latitude and longitude coordinates. We recommend that users of our study data make their own effort to verify the location of wells. All the source databases used in this study are updated on a regular basis by their respective agencies so new well data will become available in the study area in the future.

7 Hydrogeology

In addition to the groundwater studies reviewed in Section 5, there exists extensive literature relating to the geology and depositional framework of the Trinity Group formations within the study area. For this study, we have been able to utilize this large body of work to support our interpretation and analysis of the hydrogeologic setting of the Hill Country Trinity aquifer. The hydrogeologic framework and interpretations that we developed are based upon geophysical well logs, drillers descriptive logs, and published literature.

The earliest detailed geologic discussion of the Trinity Group formations is that of Hill and Vaughn (1889). This was followed by Hill (1901) which provided a detailed geologic description of the Trinity Group both surface and subsurface. Imlay (1945) provided a regional analysis of how the Lower Cretaceous formations are stratigraphically related from Louisiana, across Texas, and into Northern Mexico. Imlay was able to use geophysical well logs to supplement drillers logs and outcrop data. During the 1940s, the Lower Cretaceous formations in south-central Texas were found to be hydrocarbon rich. As a result, a significant number of oil and gas wells were drilled and the resulting data supported numerous published studies (Forgotson, 1957; Tucker, 1962; Forgotson, 1963; Stricklin and others, 1971). Perkins (1974) compiled the results of a Society of Economic Paleontologists and Mineralogists symposium dedicated to the geology of the Trinity Group formations. Bebout and Loucks (1977) edited a collection of papers presented during a symposium on the Cretaceous Carbonates in Texas and Mexico with specific attention to applications related to subsurface hydrocarbon exploration.

We used surface geological contacts published by the Texas Bureau of Economic Geology as a large-scale digital map dataset for the surface geology of Texas (Barnes, 1965). Figure 7-1 is a simplified version of this dataset showing the extent of Lower Cretaceous formations that outcrop in the study area. A continuing effort by the United States Geological Survey to map Central Texas geology has provided us with valuable information on the surface expression of the Trinity Group formations (Clark and others, 2009; Clark and Morris, 2015; Clark and others, 2016; Clark and others, 2018).

7.1 Stratigraphic framework

The Hill Country Trinity study area has outcrops ranging in age from Precambrian granites and schists to recent alluvial sediments. This report will focus on the Trinity Group formations which are Lower Cretaceous in age and outcrop in approximately 30% of the study area. Rose (1972) summarized the history behind the naming of the Trinity Group which he traced back to Hill (1889) who described outcrops of the formation in the Trinity River Valley in North Central Texas.

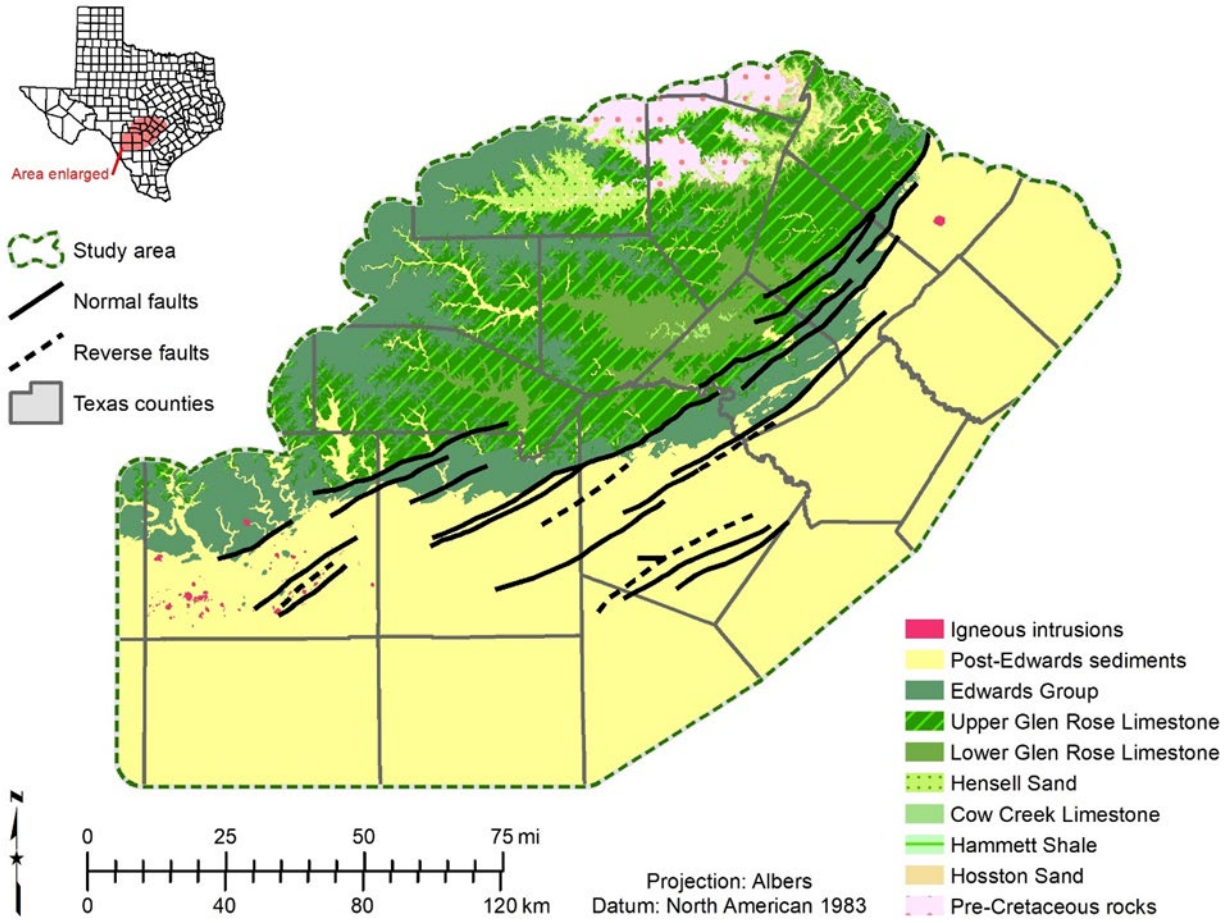

Figure 7-1 Surface geology in the Hill Country Trinity study area. Modified from Barnes (1965).

The stratigraphic framework and geologic column used for this study is shown in Figure 7-2. The terminology for mappable geologic units of the Trinity Group varies according to geographic location. We decided to utilize the stratigraphic terminology in general use to describe the Trinity Group in the subsurface and in outcrops by previous studies in Hays, Travis, Blanco, and Gillespie counties (Wierman, 2010; Hunt and others, 2020). The hydrologic unit designations of upper, middle, and lower Trinity were first utilized by Ashworth (1983) based upon observed differences in groundwater heads in wells that were completed in different portions of the Trinity Aquifer. From these observations, Ashworth proposed the existence of aquitards between the 1) Upper Glen Rose limestone and Lower Glen Rose limestone and 2) between the Cow Creek limestone and Sligo limestone.

The Trinity Group is a depositional sequence whose basal units represent a lowstand system tract overlain by a transgressive system tract which in turn is overlain by a highstand system tract. These sediments record a major transgression of the ancestral Gulf of Mexico during early Cretaceous time. There are minor regressions identifiable during the overall period of transgression. The minor transgressive/regressive sequence

boundaries mark the top of the Hosston sandstone, Sligo limestone, and Hensell sandstone. A maximum flooding surface for the Trinity Group is at the top of the Hammett shale, effectively separating the middle and lower Trinity hydrologic units. A major transgression occurred at the top of the Glen Rose Formation denoting the end of the Trinity Group (Culotta and others, 1992).

<table>
<tr><th rowspan="2">Age
m.y.</th><th rowspan="2">Period</th><th rowspan="2">Epoch</th><th rowspan="2">Group</th><th colspan="4">Formation</th><th rowspan="2">Hydrostratigraphic unit</th><th rowspan="2">Hydrologic unit</th></tr>
<tr><th colspan="2">Northern</th><th colspan="2">Hill Country</th></tr>
<tr><td colspan="8">Undifferentiated post Buda formations and sediments</td><td rowspan="4"></td></tr>
<tr><td>95

100</td><td rowspan="2">Upper
Cretaceous</td><td>Cenomanian</td><td rowspan="3">Washita</td><td colspan="2">Grayson

Mainstreet
Papaw
Weno
Denton
Fort Worth
Duck Creek</td><td colspan="2">Buda
Del Rio

Georgetown</td><td></td></tr>
<tr><td>Upper Albian</td></tr>
<tr><td>110</td><td rowspan="4">Lower
Cretaceous</td><td rowspan="2">Lower Albian</td><td rowspan="4">Fredericksburg</td><td colspan="2">Kiamichi
Edwards
Comanche Peak
Walnut</td><td colspan="2">Kiamichi
Edwards
Comanche Peak
Walnut</td><td>Edwards</td><td></td></tr>
<tr><td rowspan="3">113</td><td rowspan="3">Trinity</td><td colspan="2">Paluxy

Glen Rose</td><td colspan="2">Glen Rose</td><td>Upper Glen Rose</td><td>Upper Trinity</td></tr>
<tr><td rowspan="2">Upper Aptian</td><td rowspan="2">Twin
Mountains</td><td rowspan="2">Hensell

Pearsall</td><td rowspan="2">Travis
Peak</td><td rowspan="2">Hensell
(Bexar Shale)
Cow Creek
Hammett
(Pine Island)
Sligo</td><td>Lower Glen Rose</td><td rowspan="3">Middle Trinity</td></tr>
<tr><td>Hensell</td></tr>
<tr><td>125</td><td>Lower Aptian</td><td>Cow Creek</td></tr>
<tr><td>129</td><td></td><td>Hauterivian-
Valanginian</td><td></td><td>Hosston</td><td>Hosston</td><td>Hammett</td><td></td></tr>
<tr><td></td><td></td><td></td><td></td><td></td><td></td><td></td><td>Sligo</td><td rowspan="2">Lower Trinity</td></tr>
<tr><td colspan="8">Pre-Cretaceous</td><td>Hosston</td></tr>
</table>

Figure 7-2 **Stratigraphic column of geological units identified within the Hill Country Trinity aquifer study area. Geologic epochs and ages are defined by the International Commission on Stratigraphy Chronostratigraphic Chart (modified from Gradstein and others, 2012). Hydrologic units from Ashworth (1983). Geological units that produce water from the Hill Country Trinity aquifer are highlighted in blue.**

In the western portions of the study area, the contact between the Trinity Group and the underlying Paleozoic rocks is an erosional angular unconformity. Along the eastern portions of the study area, the Trinity Group is unconformably deposited upon Jurassic sands and shales. Because the Hosston sandstone is largely composed of sands and shales, it is easier to identify the base of the Trinity Group in updip portions of the study area in both drillers logs and geophysical well logs than in the downdip eastern portions of the study area.

7.2 Structural features

The Lower Cretaceous Trinity Group formations in the study area were deposited in a generally shallow marine environment whose character and extent were controlled by three dominant structural features, 1) the Llano Uplift, 2) the San Marcos Arch, 3) and the Stuart City Reef Trend. The Llano Uplift and the San Marcos Arch are remnant Paleozoic features that were created long before the Cretaceous period (Flawn and others, 1961; Rose, 2016). The Stuart City Reef Trend represents a syndepositional feature (Tucker, 1962) that formed during deposition of the Trinity Group in the Early Cretaceous period along the seaward edge of the ancient Central Texas Platform (Figure 7-3).

The Llano Uplift has a core of Precambrian granitic rocks that have been a regional high since the lower Paleozoic Period. This is evidenced in the way that the Paleozoic formations of the Ouachita Structural Belt have been "wrapped" around the older Precambrian rocks at the core of the Llano Uplift (Flawn and others, 1961; Rose, 2016). Since the Cretaceous Period, the Llano Uplift has been a positive structural feature. As a result, the Llano Uplift was the source for much of the argillaceous material found in the Trinity Group formations and is onlapped by many of the Trinity Group strata.

The San Marcos Arch forms a broad regional platform extending southeast from the Llano Uplift (Rose, 2016). It is evidenced in the subsurface by facies changes and stratigraphic thinning of Trinity and other overlying formations (Stricklin and others, 1971). This feature provided a shallow marine platform that dipped gently towards the southeast upon which Trinity Group sediments were deposited (Rose, 2016).

The Stuart City Reef Trend is thought to have developed upon the lower Trinity Sligo Formation and grown syndepositionally with the middle and upper Trinity formations (Tucker, 1962). This feature created the restricted shallow water environment where evaporites were extensively precipitated during deposition of the Glen Rose Formation. The combination of the San Marcos Arch and the Stuart City Reef Trend created the low-relief carbonate shelf environment present during middle and upper Trinity deposition (Stricklin and Amsbury, 1974; Bay,1977).

Major faulting of the Trinity Group occurred post deposition along the Balcones and Luling fault zones. The faulting along the Balcones Fault Zone is thought to have occurred approximately 25 million years ago during the latest Oligocene or early Miocene (Rose, 2016) with up to 1,600 feet of total vertical offset. The Luling Fault Zone is thought to have been active during the same time as the Balcones Fault Zone with total vertical offsets of no more than 1,500 feet. Neither of these fault zones is considered active at this time. Large fault offsets and the presence of impermeable material within fault planes presents challenges to the downdip migration of water (Amsbury, 1974).

Throughout the Lower Cretaceous the depositional accommodation was towards the southeast into the ancestral Gulf of Mexico. Present day structural dip is still towards the southeast where west of the Balcones Fault Zone the Cretaceous formations dip towards

the south-southeast at approximately 12 feet per mile compared to east of the Balcones Fault Zone where the dip increases to approximately 125 feet per mile.

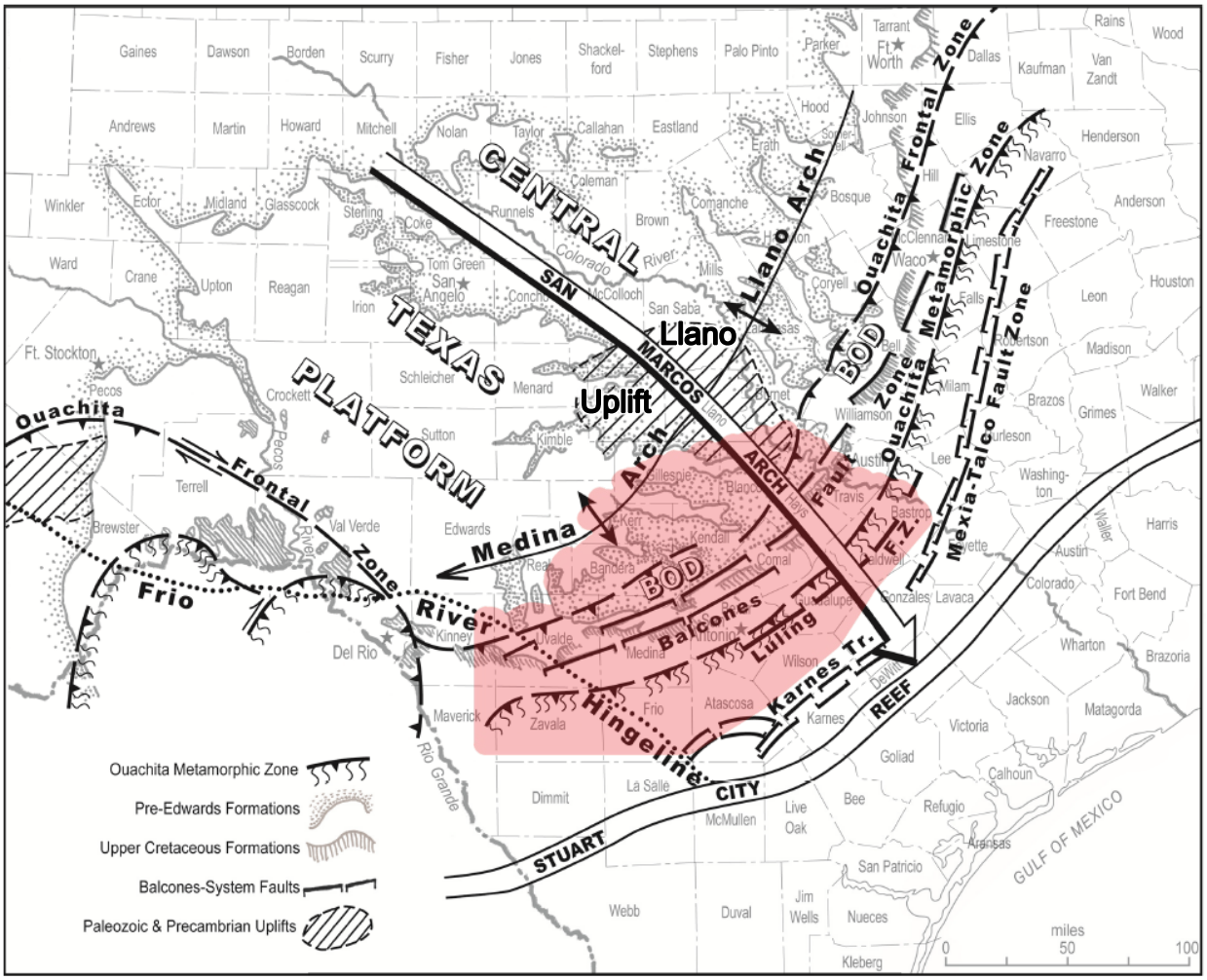

Figure 7-3 Major structural features (modified from Rose, 2016). The Hill Country Trinity aquifer study area is shown in red. (BOD= Balcones/Ouachita Downwarp.)

7.3 Hydrologic impact of relay ramp faults

Overall, the Balcones Fault Zone is a 10- to 12-mile wide band of subparallel, high angle, down towards the coast, predominantly normal faults trending from northeast to southwest across the study area. In detail, the faults are manifested by a complex pattern of closely spaced faults of varying offsets, many of which are subparallel to the primary regional trend (Collins and Hovorka, 1997). Additionally, the Trinity Group is composed of alternating beds of varying lithology which results in complex fault propagation patterns (Ferrill and Morris, 2008). Many of the fault traces show evidence of cementation and solution deformation which can inhibit the flow of fluids across them. Despite these observations, groundwater flow as determined by hydrostatic groundwater elevations appears to move through the Trinity Aquifer in a generally downdip direction (Martin and others, 2019).

A likely structural element of the faulting in the Balcones Fault Zone has been described as a relay ramp (Figure 7-4), which is thought to provide a means for groundwater to move in a downdip direction bypassing potentially impermeable faults (Grimshaw and Woodruff, 1986; Collins and Hovorka, 1997; Hunt and others, 2015). The factors leading to the development of relay ramps include the heterolithic character of the Lower Cretaceous carbonate formations which are composed of competent massive carbonate beds separated by less competent clay rich shale intervals (Ferrill and Morris, 2008). This allows for fault displacement to propagate at variable rates laterally, so that between two fault traces a monoclinal ramp may develop that provides for the necessary vertical displacement. This provides continuous flow paths for groundwater to move downdip albeit increasing transit distances.

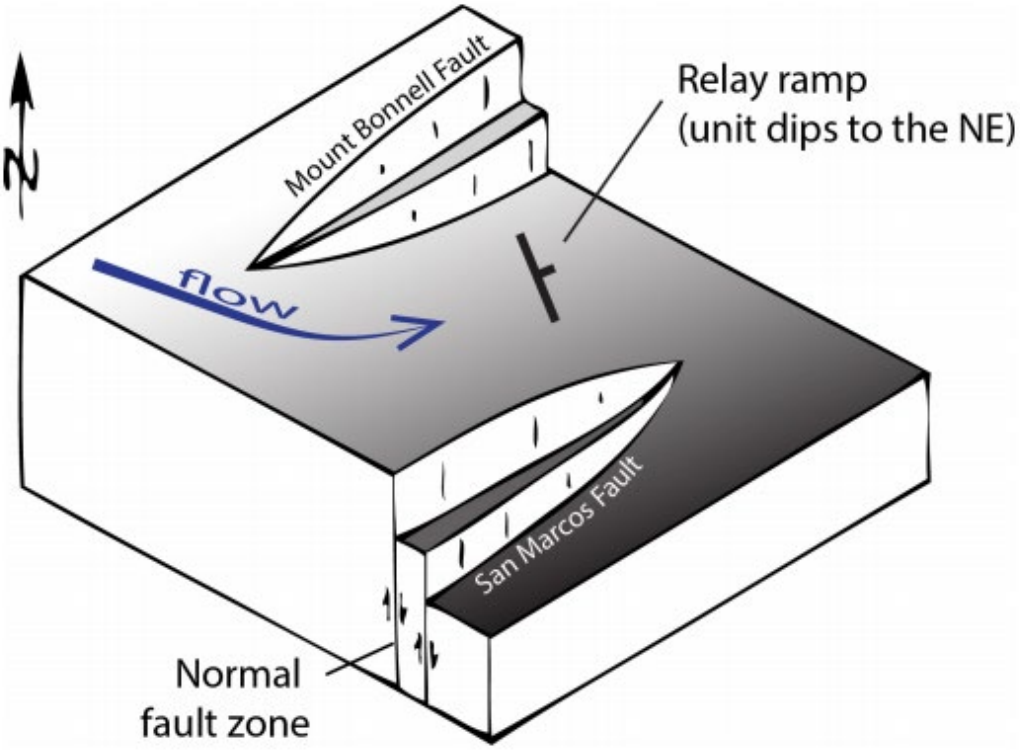

Figure 7-4 Schematic block diagram of a relay ramp. (Hunt and others, 2015)

7.4 Surface creation process

The Hill Country Trinity aquifer represents a challenging problem when it comes to creating a digital stratigraphic framework. The challenges include the presence of significant topographic features, extensive and complex faulting, lithologic variations within formations, and large areas without available geophysical well logs. Many of the previous stratigraphic frameworks developed over the last twenty years (Ferrill and others, 2003; Ferrill and others, 2005) are limited in areal extent to a county or smaller

area. Several regional frameworks were developed for the purpose of supporting groundwater availability models of the Hill Country Trinity Aquifer, (Mace and others, 2000; Jones and others, 2011; Toll and others, 2018)

Surfaces utilized in BRACS studies must meet several criteria related to 1) data transparency, 2) reproducibility, and 3) technical defensibility. Data transparency requires that all of the data used in the study and in the generation of the surfaces must be public and available for inclusion in the BRACS database. Reproducibility addresses the need for the surface generation methodology to use commonly available tools and well-defined processes so that the surfaces can be generated by other agencies or individuals if necessary. Finally, it is important that all aspects of the surface generation process be technically defensible. This requires that the stratigraphic interpretations from well logs must generally agree with previously published studies and that the surfaces generated intersect the wells at the appropriate depths in the interpreted wells.

In addition to meeting the surface generation criteria outlined above, we were able to incorporate into the current study a significant amount of new data not previously used. We performed stratigraphic interpretations on over 1,200 geophysical well logs and drillers logs in order to model the depositional surfaces of the seven hydrostratigraphic units defined for the Hill Country Trinity aquifer. Additionally, we also interpreted the top of the Buda Formation and the base of the Trinity Group.

We used the IHS-Markit Kingdom® geological software to interpret 1,266 geophysical well-logs and drillers logs. This software uses depth-calibrated images of geophysical well logs and provides efficient tools for their visualization and interpretation. We mapped the stratigraphic units in the subsurface primarily based upon geophysical well log characteristics. Drillers logs were used when no geophysical log was available or to confirm stratigraphic interpretations. The use of well logs from both water wells and deeper oil and gas wells allowed us to correlate the hydrostratigraphic units consistently throughout the study area. The stratigraphic picks were exported to Microsoft Excel for input into ESRI ArcMap® mapping software which was used to interpolate the geologic surfaces.

Figure 7-5 and Figure 7-6 show the correlation of four geophysical well logs using the cross-section feature of the IHS-Markit Kingdom® geological application software. These correlation examples are displayed so that the top of the Hammett shale is set at the same level for all four wells. This is known as “flattening” and frequently used for stratigraphic cross sections.

Outcrop locations provided by the USGS (A.K. Clarke, unpub. data, 2019) and Hays Trinity Groundwater Conservation District (Wierman, 2010) were combined with the Geological Atlas of Texas (Barnes, 1965) contacts to define the formation at the ground surface. We resampled the vertex points from the Geological Atlas of Texas contacts to 250 feet so that they would more closely reflect the accuracy of the modeled surfaces. The points for the surface contacts were included with the well log correlations in the surface generation calculations.

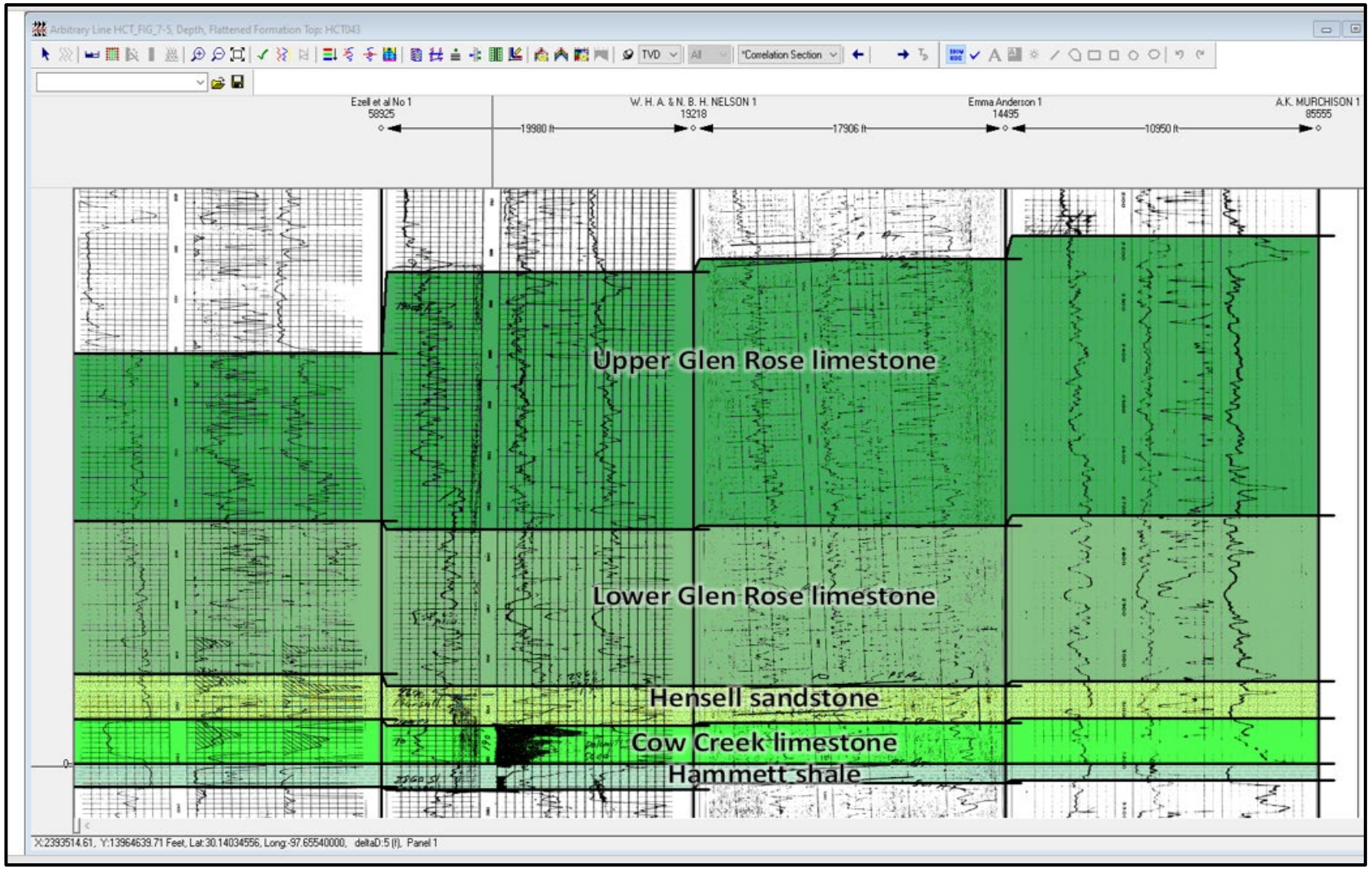

Figure 7-5 **Correlation section showing stratigraphic picks for the upper Trinity (Upper Glen Rose formation) and middle Trinity (Lower Glen Rose, Hensell and Cow Creek formations) from geophysical logs flattened on the top of the Hammett shale.**

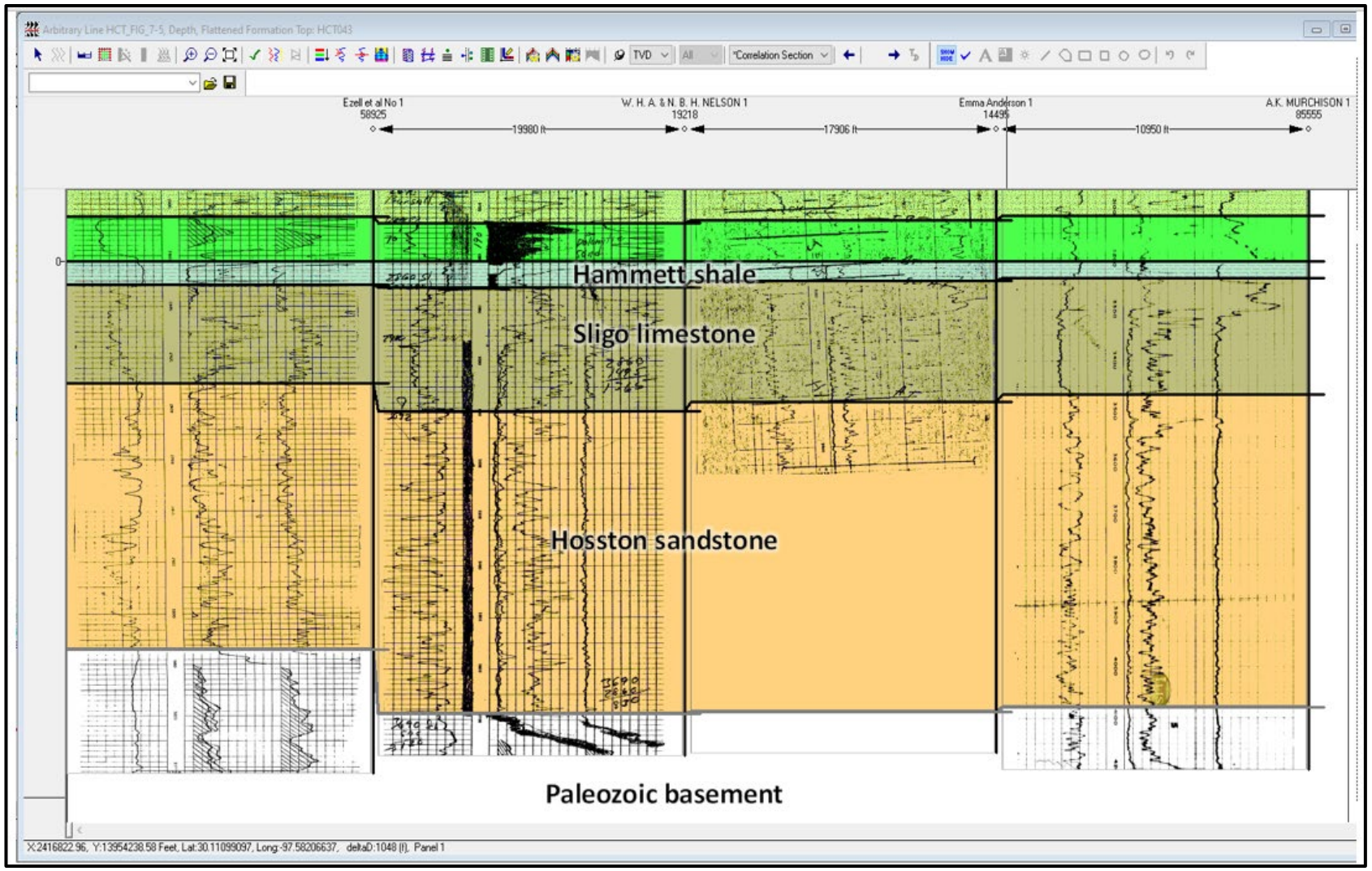

Figure 7-6 **Correlation section showing stratigraphic picks for the lower Trinity (Sligo and Hosston formations) from geophysical well logs flattened on the top of the Hammett shale.**

Faults are an important geological feature of the Trinity Group in the study area. The Balcones Fault Zone consists of hundreds of individual faults with vertical offsets of 10 feet to more than 1,000 feet. However, for this study we have identified 21 faults with significant offsets and nearby well control, thereby allowing us to use them in the surface interpolation process. Four of these faults are identified as reverse faults where the downthrown side is on the north. The remaining 17 faults are normal with the downward displacement on the southern side. Our inclusion of faults into the model is not comprehensive but does provide some insight into how the Trinity Group formations have been offset by faulting.

The Buda Formation is an Upper Cretaceous unit that is regionally identifiable in well logs across the study area. We correlated the Buda Formation surface to provide structural control in several areas where there were few wells that penetrated the Trinity Group. This was particularly important in northern Bexar County were several large faults offset the Cretaceous formations. We then used correlations in deeper wells to define stratigraphic thicknesses to project the depth of the Trinity Group correlations beneath the Buda Formation in shallow wells.

We used ESRI ArcGIS® release 10.7 to generate the geologic surfaces. The resulting surfaces are raster grids consisting of 250-foot square cells. We choose the "TopoToRaster with Cliffs" interpolation toolbox to create the surfaces since it is able to incorporate the offsets associated with large displacement faults. The large number of smaller faults could not be modeled at the scale used for this project and their effects can be considered as averaged within the modeled surfaces. Several Python scripts were developed to ensure that a standardized and repeatable process was used in generating the surfaces (Appendix 19.1). These scripts take the hydrostratigraphic unit picks from well logs correlated in Kingdom and generate the final surfaces developed for the project.

7.5 Hydrostratigraphic units

We followed the precedent established in previous studies (Ashworth, 1983; Wierman and others, 2010; Hunt and others, 2020) and divided the Hill Country Trinity aquifer into seven hydrostratigraphic units, six of which have the potential to be water producing. The six units capable of producing significant quantities of water are the Upper Glen Rose limestone, Lower Glen Rose limestone, Hensell sandstone, Cow Creek limestone, Sligo limestone, and Hosston sandstone. The seventh unit is the Hammett shale which is persistent throughout much of the project area and can be considered an aquitard because of its lithologic composition. We have in this study attempted to map and quantify the distinct properties of each of the hydrostratigraphic units commonly defined for the Hill Country Trinity aquifer. In some cases it was necessary to utilize the hydrologic units (upper Trinity, middle Trinity, and lower Trinity) when assigning certain measured properties because few or no measurements were available at the hydrostratigraphic unit level.

Our use of geophysical well logs to define the subsurface expression of the hydrostratigraphic units is an allostratigraphic approach (Bhattacharya and Walker, 1991) that tends to better reflect the depositional units rather than the named

lithostratigraphic units. For this reason, we have refrained from designating the units as recognized formations and utilize the informal naming convention shown in Figure 7-2.

We synthesized a number of references to provide the following brief descriptions of the Trinity Group hydrostratigraphic units within the study area. These were presented earlier in Section 7. Of particular note would be Ashworth (1983), Tucker (1962), Stricklin and others (1971), Perkins (1974), Bebout and Loucks (1977), and Wierman (2010).

7.5.1 Pre-Cretaceous formations

Rocks of Paleozoic sandstone, shale, and carbonate along with Precambrian granite, schist, and gneiss associated with the Ouachita Metamorphic Zone underlie much of the Trinity Group within the northern half of the study area. Precambrian granites that form the core of the Llano Uplift are located in the northeastern corner of the study area (Figure 7-1). These geologic formations represent the primary source rocks for the argillaceous material and rock fragments found in the sand and conglomeritic beds of the Trinity Group. They have been exposed to extensive erosional processes that have resulted in an irregular surface upon which Early Cretaceous sediments have been deposited. The Pre-Cretaceous formations have generally very low transmissivities compared to the Trinity Group and can generally be treated as an aquitard. There are exceptions to this as several of the pre-Cretaceous formations are known to contain moderate amounts of groundwater that is primarily used for domestic and agricultural purposes (Preston and others, 1996).

The southeastern half of the study area is underlain by Jurassic sands and shales of the Cotton Valley Group which onlaps the previously mentioned Paleozoic rocks. This contact can be observed on geophysical well logs several thousand feet below the ground surface where a significant shale unit separates the Trinity Group from the underlying Jurassic formations (Figure 7-6). The Cotton Valley Group is not a source for water in the study area.

A structure map showing the elevation of the base of the Cretaceous formations is shown in Figure 7-7. A structure map showing the depth to the base of the Cretaceous formations is shown in Figure 7-8.

7.5.2 Hosston sandstone

The Hosston sandstone is composed of alternating layers of sandstone and shale. The sandstones are fine grained, are generally calcite cemented, can be massive, and contain various amounts of silt and clay. The shales are calcareous and frequently identified as marly. Conglomerates have been noted in the basal portions of the Hosston sandstone. The Sycamore sand is considered part of the basal Hosston sandstone and is noted for being highly conglomeritic. The Hosston sandstone sits unconformably upon the Pre-Cretaceous units. The Hosston sandstone is considered the basal member of the lower Trinity hydrologic unit.

The Hosston sandstone is dominated by fluvial and fluvial-deltaic sediments that were deposited during a low stand of the ancestral Gulf of Mexico and is characterized by a fining upwards succession that records a rise in sea level that pushed the shoreline westward onto the Llano Uplift. The Llano Uplift is considered the primary source for the silicious components of the Hosston sandstone.

Figure 7-9 is a structure map showing the elevation of the top of the Hosston sandstone. The depth to the top of the Hosston sandstone is shown in Figure 7-10. A thickness map of the Hosston sandstone is shown in Figure 7-11.

7.5.3 Sligo limestone

The Sligo limestone conformably overlies the Hosston sandstone and represents a transgressive sequence of sediments composed of sand, shales, and carbonates. The carbonate beds within the Sligo limestone are often dolomitized with moderate porosity and are sources of groundwater. The Sligo limestone is the upper member of the lower Trinity hydrologic unit.

Figure 7-12 is a structure map showing the elevation of the top of the Sligo limestone. The depth to the top of the Sligo limestone is shown in Figure 7-13. A thickness map of the Sligo limestone is shown in Figure 7-14.

7.5.4 Hammett shale

Deposition of the Hammett shale represents the maximum sea level rise or "high-stand" during the Trinity Group time period. It is composed of thinly bedded shallow marine calcareous shales and silty shales. The Hammett shale is conformable with the underlying Sligo limestone. The Hammett shale is not a water bearing unit because of its fine-grained character resulting in very low permeability. The Hammett shale is roughly 35 to 50 feet thick throughout the study area and is a significant aquitard throughout the study area that restricts groundwater flow between the lower Trinity hydrostratigraphic units and the Cow Creek limestone. The Hammett shale is stratigraphically equivalent to the Pine Island Shale in downdip portions of the study area (Forgotson, 1957).

Figure 7-15 is a structure map showing the elevation of the top of the Hammett shale. The depth to the top of the Hammett shale is shown in Figure 7-16. A thickness map of the Hammett shale is shown in Figure 7-17.

7.5.5 Cow Creek limestone

The Cow Creek limestone is a significant aquifer for shallow domestic and agricultural water wells. In the updip portions of the study area the Cow Creek limestone is often a highly porous calcareous grainstone exhibiting dissolution channels and vugs. Downdip the Cow Creek limestone becomes increasingly dolomitic and is known as the James Lime, a potential petroleum bearing formation (Forgotson, 1957). The Cow Creek limestone is the basal member of the middle Trinity hydrologic unit.

Figure 7-18 is a structure map showing the elevation of the top of the Cow Creek limestone. The depth to the top of the Cow Creek limestone is shown in Figure 7-19. A thickness map of the Cow Creek limestone is shown in Figure 7-20.

7.5.6 Hensell sandstone

The Hensell sandstone was named by Hill (1901, page 131, 143) and the name is recognized by the United States Geological Survey. However, locally it is believed that Hill misspelled the name Hensel, which is the name of the family upon whose property the type location is located. Many groundwater conservation districts' use the spelling Hensel Sand in their reports. This study will use the name Hensell sandstone in order to conform with the USGS and with many previously published reports and studies.

Hensell sandstone is a stratigraphic name used to identify sand and conglomerate beds that outcrop in the northern portion of the study area that directly overlie the Paleozoic basement rocks of the Llano Uplift. The basal conglomerate and sand beds are of mixed age with the lower beds potentially equivalent to the Hosston sandstone. Because both the Hosston sandstone and the Hensell sandstone are sourced from the same basement rocks and the sandstones contains few fossils, they can be differentiated only with very careful and detailed analysis. A similar relationship exists with the Glen Rose Formation which overlies the Hensell sandstone. As the limestone beds of the Glen Rose Formation onlap in the western part of the study area, they become more argillaceous and it becomes difficult to separate the basal Glen Rose Formation from the Hensell sandstone which often includes interbedded carbonates (Wierman, 2010; Alex S. Broun, personal communication, 2019).

The Hensell sandstone becomes finer grained in a downdip eastward direction. In deep oil and gas wells, the Hensell sandstone is called the Bexar Shale where the depositional facies changes from a fluvial to a marine environment (Forgotson, 1957). The Hensel sandstone is the middle member of the middle Trinity hydrologic unit.

Figure 7-21 is a structure map showing the elevation of the top of the Hensell sandstone. The depth to the top of the Hensell sandstone is shown in Figure 7-22. A thickness map of the Hensell sandstone is shown in Figure 7-23.

7.5.7 Lower Glen Rose limestone

The Glen Rose Formation was deposited upon a shallow marine carbonate shelf resulting in a lithologically complex formation composed of interbedded limestones, dolomites, shales, evaporites, and sandy siltstones (Bebout, 1977). Evidence of water level fluctuations is documented by the diverse faunal associations that have been identified; reef facies, stromatolitic algae mounds, oyster beds, and plant fragments (Stricklin and others, 1971). Massive carbonate beds 10 to 20 feet thick separated by clay rich intervals that are several feet thick are common in the Lower Glen Rose limestone. Ashworth (1983) states, "Because the lower member of the Glen Rose is massive, it is more susceptible than the upper member to the development of secondary porosity which

results from jointing, faulting, and the dissolving action of ground water, and hence is generally the more prolific water-producing zone."

Because of the existence of numerous permeability barriers within the Glen Rose Formation, the Lower Glen Rose limestone has been shown to be hydrologically separated from the Upper Glen Rose limestone (Ashworth, 1983; Smith and Hunt, 2009; Smith and others, 2018). Consequently, the Lower Glen Rose limestone is the upper member of the middle Trinity hydrologic unit.

Figure 7-24 is a structure map showing the elevation of the top of the Lower Glen Rose limestone. The depth to the top of the Lower Glen Rose limestone is shown in Figure 7-25. A thickness map of the Lower Glen Rose limestone is shown in Figure 7-26.

7.5.8 Upper Glen Rose limestone

The Upper Glen Rose limestone represents the top of the Trinity Group. This unit is depositionally similar to the Lower Glen Rose limestone and is also composed of interbedded limestones, dolomites, shales, evaporites, and sandy siltstones. Important differences from the Lower Glen Rose limestone include fewer massive carbonate units, the carbonate beds are generally thinner, and there are a greater number of evaporite deposits towards the base of the Upper Glen Rose limestone.

Directly above the Upper Glen Rose limestone is the Walnut Clay of the Fredericksburg Group. The Walnut Clay thins to the north and west within the study area and does not appear to be an effective barrier to cross-formational flow between the basal Fredericksburg Group (which includes the Edwards Aquifer) and the Upper Glen Rose limestone as shown by the Barton Springs/Edwards Aquifer Conservation District multiport well studies (Wong and others, 2014). The Upper Glen Rose limestone is also equivalent to the upper Trinity hydrologic unit.

Figure 7-27 is a structure map showing the elevation of the top of the Upper Glen Rose limestone. The depth to the top of the Upper Glen Rose limestone is shown in Figure 7-28. A thickness map of the Upper Glen Rose limestone is shown in Figure 7-29.

This page is intentionally blank.

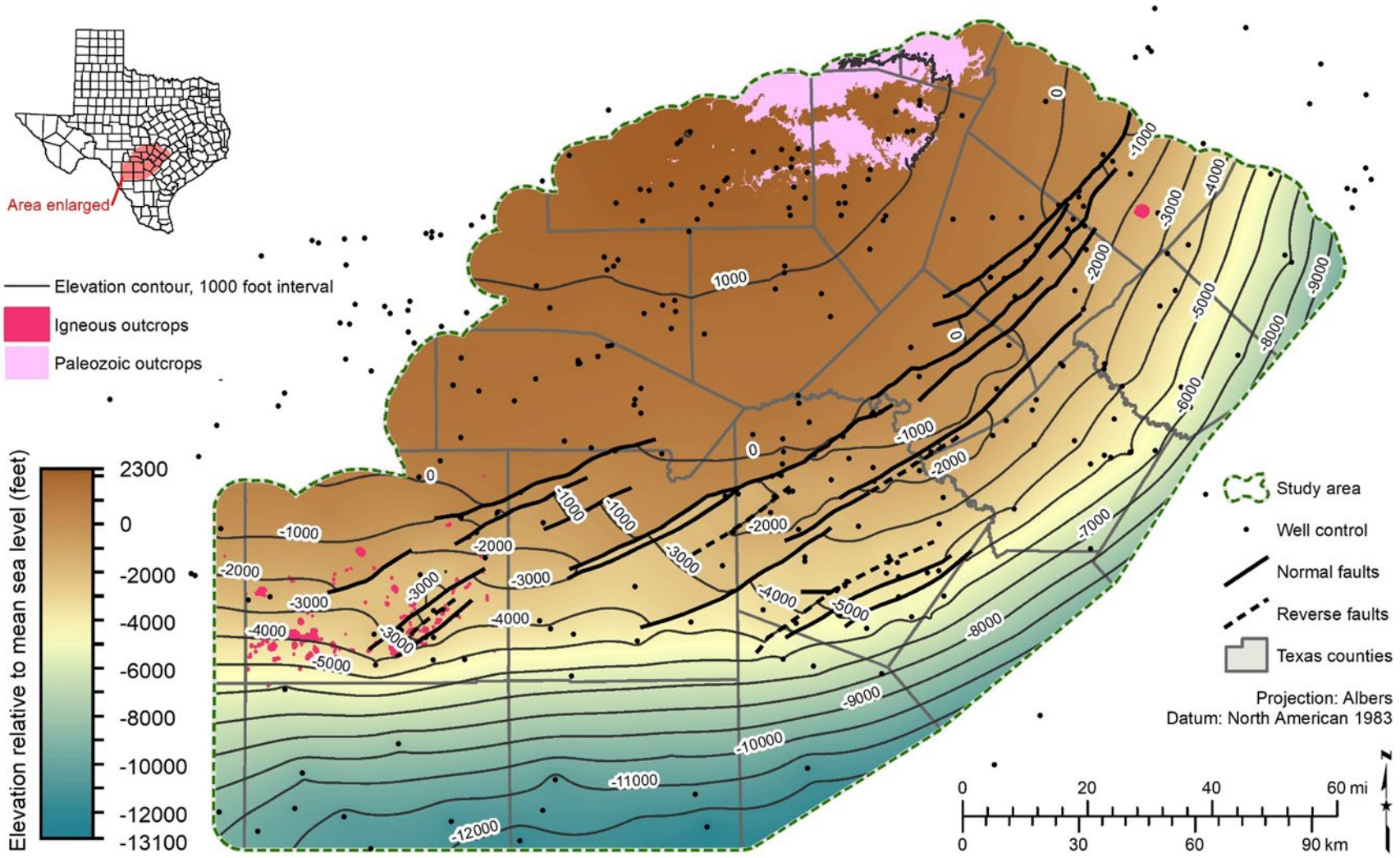

Figure 7-7 Base of Cretaceous structure map (elevation datum is mean sea level, feet).

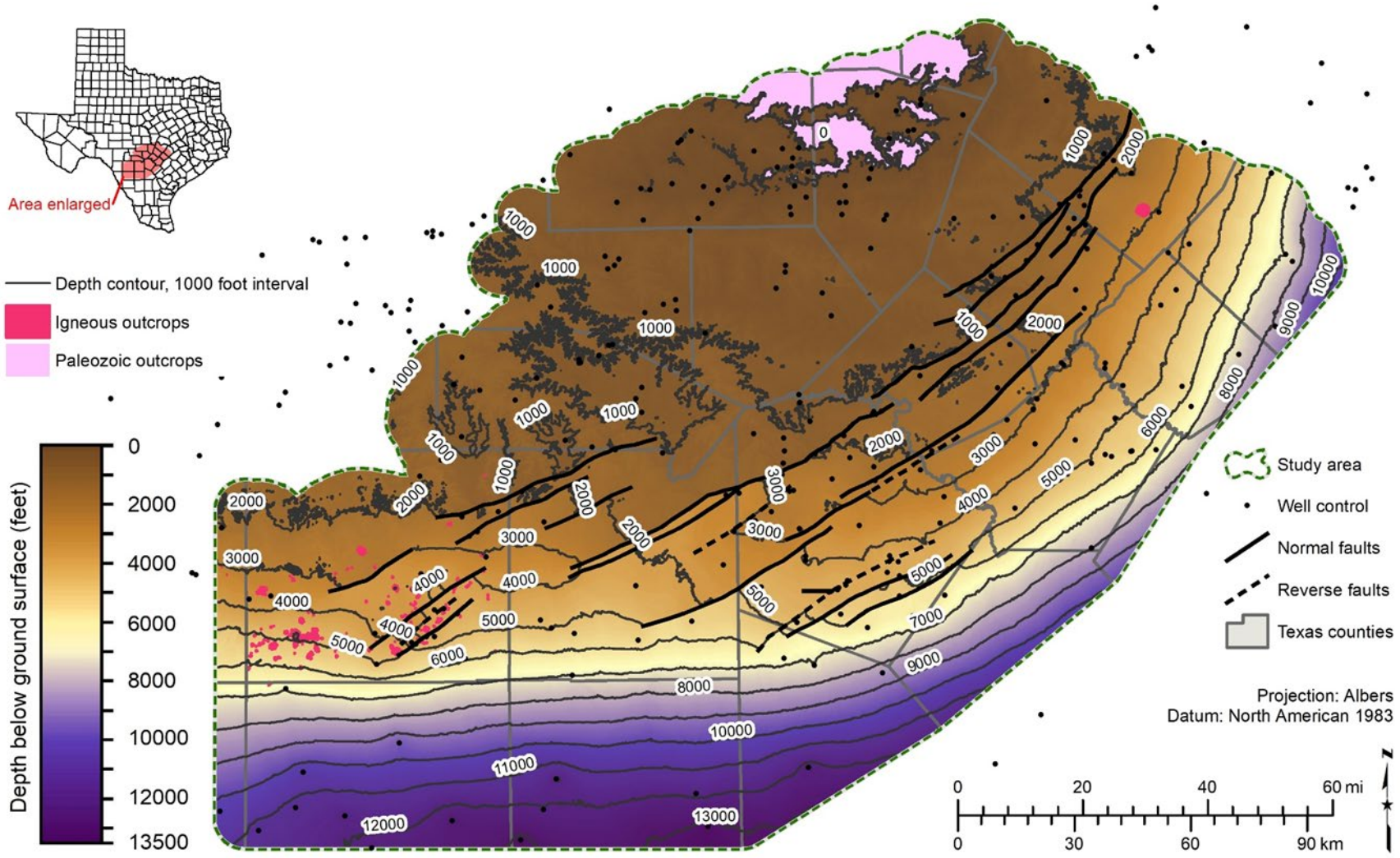

Figure 7-8 Base of Cretaceous depth surface map (depth below ground surface, feet).

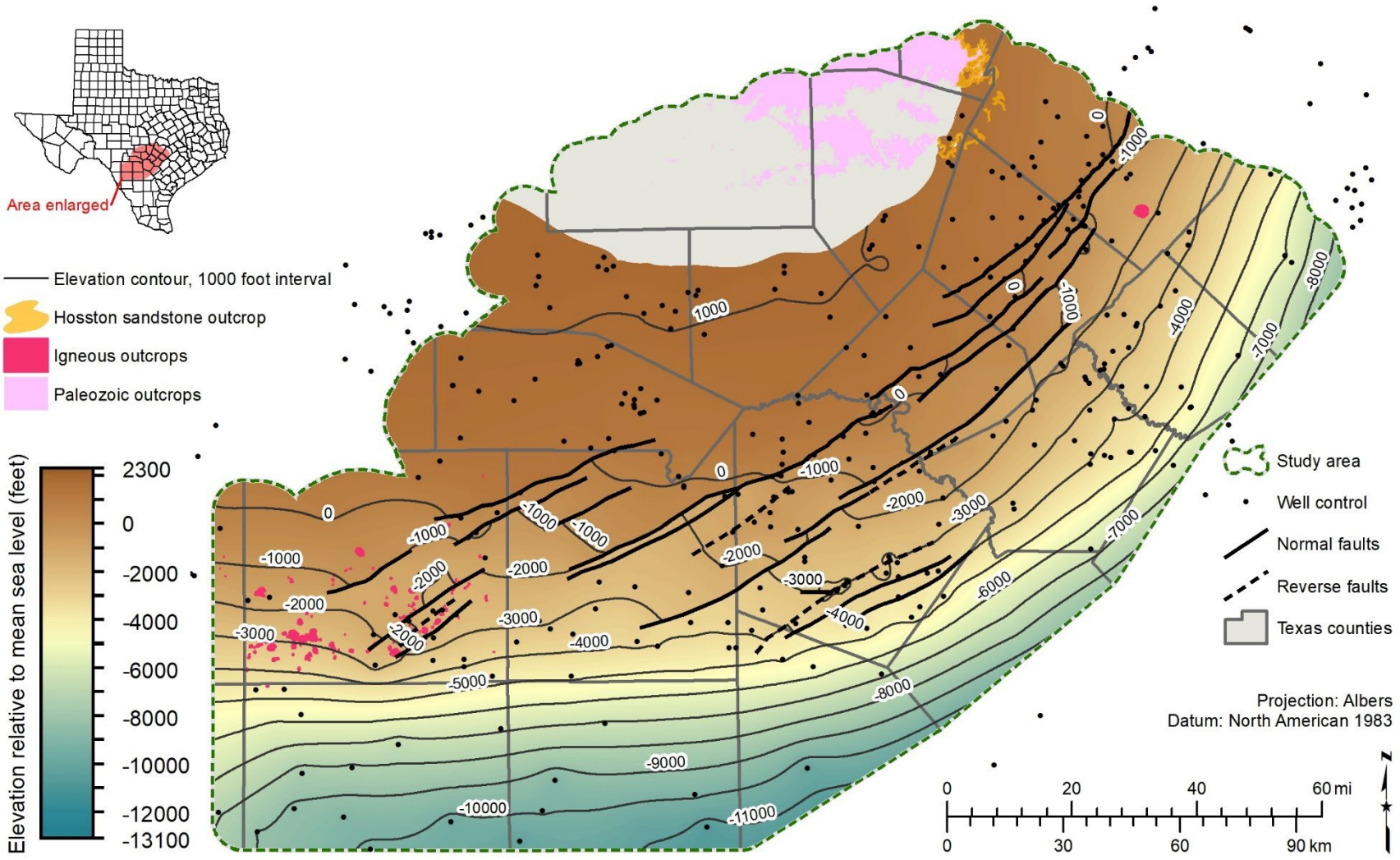

Figure 7-9 Hosston sandstone structure map (elevation datum is mean sea level, feet).

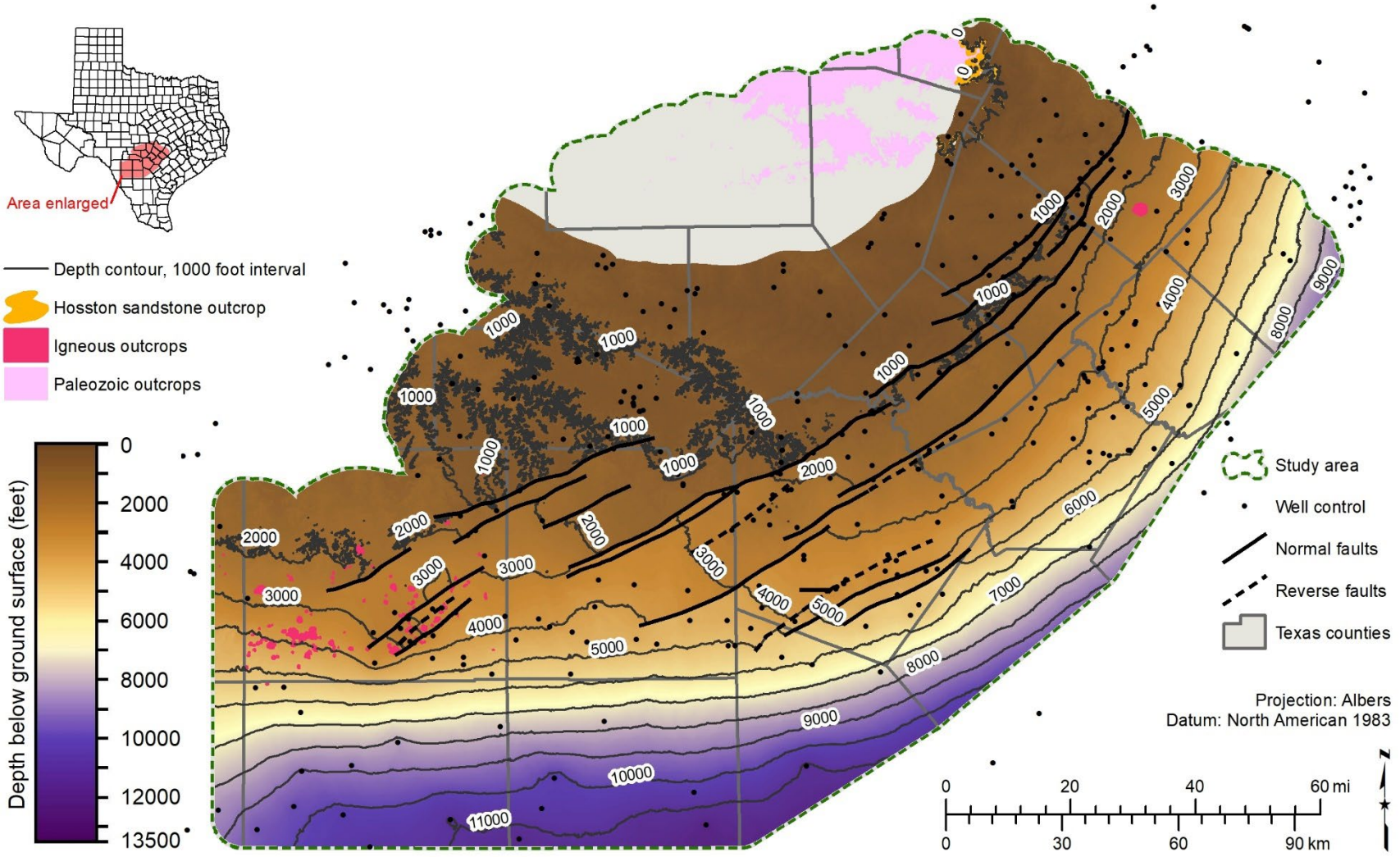

Figure 7-10 Hosston sandstone depth surface map (depth below ground surface, feet).

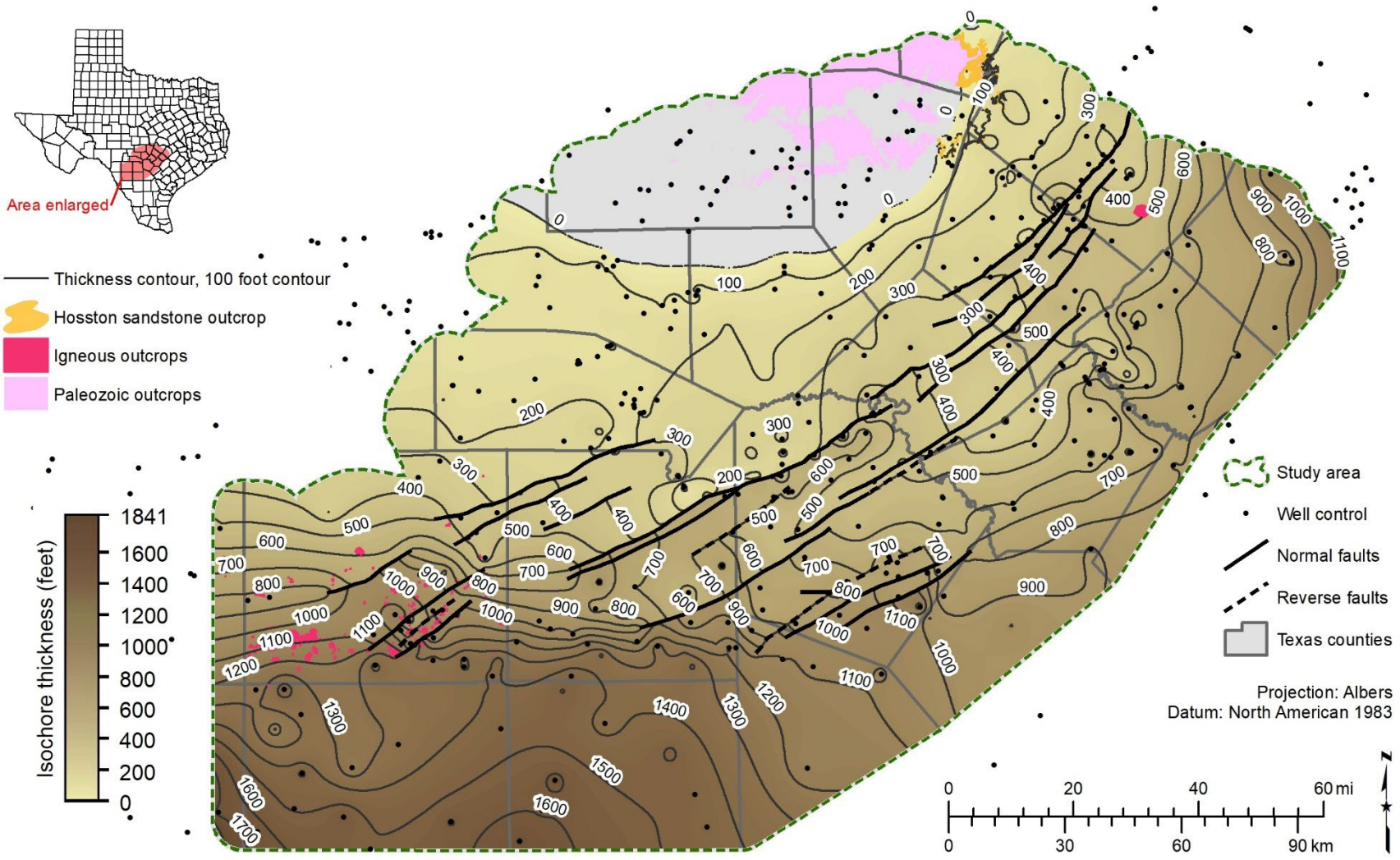

Figure 7-11 Hosston sandstone thickness map (thickness in feet). Gray areas on map indicate where the Hosston sandstone is absent.

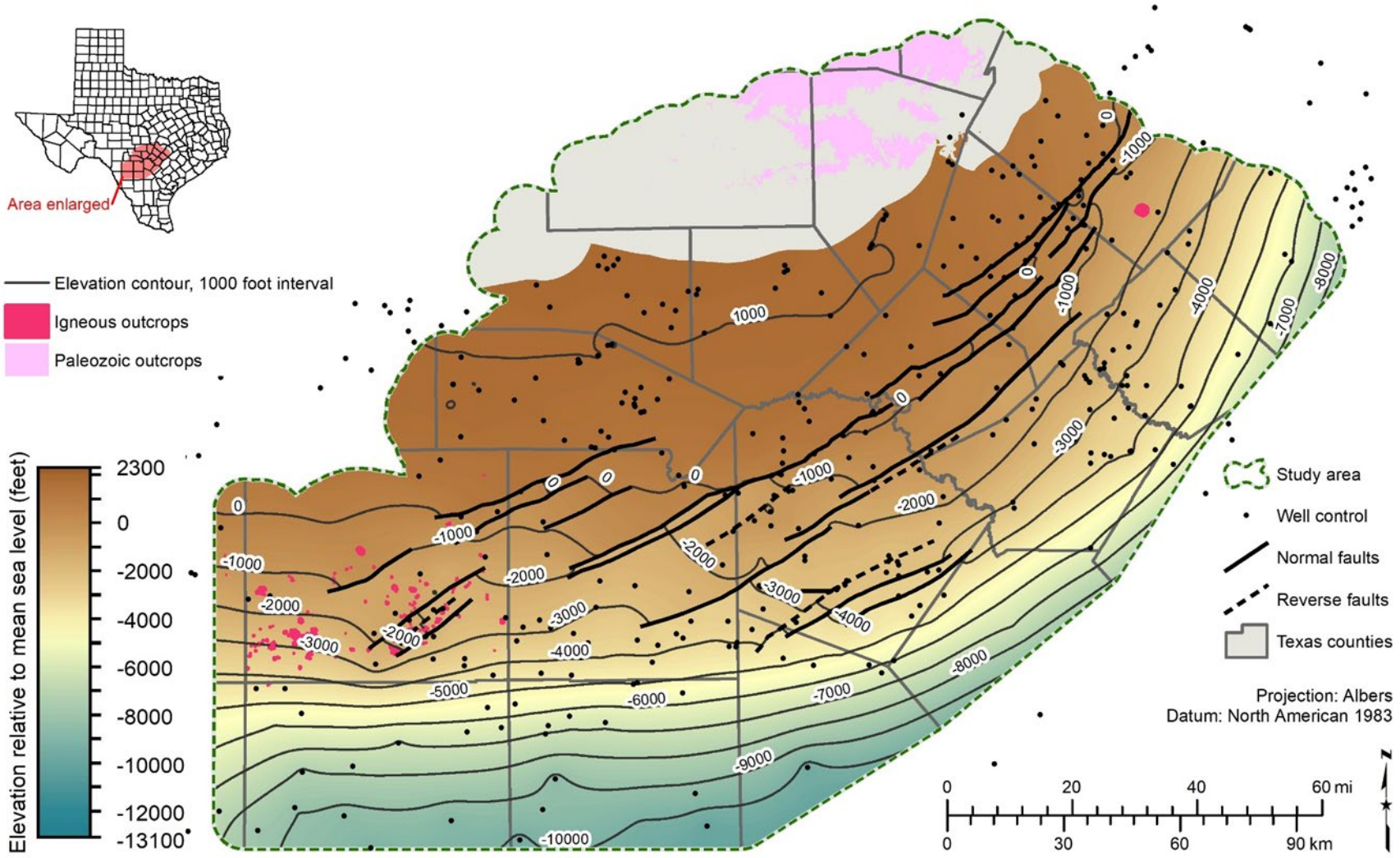

Figure 7-12 Sligo limestone structure map (elevation datum is mean sea level, feet).

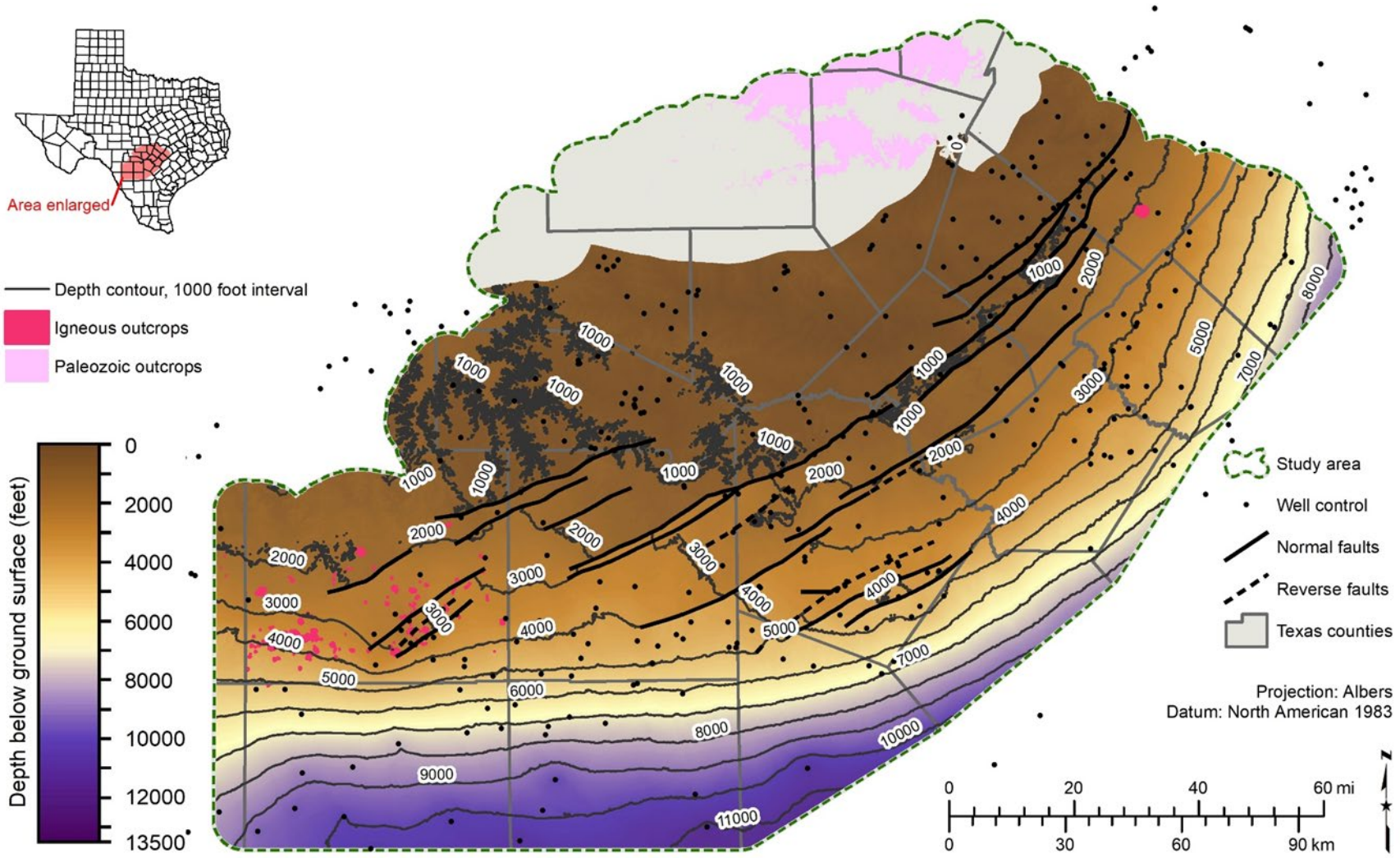

Figure 7-13 Sligo limestone depth surface map (depth below ground surface, feet).

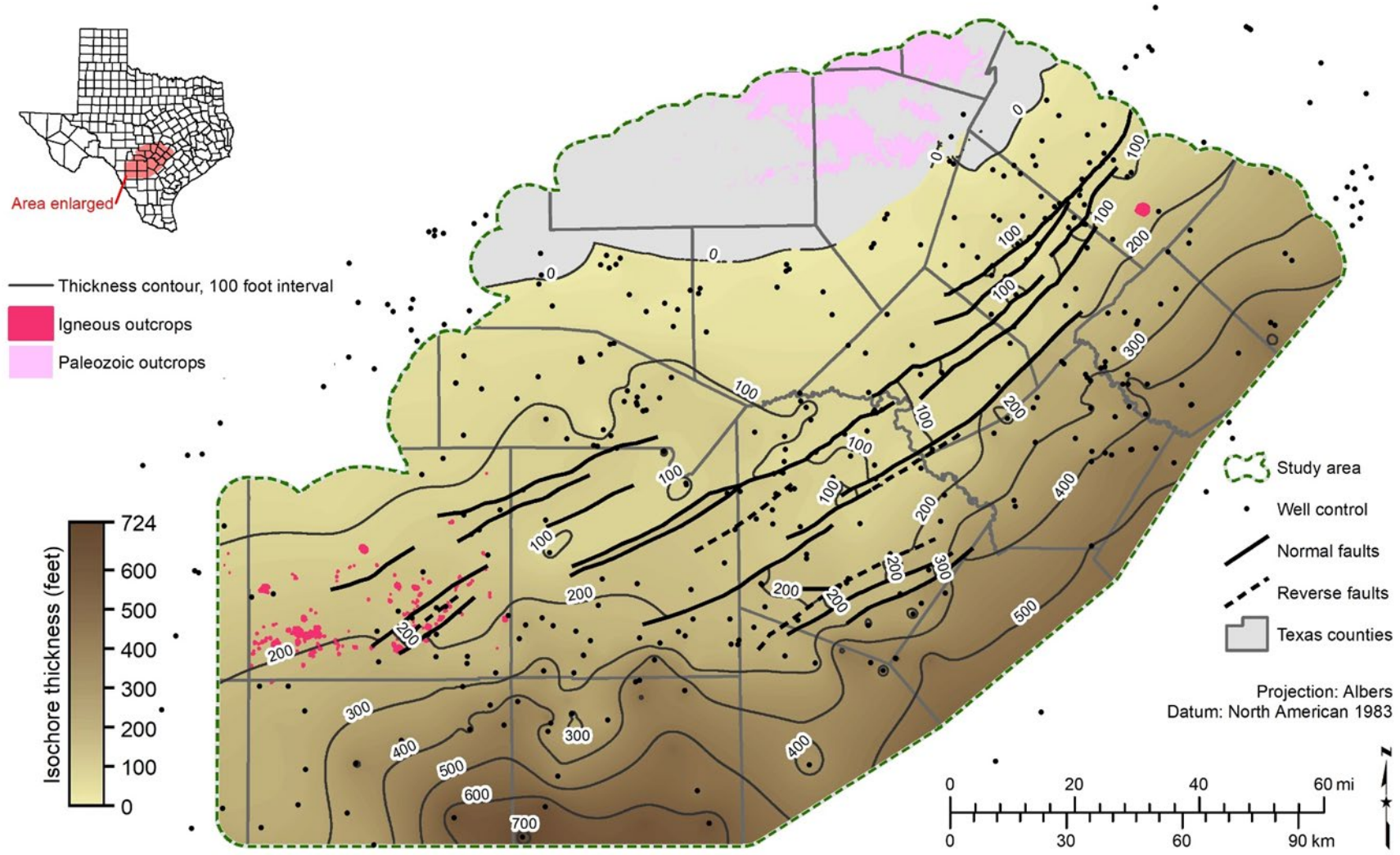

Figure 7-14 Sligo limestone thickness map (thickness in feet). Gray areas on map indicate where the Sligo limestone is absent.

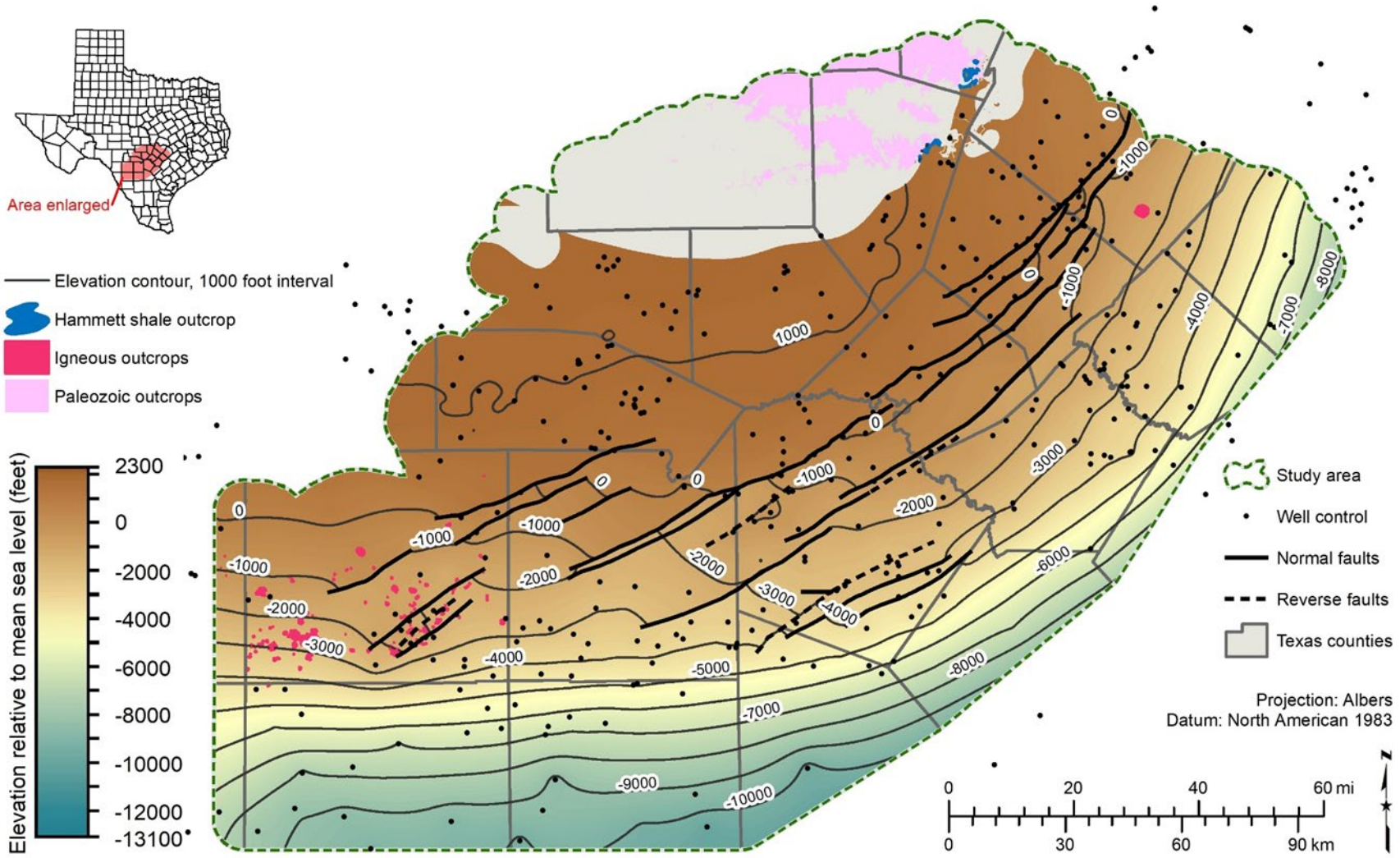

Figure 7-15 Hammett shale structure map (elevation datum is mean sea level, feet).

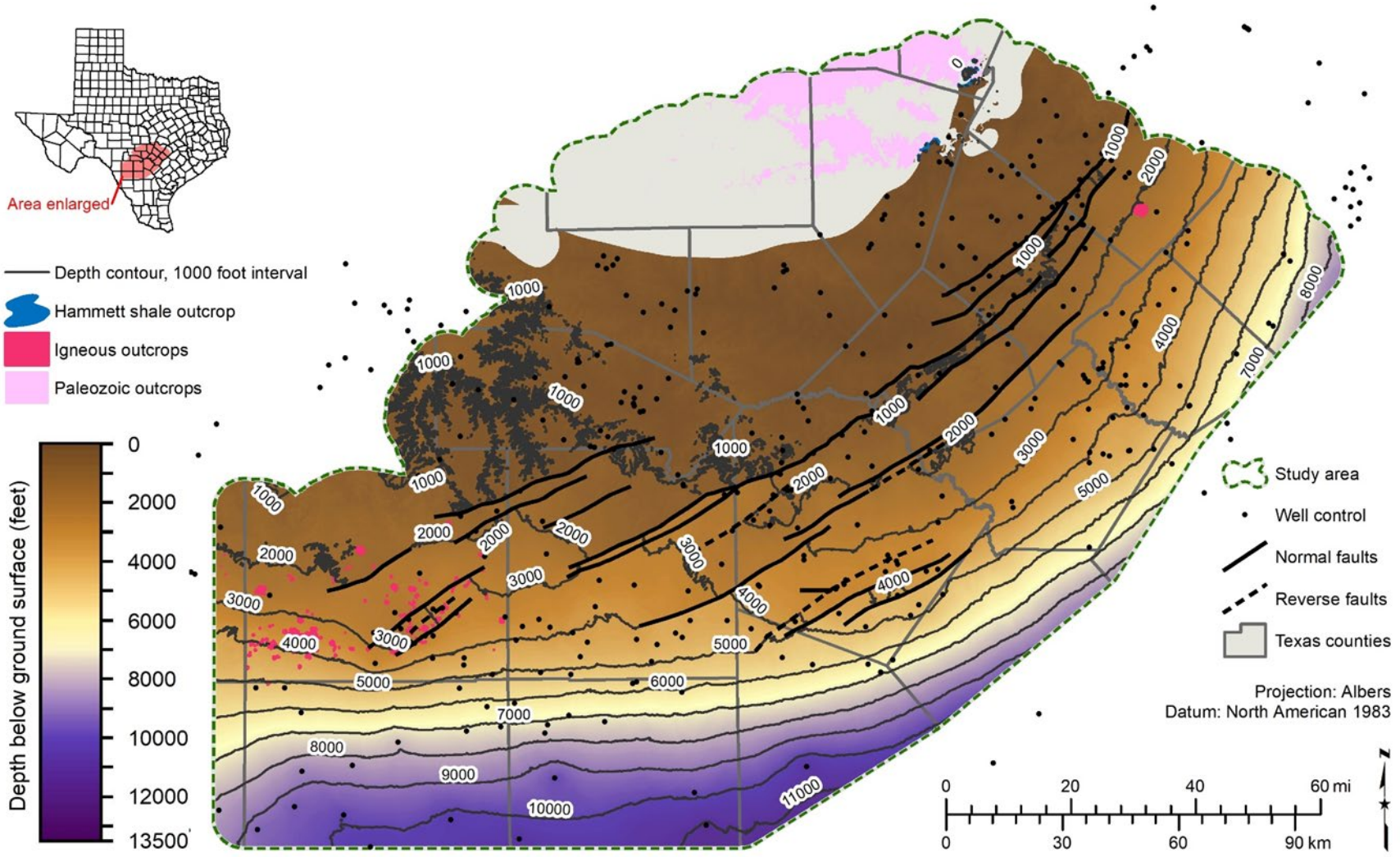

Figure 7-16 Hammett shale depth surface map (depth below ground surface, feet).

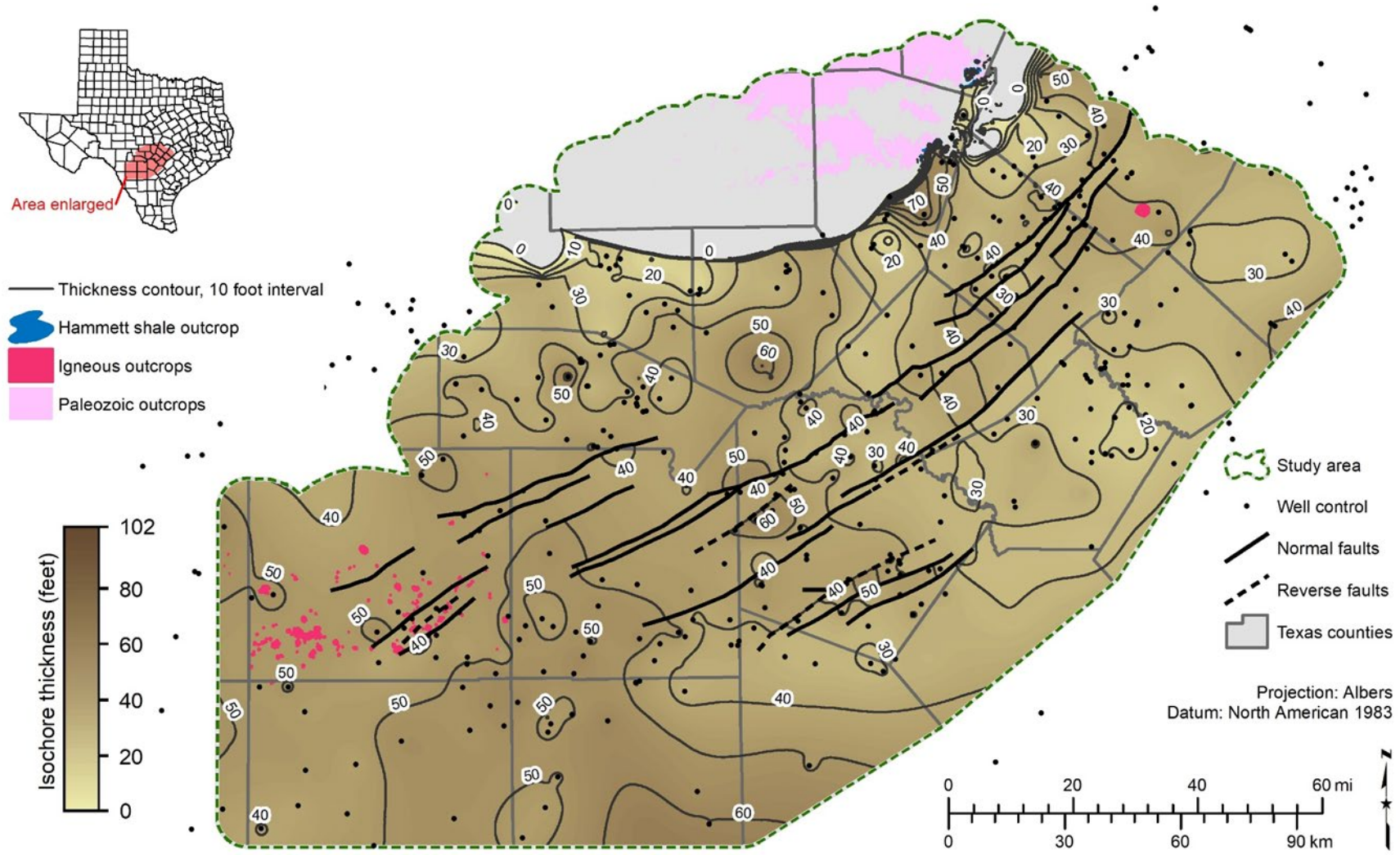

Figure 7-17 Hammett shale thickness map (thickness in feet). Gray areas on map indicate where the Hammett shale is absent.

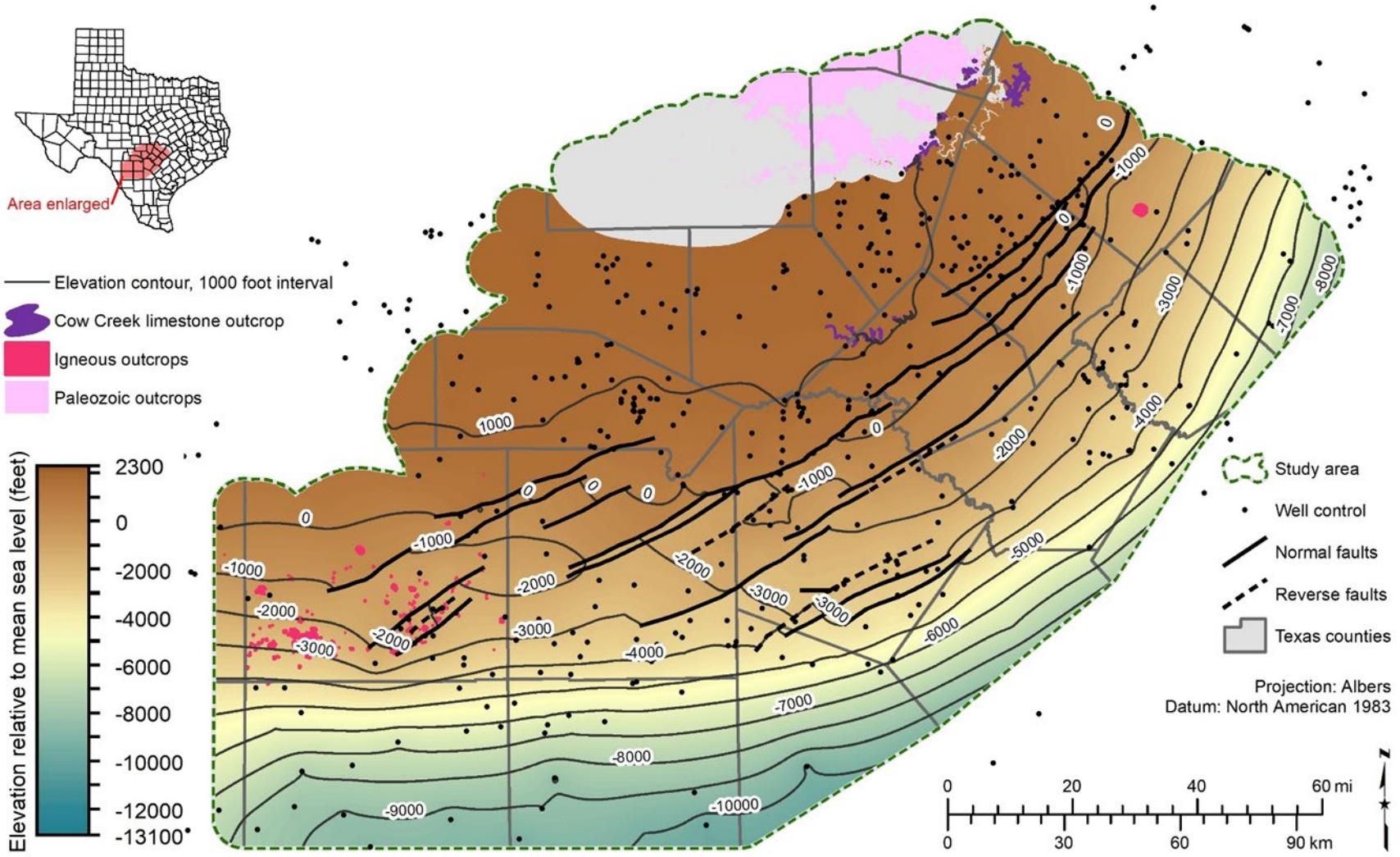

Figure 7-18 Cow Creek limestone structure map (elevation datum is mean sea level, feet).

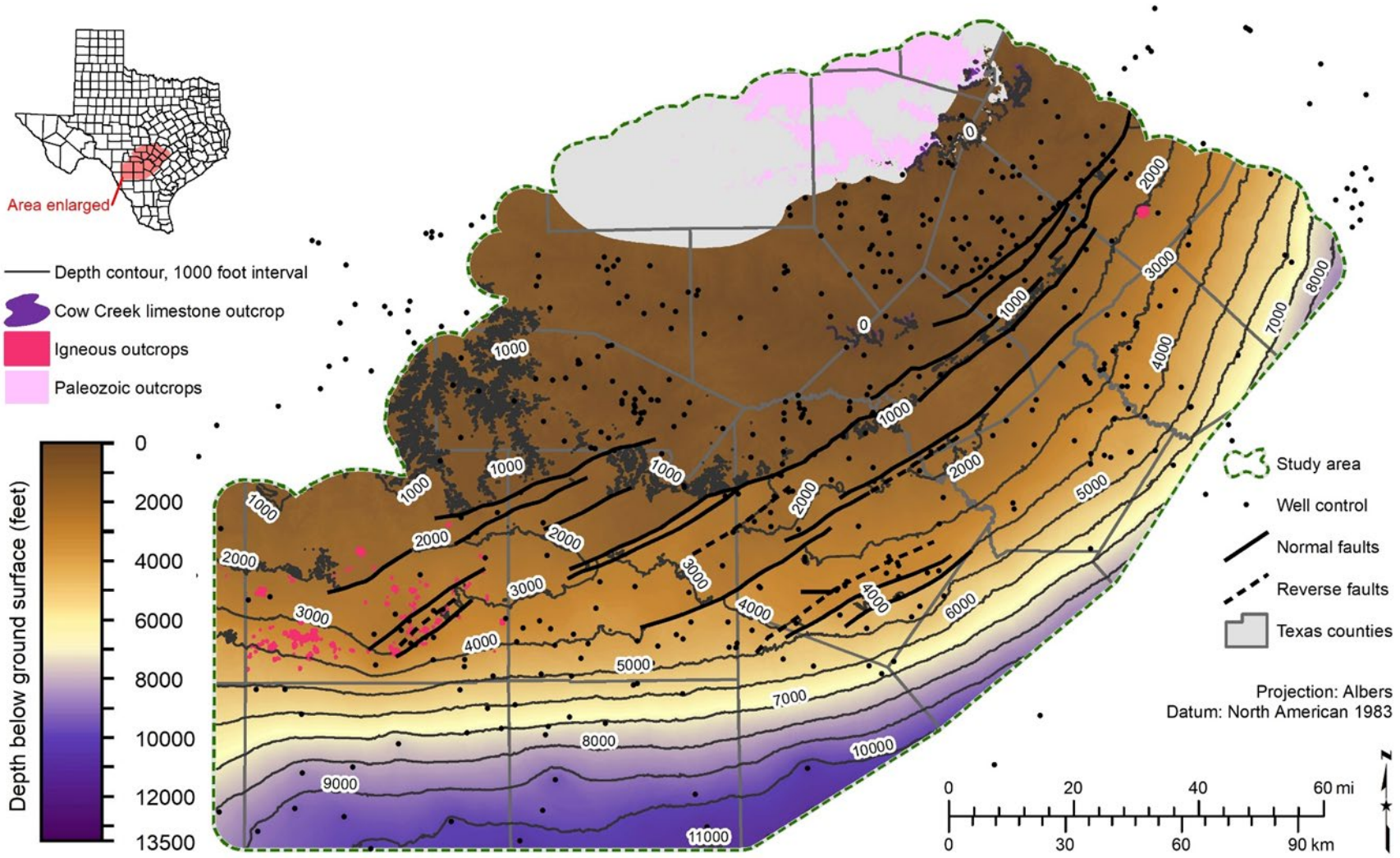

Figure 7-19 Cow Creek limestone depth surface map (depth below ground surface, feet).

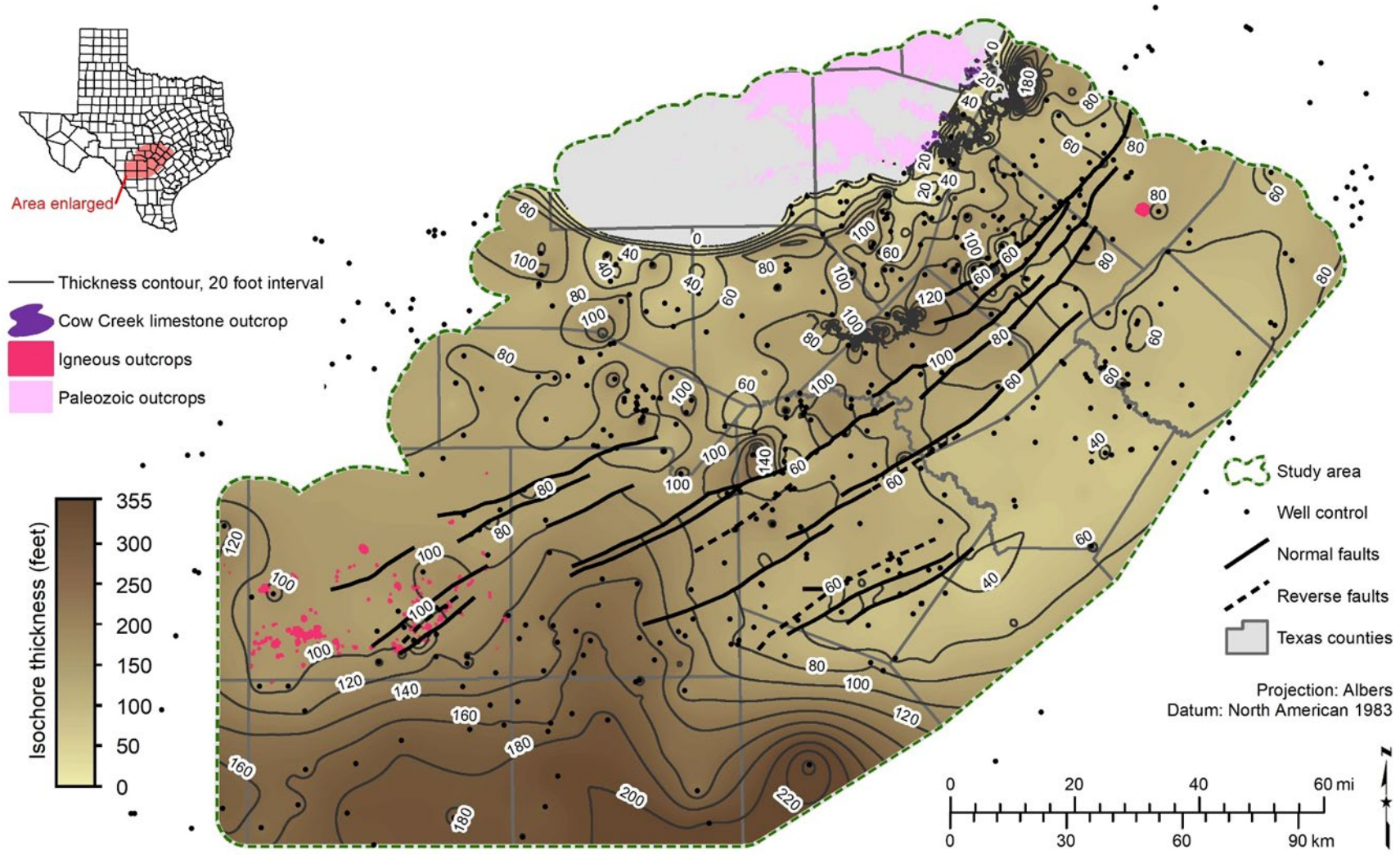

Figure 7-20 **Cow Creek limestone thickness map (thickness in feet). Gray areas on map indicate where the Cow Creek limestone is absent.**

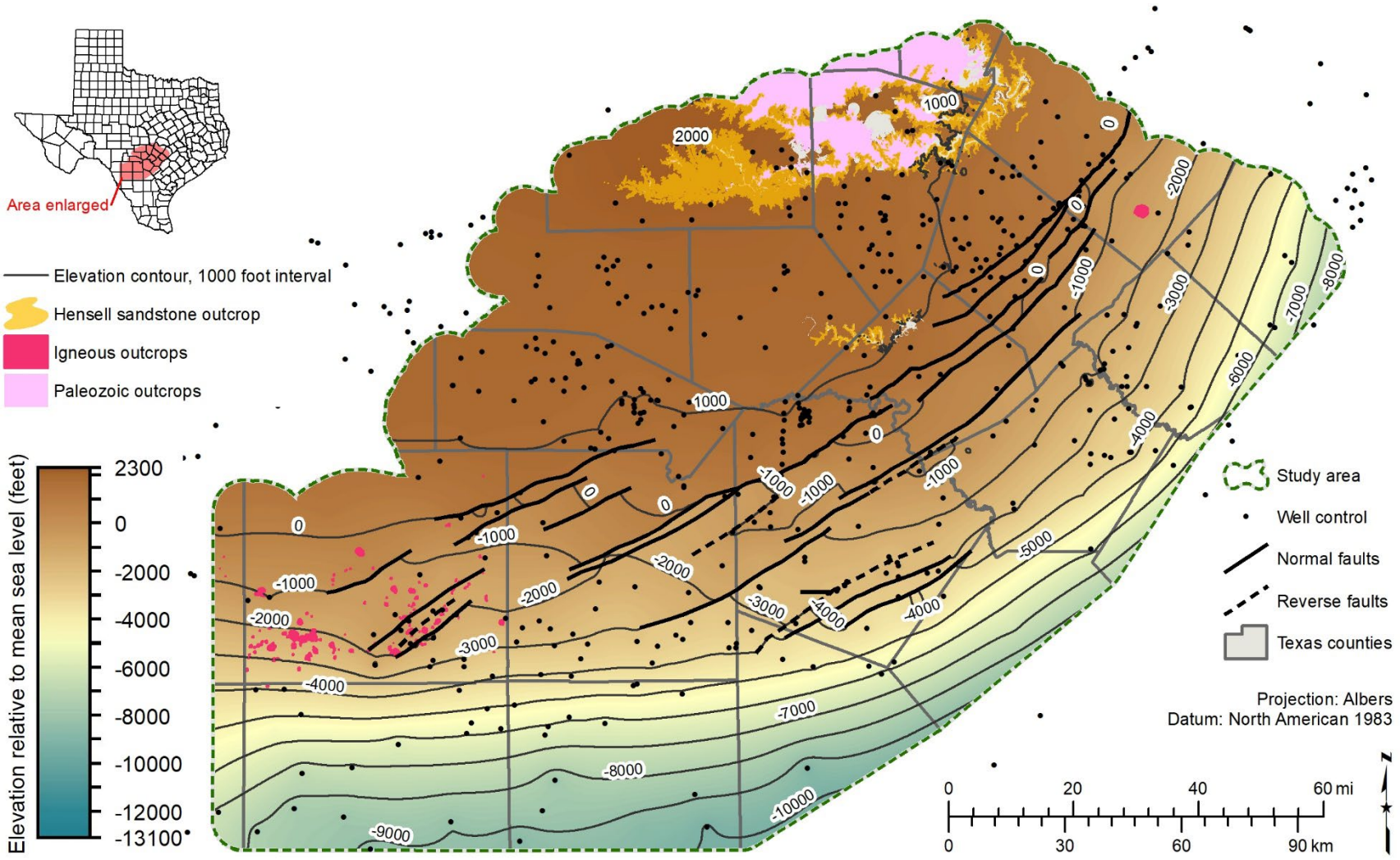

Figure 7-21 Hensell sandstone structure map (elevation datum is mean sea level, feet).

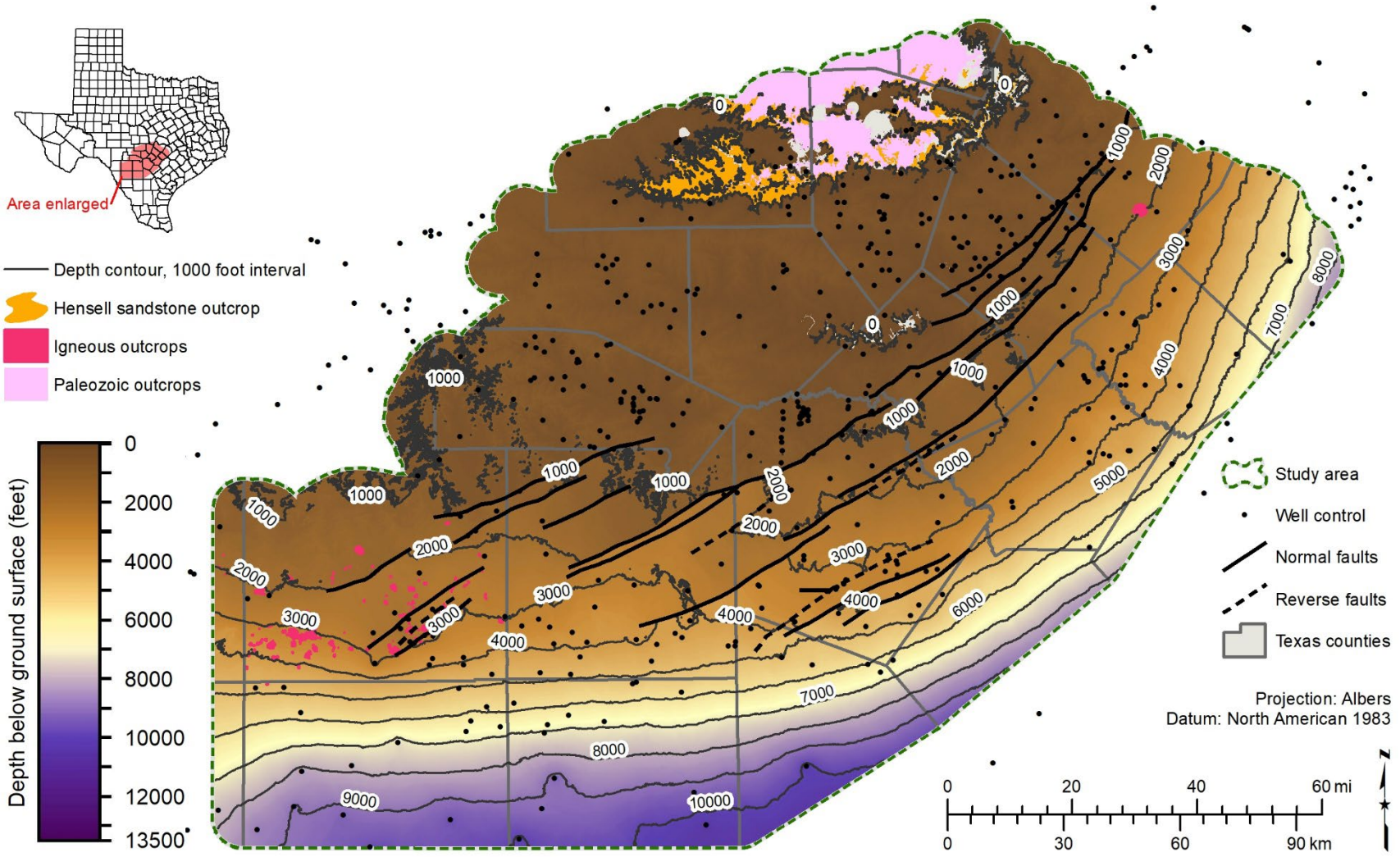

Figure 7-22 Hensell sandstone depth surface map (depth below ground surface, feet).

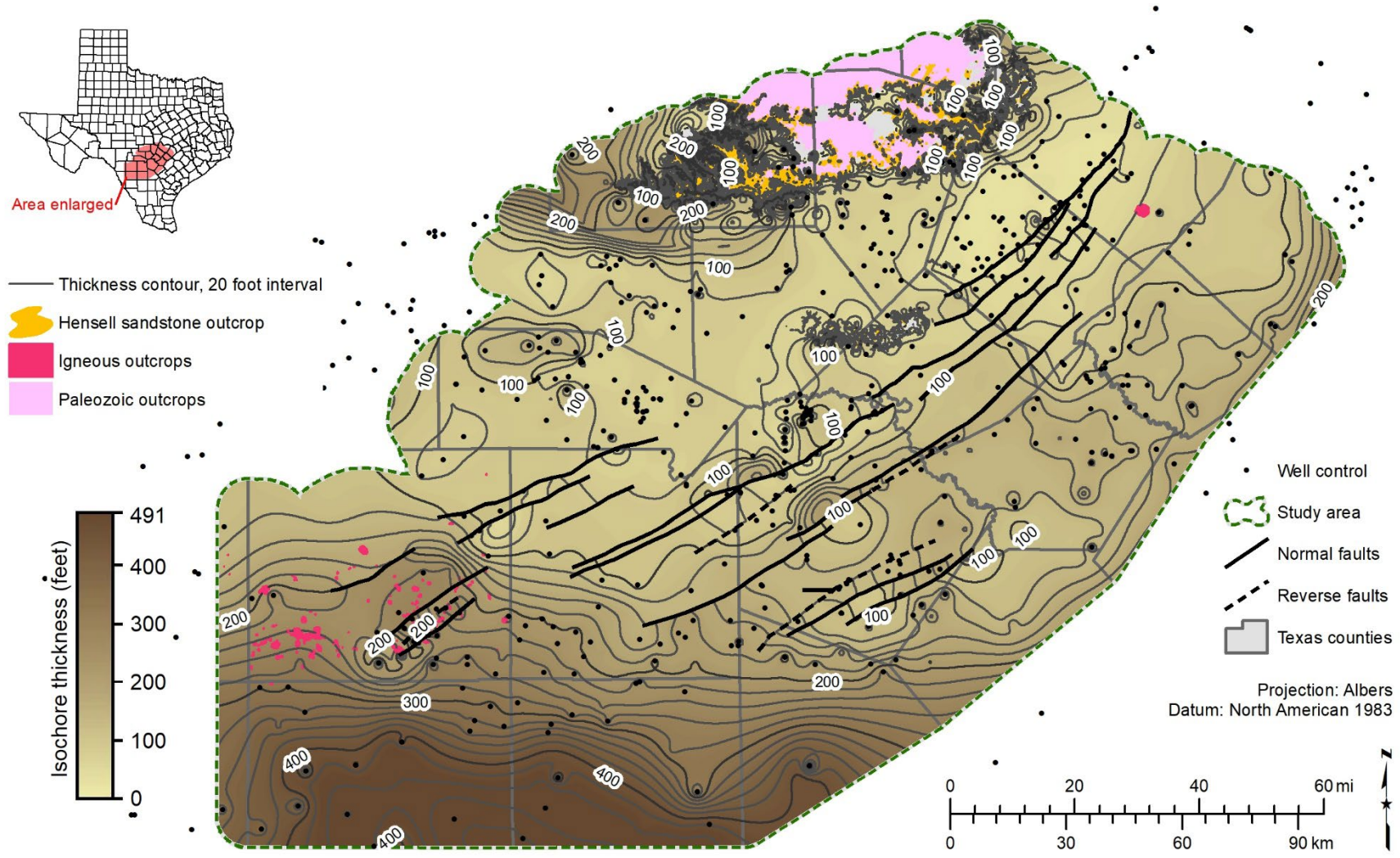

Figure 7-23 Hensell sandstone thickness map (thickness in feet). Gray areas on map indicate where the Hensell sandstone is absent.

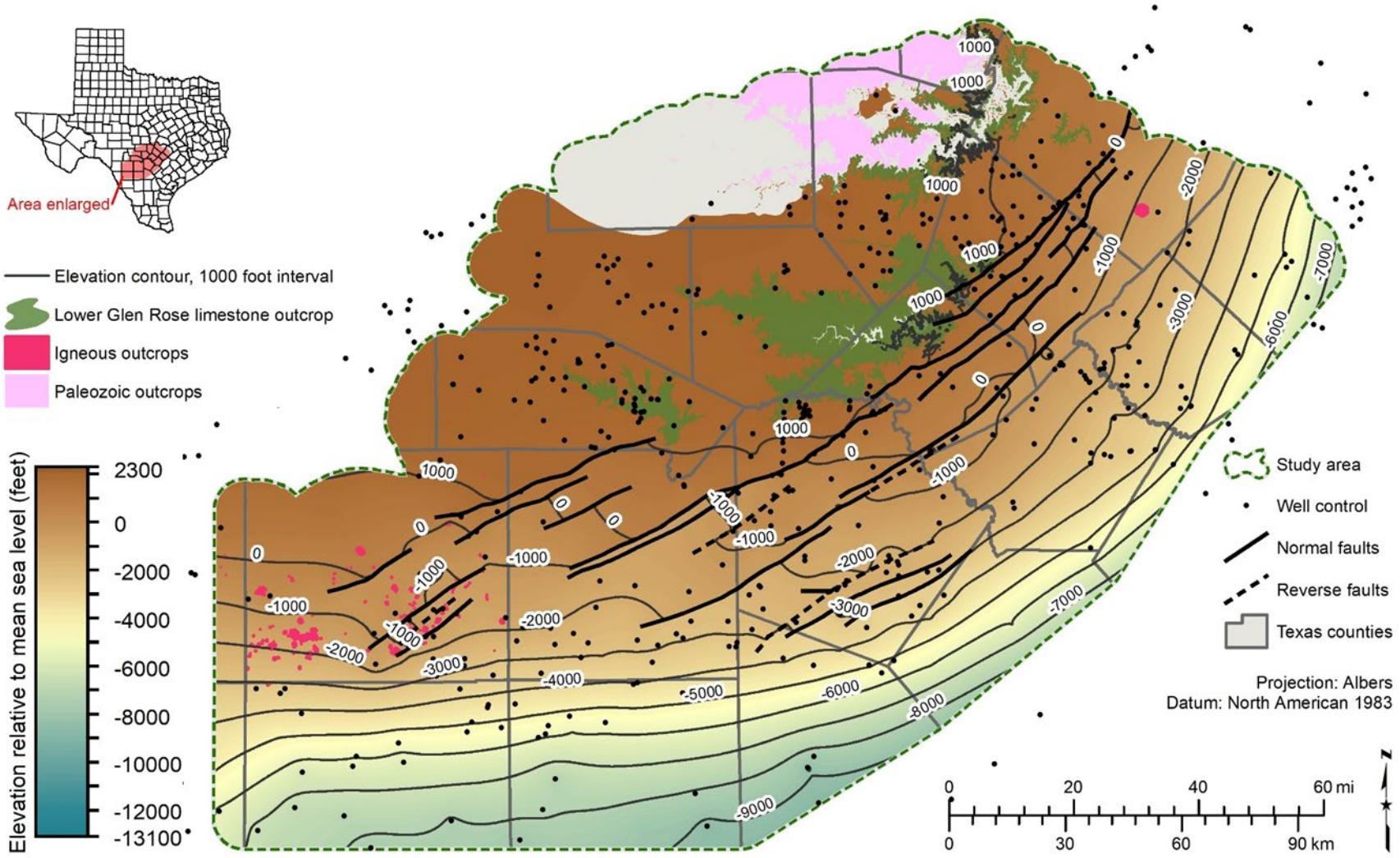

Figure 7-24 Lower Glen Rose limestone structure map (elevation datum is mean sea level, feet).

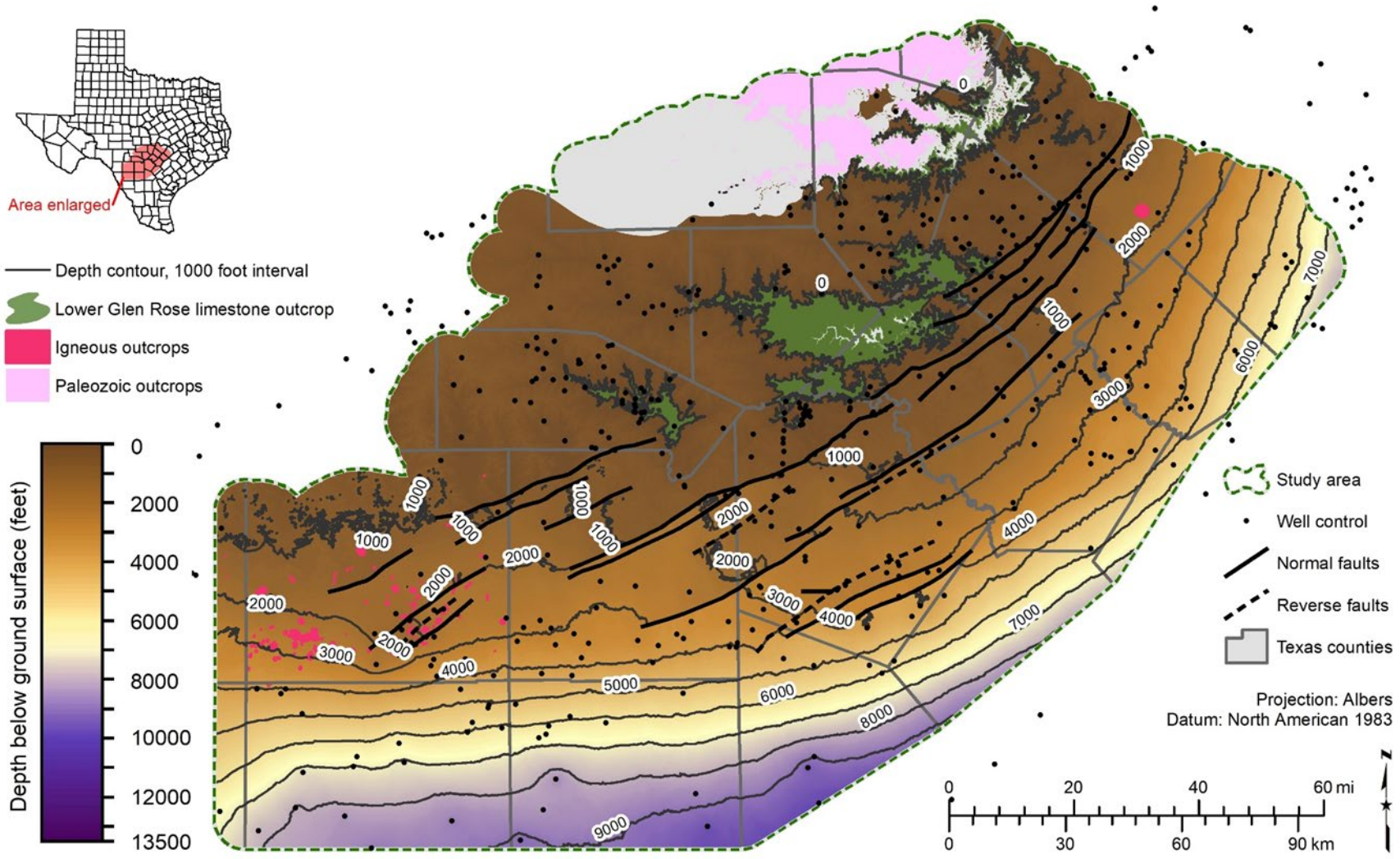

Figure 7-25 Lower Glen Rose limestone depth surface map (depth below ground surface, feet).

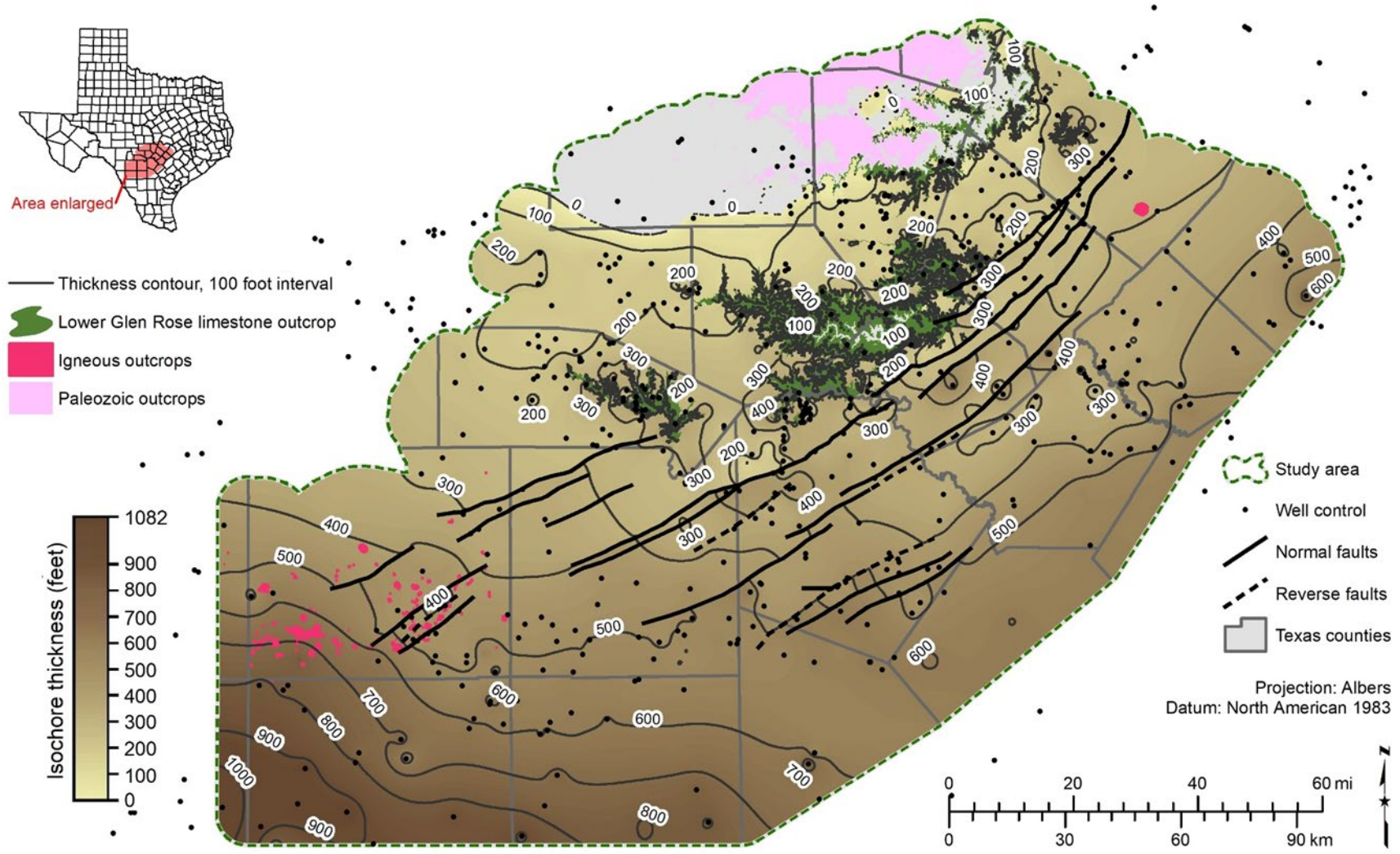

Figure 7-26 **Lower Glen Rose limestone thickness map (thickness in feet). Gray areas on map indicate where the Lower Glen Rose limestone is absent.**

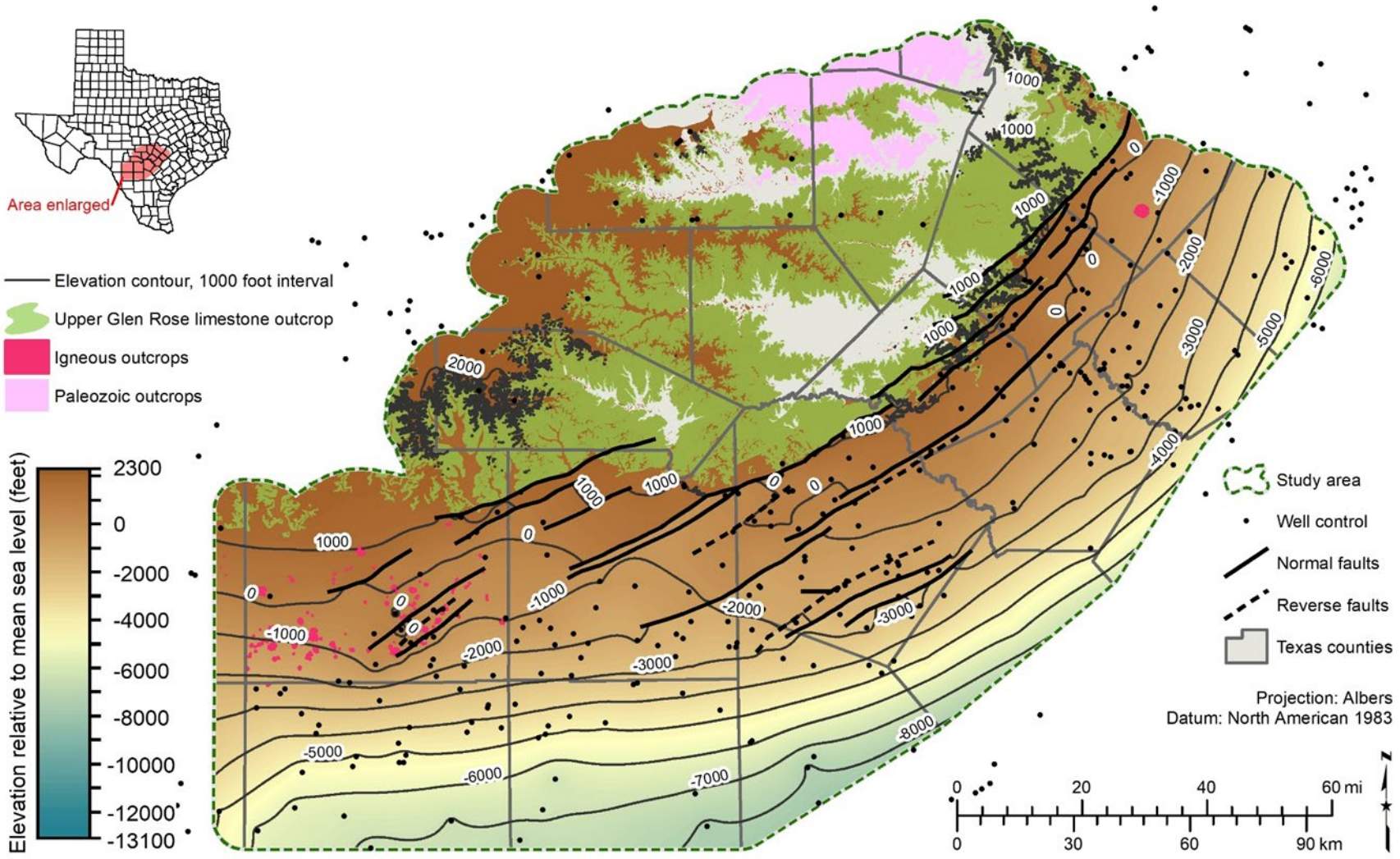

Figure 7-27 Upper Glen Rose limestone structure map (elevation datum is mean sea level, feet).

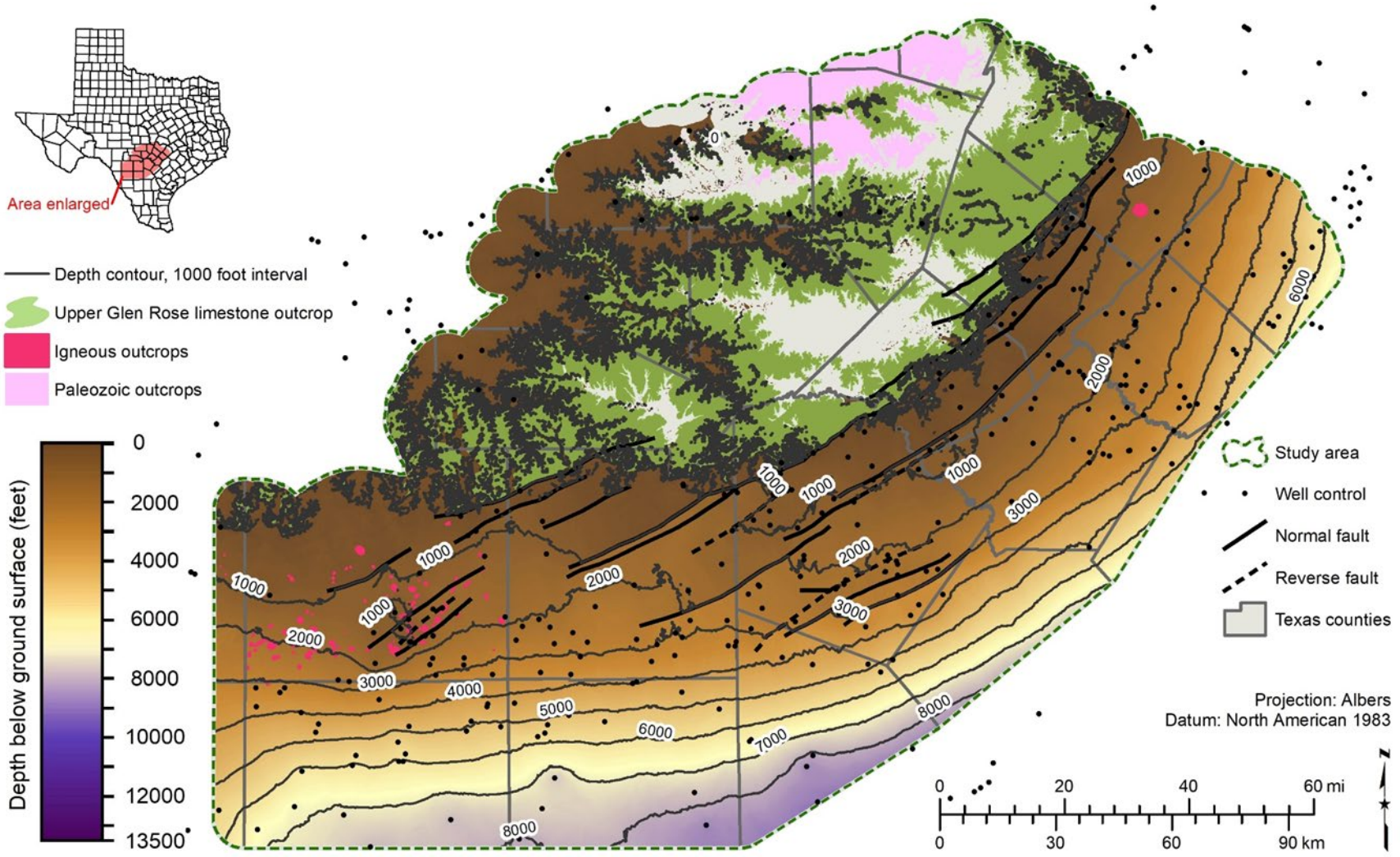

Figure 7-28 Upper Glen Rose limestone depth surface map (depth below ground surface, feet).

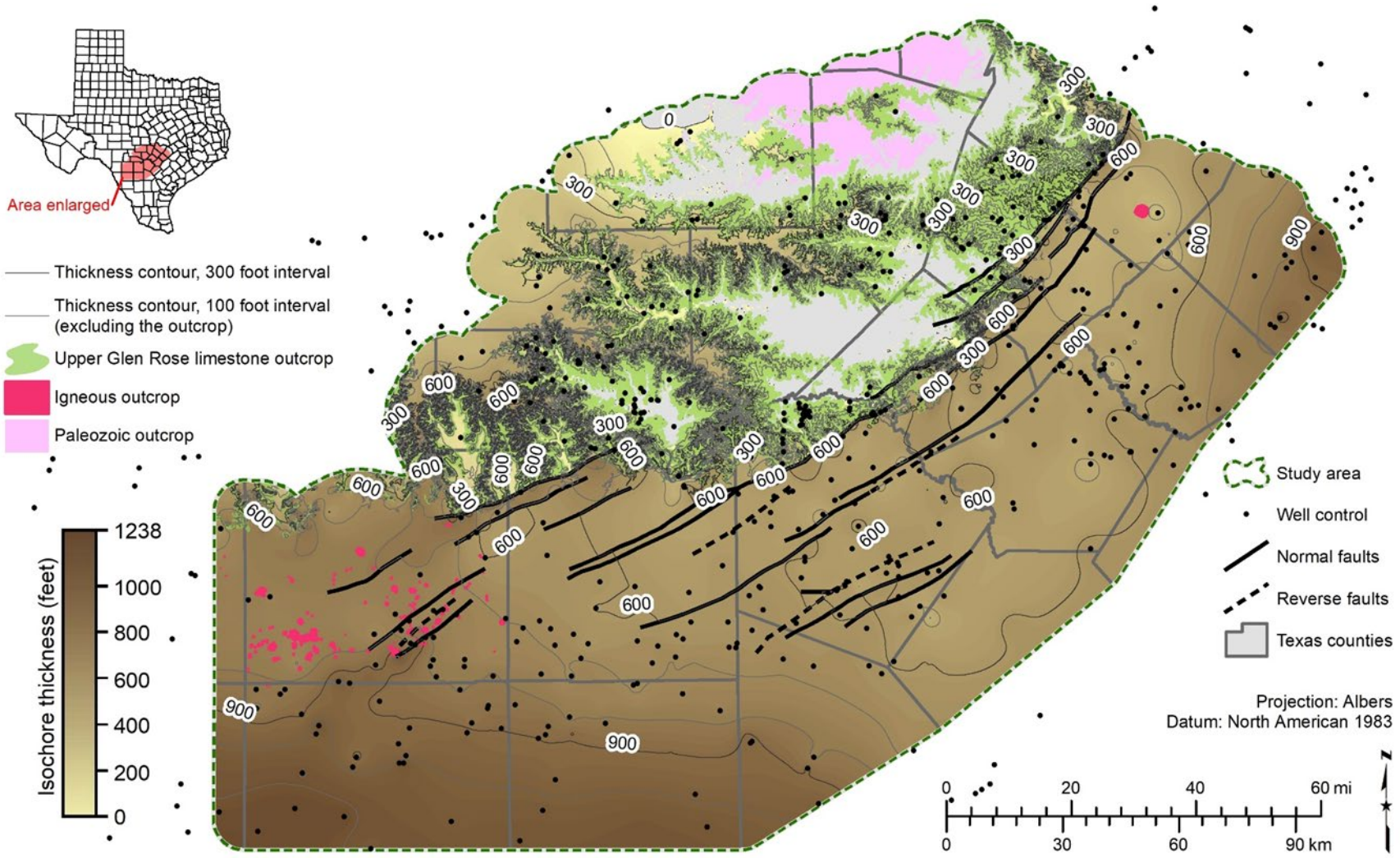

Figure 7-29 **Upper Glen Rose limestone thickness map (thickness in feet). Gray areas on map indicate where the Upper Glen Rose limestone is absent.**

This page is intentionally blank.

7.6 Stratigraphic type logs

Geophysical well log responses are a result of the lithologic and depositional characteristics of the rocks being measured and the fluids that they contain. They can be used to map geologic contacts between formations when there are significant changes in the character of the rocks because of composition, compaction, and fluid content. In the case of the Trinity Group formations, which were deposited on a broad Cretaceous shelf, we were able to map regionally correlative surfaces of the hydrogeologic units from deep in the subsurface to their outcrops. Stratigraphic correlation of well logs is a complex process that integrates numerous visual variations of the available curves within the context of the overall geologic framework.

We developed a series of type logs (Figures 7-30 to 7-43) to document the geophysical log character used to correlate the Trinity hydrostratigraphic units. Each figure contains two or three geophysical well logs from selected study area counties. Each set of wells is depicted in two figures, one for the interval between the top of the Upper Glen Rose limestone to the top of the Hammett shale and the second figure for the interval between the top of the Hammett shale to the base of the Hosston sandstone. The type logs are arranged in a roughly northwest to southeast orientation and are flattened on the top of the Hammett shale. The top of the Hammett shale generally represents a maximum flooding surface, or the deepest marine depositional environment, that can be identified in most wells throughout the study area. Locations of the wells depicted in the type logs are shown on Figure 7-44.

Each figure has been labeled and color coded to highlight the Trinity hydrostratigraphic units correlated for this study. The BRACS database well identifier is posted above the wells shown in the figures. We have noted the measured depths (below each wells reference elevation) on the well logs. Solid lines have been used to denote the surfaces that define the primary hydrostratigraphic units. Dashed lines in the Upper Glen Rose limestone, Lower Glen Rose limestone, Sligo limestone, and Hosston sandstone are shown to denote possible depositional subunits within these formations based upon changes in geophysical log character.

Most of the wells are older logs that display a spontaneous potential (SP) curve in the left-hand track and resistivity curves (RES) in the right-hand track. There are a handful of logs that have a gamma-ray curve (GR), and these have been noted in the figures. Section 11.2 of this report provides an introduction to the properties of various geophysical well logging tools.

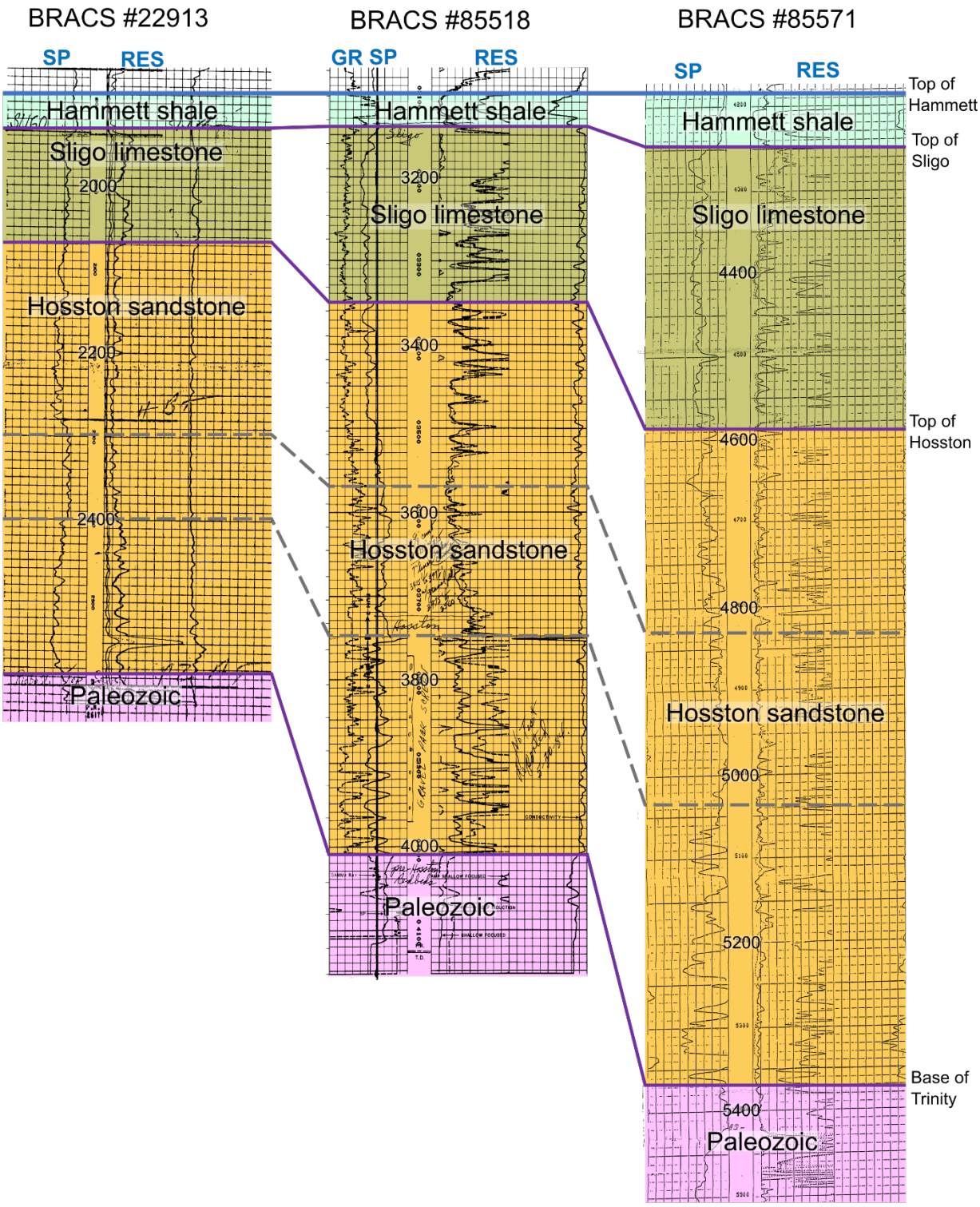

Figure 7-30 **Bexar County lower Trinity correlations for the Sligo limestone and Hosston sandstone on BRACS Database wells (identification numbers 22913, 85518, and 85571). The spontaneous potential and gamma ray tools are shown in the left track, depth (in feet below reference elevation) is shown in the middle track, and the short normal and deep induction tools are shown in the right track. (RES = resistivity, GR = gamma ray, SP = spontaneous potential)**

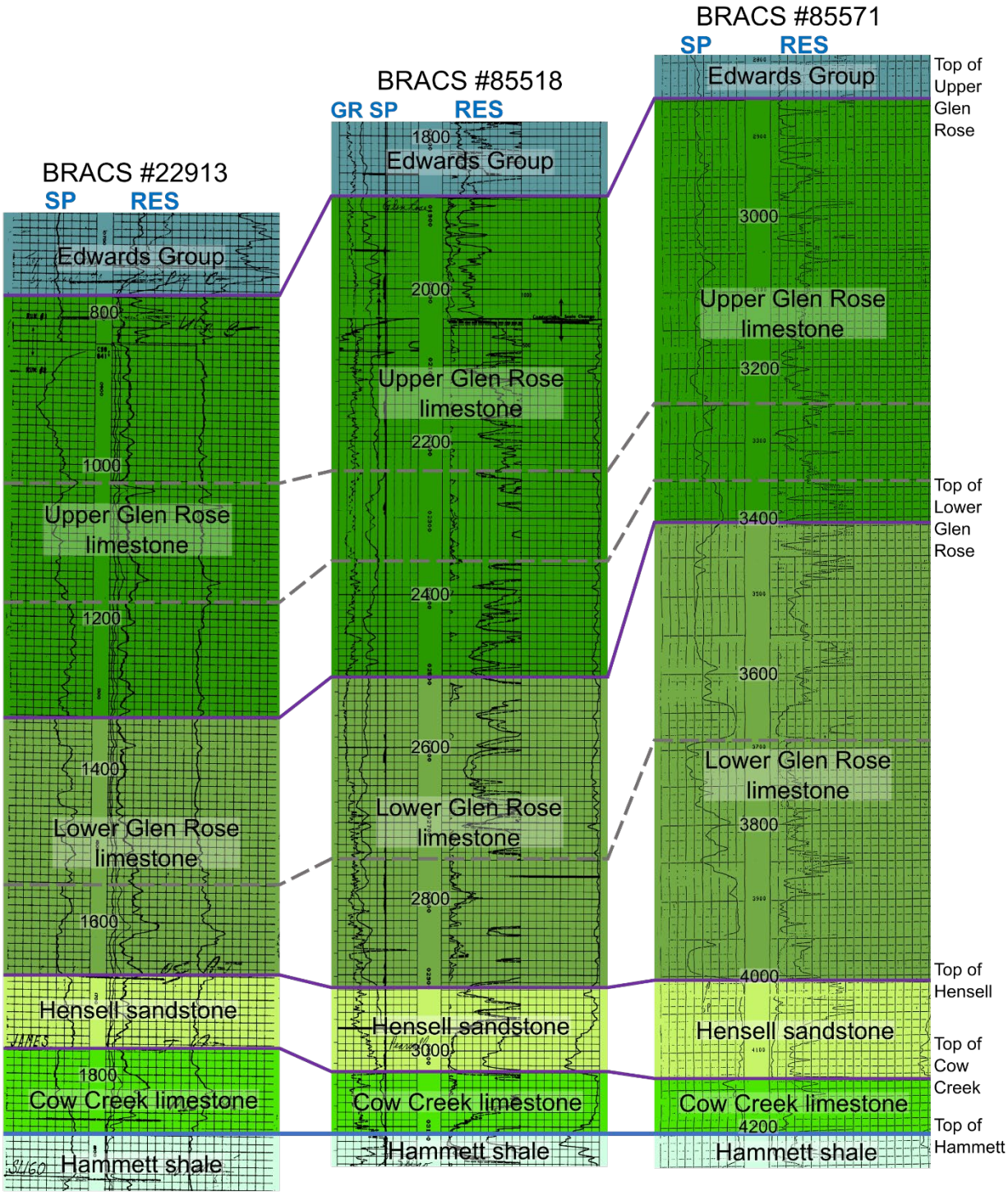

Figure 7-31 **Bexar County upper and middle Trinity correlations for the Upper Glen Rose limestone, Lower Glen Rose limestone, Hensell sandstone, and Cow Creek limestone units on BRACS Database wells (identification numbers 22913, 85518, and 85571). The spontaneous potential and gamma ray tools are shown in the left track, depth (in feet below reference elevation) is shown in the middle track, and the short normal and deep induction tools are shown in the right track. (RES = resistivity, GR = gamma ray, SP = spontaneous potential)**

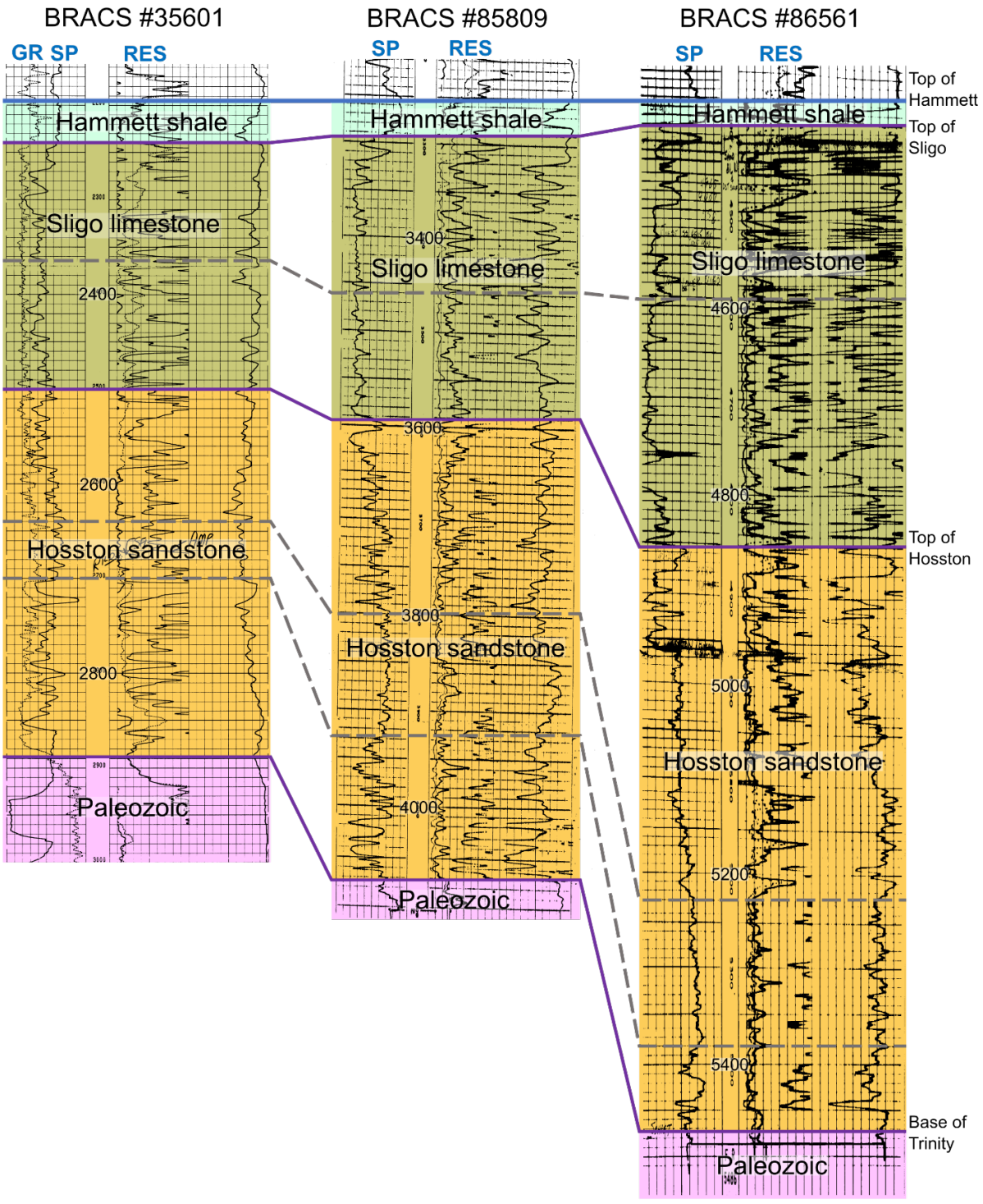

Figure 7-32 **Guadalupe County lower Trinity correlations for the Sligo limestone and Hosston sandstone on BRACS Database wells (identification numbers 35601, 85809, and 86561). The spontaneous potential and gamma ray tools are shown in the left track, depth (in feet below reference elevation) is shown in the middle track, and the short normal and deep induction tools are shown in the right track. (RES = resistivity, GR = gamma ray, SP = spontaneous potential)**

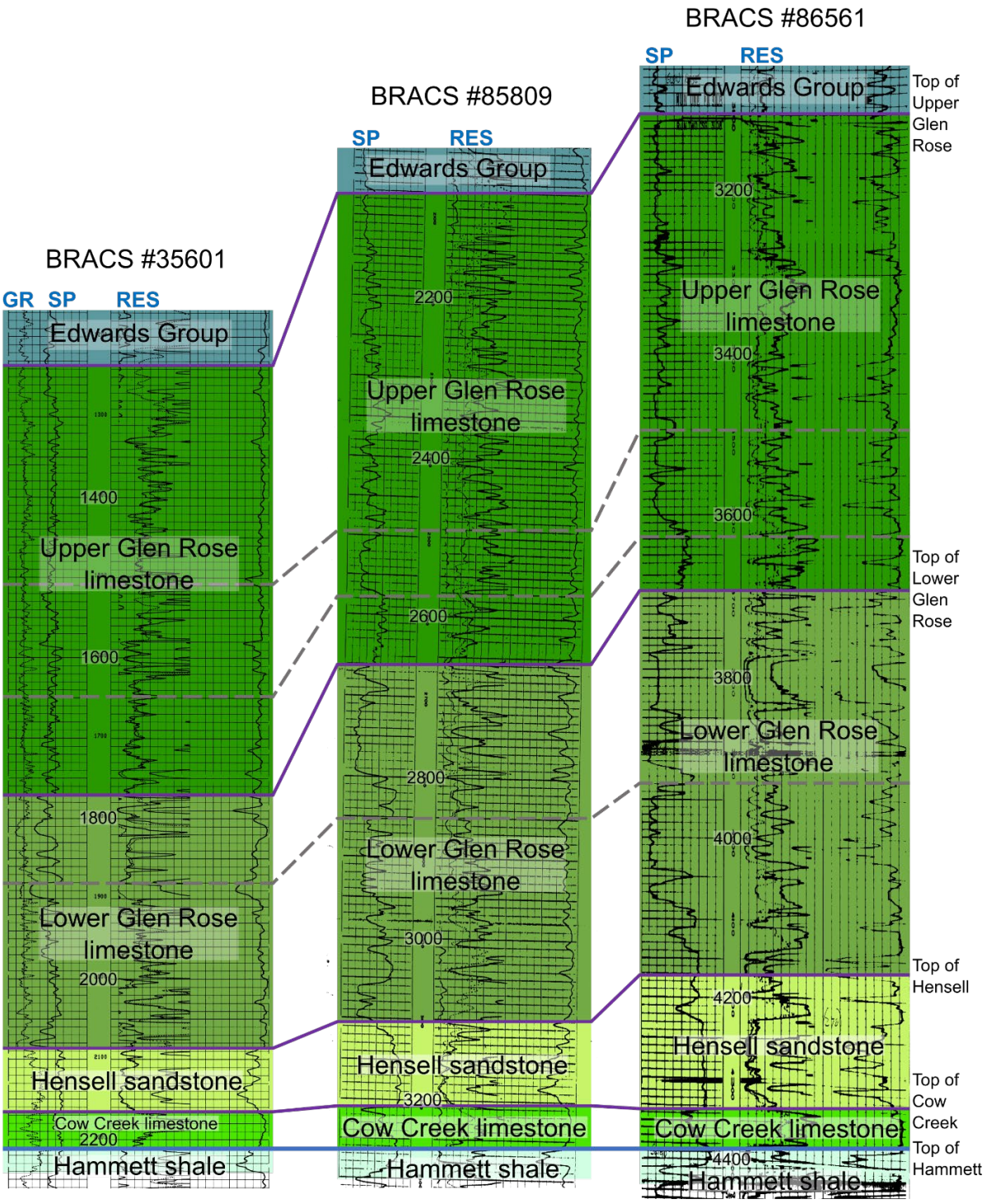

Figure 7-33 **Guadalupe County upper and middle Trinity correlations for the Upper Glen Rose limestone, Lower Glen Rose limestone, Hensell sandstone, and Cow Creek limestone on BRACS Database wells (identification numbers 35601, 85809, and 86561). The spontaneous potential and gamma ray tools are shown in the left track, depth (in feet below reference elevation) is shown in the middle track, and the short normal and deep induction tools are shown in the right track. (RES = resistivity, GR = gamma ray, SP = spontaneous potential)**

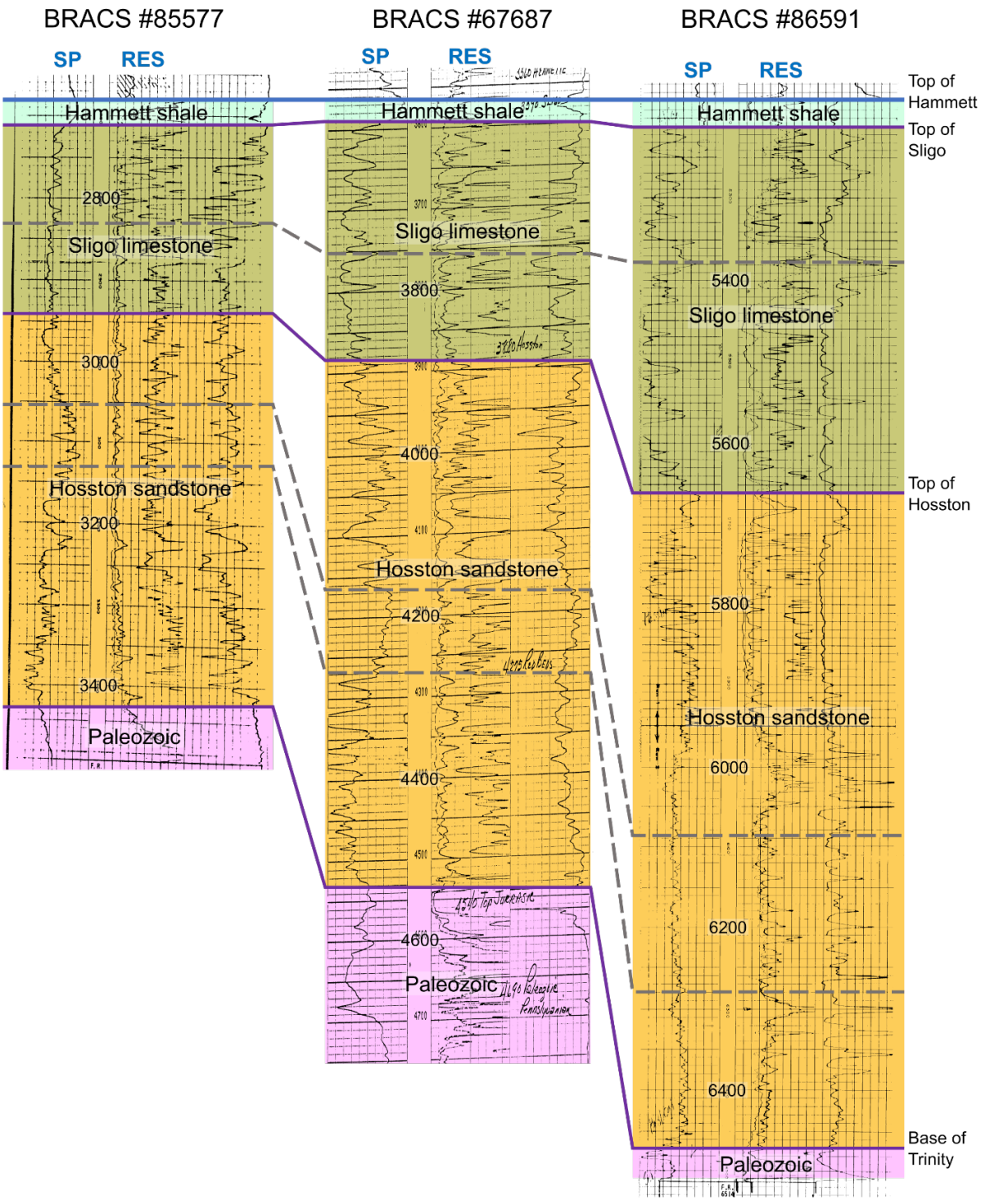

Figure 7-34 **Caldwell County lower Trinity correlations for the Sligo limestone and Hosston sandstone on BRACS Database wells (identification numbers 85577, 67687, and 86591). The spontaneous potential and gamma ray tools are shown in the left track, depth (in feet below reference elevation) is shown in the middle track, and the short normal and deep induction tools are shown in the right track. (RES = resistivity, GR = gamma ray, SP = spontaneous potential)**

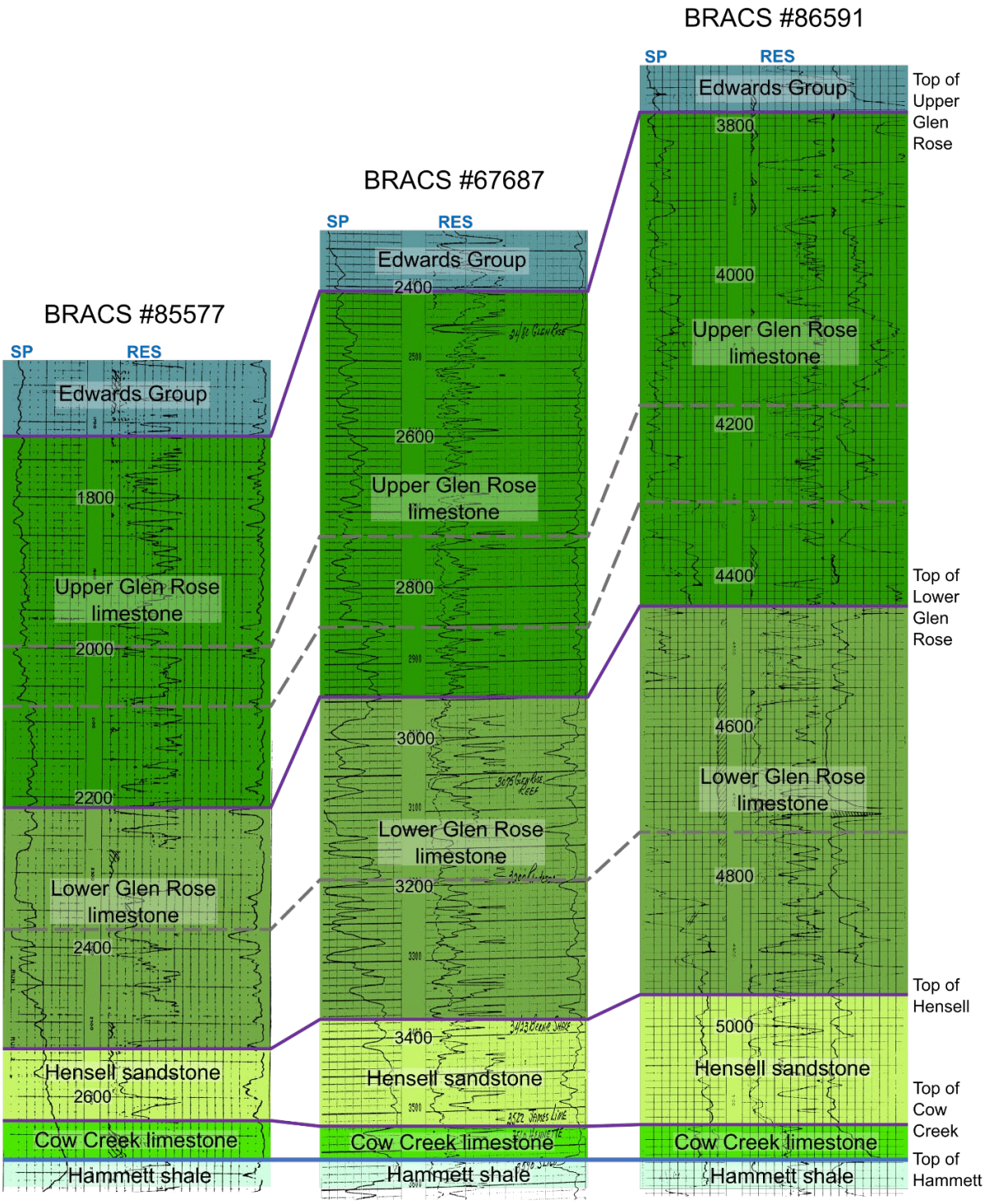

Figure 7-35 **Caldwell County upper and middle Trinity correlations for the Upper Glen Rose limestone, Lower Glen Rose limestone, Hensell sandstone, and Cow Creek limestone on BRACS Database wells (identification numbers 85577, 67687, and 86591). The spontaneous potential and gamma ray tools are shown in the left track, depth (in feet below reference elevation) is shown in the middle track, and the short normal and deep induction tools are shown in the right track. (RES = resistivity, GR = gamma ray, SP = spontaneous potential)**

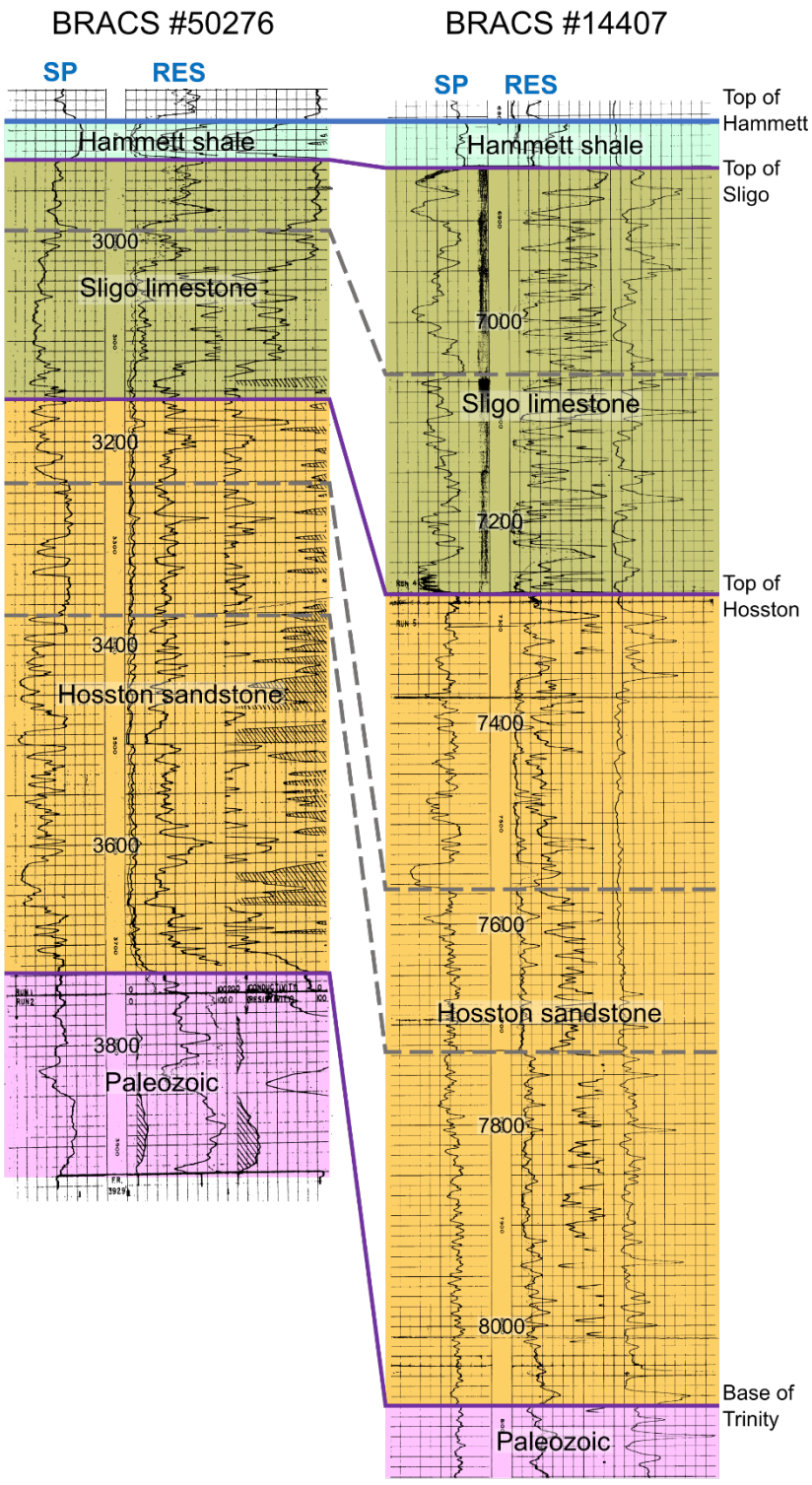

Figure 7-36 **Bastrop County lower Trinity correlations for the Sligo limestone and Hosston sandstone on BRACS Database wells (identification numbers 50276 and 14407). The spontaneous potential and gamma ray tools are shown in the left track, depth (in feet below reference elevation) is shown in the middle track, and the short normal and deep induction tools are shown in the right track. (RES = resistivity, GR = gamma ray, SP = spontaneous potential)**

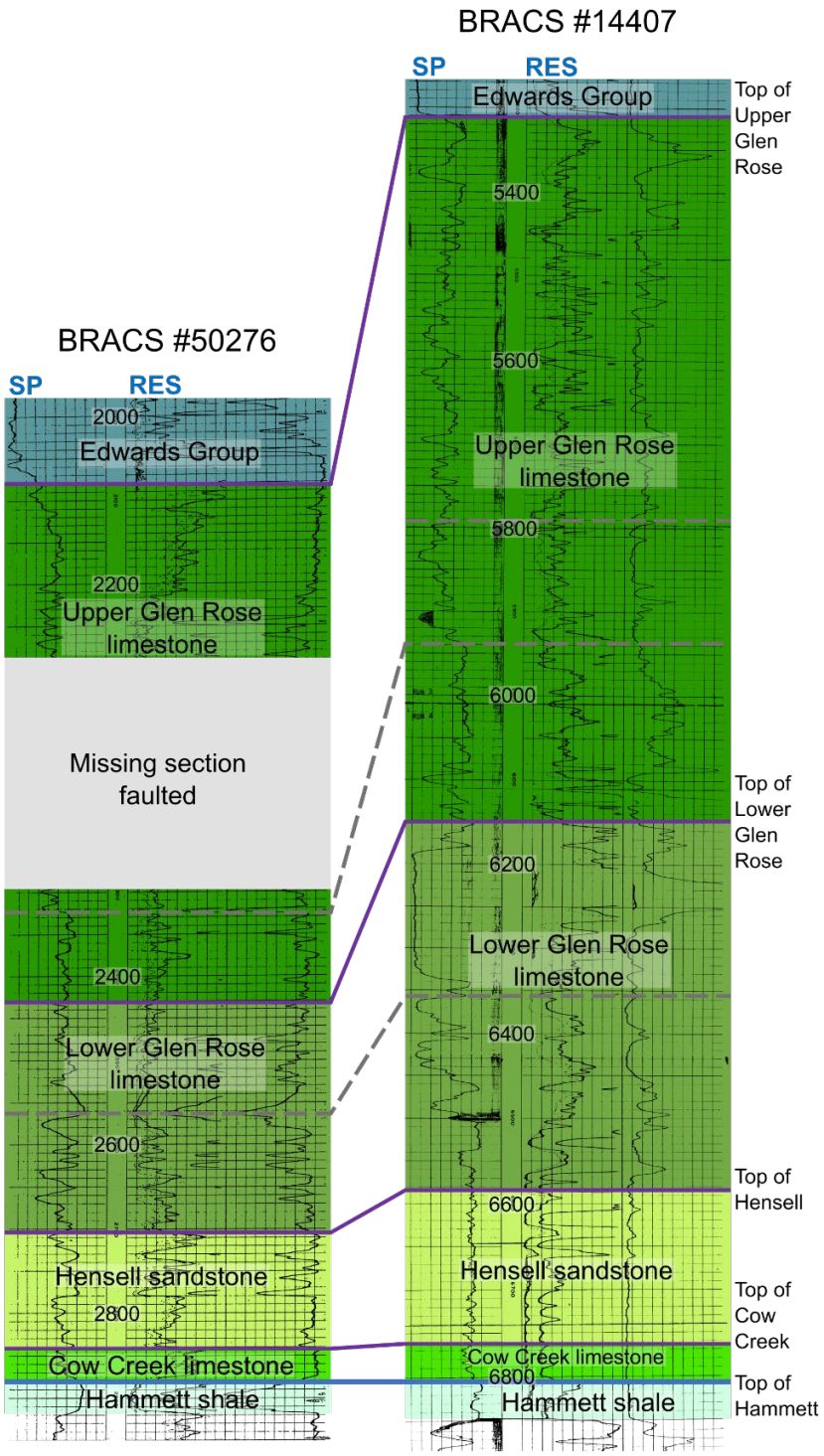

Figure 7-37 **Bastrop County upper and middle Trinity correlations for the Upper Glen Rose limestone, Lower Glen Rose limestone, Hensell sandstone, and Cow Creek limestone on BRACS Database wells (identification numbers 50276 and 14407). The spontaneous potential and gamma ray tools are shown in the left track, depth (in feet below reference elevation) is shown in the middle track, and the short normal and deep induction tools are shown in the right track. (RES = resistivity, GR = gamma ray, SP = spontaneous potential)**

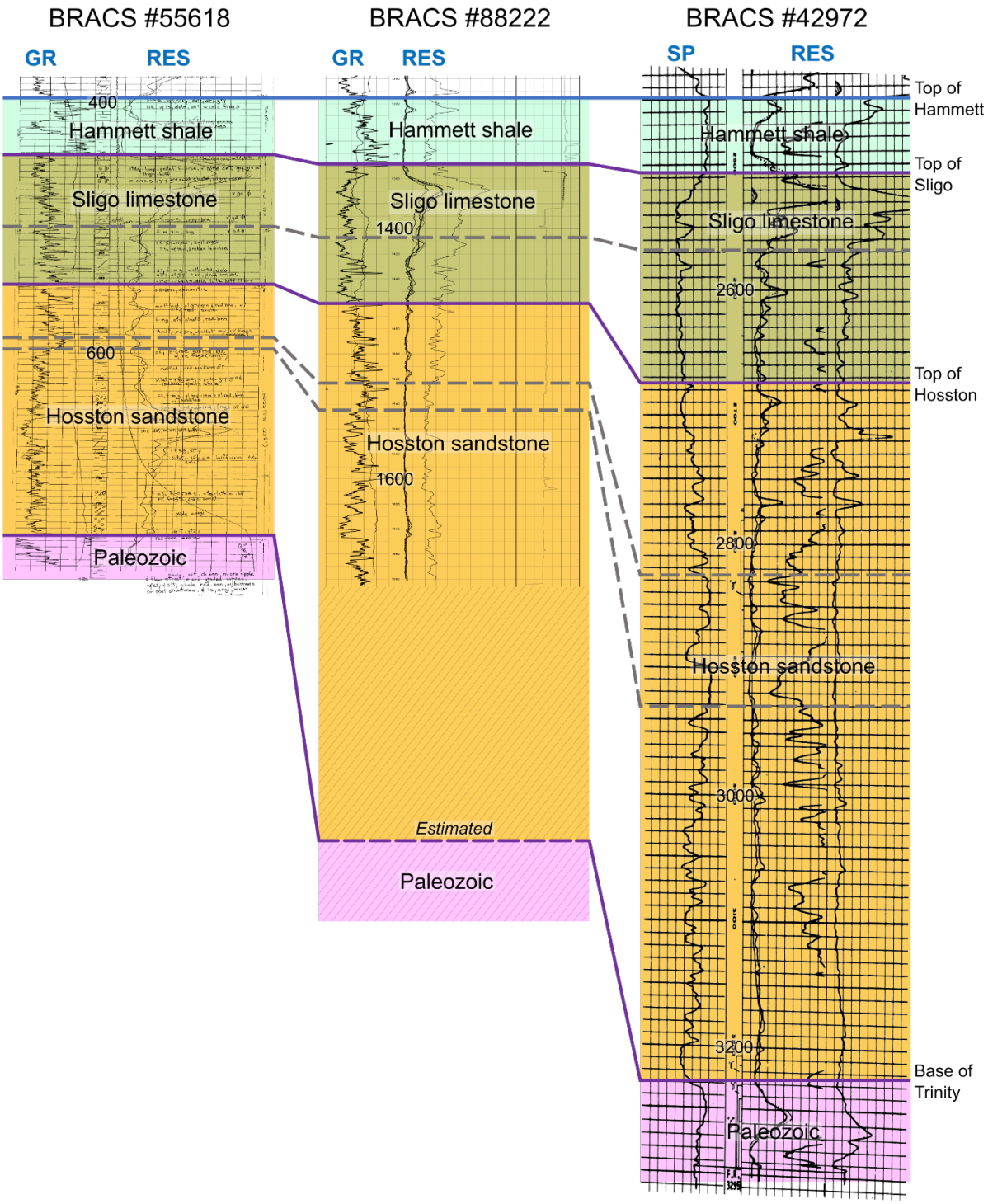

Figure 7-38 **Hays County lower Trinity correlations for the Sligo limestone and Hosston sandstone on BRACS Database wells (identification numbers 55618, 88222, and 42972). The spontaneous potential and gamma ray tools are shown in the left track, depth (in feet below reference elevation) is shown in the middle track, and the short normal and deep induction tools are shown in the right track. (RES = resistivity, GR = gamma ray, SP = spontaneous potential)**

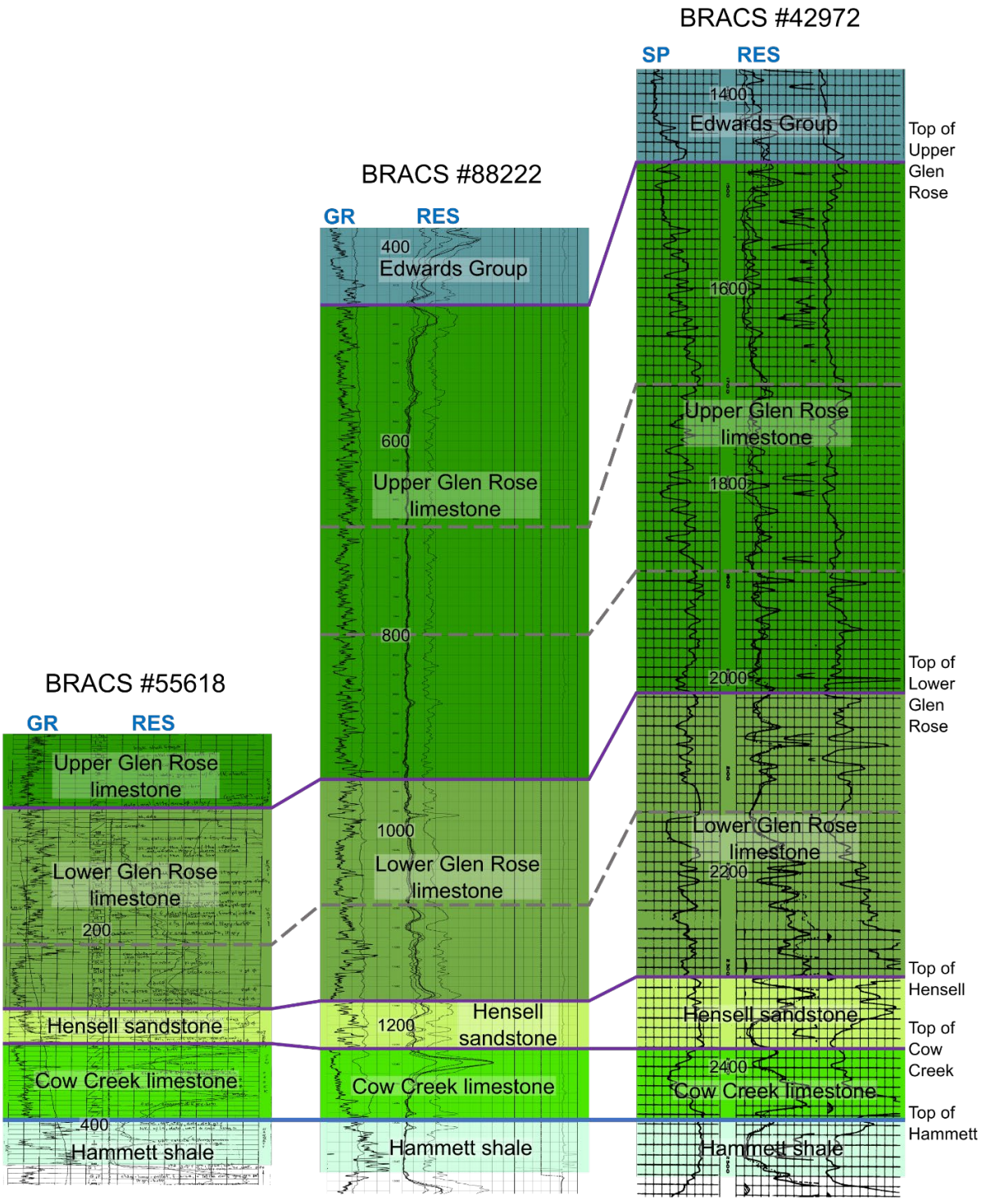

Figure 7-39 **Hays County upper and middle Trinity correlations for the Upper Glen Rose limestone, Lower Glen Rose limestone, Hensell sandstone, and Cow Creek limestone on BRACS Database wells (identification numbers 55618, 88222, and 42972). The spontaneous potential and gamma ray tools are shown in the left track, depth (in feet below reference elevation) is shown in the middle track, and the short normal and deep induction tools are shown in the right track. (RES = resistivity, GR = gamma ray, SP = spontaneous potential)**

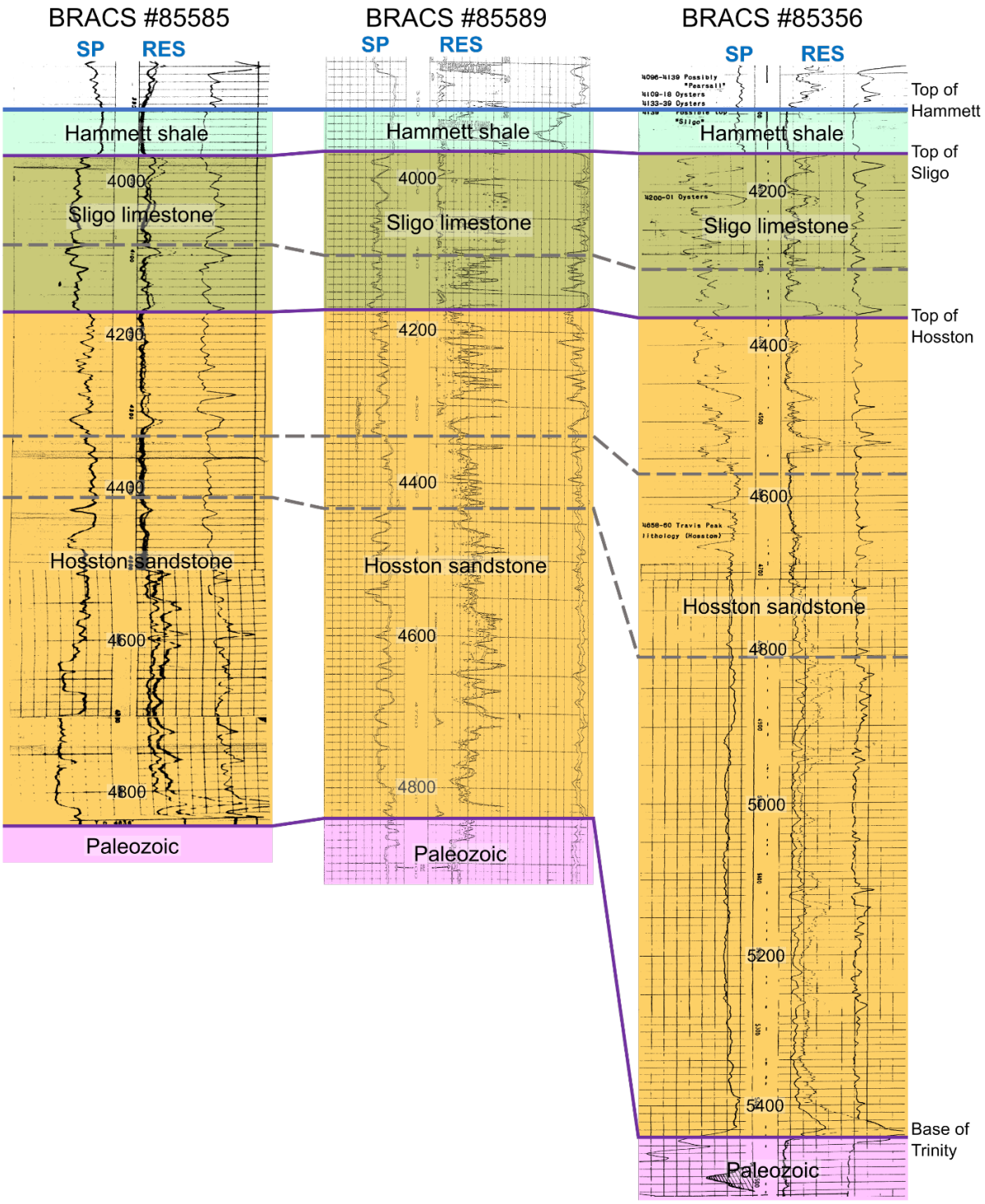

Figure 7-40 **Medina County lower Trinity correlations for the Sligo limestone and Hosston sandstone on BRACS Database wells (identification numbers 85585, 85589, and 85356). The spontaneous potential and gamma ray tools are shown in the left track, depth (in feet below reference elevation) is shown in the middle track, and the short normal and deep induction tools are shown in the right track. (RES = resistivity, GR = gamma ray, SP = spontaneous potential)**

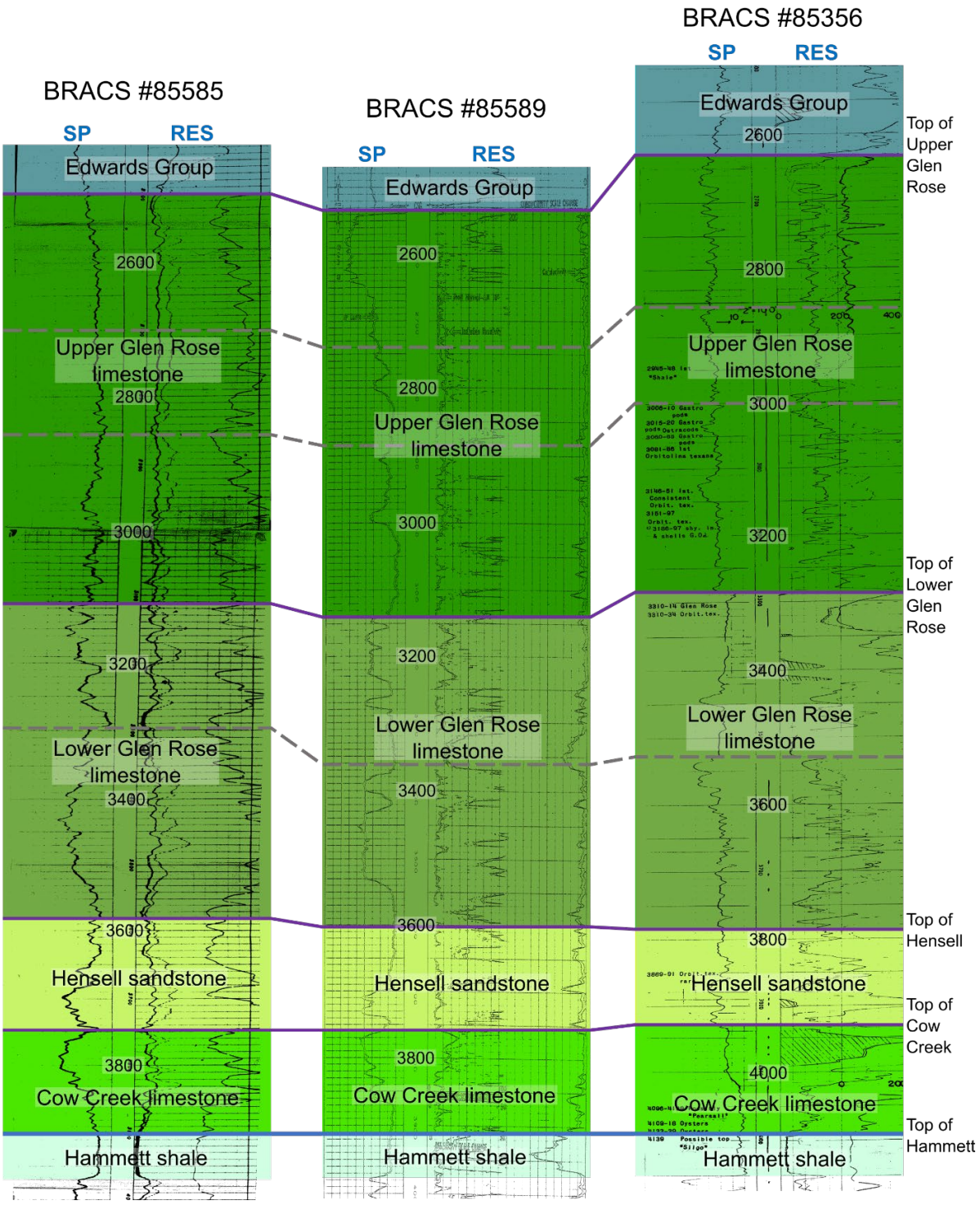

Figure 7-41 **Medina County upper and middle Trinity correlations for the Upper Glen Rose limestone, Lower Glen Rose limestone, Hensell sandstone, and Cow Creek limestone on BRACS Database wells (identification numbers 85585, 85589, and 85356). The spontaneous potential and gamma ray tools are shown in the left track, depth (in feet below reference elevation) is shown in the middle track, and the short normal and deep induction tools are shown in the right track. (RES = resistivity, GR = gamma ray, SP = spontaneous potential)**

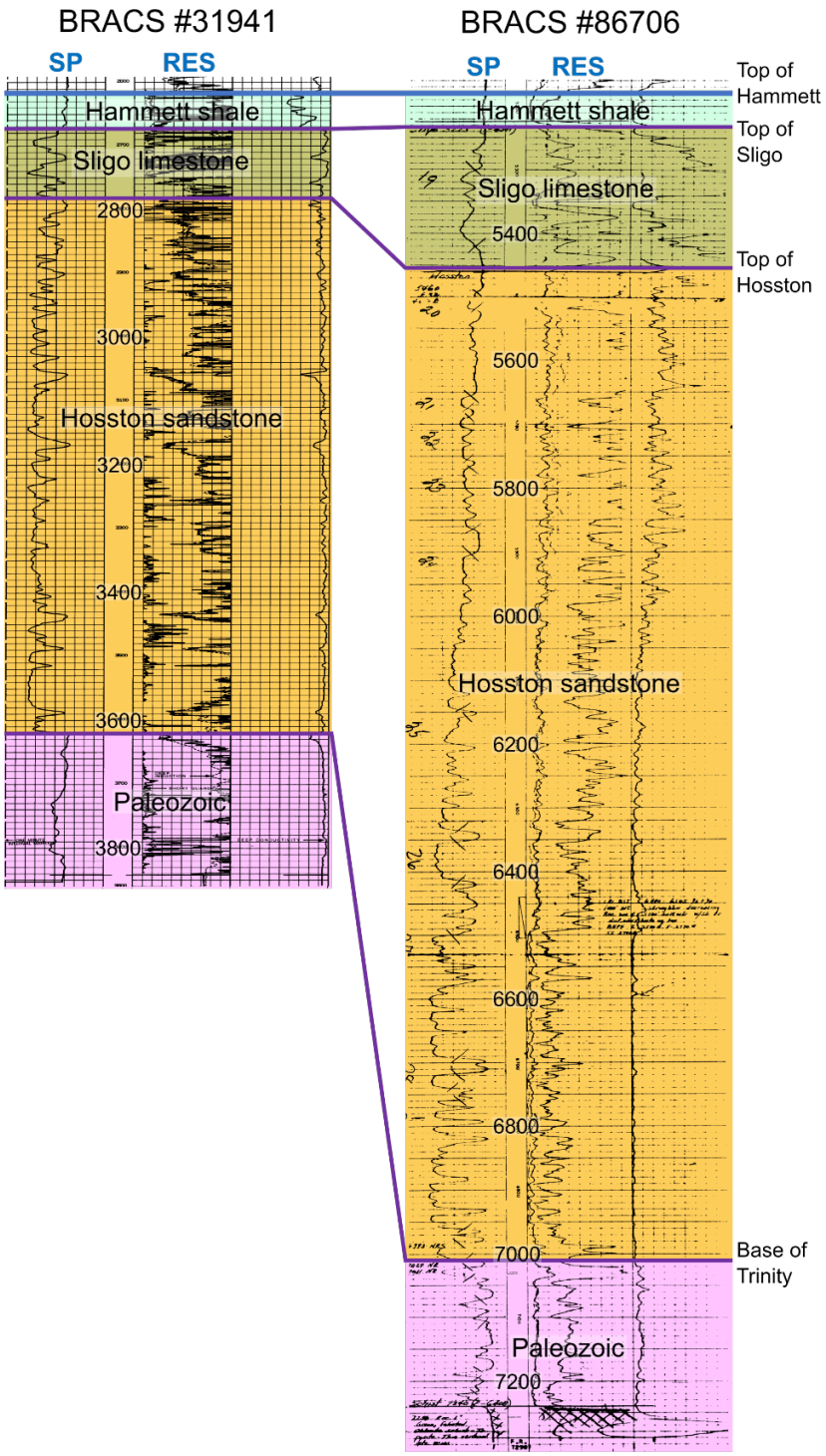

Figure 7-42 **Uvalde and Zavala Counties lower Trinity correlations for the Sligo limestone and Hosston sandstone on BRACS Database wells (identification numbers 31941 and 86706). The spontaneous potential and gamma ray tools are shown in the left track, depth (in feet below reference elevation) is shown in the middle track, and the short normal and deep induction tools are shown in the right track. (RES = resistivity, GR = gamma ray, SP = spontaneous potential)**

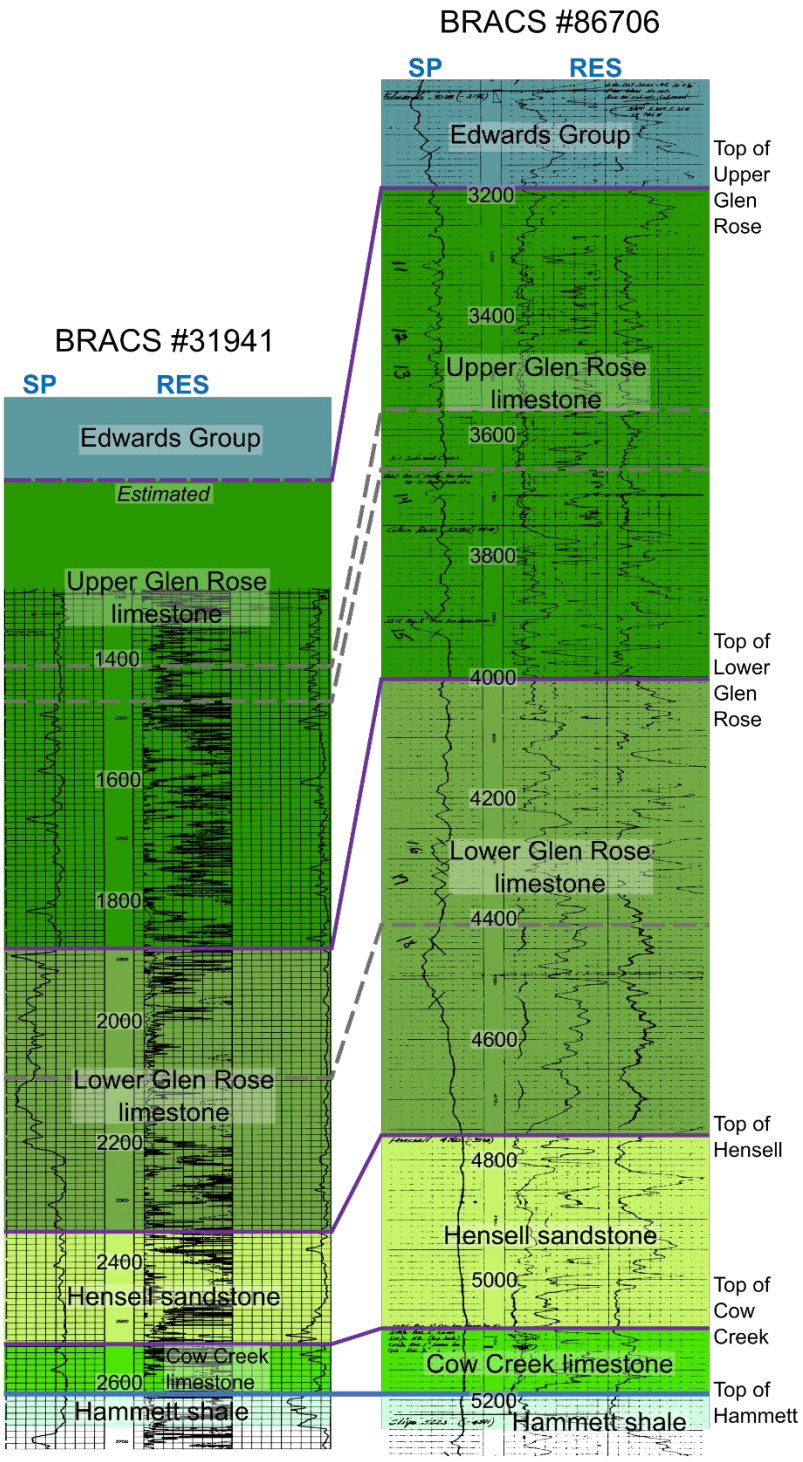

Figure 7-43 **Uvalde and Zavala Counties upper and middle Trinity correlations for the Upper Glen Rose limestone, Lower Glen Rose limestone, Hensell sandstone, and Cow Creek limestone on BRACS Database wells (identification numbers 31941 and 86706). The spontaneous potential and gamma ray tools are shown in the left track, depth (in feet below reference elevation) is shown in the middle track, and the short normal and deep induction tools are shown in the right track. (RES = resistivity, GR = gamma ray, SP = spontaneous potential)**

7.7 Study area cross sections

Four structural cross sections were constructed to illustrate the structural and stratigraphic relationships of the Hill Country Trinity aquifer hydrostratigraphic units within the study area. We used a set of Python® scripts developed in ArcGIS® at the United States Geological Survey (Thoms, 2005) to construct cross section profiles for the stratigraphic surfaces created from the well log correlations depicted in Section 7.6 of this report. The location of these cross sections is shown on the map in Figure 7-44.

The cross sections provide a powerful aid in understanding the nature of the geologic contacts between the various Trinity hydrostratigraphic units. The cross sections also illustrate the way that the Trinity hydrostratigraphic units, as a consequence of faulting, can be adjacent to overlying water bearing units which could provide a means for cross-formational flow. We used a vertical to horizontal exaggeration of approximately 40 to better visualize some of the thinner correlated units.

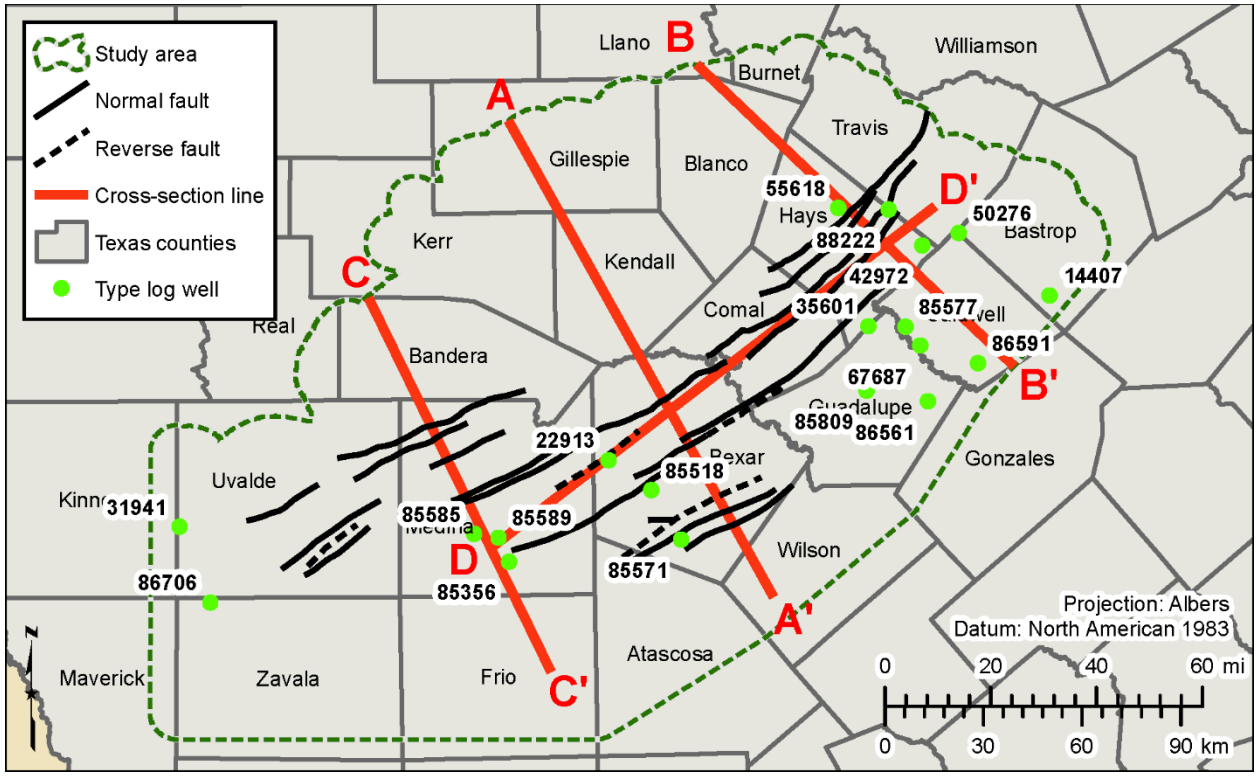

Figure 7-44 Location of cross section lines and type-log wells in the Hill Country Trinity aquifer study area.

Cross section A-A' (Figure 7-45), transects the center of the study area from the northwest to the southeast in a largely dip direction and crosses numerous faults associated with the Balcones Fault Zone. As shown, the faulting juxtaposes different units of the Trinity Group against units both younger and older. This cross section shows how the Trinity Group formations onlap upon the older Paleozoic basement as a result of the transgressive rise in sea level during deposition of the lower Trinity formations.

Cross section B-B' (Figure 7-46), is located approximately 50 miles north of line A-A' and is oriented from northwest to southeast. The Trinity Group similarly onlaps the underlying Paleozoic formations as in Figure 7-45, but the extent of the Paleozoic shelf is truncated and the onlap terminations of all Trinity Group formations are much more abrupt.

Cross section C-C' (Figure 7-47), is located approximately 40 miles south of line A-A' and is oriented from northwest to southeast. In this cross section there is significant thinning of the lower Trinity formations, but none of the Trinity Group formations terminally onlap.

Cross section D-D' (Figure 7-48), is oriented southwest to northeast and runs roughly parallel to the geological strike of the Trinity formations. This cross section includes the San Marcos Arch, which is a dominant structural feature in the study area. There is minor thinning of the lower Trinity formations across the top of the arch, but the upper Trinity formations do not show any significant thinning.

This page is intentionally blank.

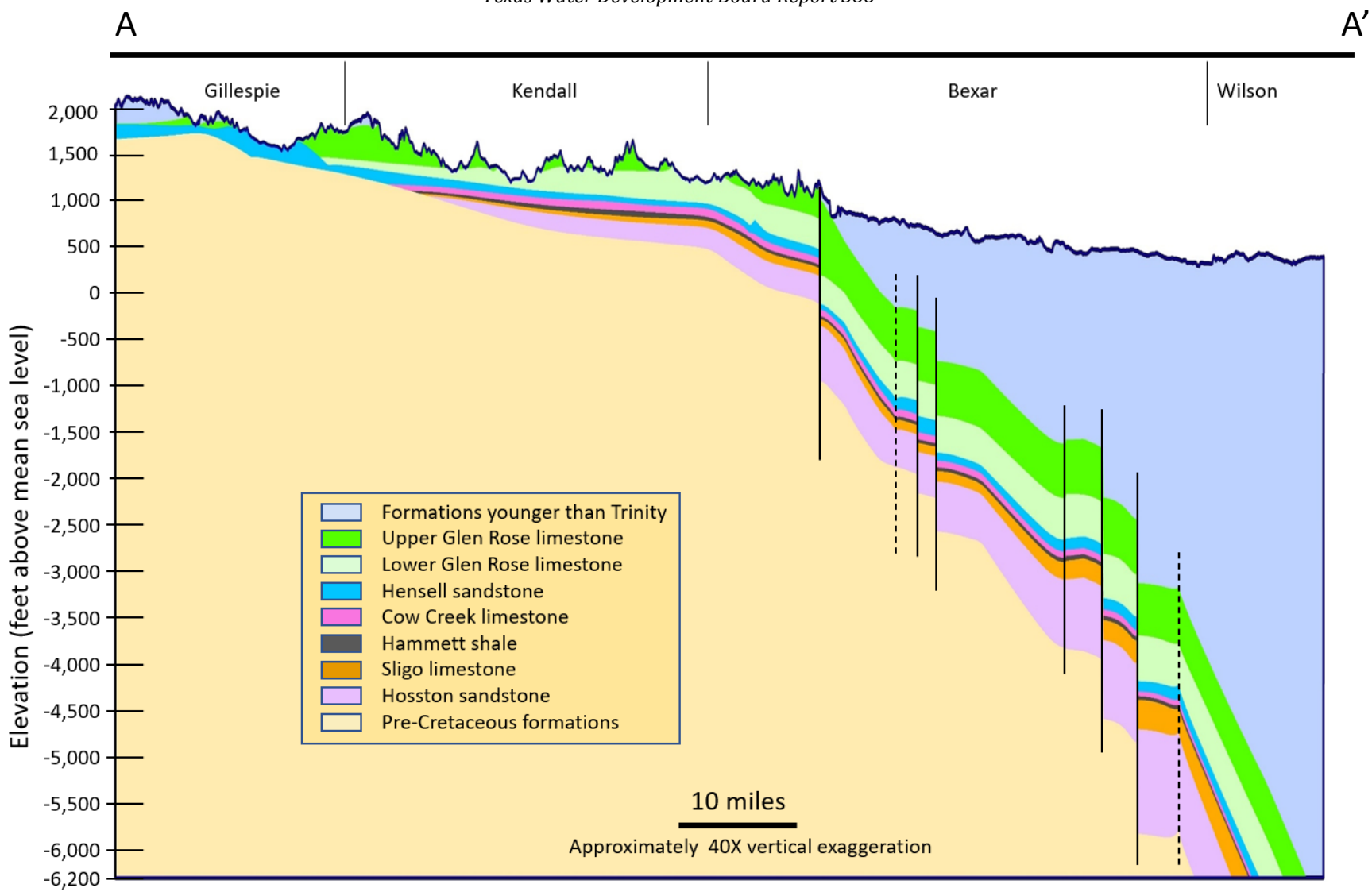

Figure 7-45 **Cross section A-A'. Refer to Figure 7-44 for cross section location. Solid vertical lines are mapped faults and dashed vertical lines are inferred faults.**

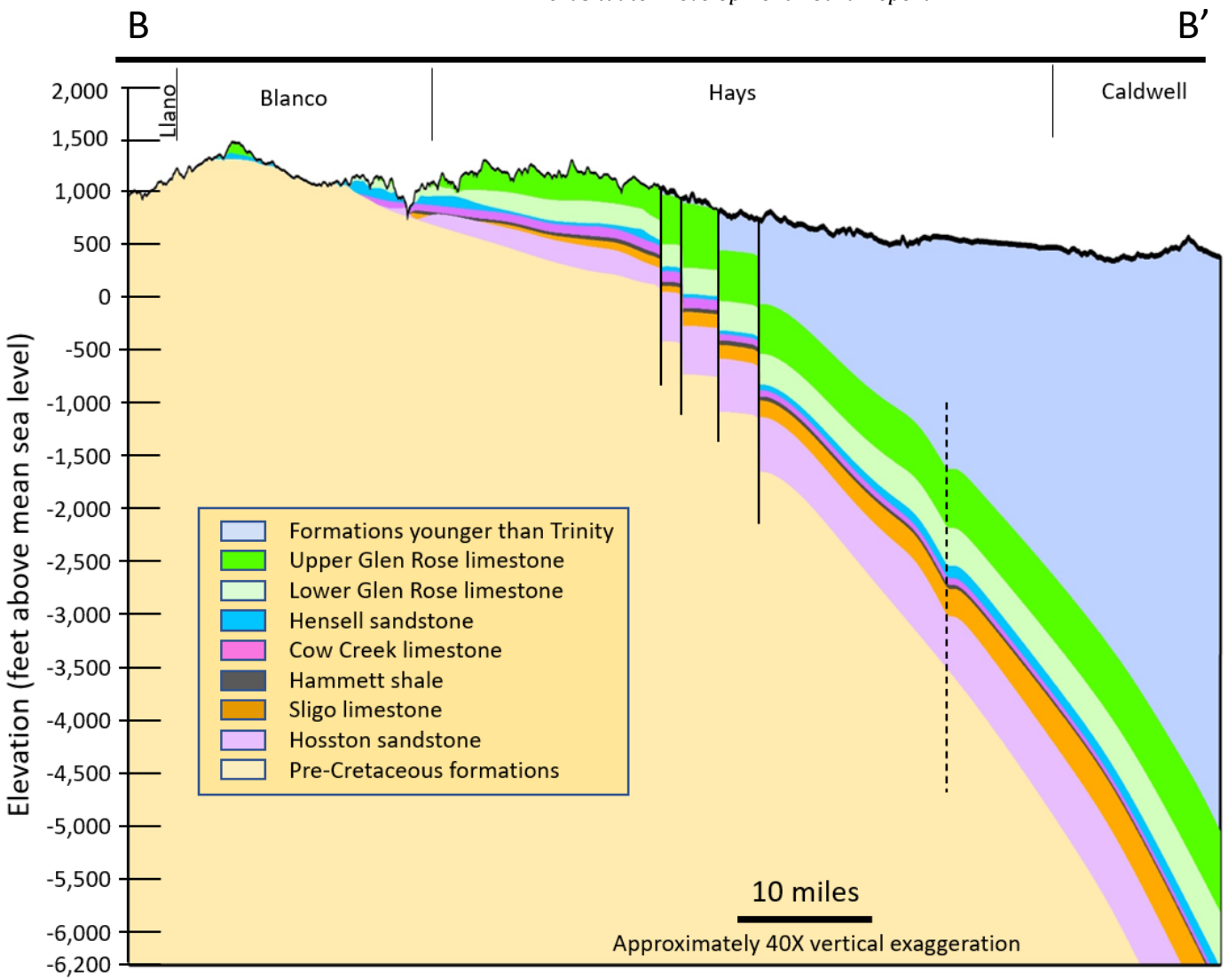

Figure 7-46 **Cross section B-B'. Refer to Figure 7-44 for cross section location. Solid vertical lines are mapped faults and dashed vertical lines are inferred faults.**

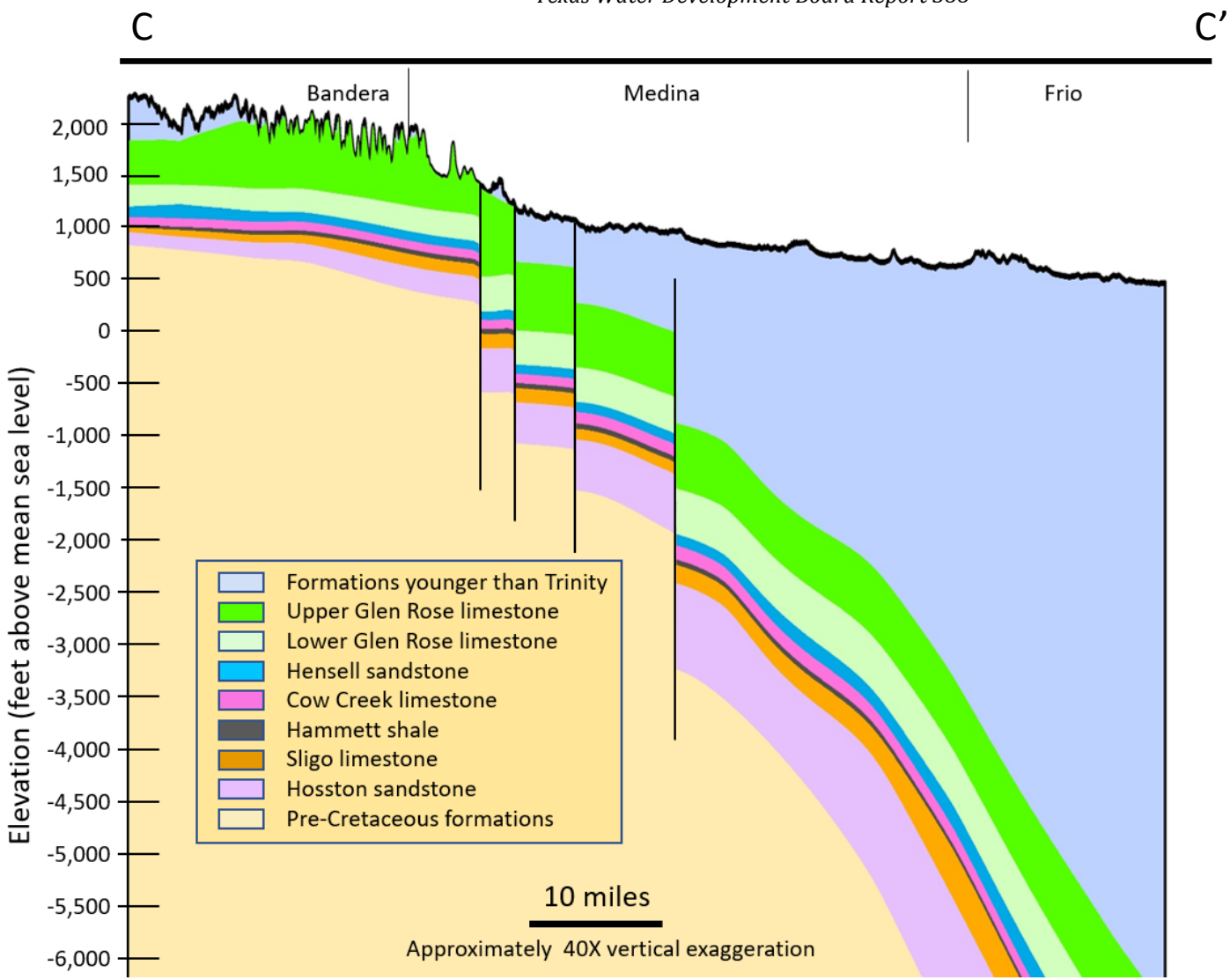

Figure 7-47 **Cross section C-C’. Refer to Figure 7-44 for cross section location. Solid vertical lines are mapped faults and dashed vertical lines are inferred faults.**

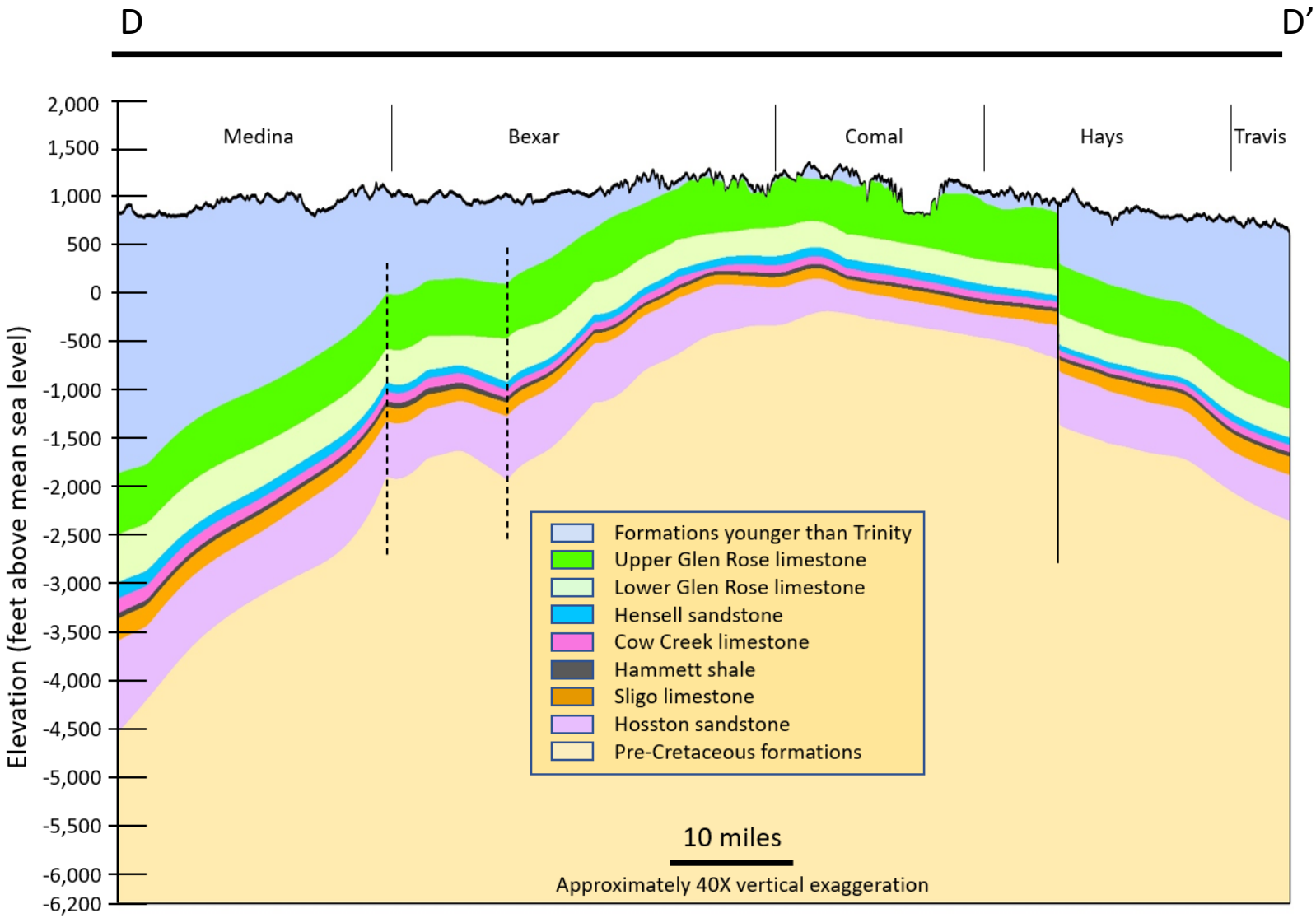

Figure 7-48 **Cross section D-D’. Refer to Figure 7-44 for cross section location. Solid vertical lines are mapped faults and dashed vertical lines are inferred faults.**

8 Aquifer determination

An important part of a BRACS study is the accurate assignment of groundwater samples and geophysical well log analyses to the correct hydrostratigraphic unit. We used the geologic surfaces created from the interpreted geophysical logs, drillers logs, and surface geologic maps to calculate their intersections with all study area wells. For wells that had reported completion intervals we determined which Hill Country Trinity aquifer hydrostratigraphic unit or units could potentially provide groundwater to the well. We used ESRI ArcMap® and Microsoft Access® to process the data.

With ESRI ArcMap® we assigned the depth value of each hydrostratigraphic surface to each study area well. The well information with the corresponding surface intersection data was then loaded into a Microsoft Access® database. We then used a series of database queries to assign appropriate bottom depths for each hydrostratigraphic surface for each well. Finally, we executed a Microsoft Visual Basic® macro that assigned an aquifer code to each well based upon the following variables: 1) total well depth, 2) top and bottom depth of screened or open intervals, and 3) top and bottom of each hydrostratigraphic unit.

8.1 Assignment of top depths

We used ESRI ArcMap® version 10.7 to assign the hydrogeologic surface values to all 65,766 wells for which aquifer determination was to be performed. Using the tool "Extract Multi Values to Points" we populated a point shape file with the raster surface elevation values of the following eight surfaces: 1) Upper Glen Rose limestone, 2) Lower Glen Rose limestone, 3) Hensell sandstone, 4) Cow Creek limestone, 5) Hammett shale, 6) Sligo limestone, 7) Hosston sandstone, and 8) base of Cretaceous. The option to use bilinear interpolation was not selected.

We linked the dBase file associated with the point shape file to a Microsoft Access® database so the records would be accessible via SQL queries. We then used a query to populate the top depth of each hydrostratigraphic unit to each study area well by subtracting its elevation value from the ground surface elevation.

8.2 Assignment of bottom depths

In general, the bottom depth of a hydrostratigraphic unit is the top depth of the underlying unit. However, the geologic history of the Trinity Group resulted in hydrostratigraphic units that have been eroded and that onlap older underlying units. As a result, the unit directly beneath a unit might be a unit lower down the stratigraphic column then generally expected. Because of this, we needed to execute an ordered sequence of programs to determine the bottom depth of a hydrostratigraphic unit in a well.

First, when a stratigraphic unit was underlain by the stratigraphic unit immediately beneath it, as expected in the stratigraphic column (Figure 7.2), we used an SQL query to populate the bottom depth with the top depth of the under lying unit. Next, working from

the next stratigraphically highest unit down we used a series of SQL queries to populate the remaining unassigned bottom depths. In this fashion we assigned a top and bottom depth to each hydrostratigraphic unit that intersected a study area well.

8.3 Aquifer code assignment

We accomplished the final step in the aquifer determination process using a Microsoft Visual Basic® macro program from within the Microsoft Access® database. This program compares the values of the total depth of a well and the top and bottom of any screened or open interval with the hydrostratigraphic units beneath each well location. The five-step process is outlined below.

Step 1: Does the well have a total depth value?

- If yes, then proceed to Step 2.
- If no, then exit with no aquifer code assigned.

Step 2: Does the well have a screened/open interval defined?

- If yes, then proceed to Step 3.
- If no, then mark aquifer code with an "X" and proceed to Step 5.

If Step 2 was "yes" then do Steps 3 and 4 for each hydrostratigraphic unit.

Step 3: Is screened/open top depth greater than unit top depth and less than unit bottom depth?

- If yes, then assign aquifer code for this unit.
- If no, then proceed to Step 4.

Step 4: Is the unit top depth greater than the screened/open top depth and less than the screened/open bottom depth?

- If yes, then assign aquifer code for this unit.
- If no, then do not assign aquifer code for this unit.

If Step 2 was "no", then do Step 5 for each hydrostratigraphic unit.

Step 5: Is total depth of well greater than unit top depth?

- If yes, then assign aquifer code for this unit.
- If no, then do not assign aquifer code for this unit.

With the results of the aquifer determination analysis, we assigned a standardized set of aquifer codes for the groundwater quality samples, aquifer test results, and salinity calculations. Throughout this report the aquifer codes assigned were used to classify data and analyses in a uniform and consistent manner.

The newly assigned aquifer codes were compared to aquifer assignments of wells in the TWDB Groundwater Database and to water sample data in published reports. In many cases, the aquifer codes previously assigned to a well were different from our aquifer determination result. We reviewed many of these by reexamining the water well report lithology, well screen, and formation surface datasets. We concluded that the aquifer codes assigned in this study represent an accurate classification.

While the aquifer determination process described here was written specifically for this study area, the methodology can be generally applied anywhere. However, it is important to understand that the dataset and series of custom queries must be individually modified for each specific study area.

9 Aquifer hydraulic properties

The ability of an aquifer to transmit and store groundwater can vary greatly depending on its individual characteristics. An aquifer's hydraulic properties refers to the physical characteristics that govern groundwater flow in the aquifer. Aquifer properties are in general determined from aquifer test data. Several methods (Theis, 1935; Cooper and Jacob, 1946) simplify the calculation of these hydraulic parameters by the analysis of drawdown measurements over time in: 1) one monitoring well or 2) in multiple monitoring wells. Analysis of these measurements allows for the calculation of the transmissivity and storativity of an aquifer. The accuracy of the results obtained from an aquifer test depend greatly upon the robustness of the aquifer test which is a function of; test duration, spacing of monitoring wells and their distances from the pumping well, and other factors. Careful scientific and logistical planning is required to maximize the accuracy of the information derived from an aquifer test.

9.1 Hydraulic property definitions

There are many factors that impact aquifer hydraulic properties and the flow of water in and between aquifers. These factors include aquifer structure, aquifer lithology, depositional environment, and the presence of fractures and faults. The primary hydraulic properties we considered in this study are:

Hydraulic conductivity – The measure of the ease with which groundwater can flow through an aquifer. Higher hydraulic conductivity indicates that the aquifer will allow more water movement under the same hydraulic gradient. Hydraulic conductivity has dimensions of length per unit time and typically is expressed in units of feet per day or gallons per day per square foot.

Transmissivity – This term is closely related to hydraulic conductivity and refers to the product of the hydraulic conductivity multiplied by the effective aquifer thickness (Equation 9-1). Transmissivity describes the ability of groundwater to flow through the entire thickness of an aquifer. As the thickness of the aquifer increases, the transmissivity increases for a given hydraulic conductivity. Transmissivity has dimensions of length squared per unit time and is typically expressed in units of square feet per day or gallons per day per foot.

$$T = K \times b \qquad \text{(Equation 9-1)}$$

Where:

T = transmissivity (feet^2/day)
K = hydraulic conductivity (feet/day)
b = aquifer thickness (feet)

Specific storage – This term describes the volume of water a unit thickness of a confined aquifer will release when the water level in the aquifer is lowered. Specific storage has dimensions of inverse length.

Storativity – This term is closely related to specific storage and refers to the product of the specific storage times the effective aquifer thickness (Equation 9-2). Also referred to

as the coefficient of storage, this term describes the volume of water a confined aquifer will release when the water level in an aquifer is lowered. Storativity is a dimensionless parameter.

$$S = Ss \times b \quad \text{(Equation 9-2)}$$

Where:

S = storativity (unitless)
Ss = specific storage (1/feet)
b = aquifer thickness (feet)

Specific capacity – This term describes the volume of water released per unit decline in water level (unit drawdown). It is a measure of the productivity of a well and is calculated by dividing the total pumping rate by the drawdown (Equation 9-3). Specific capacity is generally reported as gallons per minute per foot. However, by converting to consistent units, specific capacity can be expressed as feet squared per day. Water well drillers have historically used specific capacity to quantify the productivity of a well. In a study of the Gulf Coast Aquifer (Young and others, 2016), the relationship shown in Equation 9-4 and 9-5 was determined empirically from well test data.

$$SC = Q/s \quad \text{(Equation 9-3)}$$

$$SC = T * 0.00052 \quad \text{(Equation 9-4)}$$

$$s = Q / (T * 0.00052) \quad \text{(Equation 9-5)}$$

Where:

Q = discharge (gallons per minute)
SC = specific capacity ((gallons per minute)/feet)
s = drawdown (feet)
T = transmissivity (feet^2/day)

Several researchers have shown that there is a theoretical linear relationship between specific capacity and transmissivity (Mace, 1997; Mace, Smyth and others, 2000). These hydraulic parameters are required for calculating groundwater volume, designing a well field in a potential production area, assessing and assigning production permits, and modeling the impacts of pumping wells on other nearby wells and surface water.

9.2 Data sources and collection process

In the following section we summarize the aquifer data collected and used to determine the aquifer properties of the Hill Country Trinity aquifer. We also discuss the variety of data sources accessed during the compilation of the aquifer data.

9.2.1 Analysis criteria

Our analysis focused on the six water bearing hydrostratigraphic units of the Hill Country Trinity aquifer as discussed in the Section 7.5 of this report. We assigned a

hydrologic unit based on well depth and screen information during the aquifer determination process (Section 8 of this report). In order to include enough data points for each hydrologic unit, we considered wells producing from either a single hydrostratigraphic unit or a group of hydrostratigraphic units with similar properties or that are thought to be in communication (Table 9-1).

Table 9-1 Hill Country Trinity aquifer formations groups.

Hydrologic unit	Hydrostratigraphic units
Upper Trinity	Upper Glen Rose limestone (UG)
	Upper Glen Rose limestone (UG) and Lower Glen Rose limestone (LG)
Middle Trinity	Lower Glen Rose limestone (LG)
	Hensell sandstone (HE)
	Cow Creek limestone (CC)
	Cow Creek limestone (CC) and Hammett shale (HM)
Lower Trinity	Hammett shale (HM) and Sligo limestone (SL)
	Hosston sandstone (HO)

The Upper Glen Rose limestone is recognized as the upper Trinity hydrologic unit (Ashworth, 1983). However, for purposes of this analysis we also considered wells producing from both the Upper Glen Rose limestone and Lower Glen Rose limestone as upper Trinity because these units do share similar physical rock properties.

The Lower Glen Rose limestone, Hensell sandstone, and Cow Creek limestone comprise the middle Trinity hydrologic unit. Although these units have very different lithologic properties, water from these units is believed to be in communication based upon hydrostatic data (Ashworth, 1983, Wong and others, 2014).

The Hammett shale, also known as the Pine Island Shale, is an aquitard with no significant water production. Therefore, we considered all wells screened in both Hammett shale and Cow Creek limestone or Hammett shale and Sligo limestone to be producing from the Cow Creek limestone or Sligo limestone respectively.

The Sligo limestone and Hosston sandstone are grouped together as the lower Trinity hydrologic unit. These units do have different lithologic and physical properties but are considered to be in hydrologic communication (Ashworth, 1983).

We compiled and reviewed the hydraulic properties of discharge, specific capacity, hydraulic conductivity, and transmissivity for 167 wells in the study area. The data collected for these wells has been saved in the BRACS Database in a study specific aquifer test table (*tblBRACS_HCT_AT*).

9.2.2 Data sources

The TWDB Groundwater Database includes well test and aquifer property data for some of its wells. To supplement these records, we performed a systematic and manual review of scanned well records in the TWDB Groundwater database and were able to collect data from aquifer test spreadsheets and the well report remarks field. There were also multiple historical TWDB reports that contain compiled aquifer test results from Texas water wells (Myers, 1969; Christian and Wuerch, 2012; Daniel B. Stephens and associates, 2006).

We identified 65 public supply wells with state well numbers in the study area. These wells are included in the aquifer test table (*tblBRACS_HCT_AT*) in the BRACS database. Aquifer properties for 16 of the wells were already available in the TWDB Groundwater database. We obtained pump test reports for 20 wells from the TCEQ and collected aquifer properties for the remaining 29 wells from TWDB Groundwater database well reports.

Some of the available well reports, in both TWDB and TCEQ databases, had incomplete aquifer test data, e.g., field data but no hydraulic properties. We used the Cooper-Jacob method to calculate the transmissivity for 11 wells with available drawdown measurements over time. These wells are saved in the table (*tblBRACS_HCT_FieldData*) in the BRACS database.

9.3 Results and analysis

The number of wells with aquifer property data per county are listed in Table 9-3 and the number of wells per hydrologic unit are listed in Table 9-4. Statistics for the collected aquifer properties by hydrologic unit are listed in Table 9-5.

Table 9-2 Wells with aquifer properties per county.

County	Wells
Bandera	34
Bexar	22
Blanco	4
Comal	4
Gillespie	4
Hays	53
Kendall	17
Kerr	21
Travis	6
Uvalde	2

Table 9-3 Wells with aquifer properties per hydrologic unit.

Hydrologic unit	Wells
Upper Trinity	23
Middle Trinity	108
Lower Trinity	31

Hays County has the greatest number of wells with aquifer properties with 53 of the 170 total wells. The middle Trinity hydrologic unit has the highest number of available aquifer properties with 113 of the 170 total wells. We plotted the location of wells with

aquifer properties for each hydrologic unit in Figure 9-1 to Figure 9-12. In general, aquifer test availability distribution shows clusters in the middle and the northern part of the study area where the Trinity units are shallow, and the groundwater is predominantly fresh. This represents the portion of the aquifer that has been historically developed. Counties in the southern part of the study area overlay the deep Hill Country Trinity aquifer subcrop and generally have higher salinity groundwater. The higher well drilling costs and low quality of groundwater has resulted in few wells being drilled and a scarcity in available aquifer test information.

Transmissivity values are available for all 170 wells that we catalogued for this study. Many of the transmissivity values collected are from domestic or small capacity wells. The lowest category range in Figure 9-1 to Figure 9-3 shows typical transmissivity values for domestic uses which is generally less than or equal to 250 square feet per day. Transmissivity values greater than 2,500 square feet per day were calculated for Hill Country Trinity aquifer wells, which may indicate that they encountered portions of the aquifer with karstic porosity. Aquifer conditions are not expected to be the same everywhere and not every well will produce large amounts of water, especially if the fractured or karstic intervals are missed. Most of the wells in the highest transmissivity range have missing hydraulic conductivity information. It has been observed that aquifers with high transmissivity areas will encourage increasing production which in turn results in significant effects on water levels in nearby wells and a larger radius of influence (McWhorter and Sunada, 2010).

Table 9-4 **Aquifer property results for Hill Country Trinity hydrologic units. (Abbreviations: gpm = gallons per minute, gpm/ft = gallons per minute per foot of drawdown, ft/day = feet per day, ft^2/day = square feet per day)**

	Property	Count	Minimum	Maximum	Average	Median
Upper Trinity	**Yield** (gpm)	23	3	1,480	497	65
	Specific Capacity (gpm/ft)	23	0.01	38.04	9.65	4.88
	Hydraulic Conductivity (ft/day)	10	0.03	47.99	11.98	1.07
	Transmisisivity (ft^2/day)	23	5	27,569	3,047	601
	Storativity (unitless)	10	$9.00x10^{-6}$	$5.25x10^{-1}$	$6.99x10^{-2}$	$1.69x10^{-4}$
Middle Trinity	**Yield** (gpm)	108	3	710	88	30
	Specific Capacity (gpm/ft)	98	0.04	82.89	4.30	1.07
	Hydraulic Conductivity (ft/day)	58	0.03	512.93	13.19	2.73
	Transmisisivity (ft^2/day)	113	1	4,612	484	233
	Storativity (unitless)	80	$4.00x10^{-8}$	$3.68x10^{-1}$	$7.30x10^{-3}$	$1.5x10^{-4}$

Lower Trinity	**Yield** (gpm)	24	3	723	102	39
	Specific Capacity (gpm/ft)	23	0.03	58.33	5.07	1.46
	Hydraulic Conductivity (ft/day)	10	0.01	21.92	3.50	1.40
	Transmisisivity (ft^2/day)	31	1	1,735	344	267
	Storativity (unitless)	18	$3.00x10^{-5}$	$3.77x10^{-2}$	$4.35x10^{-3}$	$3.20x10^{-4}$

We plotted the transmissivity (Figures 9-1 to 9-3), well yield (Figures 9-4 to 9-6), hydraulic conductivity (Figures 9-7 to 9-9), and specific capacity (Figures 9-10 to 9-12) values from reported aquifer tests and determined that they show no significant distribution pattern. Variations in aquifer properties occur for many reasons including: 1) the geologic nature of the formations, 2) the intensity of aquifer use, and 3) the setting and length of the aquifer test performed to obtain these properties. The inclusion of many smaller capacity wells in the overall statistics has biased the mean and median values of the aquifer properties shown in Table 9-5. The hydraulic property data presented in this study provides a regional perspective and should not be used to replace site-specific well tests.

This page is intentionally blank.

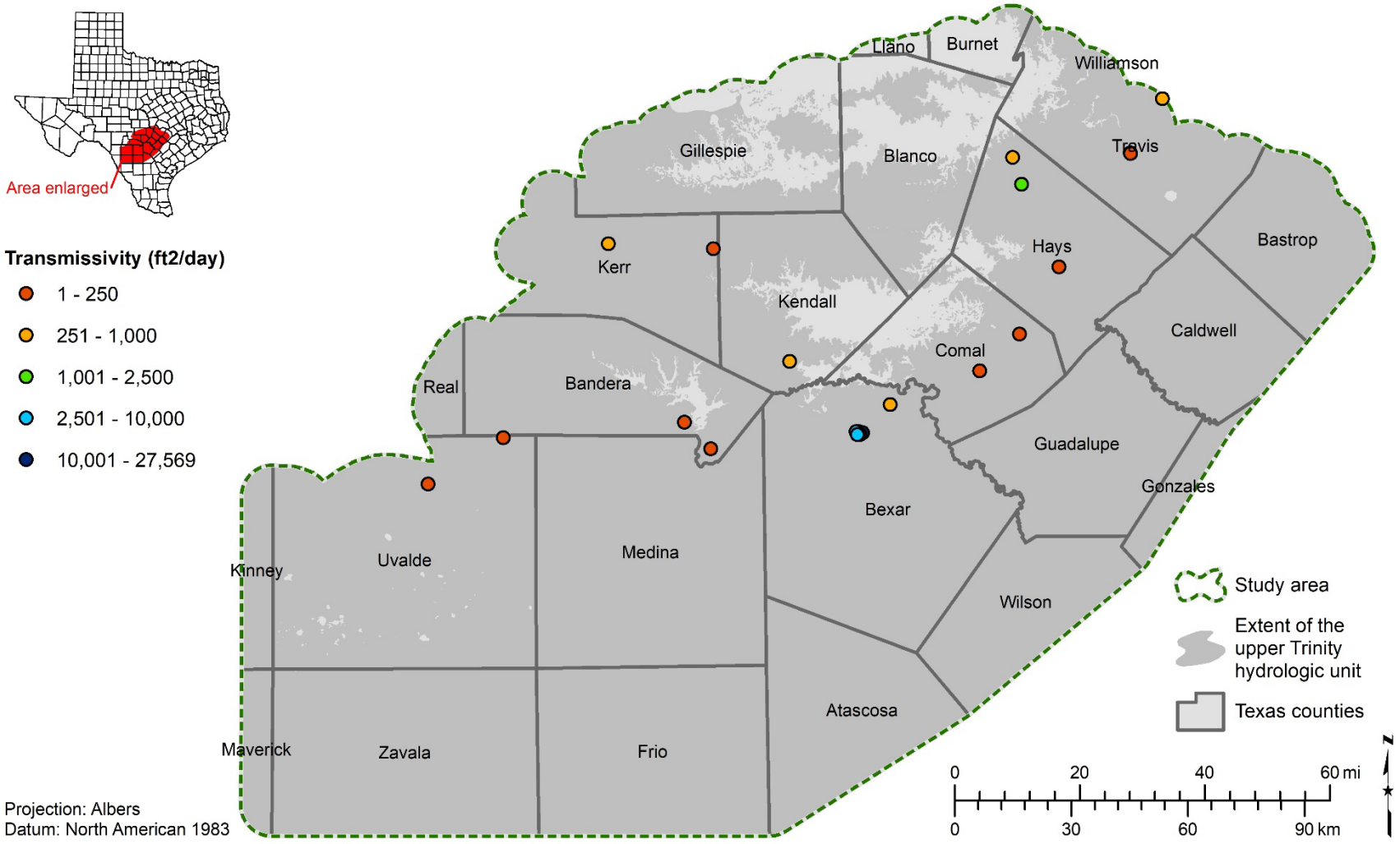

Figure 9-1 Transmissivity ranges and distribution for wells in the upper Trinity hydrologic unit. (ft2 = square feet)

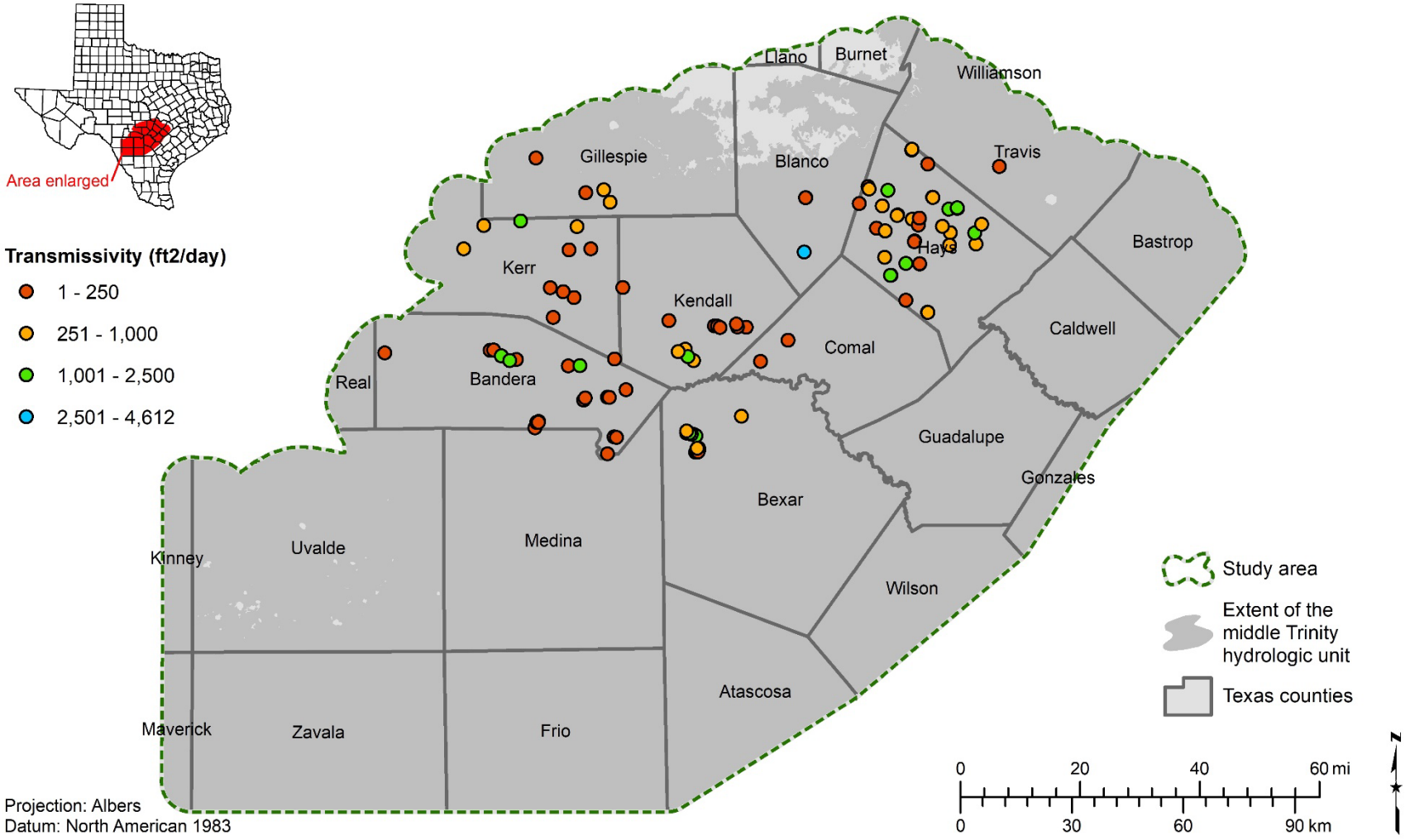

Figure 9-2 Transmissivity ranges and distribution for wells in the middle Trinity hydrologic unit. (ft2 = square feet)

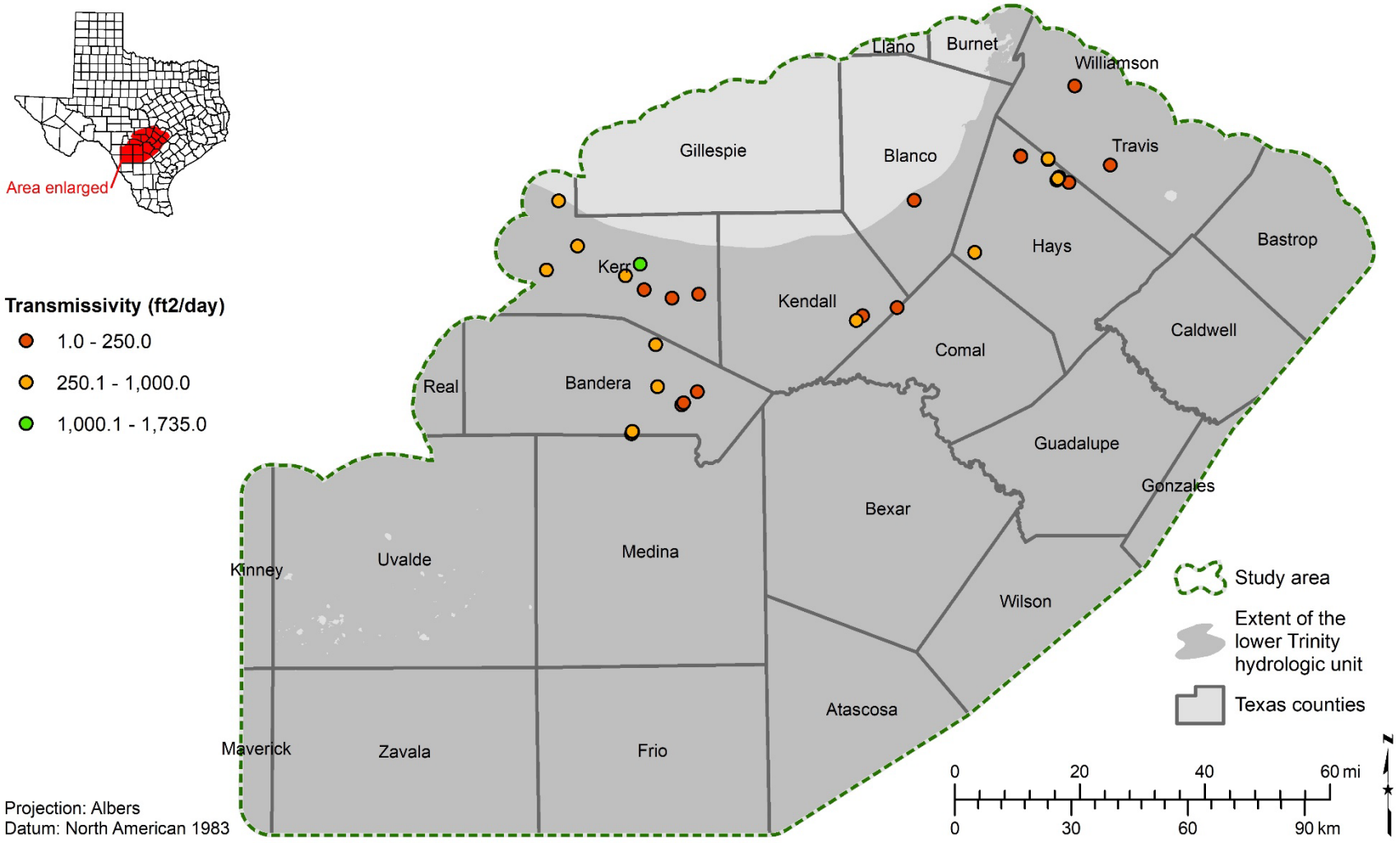

Figure 9-3 Transmissivity ranges and distribution for wells in the lower Trinity hydrologic unit. (ft2 = square feet)

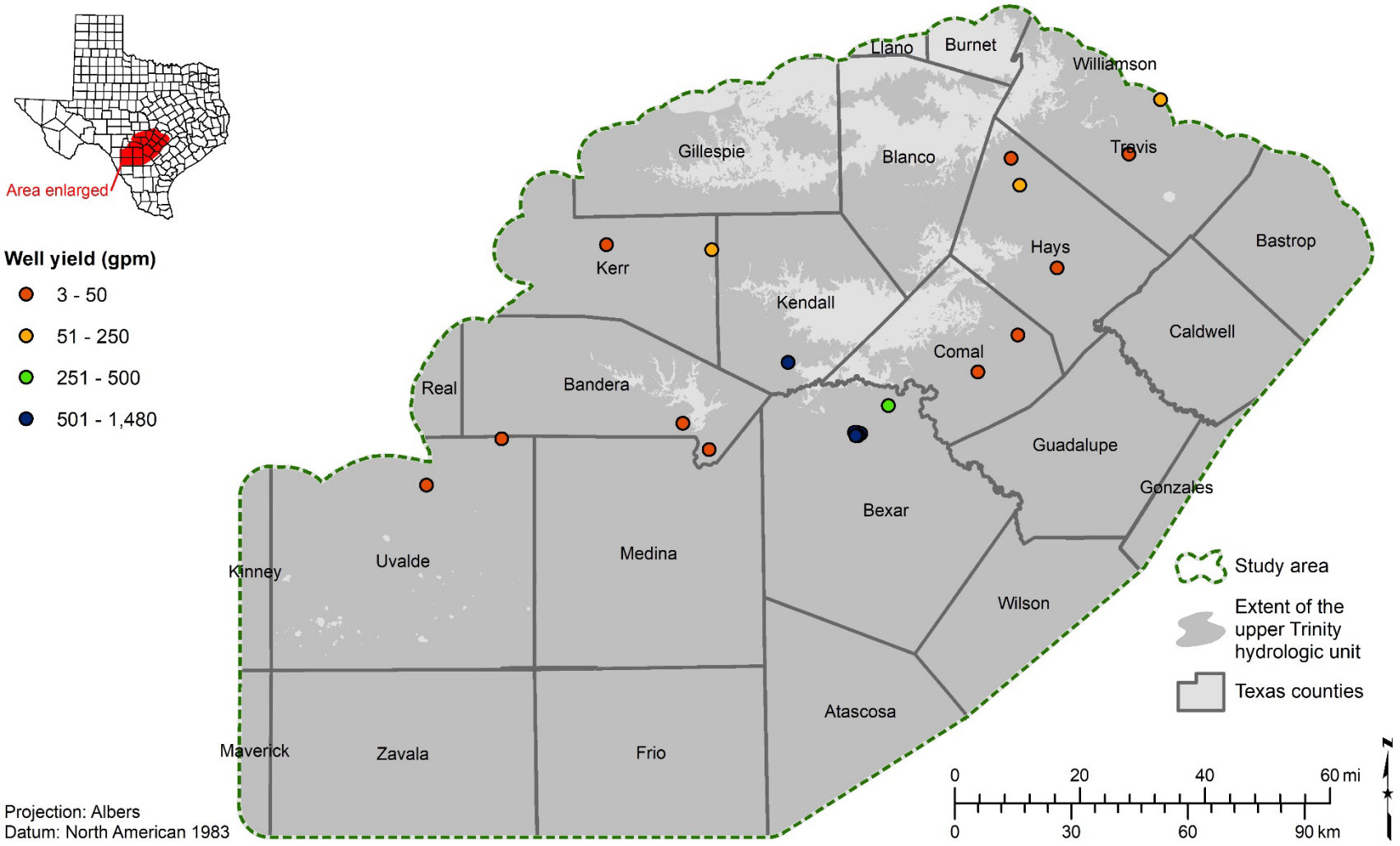

Figure 9-4 Well yield ranges and distribution for wells in the upper Trinity hydrologic unit. (gpm = gallons per minute)

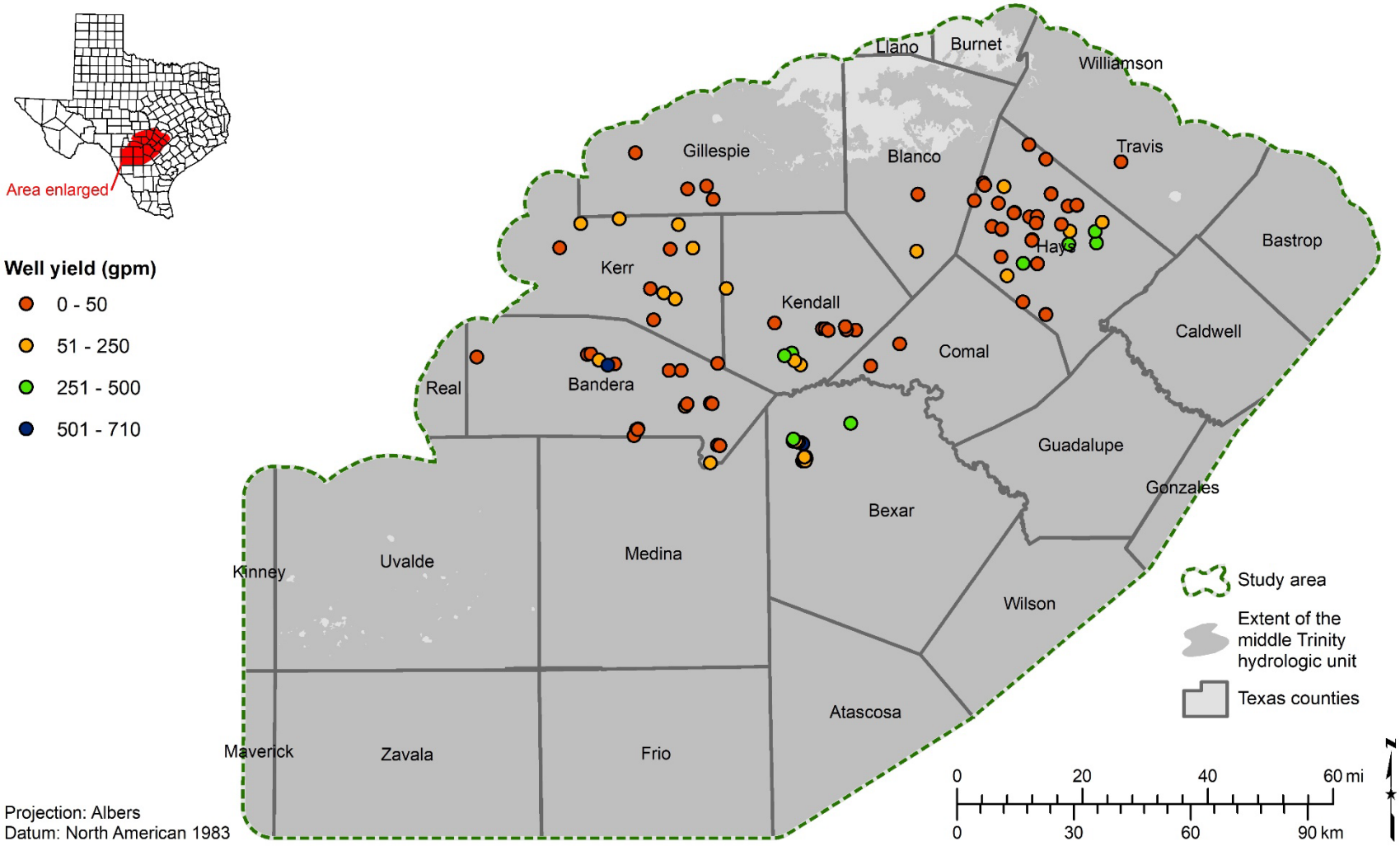

Figure 9-5 Well yield ranges and distribution for wells in the middle Trinity hydrologic unit. (gpm = gallons per minute)

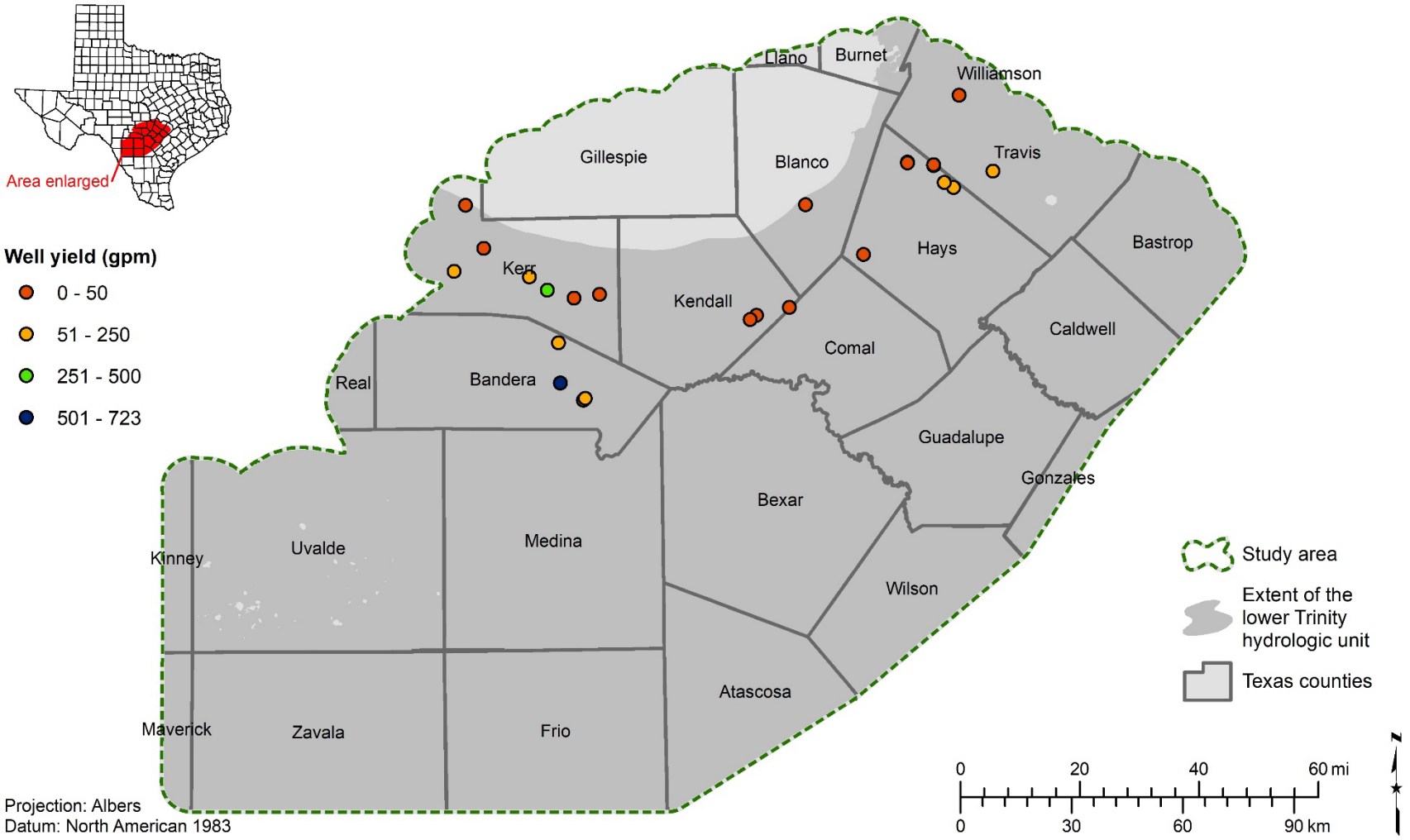

Figure 9-6 Well yield ranges and distribution for wells in the lower Trinity hydrologic unit. (gpm = gallons per minute)

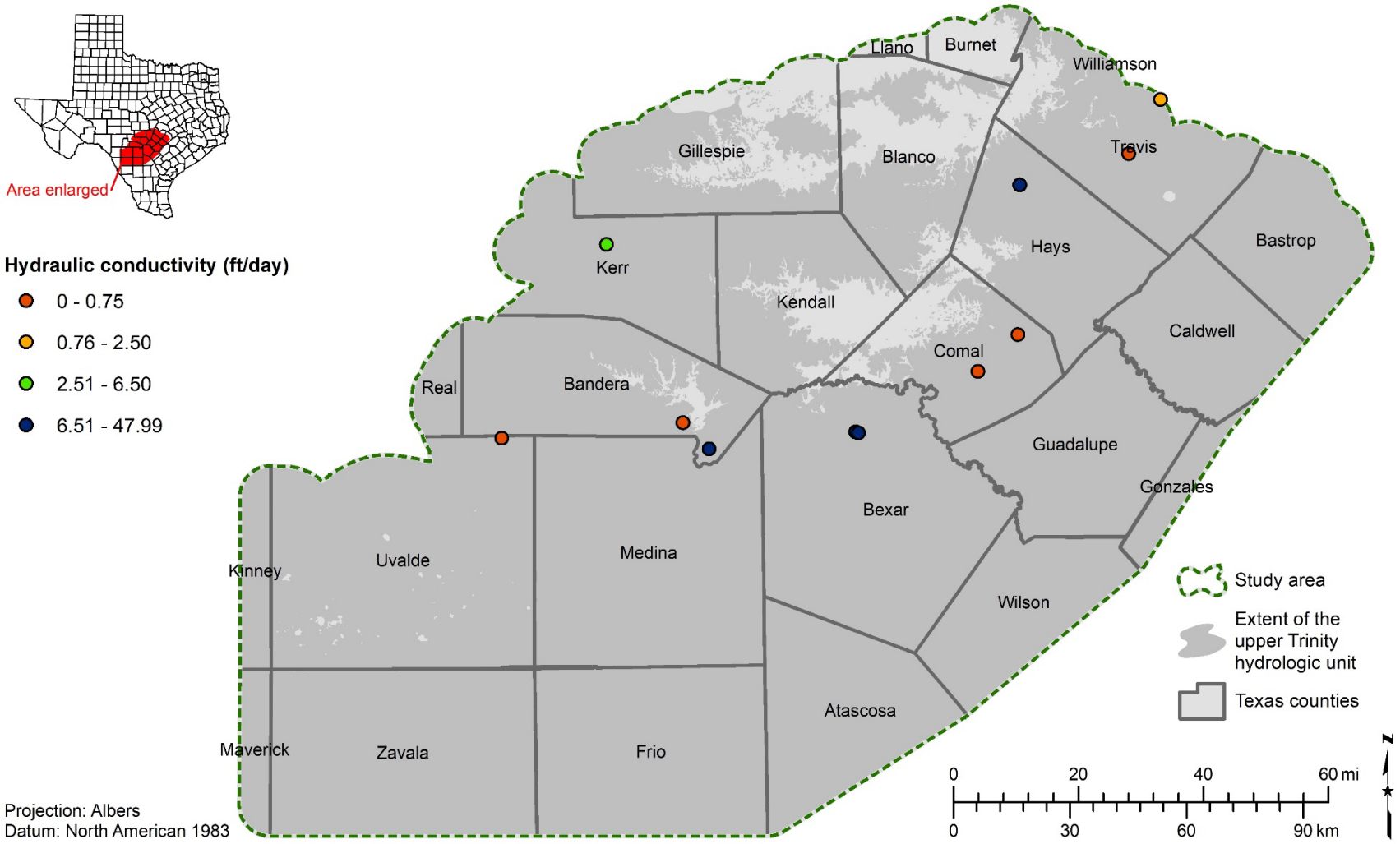

Figure 9-7 Hydraulic conductivity ranges and distribution for wells in the upper Trinity hydrologic unit. (ft = feet)

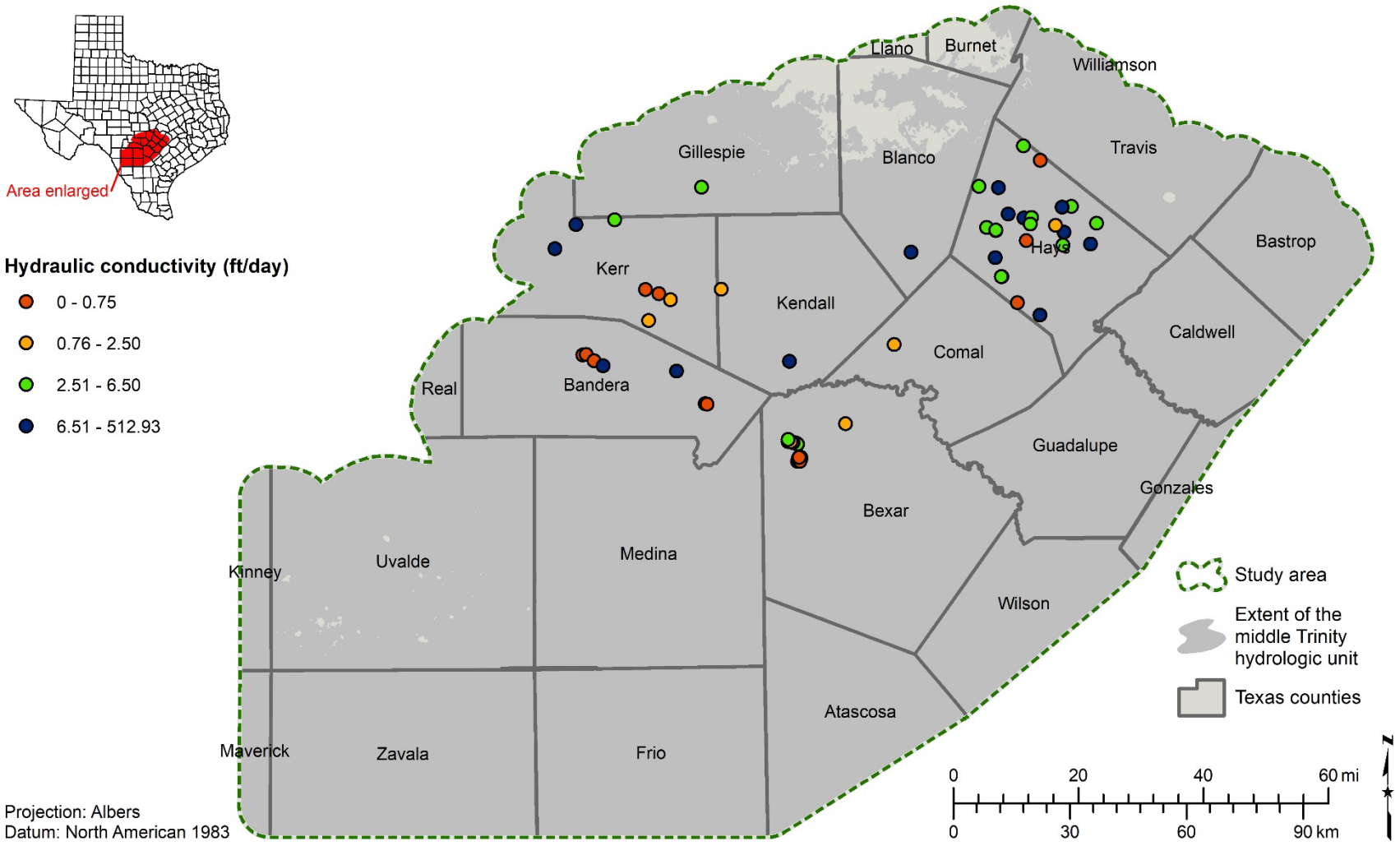

Figure 9-8 Hydraulic conductivity ranges and distribution for wells in the middle Trinity hydrologic unit. (ft = feet)

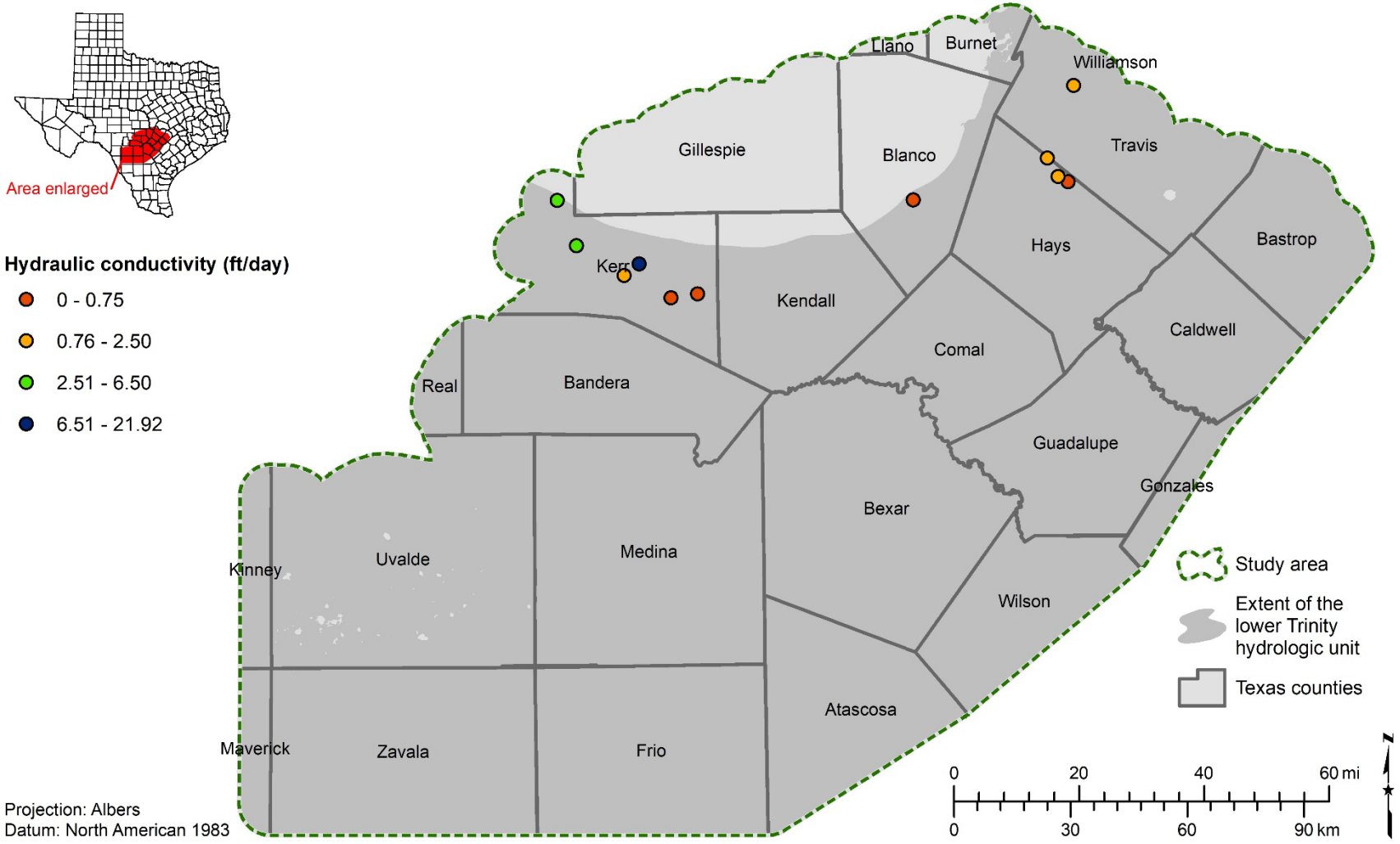

Figure 9-9 Hydraulic conductivity ranges and distribution for wells in the lower Trinity hydrologic unit. (ft = feet)

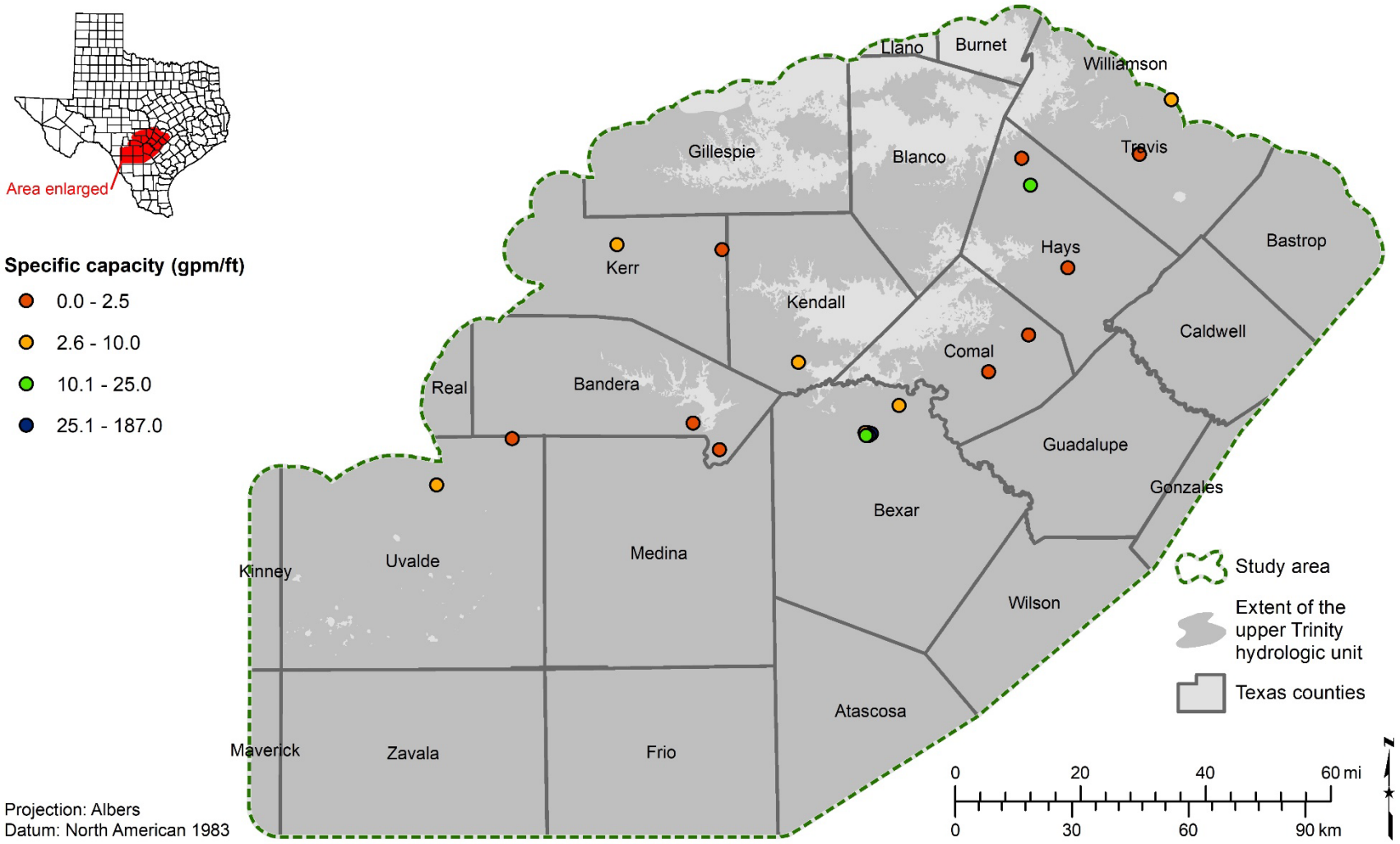

Figure 9-10 Specific capacity ranges and distribution for wells in the upper Trinity hydrologic unit. (gpm = gallons per minute, ft = feet)

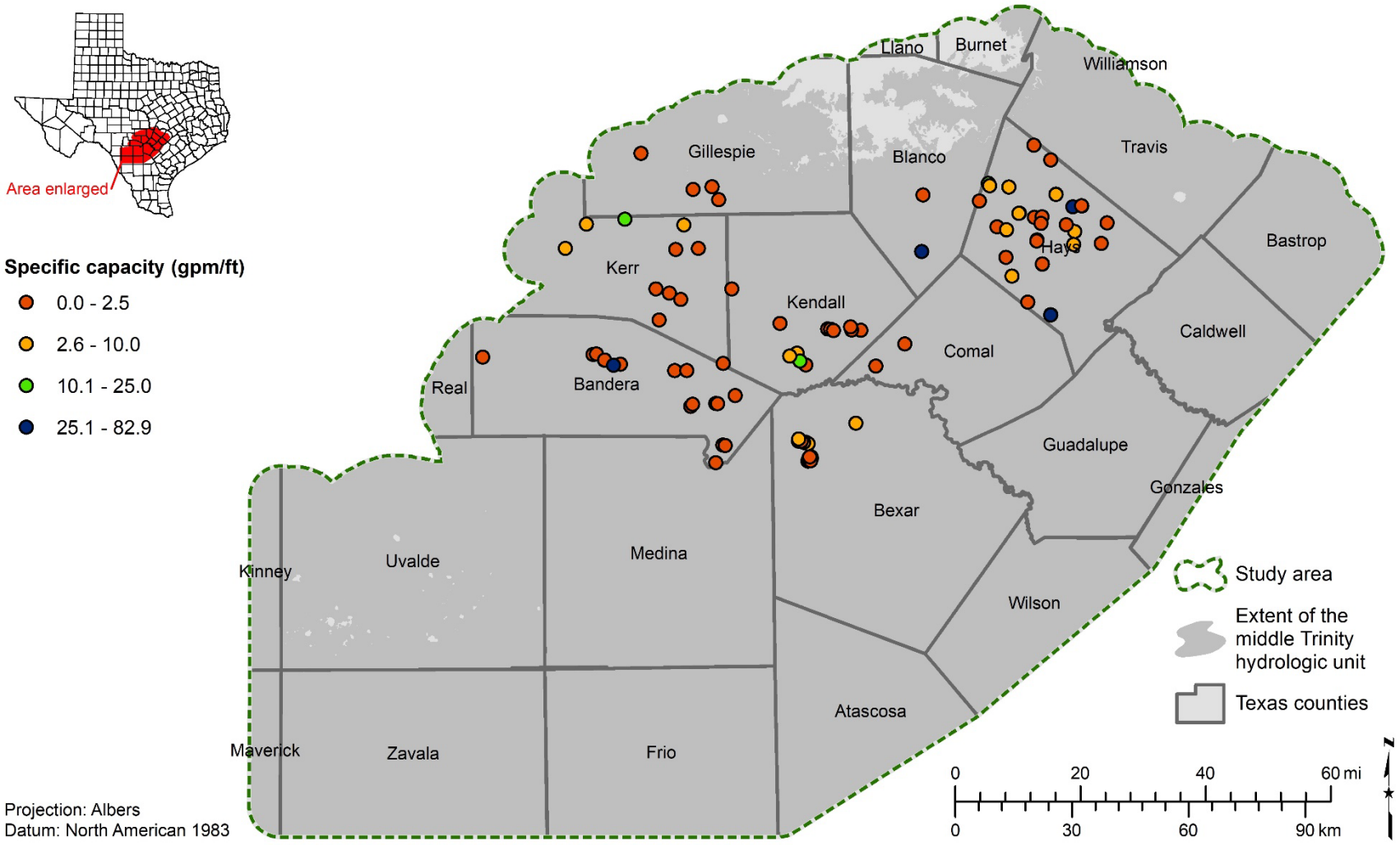

Figure 9-11 Specific capacity ranges and distribution for wells in the middle Trinity hydrologic unit. (gpm = gallons per minute, ft = feet)

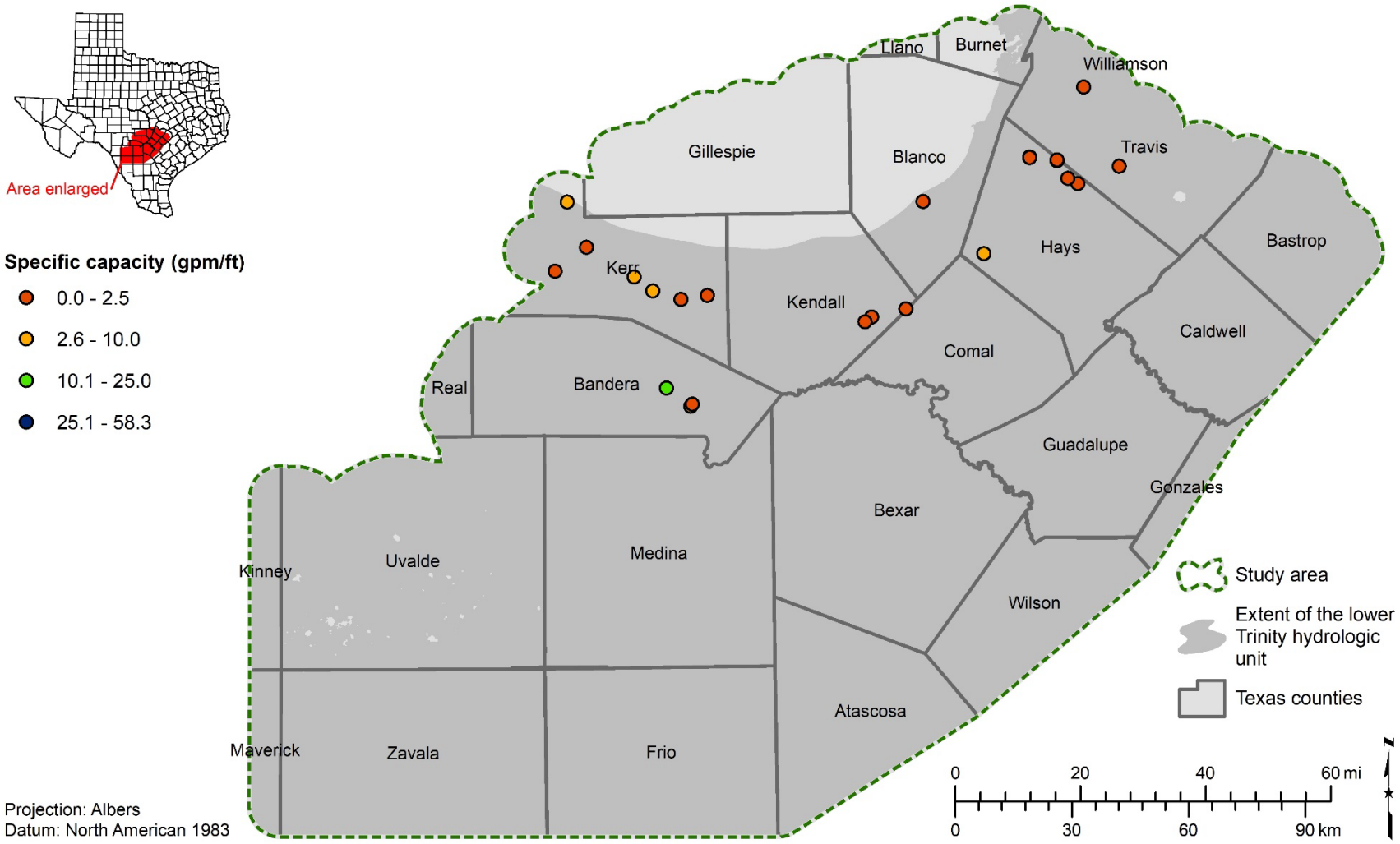

Figure 9-12 Specific capacity ranges and distribution for wells in the lower Trinity hydrologic unit. (gpm = gallons per minute, ft = feet)

10 Water quality data

Water quality broadly refers to water properties relating to the concentration of dissolved ions, turbidity (the amount of suspended sediment), pH, and the presence of bacteria and organic compounds. However, for our purposes of characterizing brackish water, water quality refers only to total dissolved solids, defined as the total concentration of all dissolved molecules and ions reported in units of milligrams per liter. Measured water quality refers to samples of water that were collected from a well with known screen or casing intervals, which were analyzed for the individual concentrations of chemical constituents. Most measured water quality data used in this report are from the digital TWDB Groundwater Database. Other sources include the USGS produced water database (Blondes and others, 2016), scanned reports in the TWDB Groundwater Database, and groundwater conservation districts.

We assigned groundwater well samples to hydrologic units by utilizing the aquifer determination results described in Section 8 of this report. This process compares the screen and casing depths of the well to formation top and bottom depths defined by our geologic model for the study. Utilizing these results, we were able to classify if water samples were sourced from individual formations or groups of formations in the upper, middle, or lower Trinity, and to verify that a sample was not a mixture between groups of hydrologic units.

Using measured water quality values, we established relationships of total dissolved solids to specific conductance. These relationships allowed us to convert our interpretations of water resistivity from geophysical log calculations to total dissolved solids more accurately. We then were able to interpret the groundwater salinity boundaries guided by values of total dissolved solids derived from measured water quality supplemented with estimated water quality from calculations on geophysical well logs.

Measured water quality values used in this study, excluding those from the TWDB Groundwater Database, were entered into the TWDB BRACS Database. All of the compiled water quality information used for the study can be accessed in the ***tblMaster_Water_Quality_HCT*** table in the TWDB BRACS database.

10.1 Sources of measured water quality

We identified 1,897 water samples from wells completed in individual Trinity hydrostratigraphic units or in the following combinations of units: 1) Upper Glen Rose limestone and Lower Glen Rose limestone, 2) Lower Glen Rose limestone, Hensell sandstone, and Cow Creek limestone, and 3) Sligo limestone and Hosston sandstone. We ignored the Hammett shale as it is considered a non-water-producing unit. The great majority of water samples with measured water quality are from the TWDB Groundwater Database (1,763 samples). Other sources of measured water quality samples are the Bandera County River Authority and Groundwater Conservation District (100 samples), Edwards Aquifer Authority (24 samples), United States Geological Survey

produced water database (5 samples), and the INTERA Northern Trinity GAM study (INTERA, 2014) (5 samples).

10.2 Total dissolved solids

The total dissolved solids value is defined as the total concentration of ions and molecules dissolved in the water and is reported in units of milligrams per liter. In this report, the total dissolved solids concentration of water is also referred to as the salinity of the water. Five salinity classes defined by total dissolved solids concentration are used throughout this report following usage in the USGS paper by Winslow and Kister (1956):

- fresh water (0 to 999 milligrams per liter total dissolved solids)
- slightly saline water (1,000 to 2,999 milligrams per liter total dissolved solids)
- moderately saline water (3,000 to 9,999 milligrams per liter total dissolved solids)
- very saline water (10,000 to 34,999 milligrams per liter total dissolved solids)
- brine (>35,000 milligrams per liter total dissolved solids)

Although brackish water can refer to total dissolved solid concentrations ranging from 1,000 to 34,999 milligrams per liter (slightly saline to very saline water), we focus on slightly saline and moderately saline water in our mapping and volume estimates. For this study, we mapped and characterized brackish water up to 35,000 milligrams per liter total dissolved solids. It is important to note that desalination often requires reducing total dissolved solids concentrations below 1,000 milligrams per liter, thus the total dissolved solids concentration of brackish water is a primary concern for desalination. That is, slightly saline and moderately saline brackish water is preferable to very saline brackish water as it requires less effort and expense to desalinate to fresh drinking water standards.

10.2.1 Contributing factors of dissolved solids in the study area

Groundwater in the study area is sourced and recharged from rainfall and to a lesser amount by losing streams (referred to collectively as meteoric water) which infiltrates the aquifers at their outcrop. Because rainwater contains very little dissolved solids, dissolved solids present in groundwater are mainly sourced from leaching of material in the soil and chemical interactions of groundwater with the aquifer material. Recharge rate, groundwater flow velocity, and groundwater residence time (the amount of time water remains underground), are important factors controlling the concentration of dissolved solids in groundwater. In general, the more time water resides underground, the greater its dissolved solids content.

A typical trend in groundwater quality is that fresh water is common at the outcrop where the aquifer is recharged by meteoric water and degrades with depth and distance from the outcrop as dissolved solids content increases and the residence time of the groundwater increases. Because most of the Trinity Group aquifer material was deposited in a shallow marine environment millions of years ago, it is possible for the

ancient sea water to remain trapped within non-connected pores in the rocks (referred to as connate water). However, connate water in the permeable intervals of the aquifers most likely was flushed out long ago from recharge by meteoric water (Winslow and Kister, 1956) and is not considered a major contributor to the dissolved solids in the study area.

Groundwater flow between aquifers may contribute dissolved solids from one aquifer to another. However, we divided the Trinity into upper, middle, and lower Trinity hydrologic units based on their separation by low-permeability aquitards, and thus we assume vertical flow between the upper, middle, and lower Trinity is minor to nonexistent. For example, Wong and others (2014) describes a prominent evaporite interval between the Upper Glen Rose limestone and Lower Glen Rose limestone which hinders vertical groundwater flow between them. However, where aquifers are juxtaposed along faults of the Balcones Fault Zone, groundwater may flow between aquifers via horizontal flow through a fault, or vertical flow along a fault. Groundwater flow along or through faults is complicated as the fault core is often impermeable, whereas the damage zone around the fault has generally higher permeability (Caine and others, 1996; Bense and others, 2013).

Senger and Kreitler (1984) noted that Trinity Aquifer groundwater is typically dominated by calcium and bicarbonate or calcium and sulfate due to chemical interaction with the carbonate host rock and dissolution of interlayered evaporite beds (primarily gypsum). Wong and others (2014) concluded the Upper Glen Rose limestone, Lower Glen Rose limestone, Hensell sandstone, and Cow Creek limestone water chemistry primarily reflect gypsum dissolution based on the relative concentrations of calcium, magnesium, bicarbonate, and sulfate. Wong and others (2014) further concluded the water chemistry of the Hensell sandstone and Cow Creek limestone reflect interaction with silicate minerals based on strontium isotope values. Sulfate concentrations in the upper, middle, and lower Trinity are similar, indicating the presence and dissolution of gypsum and anhydrite in all three, and/or possible vertical movement of water between formations (Tian and others, 2020).

Dissolved solids may also be contributed by human activity such as surface contamination or injection of wastewater into aquifers at depth. Surface contamination is assumed to not affect the deeper, brackish portions of the aquifer which are the primary concern of this study. We did not investigate injection of wastewater in detail for this study.

10.2.2 Total dissolved solids quality control

Two methods for determining milligrams per liter of total dissolved solids for a water sample include: 1) dry the sample at temperatures above 103° Celsius to as high as 180° Celsius and weigh the residue, or 2) sum the individually determined chemical constituents (Hem, 1985). Because laboratory methods for determining the weight of residue may differ and reported total dissolved solid values do not always specify whether the value is from a weighed residue or calculated, we used only total dissolved

solid values calculated from the sum of the major constituents for this study in order to assure that our values are directly comparable.

To compare values of total dissolved solids derived from the sum of major constituents to values of total dissolved solids derived from the weight of residue, the milligrams per liter of bicarbonate (HCO_3) is multiplied by 0.4917 to account for the weight of HCO_3 that volatizes to $CO_2 + H_2O$ when heated above 100° C as done to measure the weight of residue (Hem, 1985). However, because our study only utilizes total dissolved solids derived from the sum of constituents, reducing the bicarbonate value to compare with the weight of residue analyses is not required. In Section 11 of this report, the final step of estimating total dissolved solids from geophysical well logs requires establishing the relationship between total dissolved solids and specific conductance for each of the Trinity Aquifer hydrostratigraphic units. The benefit of using the full value of bicarbonate for the plots of total dissolved solids versus specific conductance is that it yields a more accurate relationship.

We summed the following major constituents to calculate total dissolved solids: Ca^{2+}, Mg^{2+}, K^{+}, Na^{+}, Sr^{2+}, SiO_2, HCO_3^{-}, CO_3^{2-}, Cl^{-}, SO_4^{2-}, F, and NO_3^{-}. We verified the accuracy of the reported major constituent values by verifying the charge balance between the major anions and cations and by comparing the total anion milliequivalents per liter to the total cation milliequivalents per liter. For accurately analyzed water quality samples, the total anion and cation milliequivalents per liter should only differ by one to two percent (Hem, 1985). We marked as balanced any sample where the percent difference between the anion and cation total milliequivalents per liter was less than or equal to five percent (positive or negative), and any sample with a percent difference greater than five percent we marked as unbalanced and excluded from our analysis. An exception are 15 unbalanced samples (unbalanced by less than 10 percent) which we manually marked as balanced, as they are particularly important for the study because their total dissolved solid concentrations are greater than 800 milligrams per liter. All balanced and unbalanced water quality analyses are available in the TWDB BRACS Database.

We calculated the total cation and anion milliequivalents per liter with the following formulas (the chemical constituents are in milligrams per liter, and the decimal fraction in the formulas is the conversion from milligrams per liter to milliequivalents per liter for each individual constituent):

Total Cation milliequivalents per liter = ((Ca * 0.0499) + (Mg * 0.08229)
+ (Na * 0.0435) + (K * 0.02557) + (Sr * 0.0228))

Total Anion milliequivalents per liter = ((CO_3 * 0.03333) + (HCO_3 * 0.01639)
+ (SO_4 * 0.02082) + (Cl * 0.02821) + (F * 0.05264) + (NO_3 * 0.01613))

Measured water quality samples from the Texas Water Development Board Groundwater Database include a flag to indicate whether they are balanced or unbalanced if the difference in the anion and cation milliequivalents per liter is less than or greater than 5 percent. However, we noted some inconsistencies between the ion concentrations and

reported balance in the groundwater database (for example, samples that appear to be balanced were flagged as unbalanced), and thus we recalculated the balance for all TWDB Groundwater Database samples and reflagged them as balanced or unbalanced.

10.2.3 Analysis of major chemical constituents

For most of our analyses we used only the most recent water sample for each well location. The exception to this is where we develop total dissolved solids versus specific conductance relationships, in which case we used all available water samples. Based on our analysis of measured water quality in the study area, the dominant water types are calcium-magnesium bicarbonate for fresh water, and calcium-magnesium sulfate for water up to 4,000 milligrams per liter total dissolved solids (Figure 10-1 to Figure 10-16). In all formations, sulfate is the dominant contributor of dissolved solids in samples with total dissolved solids greater than 1,100 milligrams per liter, while bicarbonate maintains a consistent concentration of a few hundred milligrams per liter (Figure 10-1, Figure 10-3, and Figure 10-5).

In the Upper Glen Rose limestone and Lower Glen Rose limestone, the concentration of calcium is greater than magnesium, which is greater than sodium, until beyond about 5,000 milligrams per liter total dissolved solids where sodium becomes the dominant cation (Figure 10-2). The Hensell sandstone and Cow Creek limestone have an overall similar pattern with calcium as the dominant cation followed by magnesium. However, in the Hensell sandstone and Cow Creek limestone, sodium increases rapidly for total dissolved solid concentrations up to about 900 milligrams per liter where in places sodium is the dominant cation (Figure 10-3). The Sligo limestone and Hosston sandstone have the greatest sodium concentration for any of the water bearing units, which is the dominant cation for samples with total dissolved solid concentrations above approximately 600 milligrams per liter (Figure 10-5).

One limitation of our analysis of ion concentrations is that measured water quality samples are very sparse beyond 4,000 milligrams per liter total dissolved solids. However, from the few data points above 4,000 milligrams per liter total dissolved solids in the Upper Glen Rose limestone and Lower Glen Rose limestone, we observe that sodium becomes the dominant cation in the form of sodium sulfate and that sodium chloride dominates at total dissolved solid concentrations above 10,000 milligrams per liter (Figure 10-1 and Figure 10-2). We assume the Hensell sandstone and Cow Creek limestone have similar trends in ion concentrations above 5,000 milligrams per liter total dissolved based on the similarity in their trends of ion concentrations where samples exist (Figure 10-3 and Figure 10-4). The Sligo limestone and Hosston sandstone were found to have the most sodium chloride of all the water bearing units and that below 4,000 milligrams per liter total dissolved solids, the increase in total dissolved solids is because of an increase in sulfate. Beyond 5,000 milligrams per liter total dissolved solids sodium chloride dominates in the Sligo limestone and Hosston sandstone (Figure 10-5 and Figure 10-6).

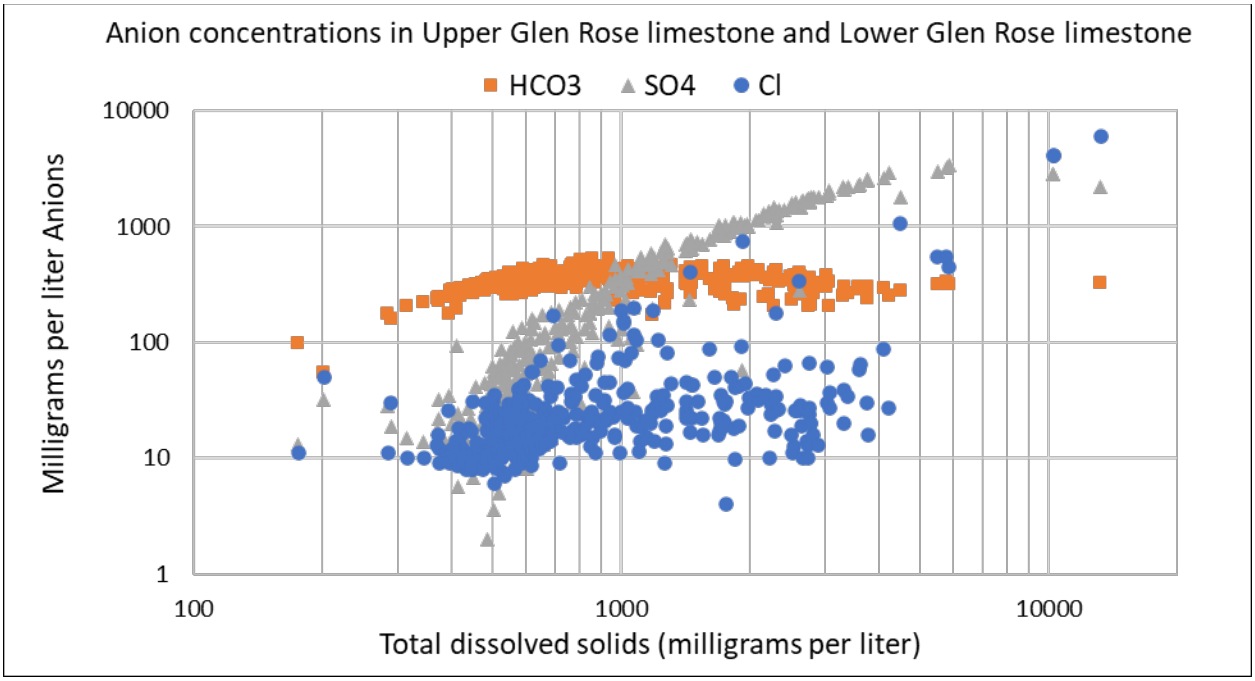

Figure 10-1 **Major anion concentration versus total dissolved solids for the Upper Glen Rose limestone and Lower Glen Rose limestone. Number of samples is 394. (HCO3 = bicarbonate, SO4 = sulfate, Cl = chloride)**

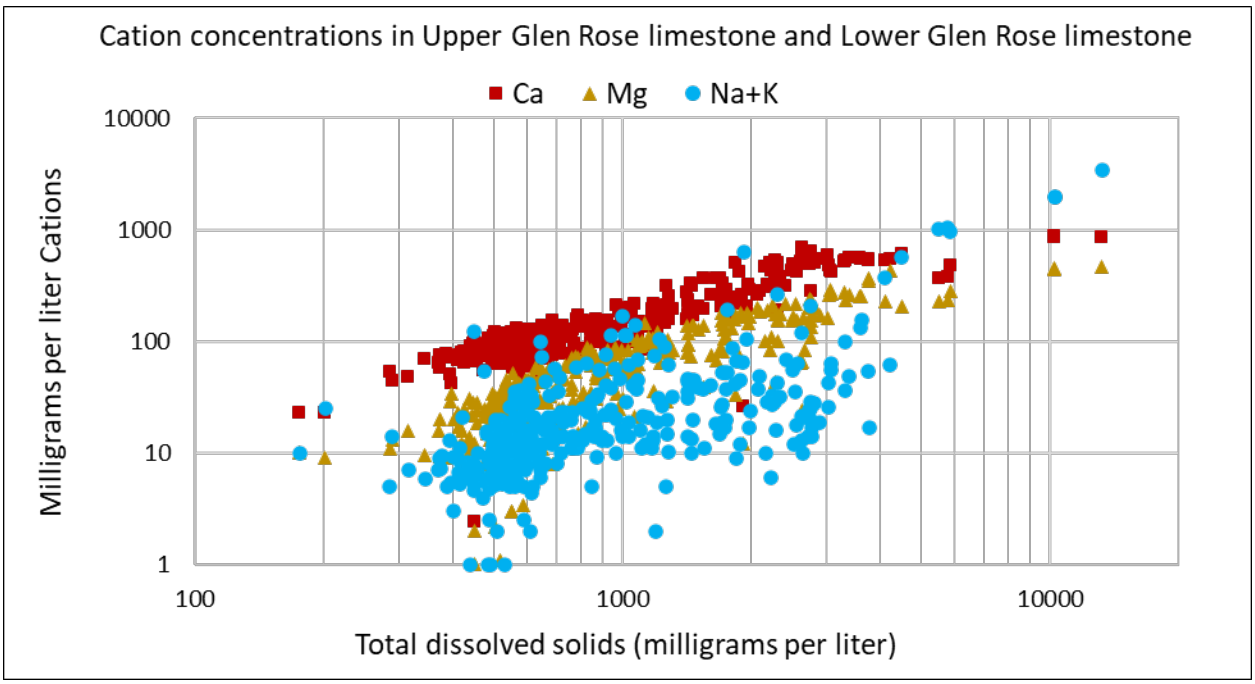

Figure 10-2 **Major cation concentration versus total dissolved solids for the Upper Glen Rose limestone and Lower Glen Rose limestone. Number of samples is 394. (Ca = calcium, Mg = magnesium, Na= sodium, K = potassium)**

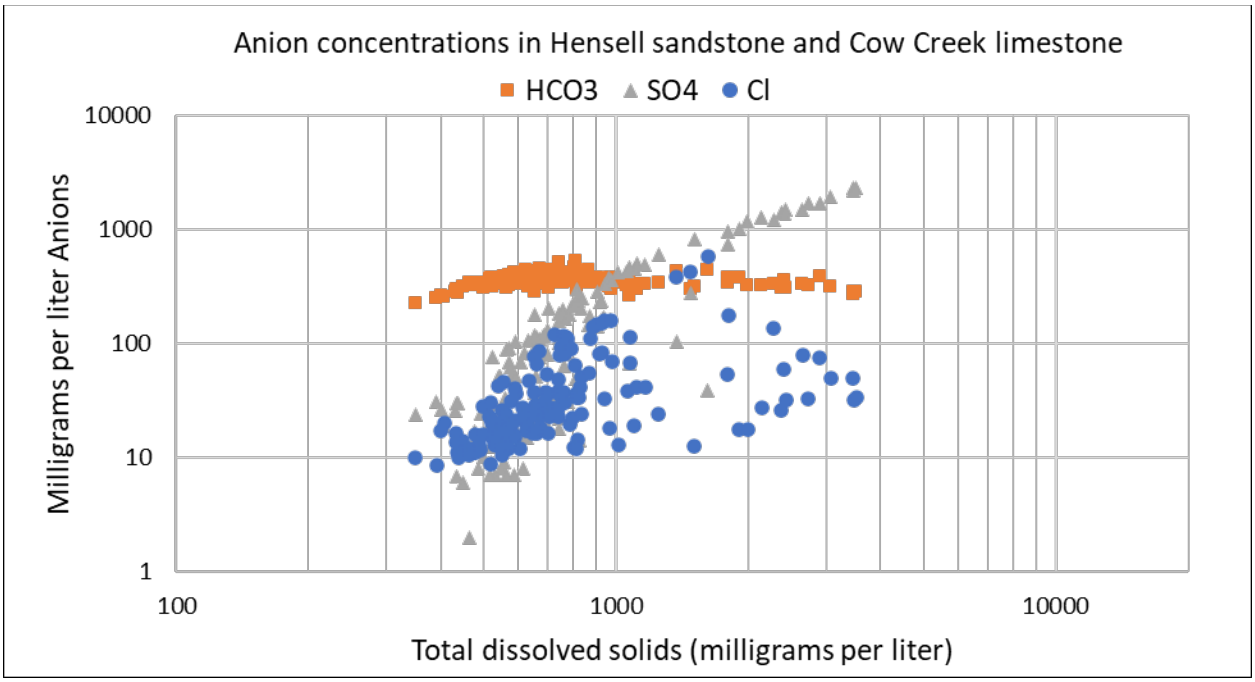

Figure 10-3 **Major anion concentration versus total dissolved solids for the Hensell sandstone and Cow Creek limestone. Number of samples is 150. (HCO3 = bicarbonate, SO4 = sulfate, Cl = chloride)**

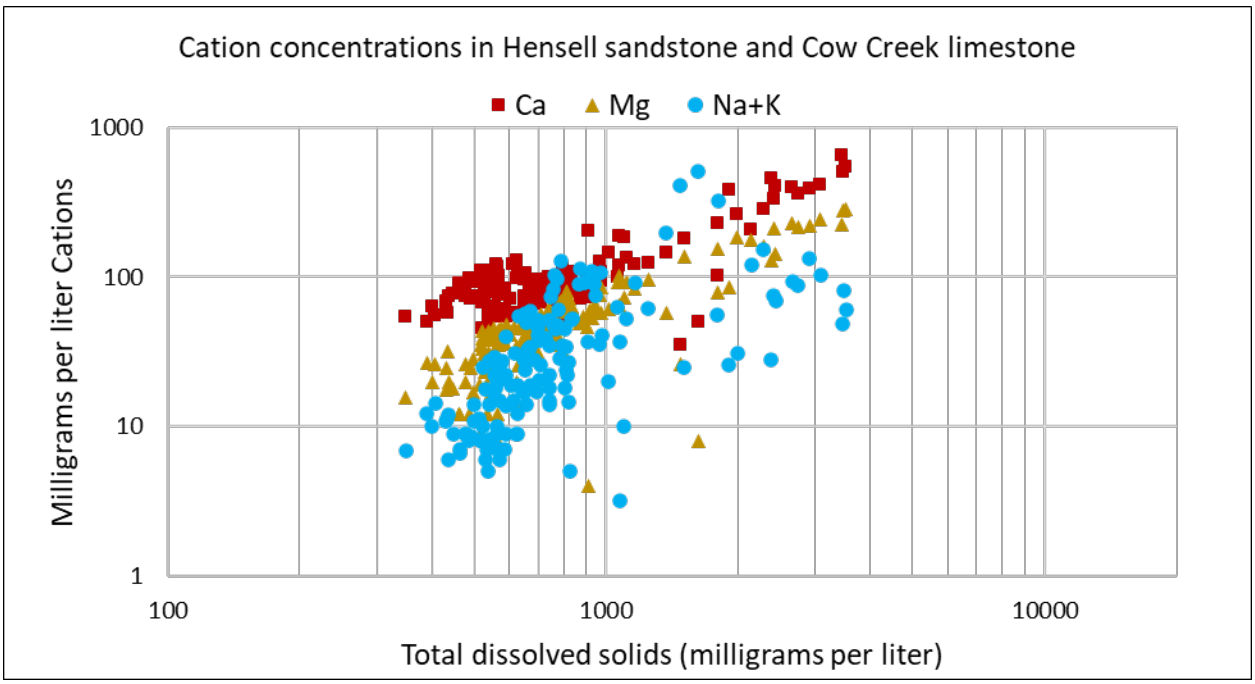

Figure 10-4 **Major cation concentration versus total dissolved solids for the Hensell sandstone and Cow Creek limestone. Number of samples is 150. (Ca = calcium, Mg = magnesium, Na = sodium, K = potassium)**

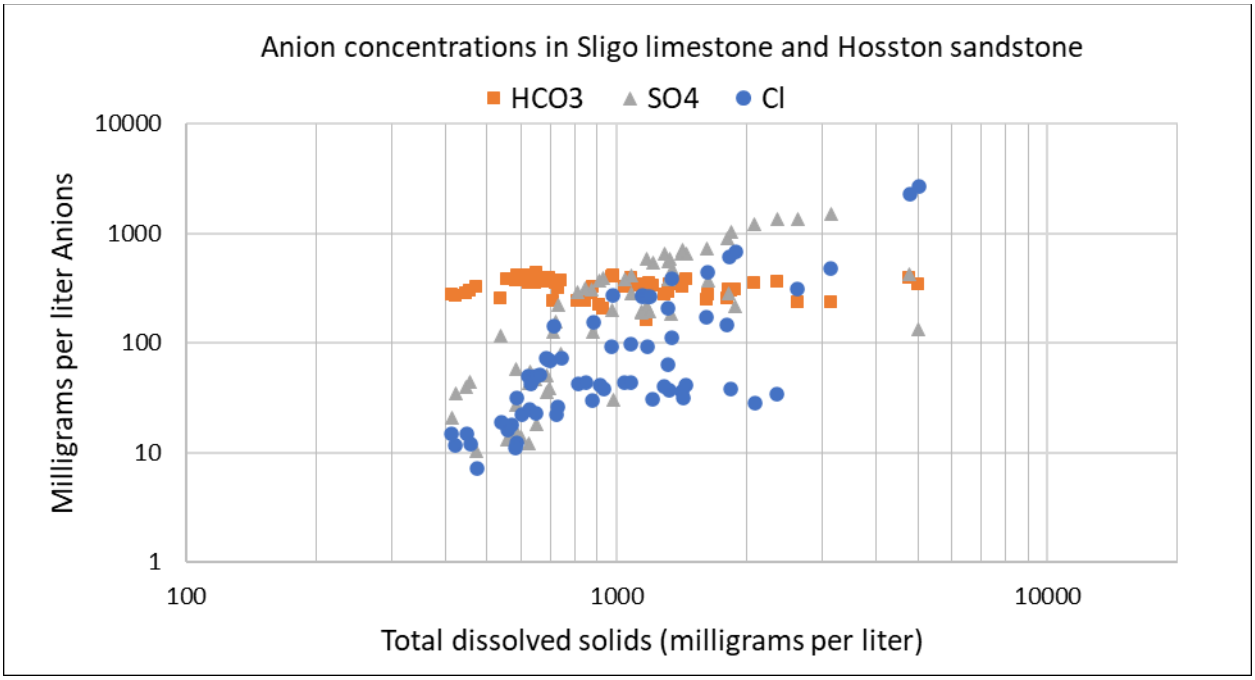

Figure 10-5 **Major anion concentration versus total dissolved solids for the Sligo limestone and Hosston sandstone. Number of samples is 64. (HCO3 = bicarbonate, SO4 = sulfate, Cl = chloride)**

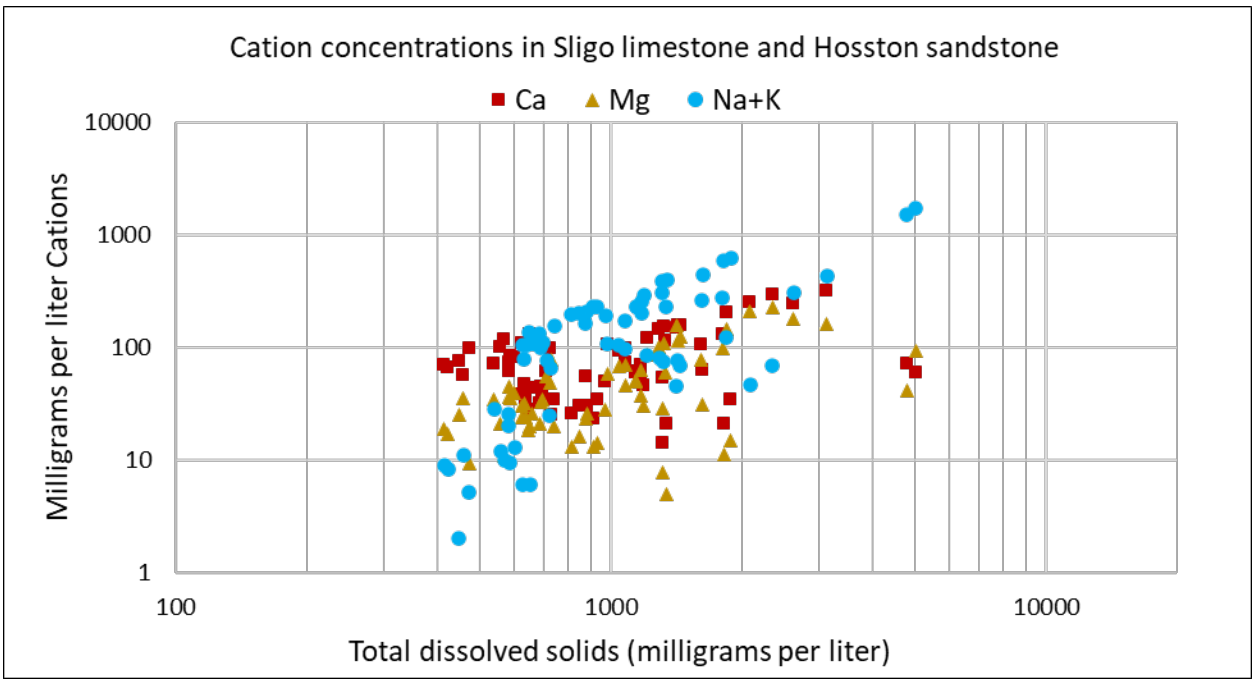

Figure 10-6 **Major cation concentration versus total dissolved solids for the Sligo limestone and Hosston sandstone. Number of samples is 64. (Ca = calcium, Mg = magnesium, Na = sodium, K = potassium)**

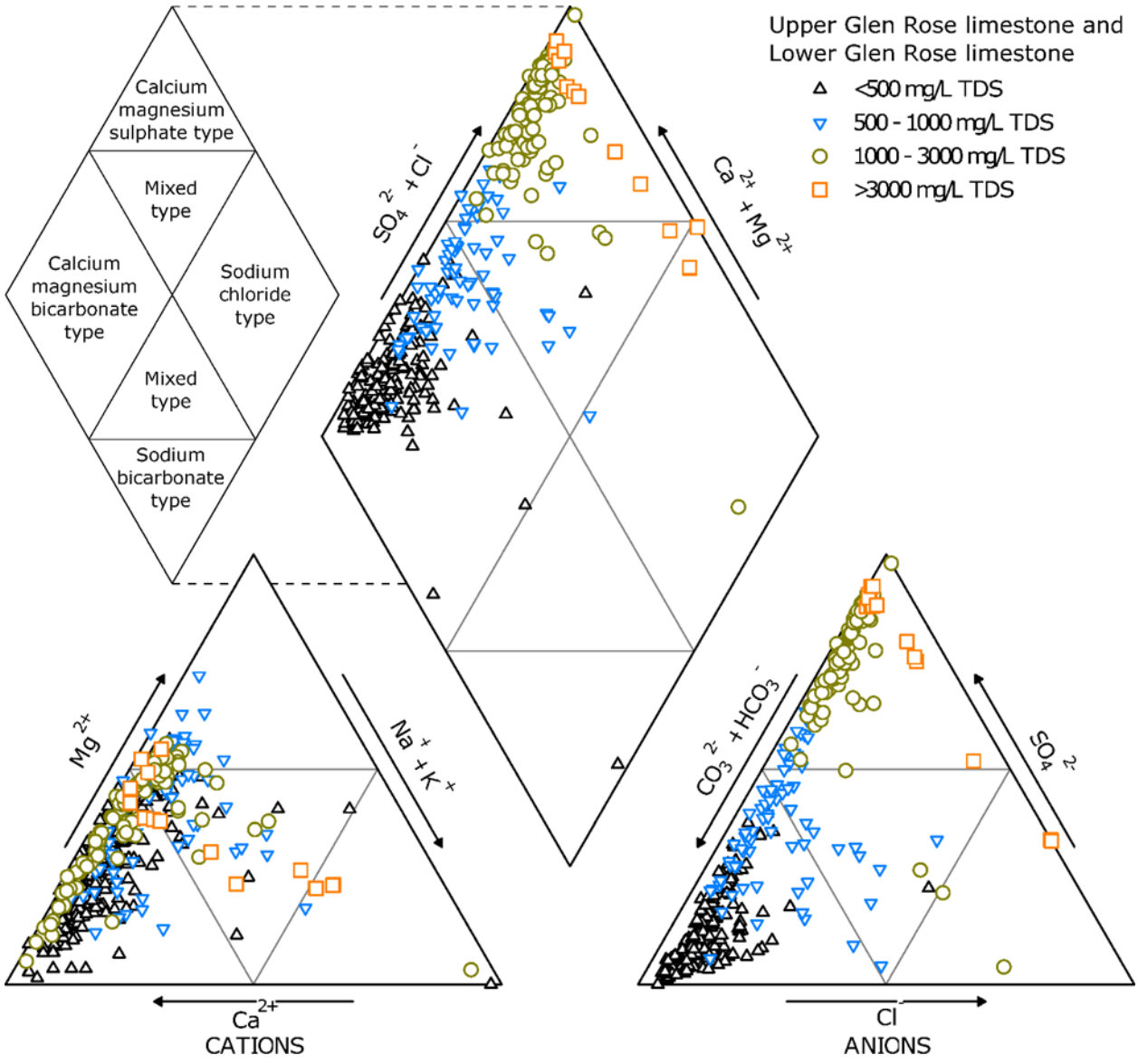

Figure 10-7 **Piper plots of the Upper Glen Rose limestone and Lower Glen Rose limestone, with data points symbolized by water quality (<500, 500-1,000, 1,000-3,000, and >3,000 milligrams per liter total dissolved solids). Number of samples is 393.**

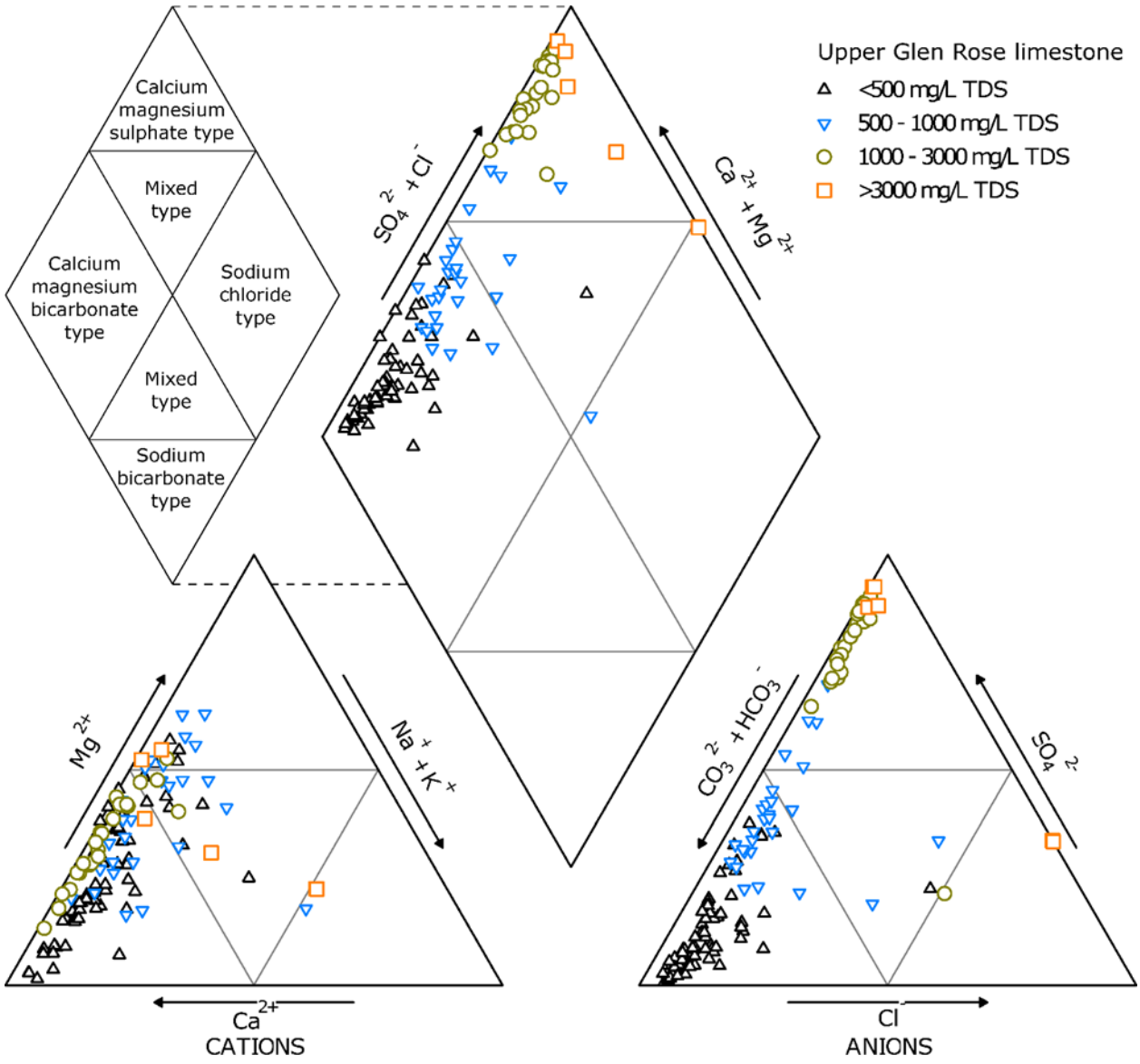

Figure 10-8 **Piper plots of the Upper Glen Rose limestone, with data points symbolized by water quality (<500, 500-1,000, 1,000-3,000, and >3,000 milligrams per liter total dissolved solids). Number of samples is 127.**

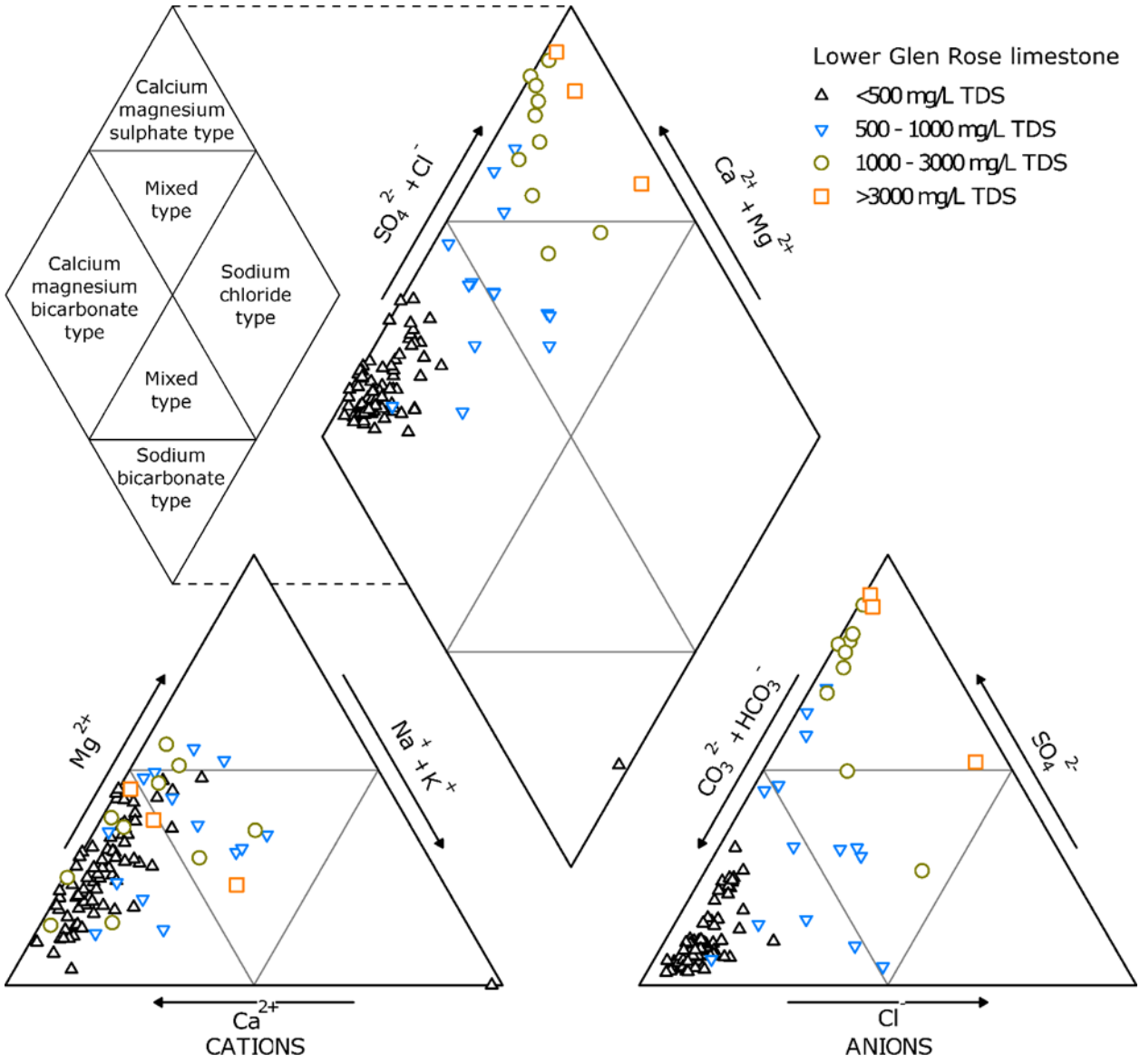

Figure 10-9 **Piper plots of the Lower Glen Rose limestone, with data points symbolized by water quality (<500, 500-1,000, 1,000-3,000, and >3,000 milligrams per liter total dissolved solids). Number of samples is 104.**

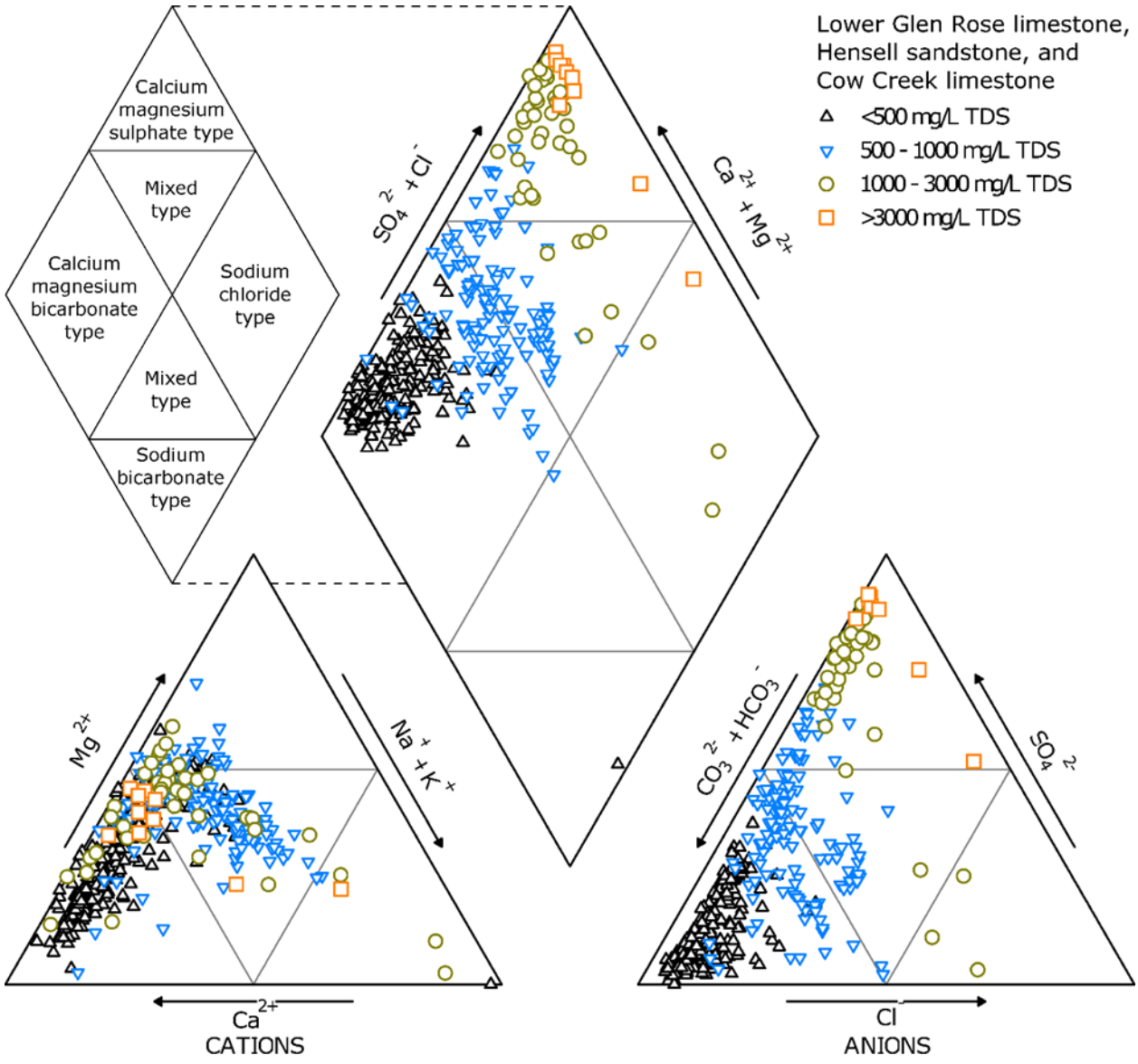

Figure 10-10 **Piper plots of the Lower Glen Rose limestone, Hensell sandstone, and Cow Creek limestone, with data points symbolized by water quality (<500, 500-1,000, 1,000-3,000, and >3,000 milligrams per liter total dissolved solids). Number of samples is 484.**

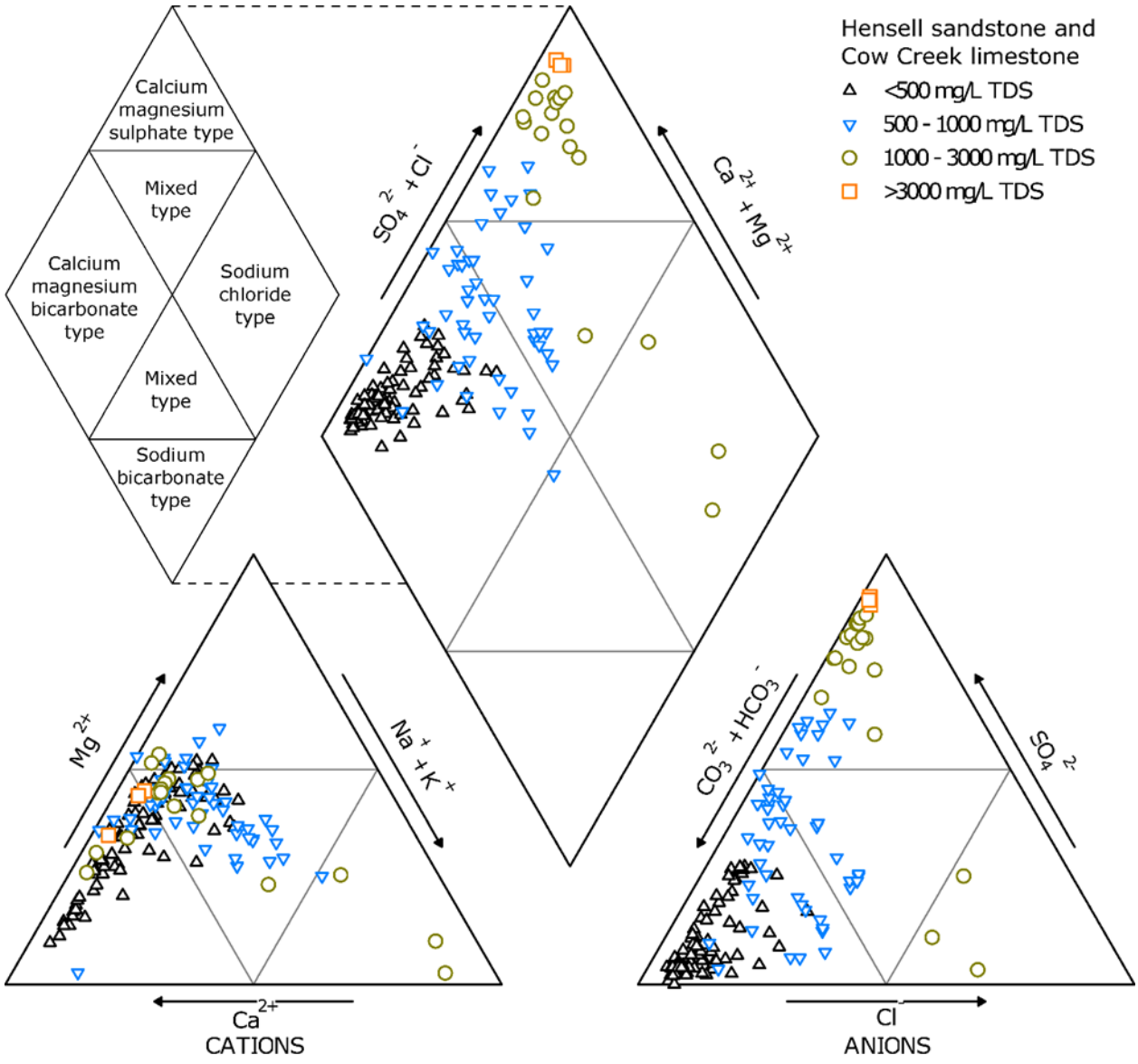

Figure 10-11 **Piper plots of the Hensell sandstone and Cow Creek limestone, with data points symbolized by water quality (<500, 500-1,000, 1,000-3,000, and >3,000 milligrams per liter total dissolved solids). Number of samples is 150.**

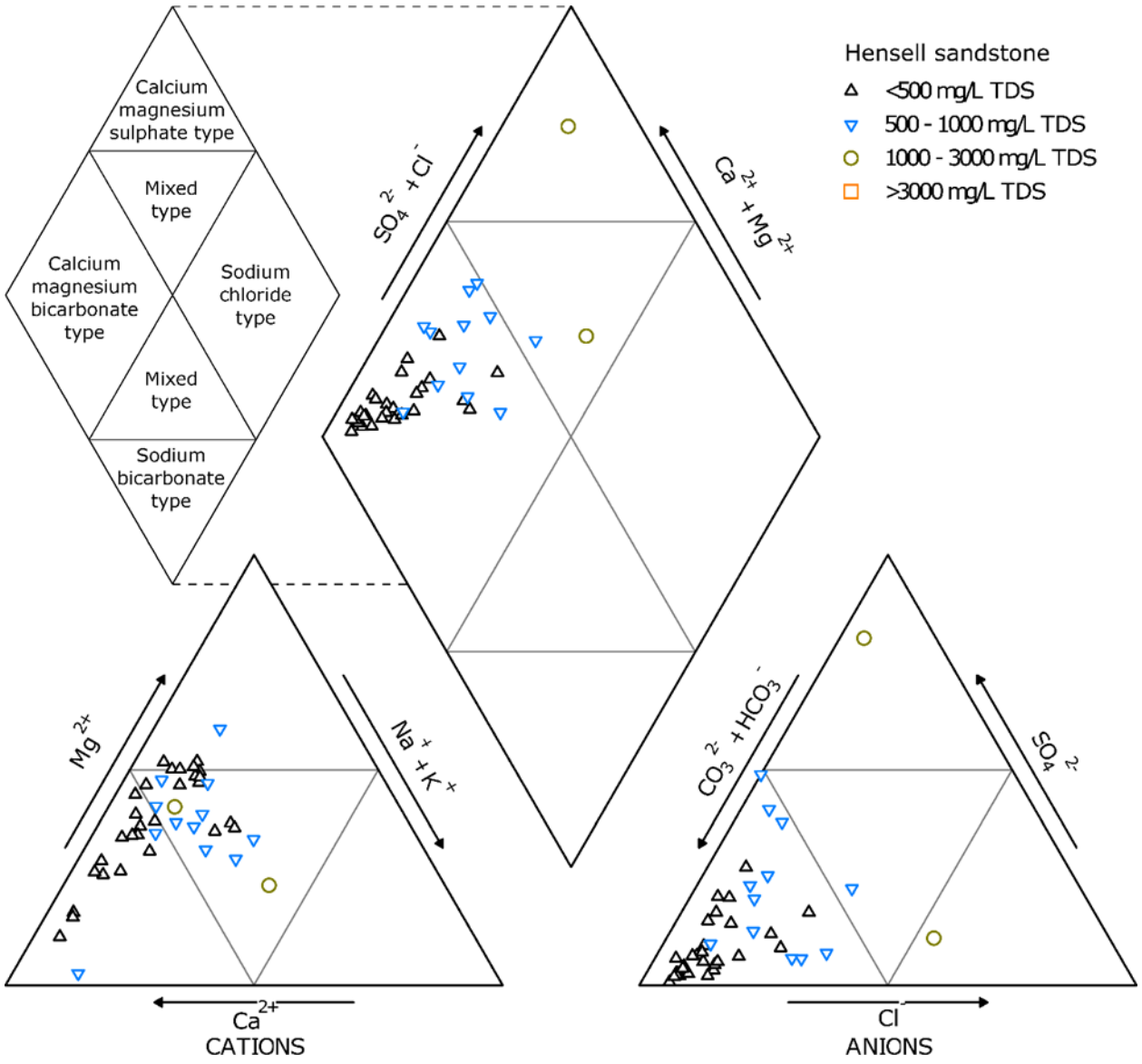

Figure 10-12 Piper plots of the Hensell sandstone, with data points symbolized by water quality (<500, 500-1,000, 1,000-3,000, and >3,000 milligrams per liter total dissolved solids). Number of samples is 43.

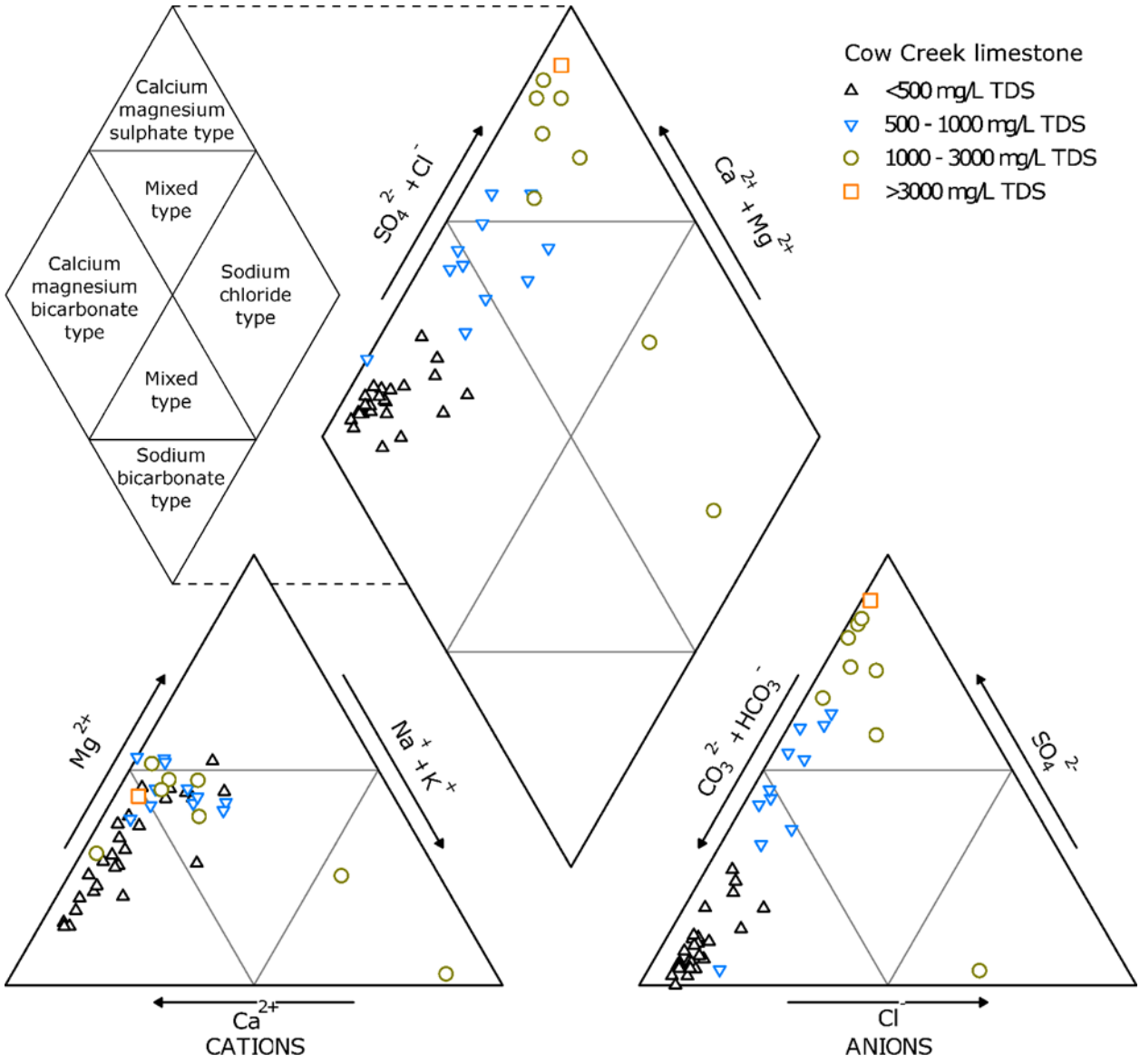

Figure 10-13 **Piper plots of the Cow Creek limestone, with data points symbolized by water quality (<500, 500-1,000, 1,000-3,000, and >3,000 milligrams per liter total dissolved solids). Number of samples is 46.**

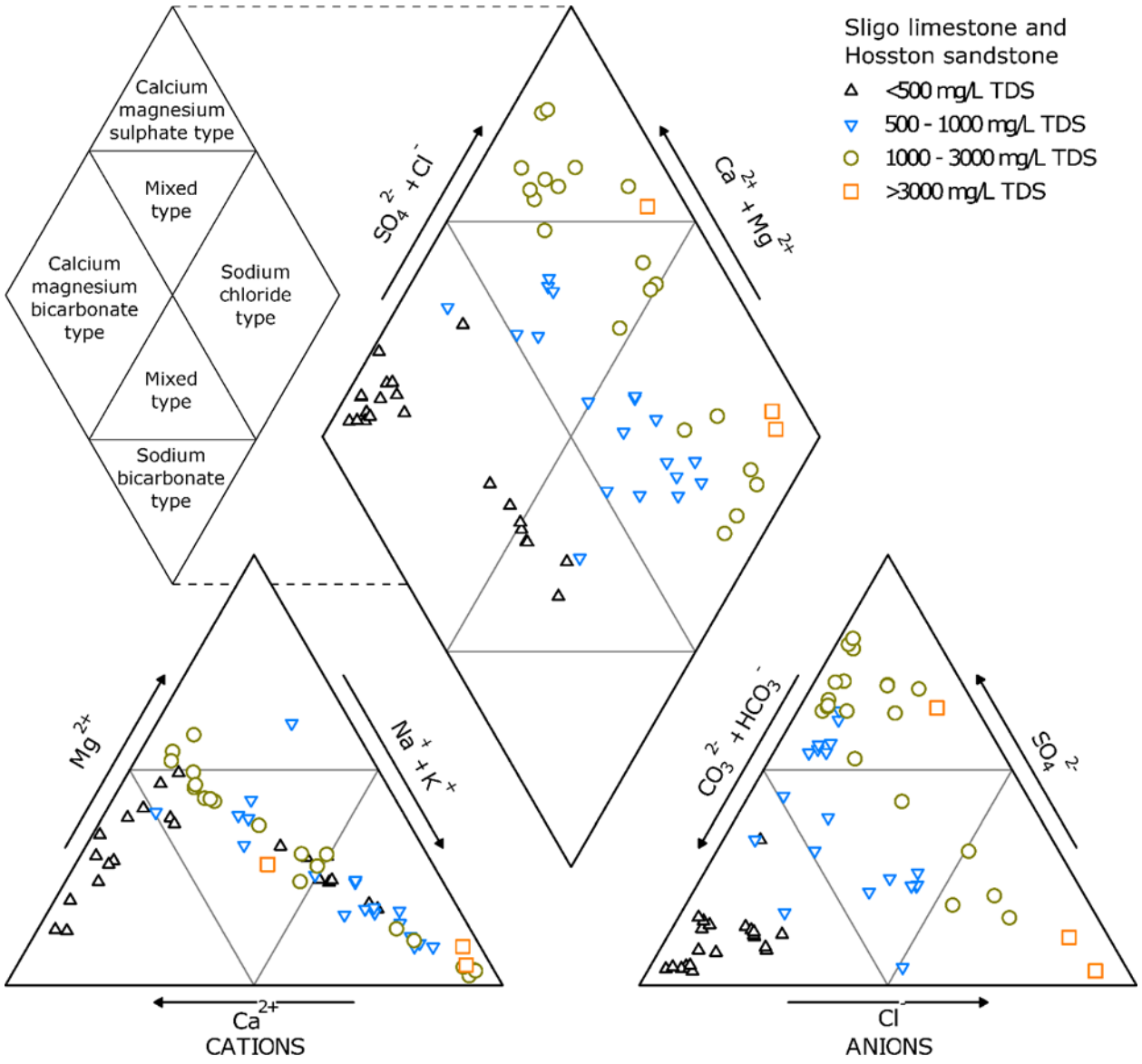

Figure 10-14 **Piper plots of the Sligo limestone and Hosston sandstone, with data points symbolized by water quality (<500, 500-1,000, 1,000-3,000, and >3,000 milligrams per liter total dissolved solids). Number of samples is 64.**

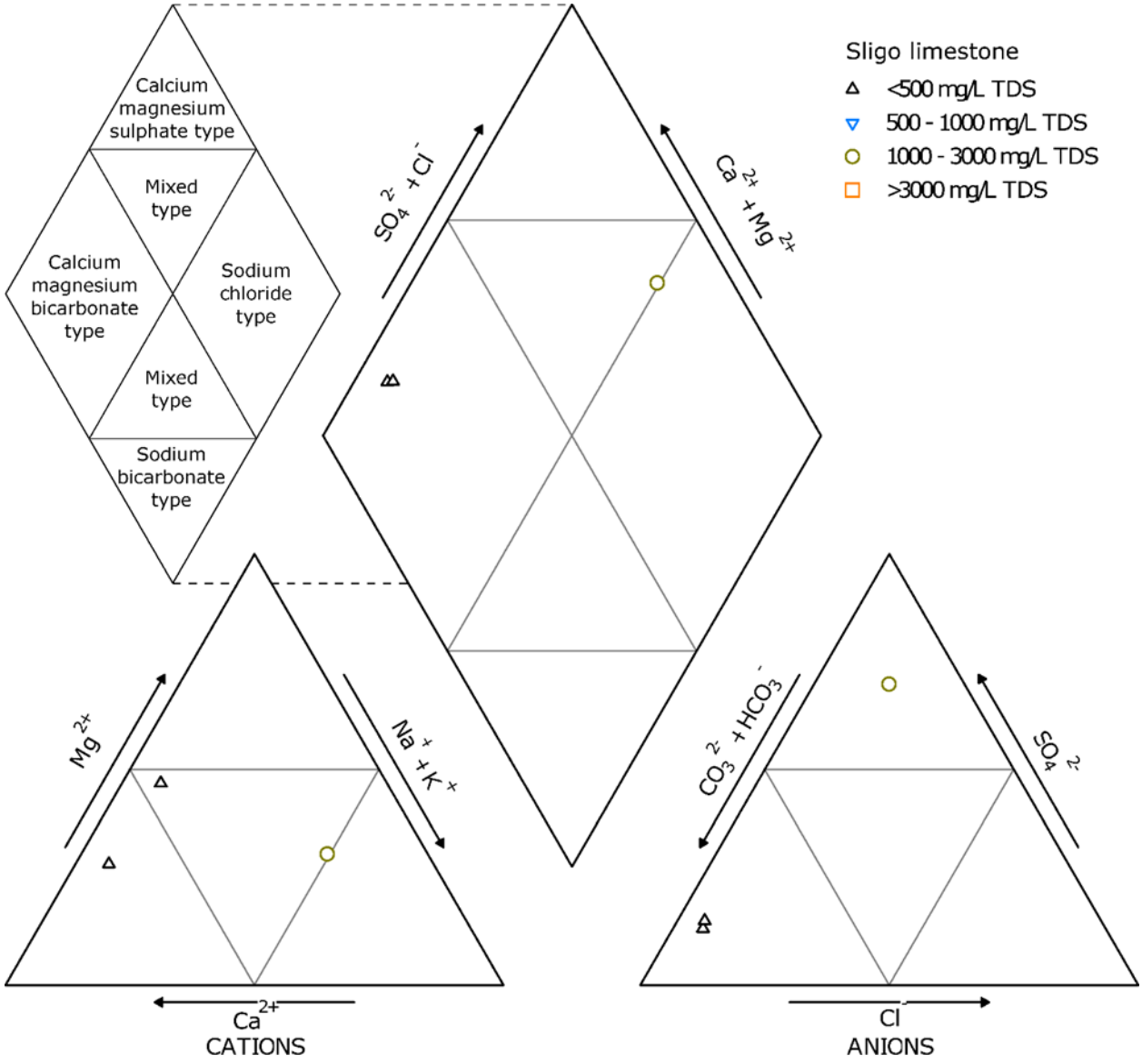

Figure 10-15 **Piper plots of the Sligo limestone, with data points symbolized by water quality (<500, 500-1,000, 1,000-3,000, and >3,000 milligrams per liter total dissolved solids). Number of samples is three.**

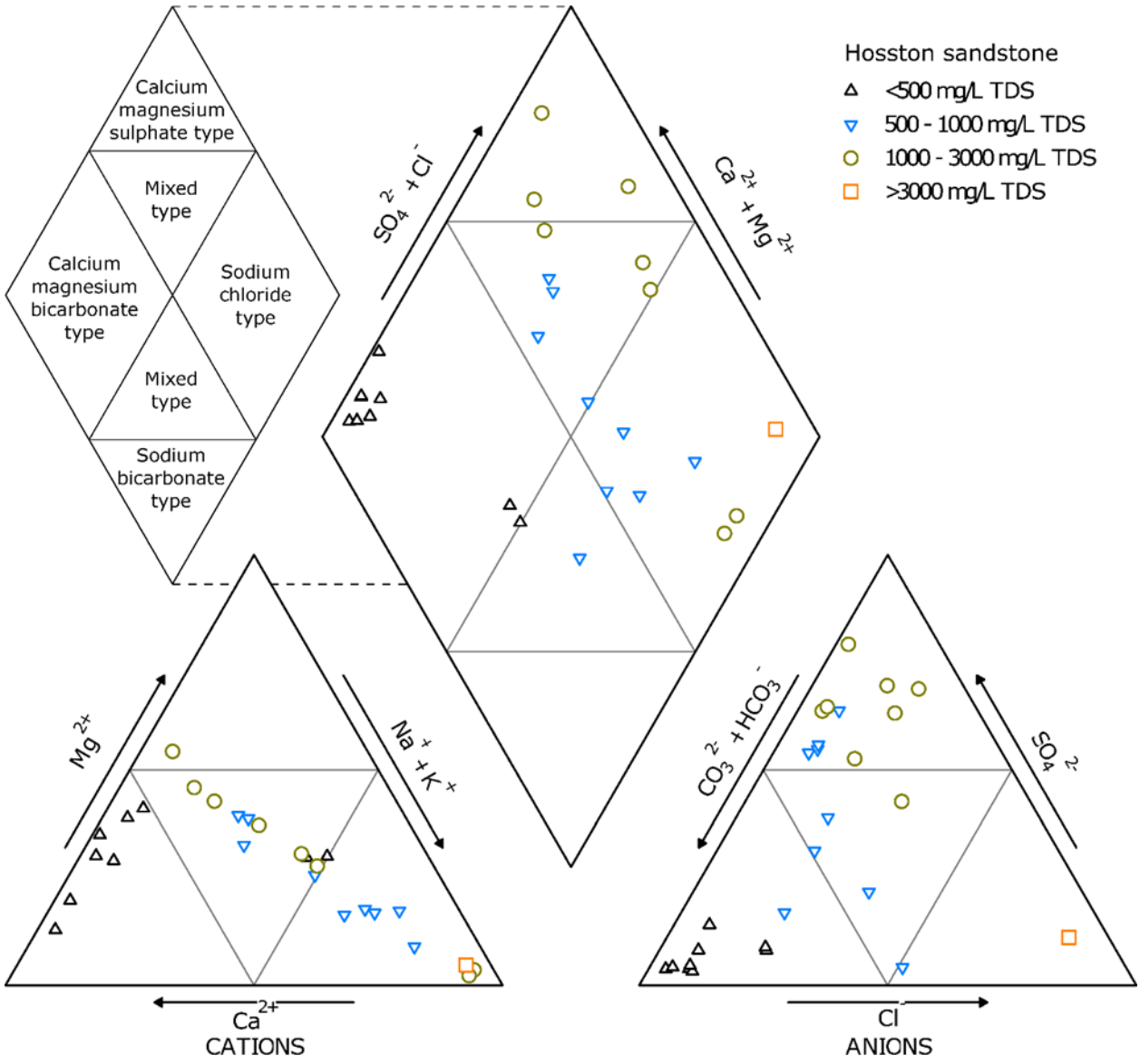

Figure 10-16 **Piper plots of the Hosston sandstone, with data points symbolized by water quality (<500, 500-1,000, 1,000-3,000, and >3,000 milligrams per liter total dissolved solids). Number of samples is 27.**

10.2.4 Spatial trends of major constituents

We graphed milligrams per liter total dissolved solids versus well depth (Figure 10-17) and mapped the concentration of the eight major ions (Ca^{2+}, Mg^{2+}, Na^{+} plus K^{+}, Cl^{-}, SO_4^{2-}, CO_3^{2-}, and HCO_3^{-}) (Figure 10-18 to Figure 10-21). Based upon these graphs and maps, sample data shows little correlation with well depth or distance from outcrop to the concentration of total dissolved solids. Figure 10-17 indicates that for all water bearing units, fresh water (<1,000 milligrams per liter total dissolved solids) occurs at depths where slightly and moderately saline water also occurs. Figure 10-18 to Figure 10-21 demonstrate that there is significant variability in the concentration of total dissolved solids with no apparent downdip trend (north to south and northwest to southeast) of increasing concentration. However, we do observe that the three deepest samples in the Upper Glen Rose limestone and Lower Glen Rose limestone do have the highest concentrations of total dissolved solids. We also observe local clusters of different water-chemistry types in all hydrostratigraphic units.

Figure 10-18 shows that salinity in the Upper Glen Rose limestone is highly variable with no apparent trend, except that the two highest salinity wells are furthest downdip to the east. A cluster of freshwater samples within the Balcones Fault Zone in northern Bexar and southeast Comal counties may be due to increased permeability of the Upper Glen Rose limestone within the fault zone due to relay ramp faulting and fracturing, and thus increased flushing of groundwater by surface water recharge. Updip of the Balcones Fault Zone, salinity is highly variable from fresh to moderately saline. The difference between freshwater wells and slightly saline to moderately saline water wells may be how they are completed, with freshwater wells completed in specific intervals, whereas the slightly saline to moderately saline wells may be completed (or open hole) through gypsum or anhydrite layers from which sulfate is readily leached.

Figure 10-19 shows that fresh water in the Lower Glen Rose limestone is much more prevalent than in the Upper Glen Rose limestone, though locally there are clusters of slightly saline water nearby the freshwater zones. The highest salinity well is furthest downdip in Bexar county.

Figure 10-20 shows that water quality in the Hensell sandstone and Cow Creek limestone is mostly fresh, with a notable exception of an approximately east-west axis of slightly saline to moderately saline water that bisects Blanco County and extends into northern Hays and western Travis counties. This axis of slightly saline to moderately saline water may indicate significant layers of gypsum or anhydrite from past depositional patterns.

Figure 10-21 shows salinity generally increases from southwest to northeast in the Sligo limestone and Hosston sandstone. Clusters of water chemistries for the Sligo limestone and Hosston sandstone hydrostratigraphic units include sodium and calcium-magnesium-bicarbonate water in the southwest, relatively high sodium chloride ratios in the central study area, calcium-magnesium-sulfate in the northeast, and three samples dominated by sodium chloride just northeast of the study area.

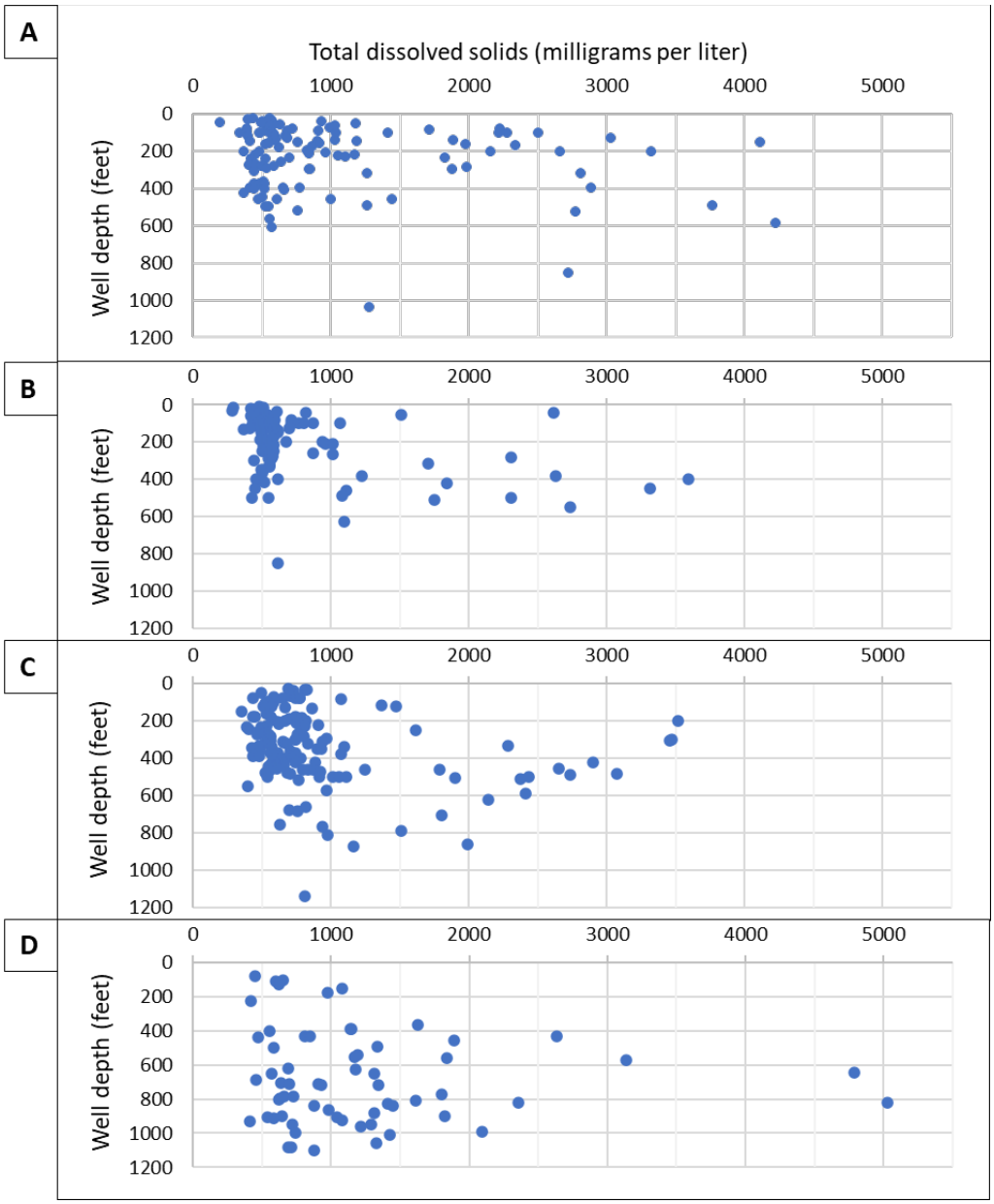

Figure 10-17 Sample depth versus total dissolved solids. A) Upper Glen Rose limestone (118 samples), B) Lower Glen Rose limestone (91 samples), C) Hensell sandstone and Cow Creek limestone (144 samples), and D) Sligo limestone and Hosston sandstone (63 samples).

From the general lack of correlation between total dissolved solids concentration with well depth, we interpret the water quality for all hydrostratigraphic units is predominantly controlled by lithology updip of the Balcones Fault Zone where most of the water wells are completed. This conclusion is supported by Wong and others (2014) in their study of ion concentrations and strontium isotopes of the Trinity formations. It is important to note that our calculations of total dissolved solids from geophysical well logs show that salinity does increase significantly downdip of the Balcones Fault Zone as expected where the residence time of groundwater is likely to have a greater influence on salinity.

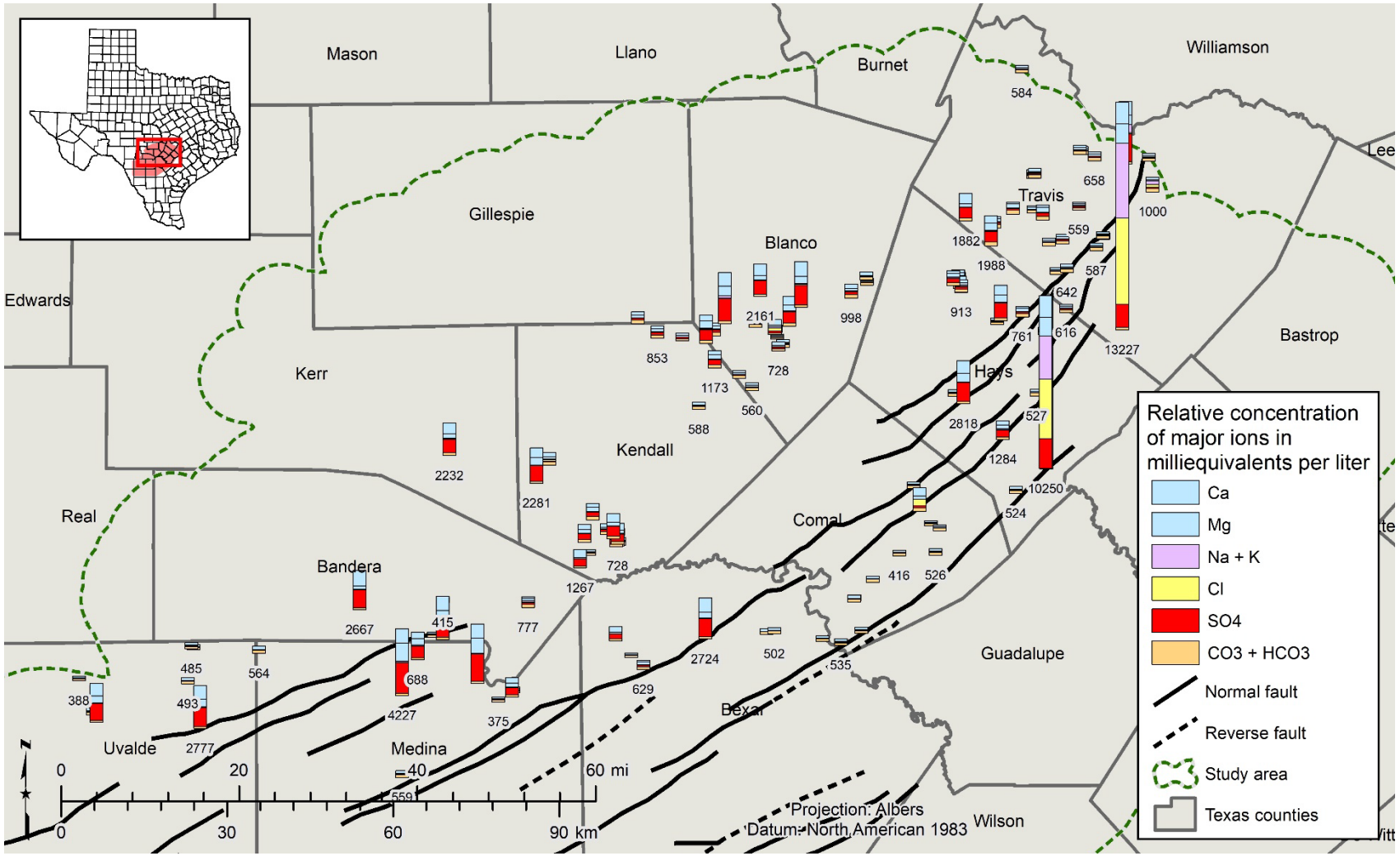

Figure 10-18 **Map of water quality samples for the Upper Glen Rose limestone showing the relative proportion of the major ions in milliequivalents per liter as a stacked bar chart for each well. Milligrams per liter total dissolved solids are labeled beneath some of the wells for reference. Number of well locations is 128. (Ca = calcium, Mg = magnesium, Na = sodium, K = potassium, Cl = chloride, SO4 = sulfate, CO3 = carbonate, HCO4 = bicarbonate)**

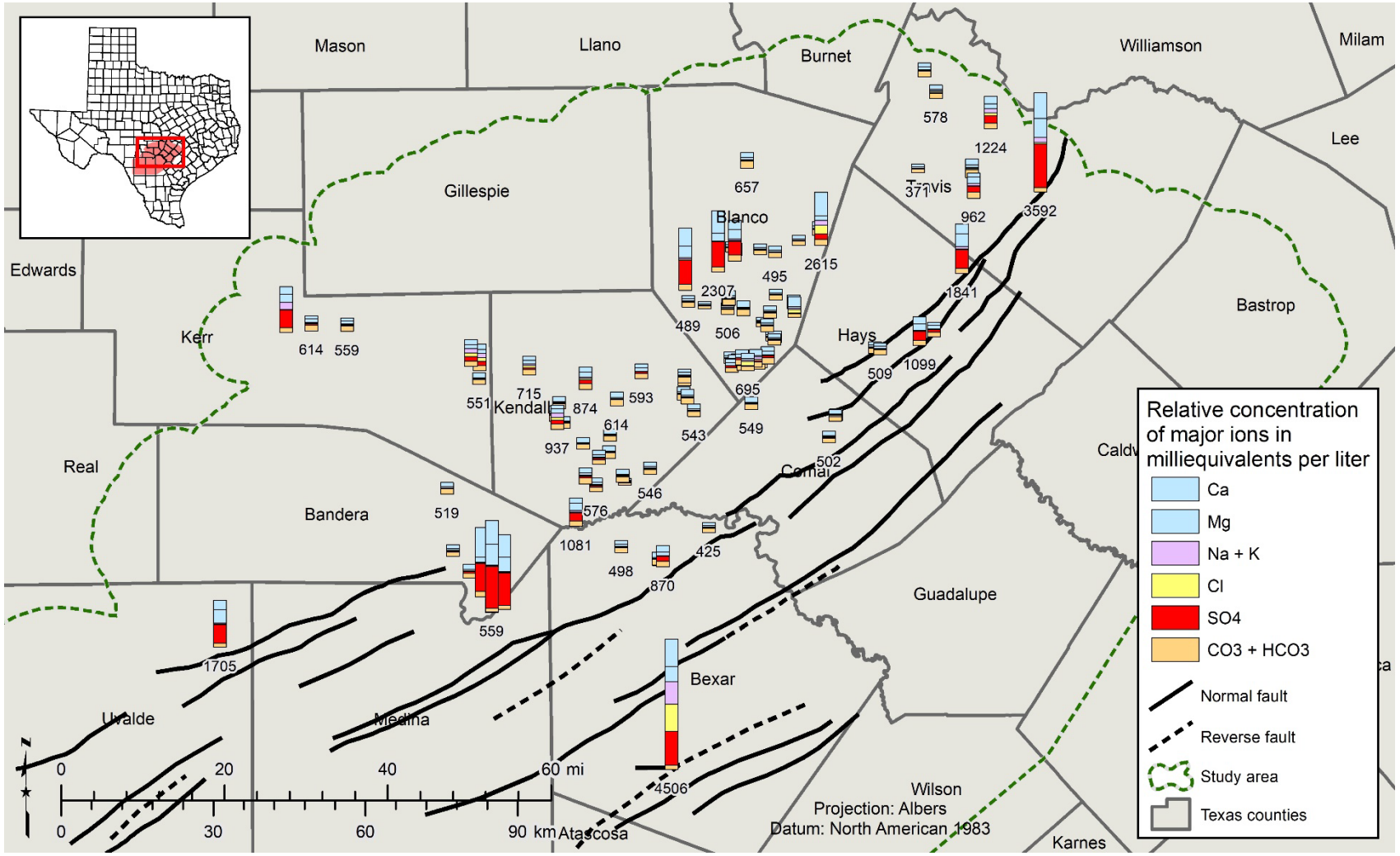

Figure 10-19 Map of water quality samples for the Lower Glen Rose limestone showing the relative proportion of the major ions in milliequivalents per liter as a stacked bar chart for each well. Milligrams per liter total dissolved solids are labeled beneath some of the wells for reference. Number of well locations is 104. (Ca = calcium, Mg = magnesium, Na = sodium, K = potassium, Cl = chloride, SO4 = sulfate, CO3 = carbonate, HCO4 = bicarbonate)

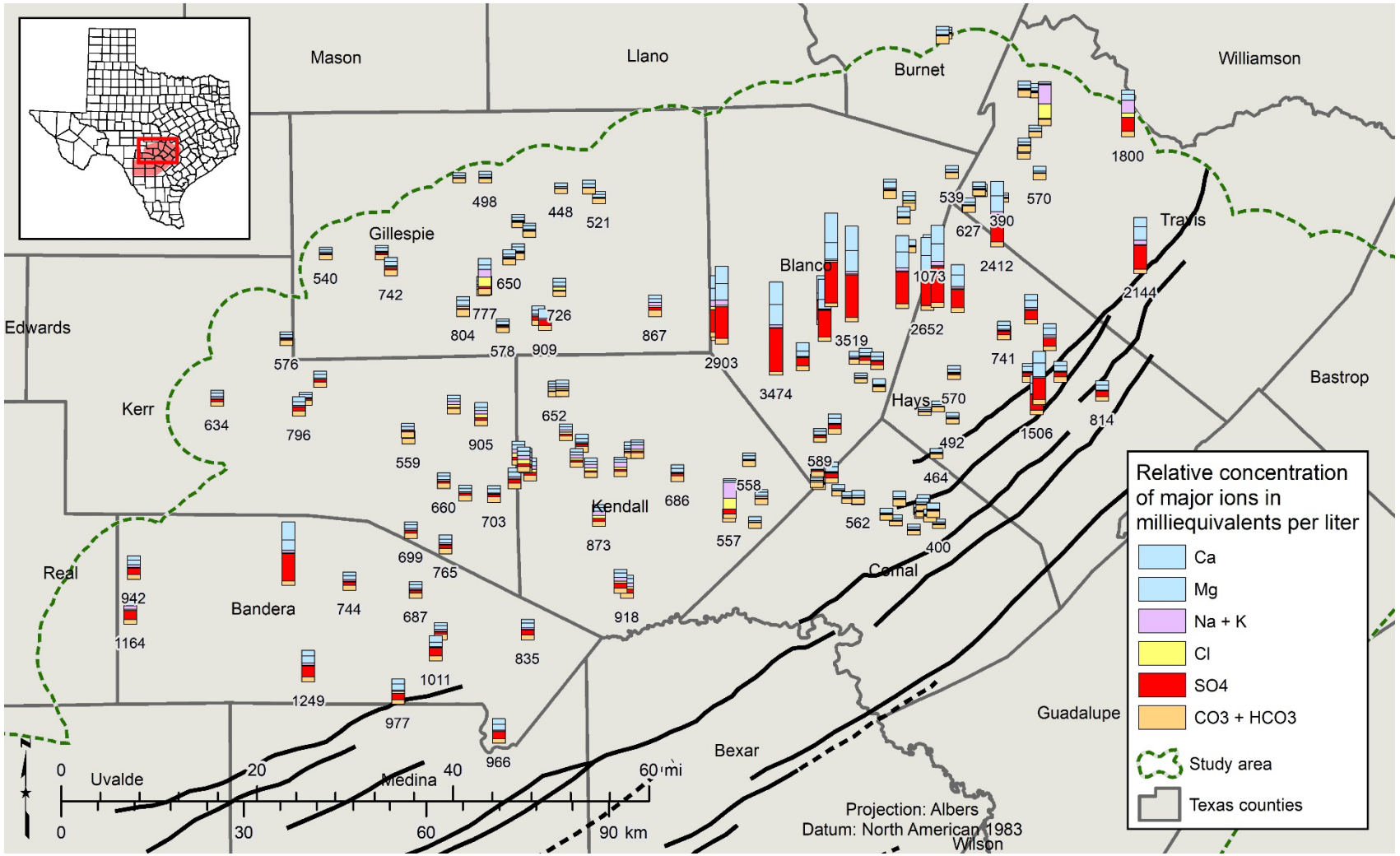

Figure 10-20 **Map of water quality samples for the Hensell sandstone and Cow Creek limestone showing the relative proportion of the major ions in milliequivalents per liter as a stacked bar chart for each well. Milligrams per liter total dissolved solids are labeled beneath some of the wells for reference. Number of well locations is 150. (Ca = calcium, Mg = magnesium, Na = sodium, K = potassium, Cl = chloride, SO4 = sulfate, CO3 = carbonate, HCO4 = bicarbonate)**

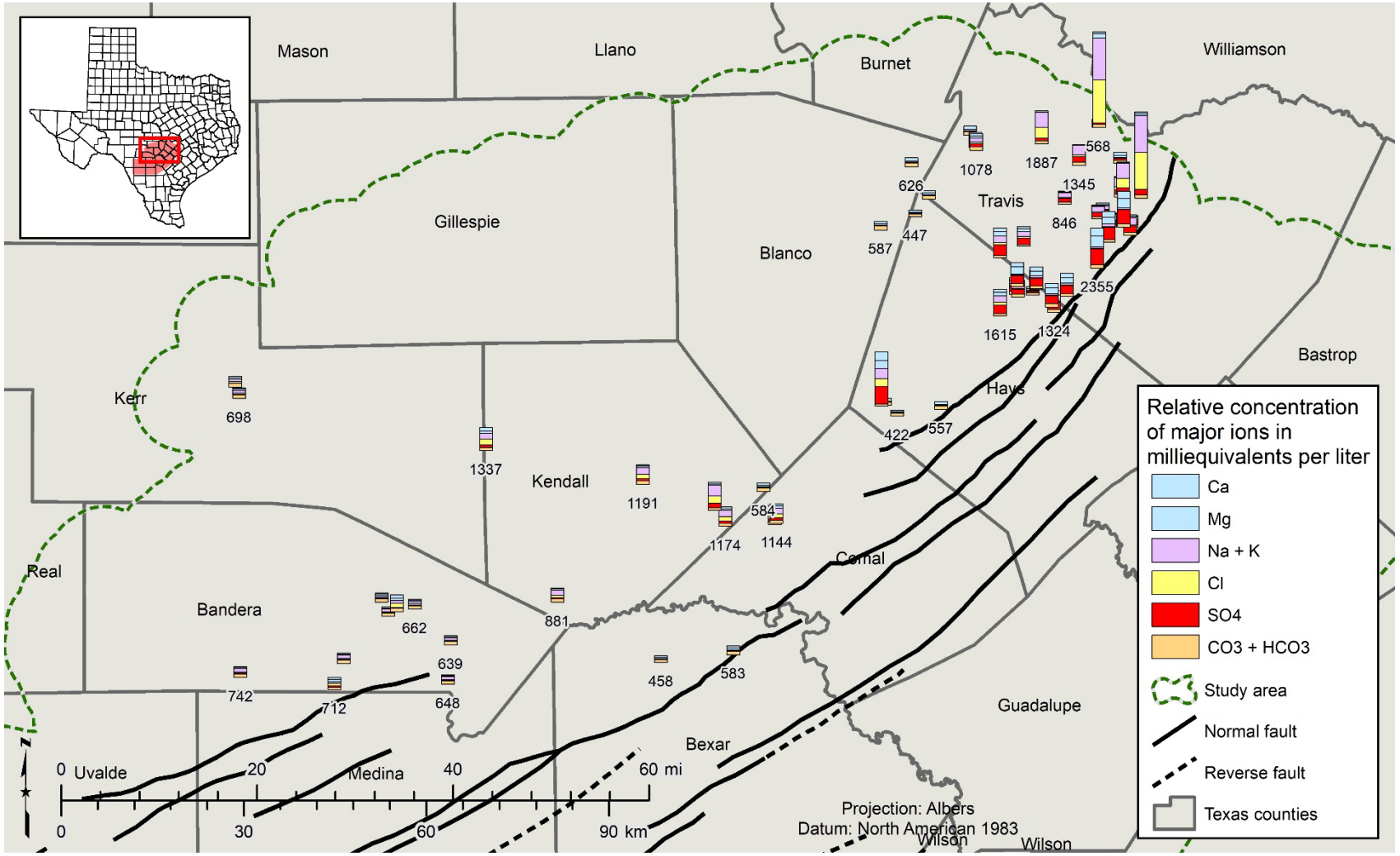

Figure 10-21 Map of water quality samples for the Sligo limestone and Hosston sandstone showing the relative proportion of the major ions in milliequivalents per liter as a stacked bar chart for each well. Milligrams per liter total dissolved solids are labeled beneath some of the wells for reference. Number of well locations is 64. (Ca = calcium, Mg = magnesium, Na = sodium, K = potassium, Cl = chloride, SO4 = sulfate, CO3 = carbonate, HCO4 = bicarbonate)

10.3 Parameters of concern for desalination

Though the concentration of total dissolved solids is the primary concern for desalination, there are also physical parameters of concern including pH, silt density, and temperature. The presence of several minor chemical constituents is also of concern because they may violate drinking water standards or lead to fouling during the desalination process even when present in relatively small amounts. The minor chemical constituents of concern include arsenic, iron, barium, and radionuclides, which are discussed in the following sections. For the number of water quality records reported below, any water quality record from a well screened within or intersecting the Trinity hydrostratigraphic units (including open hole) were included.

10.3.1 Arsenic

Arsenic is a human health concern and has a standard defined by the Texas Commission on Environmental Quality (TCEQ). For dissolved arsenic, 596 water quality analyses of the Hill Country Trinity aquifer from 320 wells are available in the study area (Figure 10-22). Two wells have water quality samples that exceed the TCEQ maximum contaminant level for arsenic of 0.010 milligrams per liter (TCEQ, 2015), with a maximum concentration of 0.0132 milligrams per liter.

10.3.2 Iron

Iron is not a human health concern but is considered a nuisance contaminant. Iron in groundwater can become oxidized and will precipitate when it reaches ground surface. To avoid fouling reverse osmosis membranes, water with elevated levels of iron must be pre-treated. For dissolved iron, 906 water quality analyses of the Hill Country Trinity aquifer from 449 wells are available in the study area (Figure 10-23). 112 wells have water quality samples that exceed the TCEQ secondary maximum contaminant level for iron of 0.3 milligrams per liter (TCEQ, 2015), with a maximum concentration of 21 milligrams per liter.

10.3.3 Barium

Barium is a human health concern and regulated by the TCEQ. For dissolved barium, 539 water quality analyses of the Hill Country Trinity aquifer from 311 wells are available in the study area. No water quality samples exceed the TCEQ secondary maximum contaminant level for barium of 2 milligrams per liter (TCEQ, 2015). The maximum concentration of dissolved barium in the Trinity aquifers in the study area is 0.3 milligrams per liter. The low levels of dissolved barium are expected as barium readily combines with sulfate (forming barium sulfate; Hem, 1985), which is abundant in the study area.

10.3.4 Radionuclides

The radionuclides uranium, radium-228 and radium-226 are human health concerns and regulated by the TCEQ. Radionuclides are unstable atoms which release gamma radiation or alpha and beta particles (also types of radiation) as the atoms undergo radioactive decay. The presence of radionuclides in groundwater is important when selecting screen

zone(s) for a well, as elevated naturally occurring radiation should be avoided. Test wells should always be logged with a gamma ray tool to identify elevated radionuclides (specifically gamma radiation) in formation materials. There are no water quality samples from wells completed in the Hill Country Trinity aquifer with measured alpha and beta radiation.

Uranium is a radionuclide which emits alpha particles and gamma radiation. For dissolved uranium, 421 water quality analyses of the Hill Country Trinity aquifer from 233 wells are available in the study area. No water quality samples exceed the TCEQ maximum contaminant level for dissolved uranium of 30 micrograms per liter (TCEQ, 2015). The maximum concentration of dissolved uranium in the Hill Country Trinity aquifer is 13.8 micrograms per liter.

Radium-228 and radium-226 are radionuclides which emit alpha and beta particles and gamma radiation. For dissolved radium-228 plus radium-226, 134 water quality analyses of the Hill Country Trinity aquifer from 127 wells are available in the study area (Figure 10-22). Six wells have water quality samples that exceed the TCEQ maximum contaminant level for radium-228 plus radium-226 of 5 picocuries per liter (TCEQ, 2015), with a maximum concentration of 19 picocuries per liter

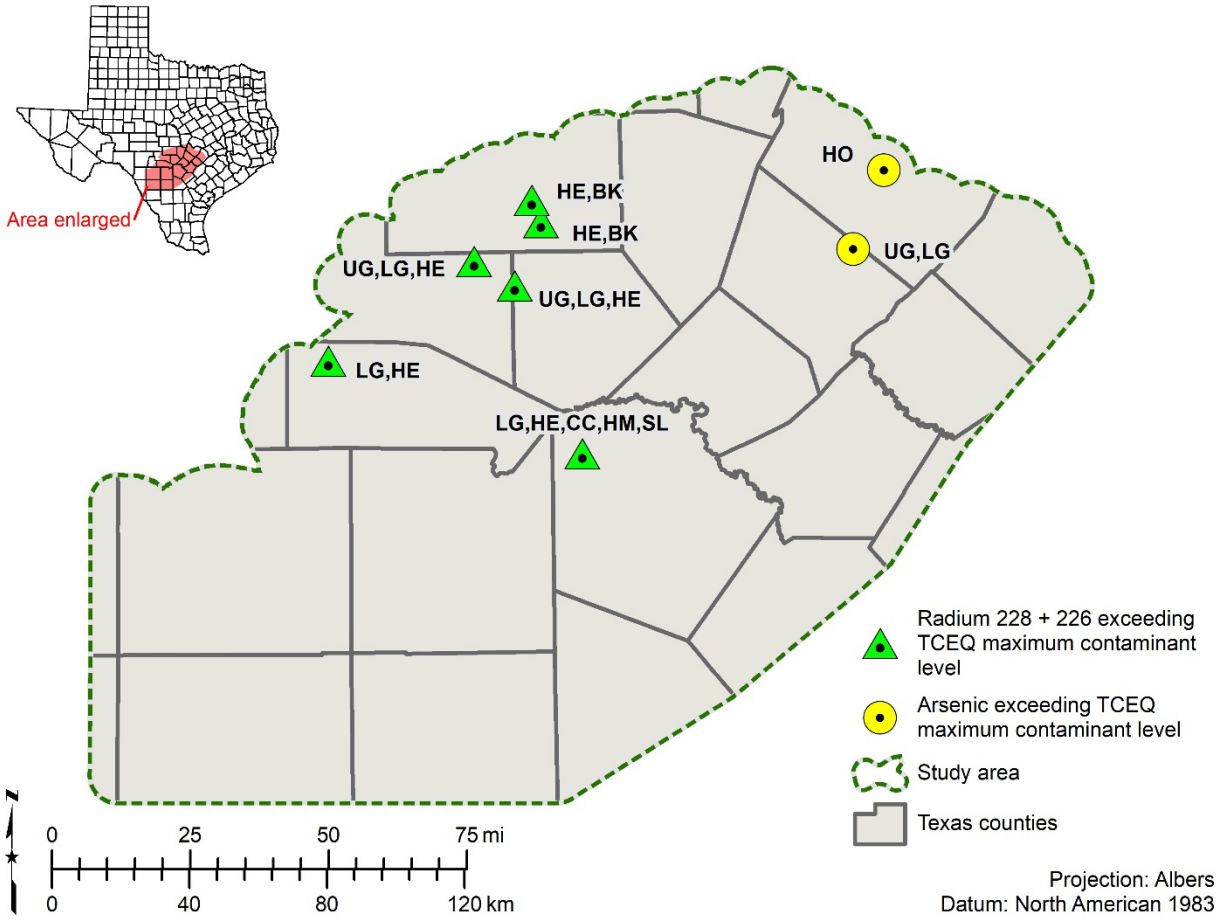

Figure 10-22 **Map of well locations with water quality samples exceeding arsenic (two wells) or radium-228 plus radium-226 (six wells) maximum contamination levels (0.010 milligrams per liter for arsenic and 5 picocuries per liter for radium-228 plus radium-226). Well locations are labeled with abbreviations of the formations they are completed in. UG = Upper Glen Rose limestone, LG = Lower Glen Rose limestone, HE = Hensell sandstone, CC = Cow Creek limestone, HM = Hammett shale, SL = Sligo limestone, HO = Hosston sandstone, and BK = formations below the Cretaceous Trinity Group. (TCEQ = Texas Commission on Environmental Quality)**

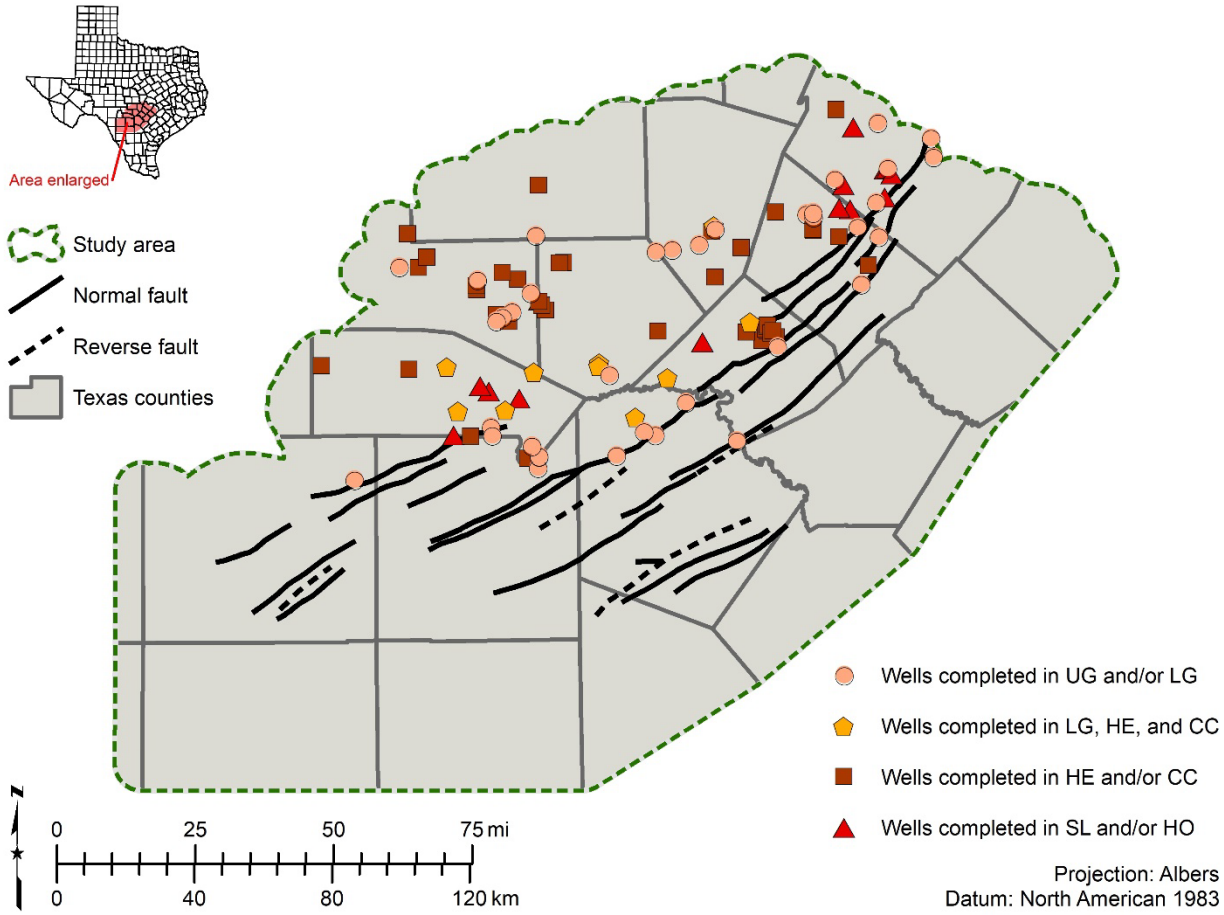

Figure 10-23 **Map of well locations with water quality samples exceeding iron secondary maximum contamination levels (0.3 milligrams per liter) symbolized by groups of Hill Country Trinity hydrostratigraphic units sampled. Number of wells in the map with water quality analyses exceeding iron maximum contamination levels is 99. (UG = Upper Glen Rose limestone, LG = Lower Glen Rose limestone, HE = Hensell sandstone, CC = Cow Creek limestone, SL = Sligo limestone, HO = Hosston sandstone)**

10.4 Relationship of total dissolved solids to specific conductance

In Section 11 of this report, we describe our methodology for calculating concentrations of total dissolved solids from geophysical well logs in portions of the Hill Country Trinity aquifer where measured water quality samples are not available. Because the resistivity of the formation water is a function of the dissolved solids concentration, we can calculate the dissolved solids concentration by using the resistivity measurements from geophysical well logs. Measured water quality often includes a measurement of specific conductance in units of micromhos per centimeter, which is the inverse of resistivity in ohm-meters multiplied by 10,000. In this section, we present relationships of groundwater total dissolved solid concentrations to measured and calculated specific conductance values of the Hill Country Trinity hydrostratigraphic units grouped as, 1) Upper Glen Rose limestone and Lower Glen Rose limestone, 2) Hensell sandstone and

Cow Creek limestone, and 3) Sligo limestone and Hosston sandstone. These groups are based on the similarities in their relationship of total dissolved solid concentrations to specific conductance which results from similarities in lithology.

10.4.1 Erroneous specific conductance measurements

We plotted total dissolved solids versus specific conductance for all samples recorded in the TWDB Groundwater Database, which yielded two trends, an "upper trend" and a "lower trend" labeled in Figure 10-24. We determined the lower trend is composed predominantly of samples analyzed by the Texas Department of Health, as illustrated in Figure 10-25 where we separated the data based on whether a sample was analyzed by the Texas Department of Health versus any other laboratory. In the study area, the Texas Department of Health was the primary laboratory used for water analyses between 1969 and 1988 (Figure 10-26).

Collier (1993) notes that conductance measurements by the Texas Department of Health analyses between 1960 and 1988 are "diluted conductance" measurements, which are not equivalent to specific conductance and cannot be used to determine relationships of total dissolved solids versus specific conductance. Specific conductance is ideally measured in the field using a conductivity meter of the natural water sample. Diluted conductance however is a laboratory procedure where the water sample is diluted to a specific conductance of approximately 100 micromhos per centimeter, and the diluted conductance is calculated from the specific conductance, resistivity, and dilution ratio of the sample (Rossum, 1949). This procedure in effect projects the conductance from very low total dissolved solids concentrations (diluted to approximately 50 milligrams per liter) to higher values of total dissolved solids by multiplying by the dilution ratio. The consequence of this procedure is it negates the effects of ion pairing that occurs in true concentrations of dissolved solids in the natural water. Ion pairing has the effect of reducing the conductance of the water, thus the diluted conductance procedure yields a conductance of the water that is too high.

The conductance of water is a result of dissolved charged ions. When the ions form pairs or complexes, there is no intervening H_20 between the paired ions (Hem, 1985). Thus, the charges of the paired ions are neutralized and do not contribute to the conductance of the water. Ion pairing is prevalent in calcium-magnesium-bicarbonate and calcium-magnesium-sulfate water (Miller and others, 1988), which are the dominant water types in the study area. In Figure 10-24 and Figure 10-25, the upper trend represents the effects of ion pairing and has a lower conductance value for a given concentration of totals dissolved solids than the lower trend in which ion pairing has been negated by the diluted conductance procedure. Because the lower trend derived from diluted conductance values is not representative of the conductance of the formation water, we did not use conductance values from the Texas Department of Health for developing relationships of total dissolved solids versus specific conductance. However, for the analyses in Section 10.2, we did use the concentrations of major and minor ions determined by the Texas Department of Health as those values do appear accurate.

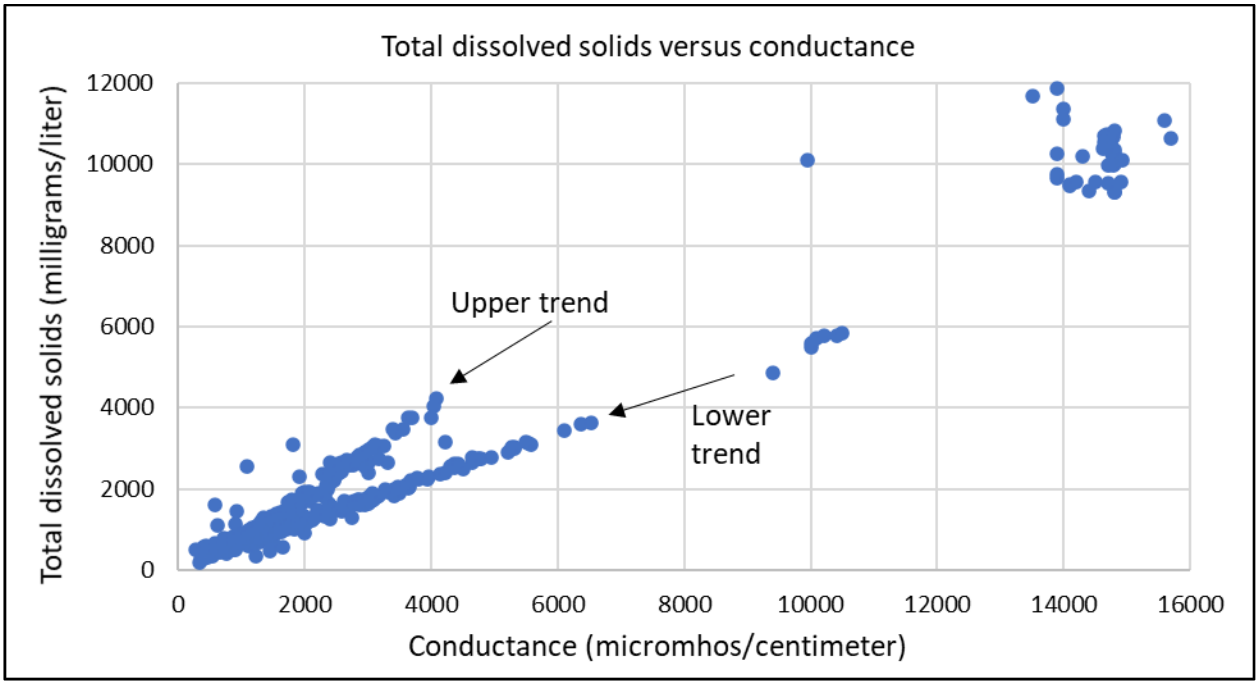

Figure 10-24 **Graph of total dissolved solids versus specific conductance for all water quality analyses of the Hill Country Trinity aquifer. For a given concentration of total dissolved solids, the "upper trend" has a lower conductance value that the "lower trend." Number of samples is 1300.**

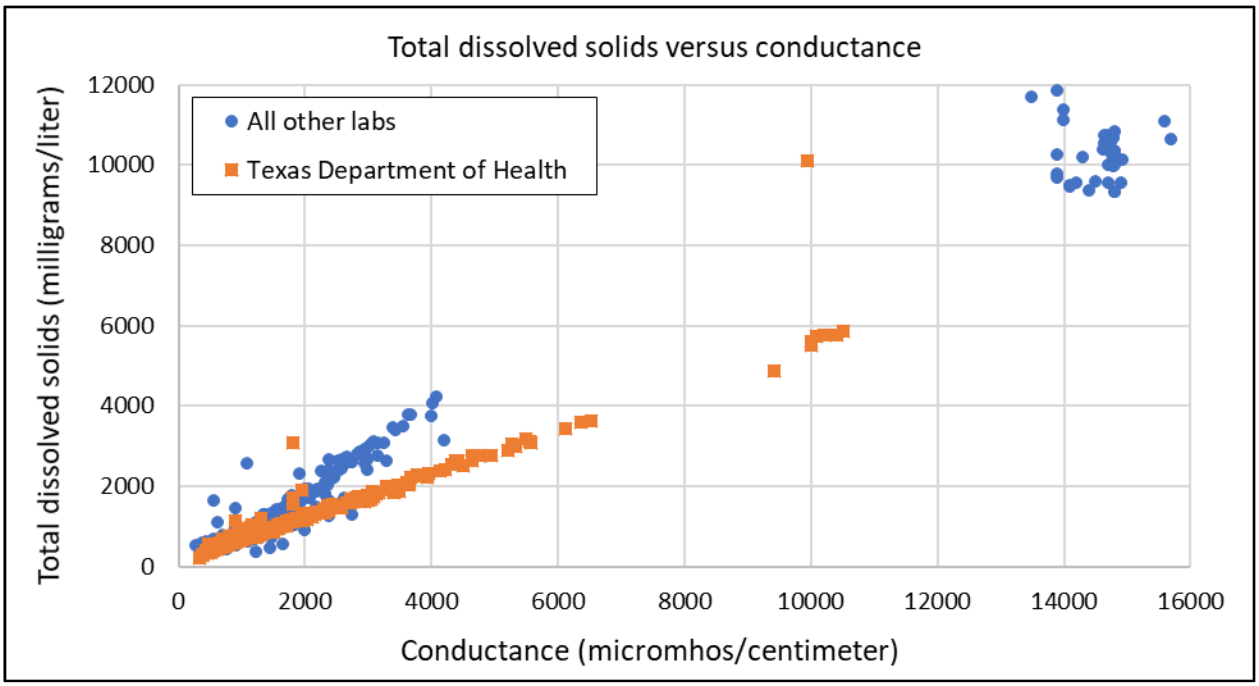

Figure 10-25 **Graph of total dissolved solids versus specific conductance for all water quality analyses of the Hill Country Trinity aquifer, symbolized by whether the analysis was conducted by the Texas Department of Health (orange squares, 649 samples) or another lab (blue circles, 651 samples).**

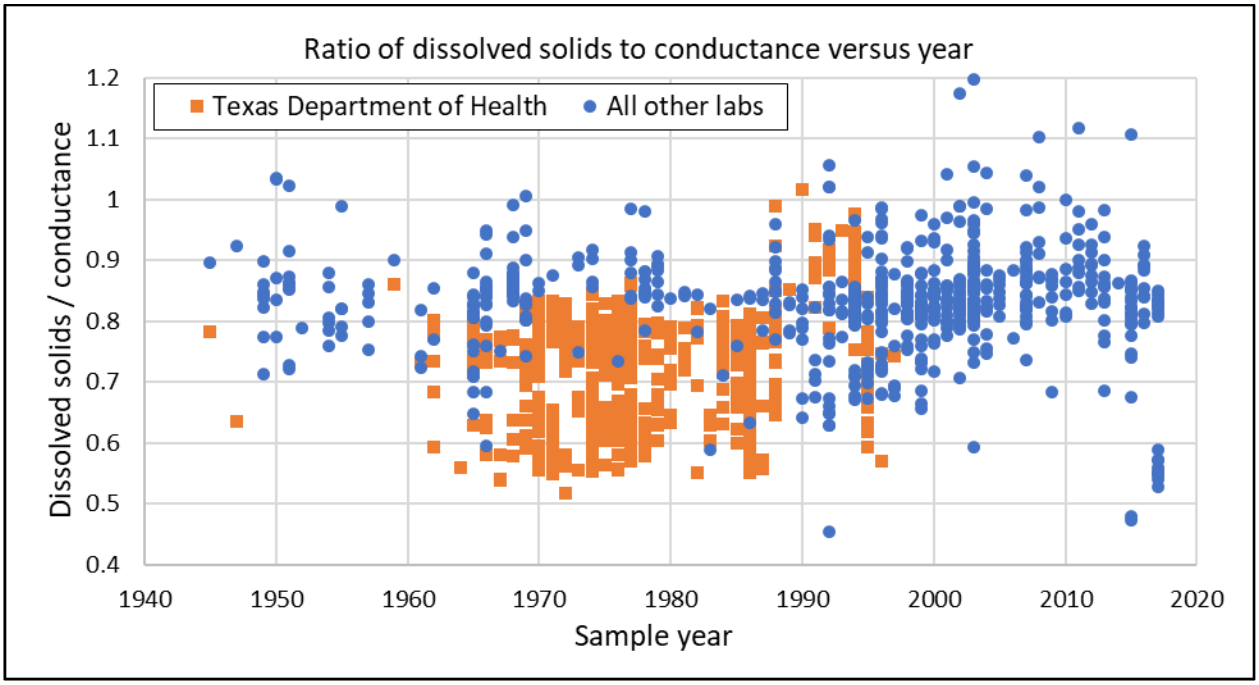

Figure 10-26 **Graph of the ratio of dissolved solids to conductance versus the sample year of all water quality samples for the Hill Country Trinity aquifer. The low ratio of dissolved solids to conductance between 1969 and 1988 correspond to measurements of diluted conductance by the Texas Department of Health, which analyzed most of the samples between those years.**

10.4.2 Final total dissolved solids versus specific conductance relationships

In the study area, samples of measured water quality with measured specific conductance values generally have dissolved solid concentrations less than 4,000 milligrams per liter, except for a few wells. To develop relationships of concentration of total dissolved solids versus specific conductance up to approximately 35,000 milligrams per liter, we supplemented measured specific conductance values in two ways:

1) Specific conductance values calculated from the concentrations of the major ions from measured water quality samples.
2) Specific conductance values calculated from modeled ion concentrations extrapolated between and beyond known concentrations of measured water quality samples.

We calculated specific conductance with the United States Geological Survey software PHREEQC version 3.

Upper Glen Rose limestone and Lower Glen Rose limestone

Figure 10-27 and Figure 10-28 show the relationship of total dissolved solids to specific conductance for the Upper Glen Rose limestone and Lower Glen Rose limestone. Figure 10-27 covers the range of available water quality measurements, while Figure 10-28 shows the relationship extrapolated to much higher TDS and conductance values. Up to about 4,000 micromhos per centimeter, the relationship is best approximated by a polynomial. We extrapolated modeled ion concentrations between the last sample of the

polynomial at about 4,000 micromhos per centimeter to the center of the cluster of values at about 14,500 micromhos per centimeter and calculated specific conductance for the hypothetical concentrations. We further extrapolated ion concentrations beyond about 14,500 micromhos per centimeter to about 50,000 micromhos per cm, or about 35,000 milligrams per liter total dissolved solids. For the modeled ion concentrations (Appendix 19.2), the ion concentrations slowly decrease in sulfate and rapidly increase in sodium chloride. In Figure 10-27, the green diamonds at about 6,500 micromhos per centimeter are measured water quality samples for which we calculated specific conductance from their ion concentrations. These three points fall along the trend defined by the modeled concentrations, giving us confidence this trend from the end of the polynomial to the cluster of high total dissolved solid values is a good representation of the evolution of the actual ion concentrations. In Figure 10-28, we identified the one measured water quality sample at about 20,000 micromhos per centimeter after we had already finalized these relationships. This sample also falls along the projected trend, giving us confidence the hypothetical concentrations we developed beyond approximately 14,500 micromhos per centimeter are also valid.

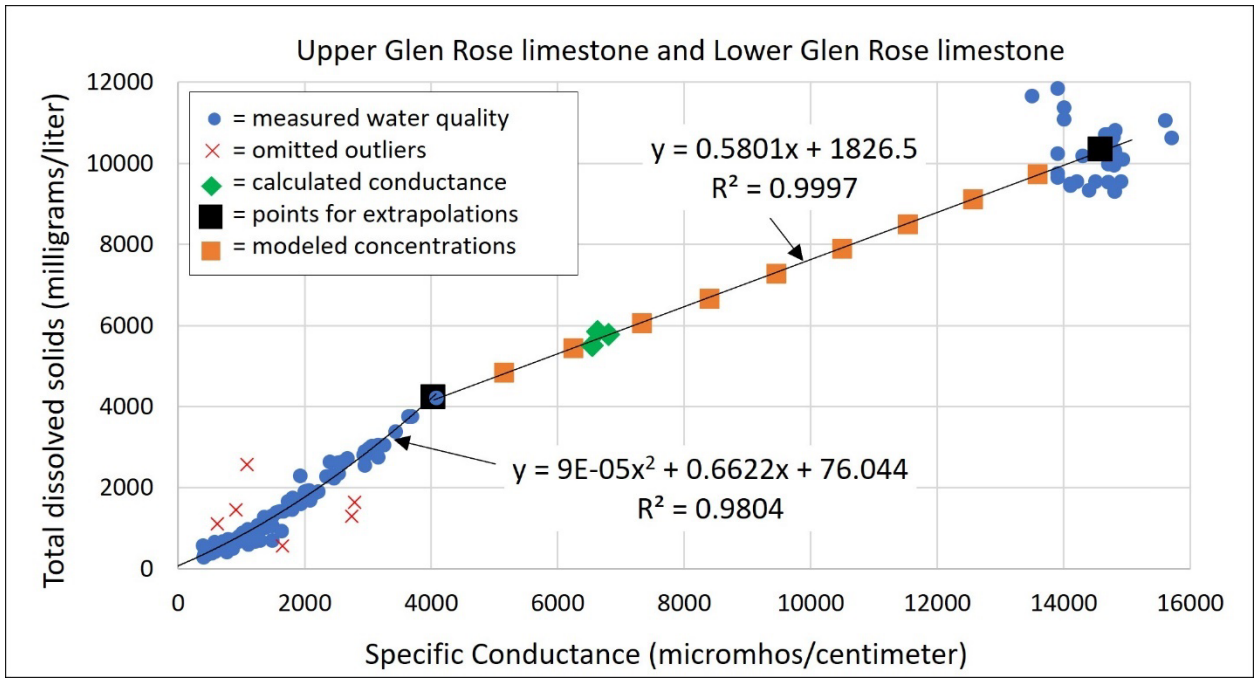

Figure 10-27 Plot of total dissolved solids versus specific conductance for the Upper Glen Rose limestone and Lower Glen Rose limestone (295 measured water samples).

A note about the cluster of points in Figure 10-27 and Figure 10-28 centered around 14,500 micromhos per centimeter: our stratigraphic surface analysis places the screen of these two wells in the very uppermost Upper Glen Rose limestone (only about 50 feet below the base of the Edwards Group). These two wells are supposedly monitoring wells for the Edwards Group, and thus we may have miss attributed them to the Upper Glen Rose limestone during our Aquifer Determination process. However, in Figure 10-28 the sample at about 20,000 micromhos per centimeter is from a multiple port well, and this sample was specifically collected from in the Upper Glen Rose limestone, giving us

confidence that even if the cluster of points is of the Edwards Group that their water chemistries are similar to that of the Upper Glen Rose limestone at these high concentrations of total dissolved solids.

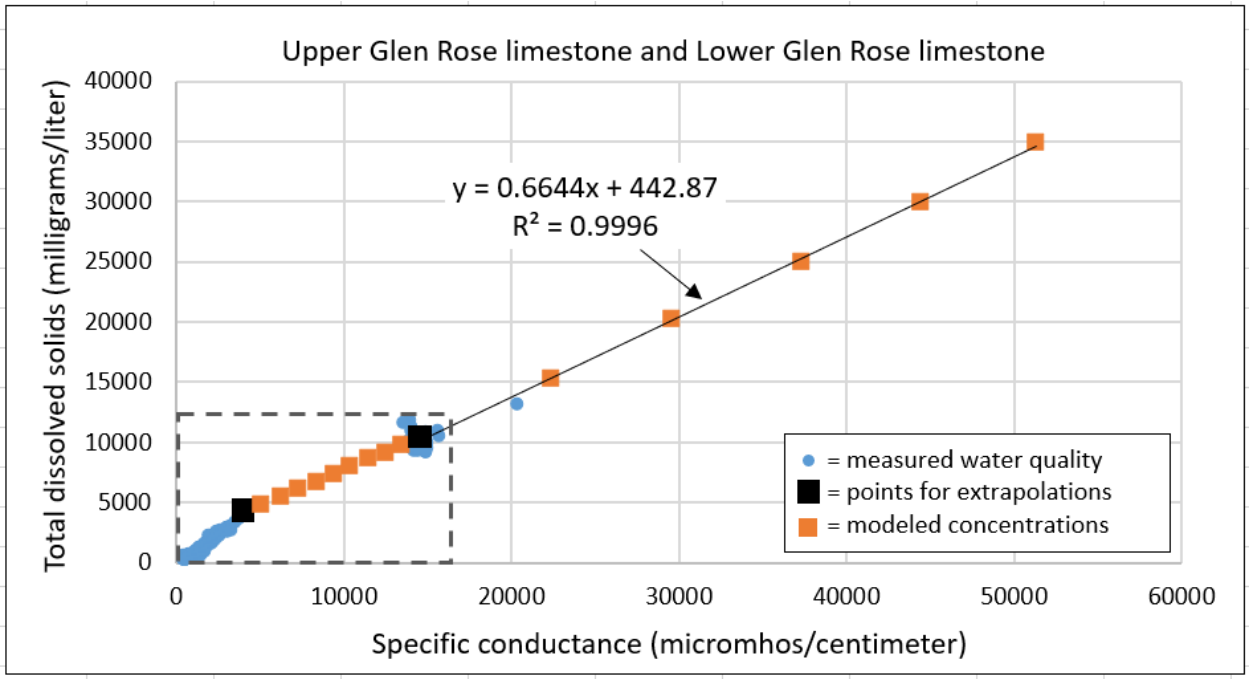

Figure 10-28 Plot of total dissolved solids versus specific conductance for the Upper Glen Rose limestone and Lower Glen Rose limestone (296 measured water samples). Dashed rectangle is the extent of Figure 10-27.

Hensell sandstone and Cow Creek limestone

Figure 10-29 shows the relationship of total dissolved solids to specific conductance for the Hensell sandstone and Cow Creek limestone. Up to about 4,000 micromhos per centimeter, the relationship is best approximated by a polynomial and is nearly identical to the polynomial relationship of the Upper Glen Rose limestone and Lower Glen Rose limestone. Because there were no other samples beyond 4,000 micromhos per centimeter, we were unable to derive an extrapolated line for higher concentrations. However, because the polynomial relationship is nearly identical to that of the Upper Glen Rose limestone and Lower Glen Rose limestone, we assumed the evolution in the water chemistry of the Hensell sandstone and Cow Creek limestone at higher total dissolved solid values are similar to the Upper Glen Rose limestone and Lower Glen Rose limestone. Therefore, the relationships we used for the Hensell sandstone and Cow Creek limestone beyond 4,000 micromhos per centimeter are identical to the relationships we developed for the Upper Glen Rose limestone and Lower Glen Rose limestone.

Sligo limestone and Hosston sandstone

Figure 10-30 and Figure 10-31 show the relationship of total dissolved solids to specific conductance for the Sligo limestone and Hosston sandstone. Figure 10-30 covers the range of available water quality measurements and calculated conductance values, while

Figure 10-31 shows the relationship extrapolated to much higher TDS and conductance values. The relationship between total dissolved solids and specific conductance can be best approximated by three linear trends. We extrapolated modeled ion concentrations between measured water quality samples at 4,500 and 8,900 micromhos per centimeter (black squares), and further projected ion concentrations to 50,000 micromhos per centimeter for which we calculated specific conductance. Our extrapolations of ion concentrations assume the groundwater is dominated by sodium chloride as detailed in Appendix 9.2. In Figure 10-30, the blue diamonds at 8,000 micromhos per centimeter are two measured water quality samples for which specific conductance was calculated, which fall along the extrapolated trend, giving us confidence that our extrapolated relationships are reasonable.

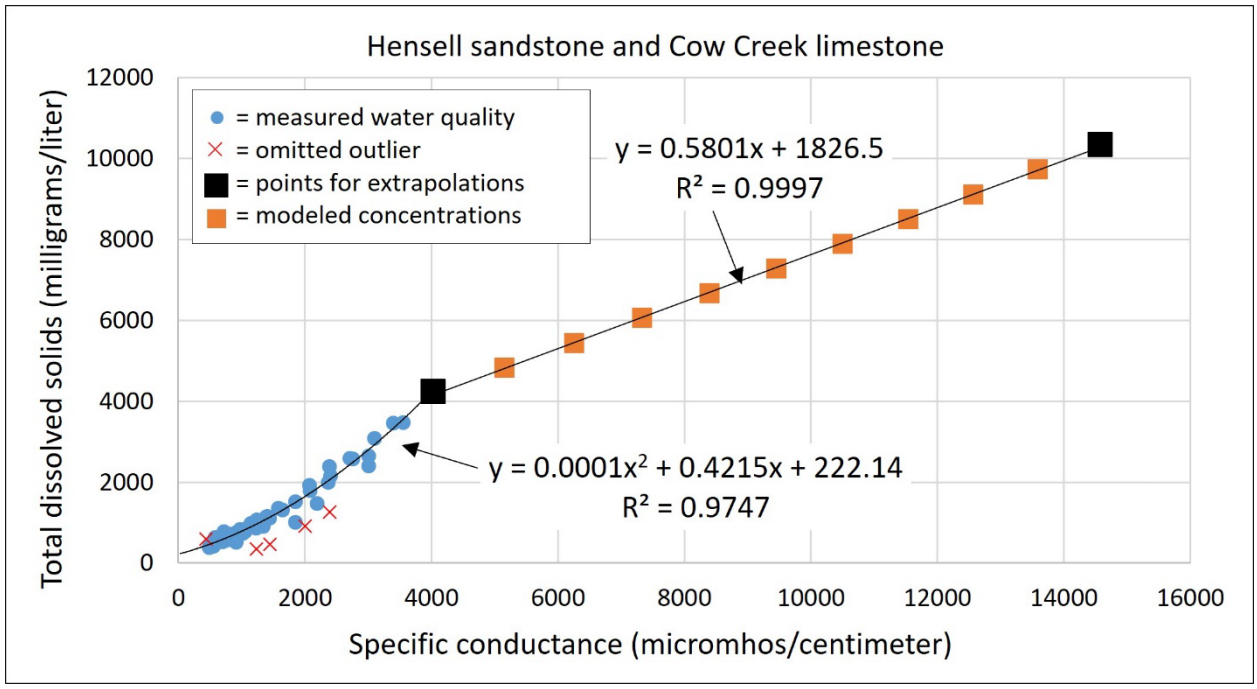

Figure 10-29 Plot of total dissolved solids versus specific conductance for the Hensell sandstone and Cow Creek limestone (106 measured water samples).

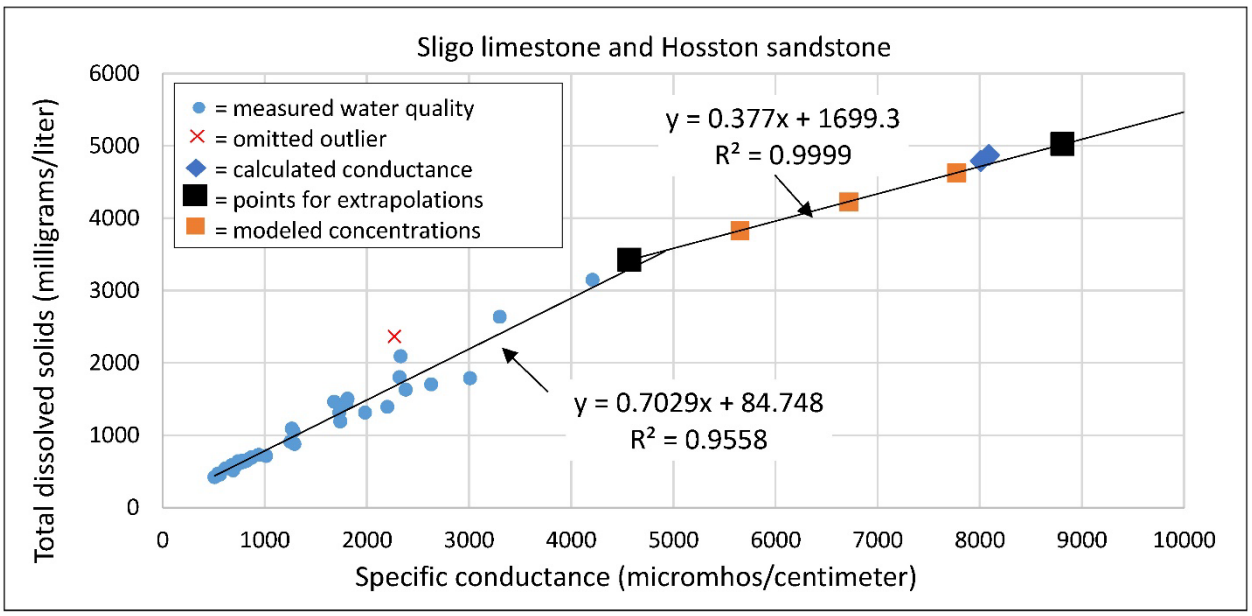

Figure 10-30 **Plot of total dissolved solids versus specific conductance for the Sligo limestone and Hosston sandstone (41 measured water samples).**

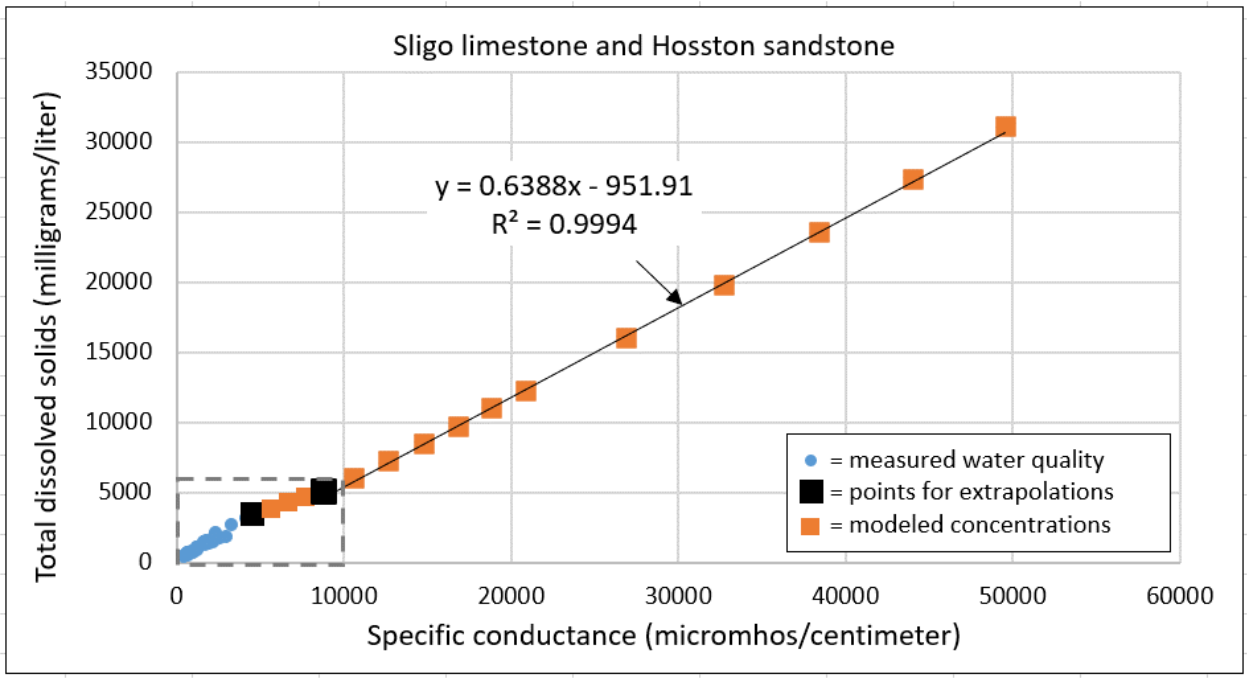

Figure 10-31 **Plot of total dissolved solids versus specific conductance for the Sligo limestone and Hosston sandstone (41 measured water samples). Dashed rectangle is the extent of Figure 10-30.**

11 Salinity calculations from geophysical well logs

Because of the scarcity of measured water quality values, particularly in downdip brackish formations, we supplemented this data with salinity calculated from geophysical well logs. We were then able to more accurately map groundwater salinity for the six water-bearing hydrostratigraphic units we defined for the Hill Country Trinity aquifer in the project study area. In this chapter, we will discuss how we increased spatial coverage using salinity calculations from geophysical well logs and how we tested and applied the Alger-Harrison (Alger and Harrison, 1989) method to estimated salinity from well logs for this study. Without calculating groundwater salinity estimates, the Upper Glen Rose limestone and Lower Glen Rose limestone would have insufficient data to map salinity zones in the southern half of the study area (Figure 11-1), the Hensell sandstone and Cow Creek limestone would also have insufficient data for mapping in the southern half of the study area (Figure 11-2), and the Sligo limestone and Hosston sandstone would have insufficient data for mapping the entire study area (Figure 11-3).

Previous BRACS studies have utilized various salinity calculation techniques in predominantly clastic aquifers. Meyer and others (2012) used the SP method (Estepp, 1998), Wise (2014) used the Rwa Minimum method (Estepp, 1998) and the Modified Alger-Harrison (Alger and Harrison, 1989) method, Meyer and others (2014) used the Rwa minimum method, Young and others (2016) used both Mean Ro (Estepp, 1998) and Rwa minimum methods (Young and others, 2016), Croskrey and others (2019) used the Rwa minimum method, and Andrews and Croskrey (2019) used the Rwa minimum method. BRACS studies that include significant carbonates and/or evaporites used the Rwa minimum method (Lupton and others, 2016) or the modified Alger-Harrison method (Robinson and others, 2018; Robinson and others, 2019). The authors of the Blaine study found calculating TDS estimates from logs impractical given data availability and the complexity of the Blaine Aquifer system (Finch and others, 2016).

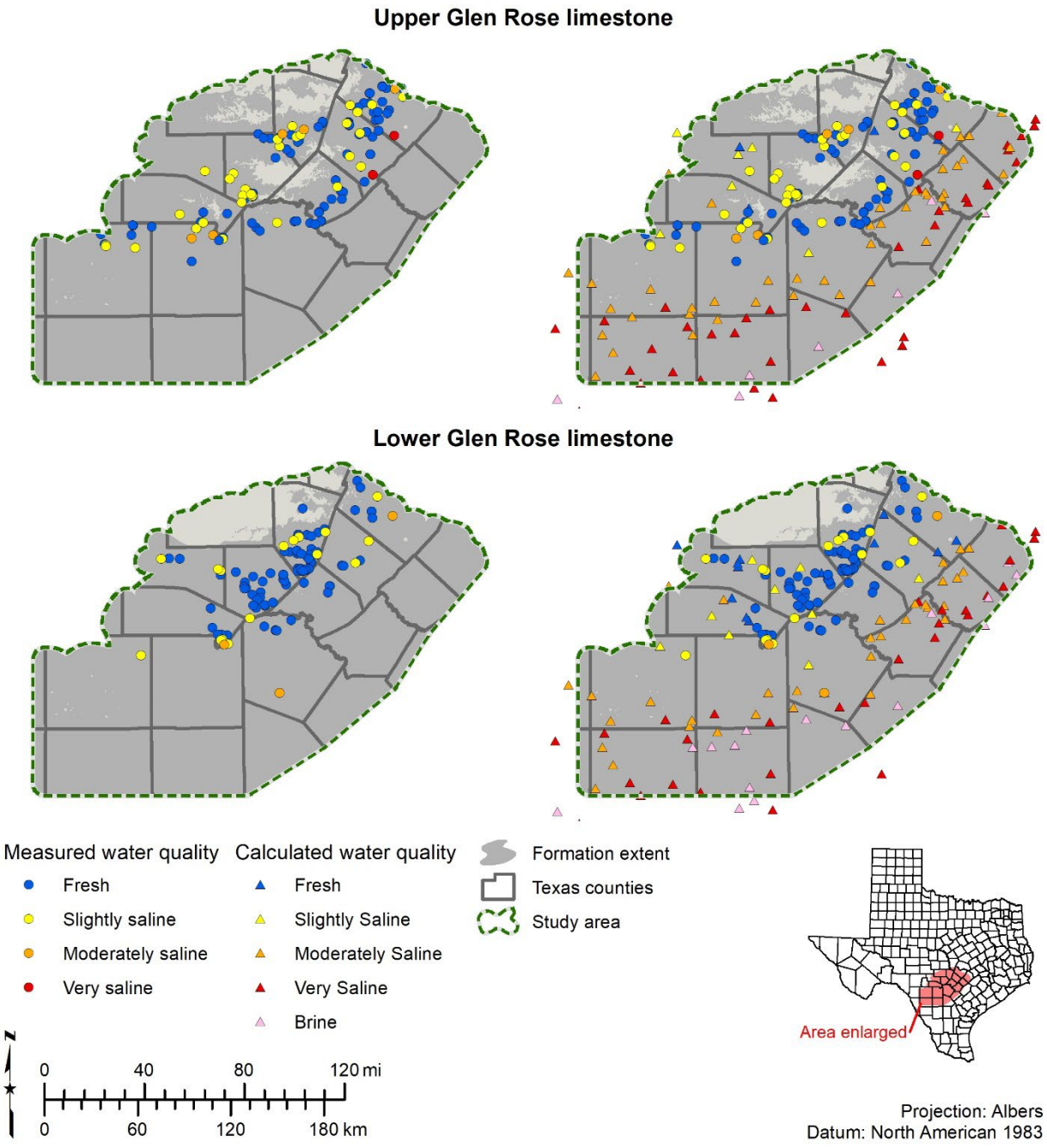

Figure 11-1 **Locations of measured water quality (left) and combined locations of measured water quality and calculated water quality (right) for the Upper Glen Rose limestone (top) and Lower Glen Rose limestone (bottom).**

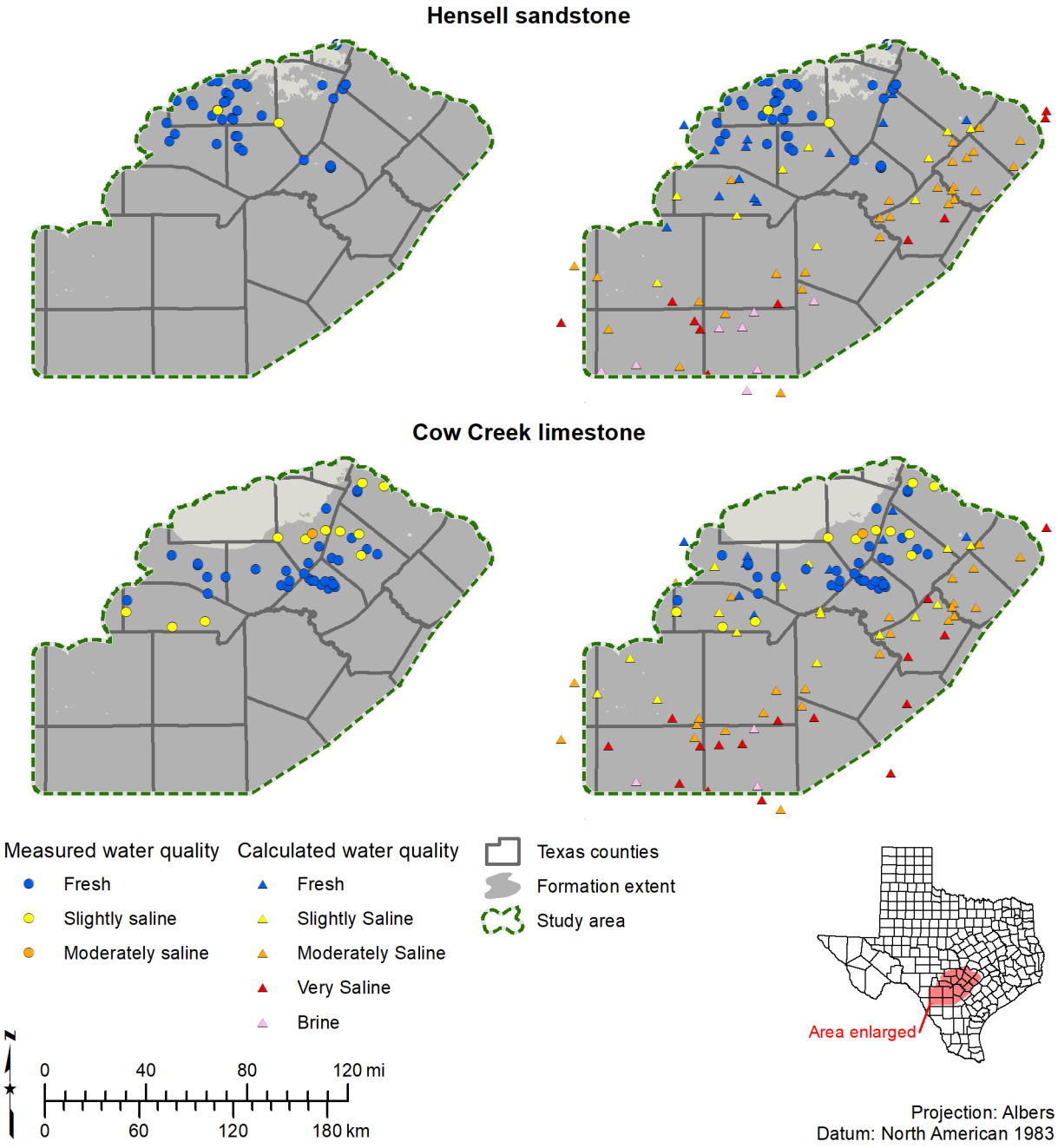

Figure 11-2 **Locations of measured water quality (left) and combined locations of measured water quality and calculated water quality (right) for the Hensell sandstone (top) and Cow Creek limestone (bottom).**

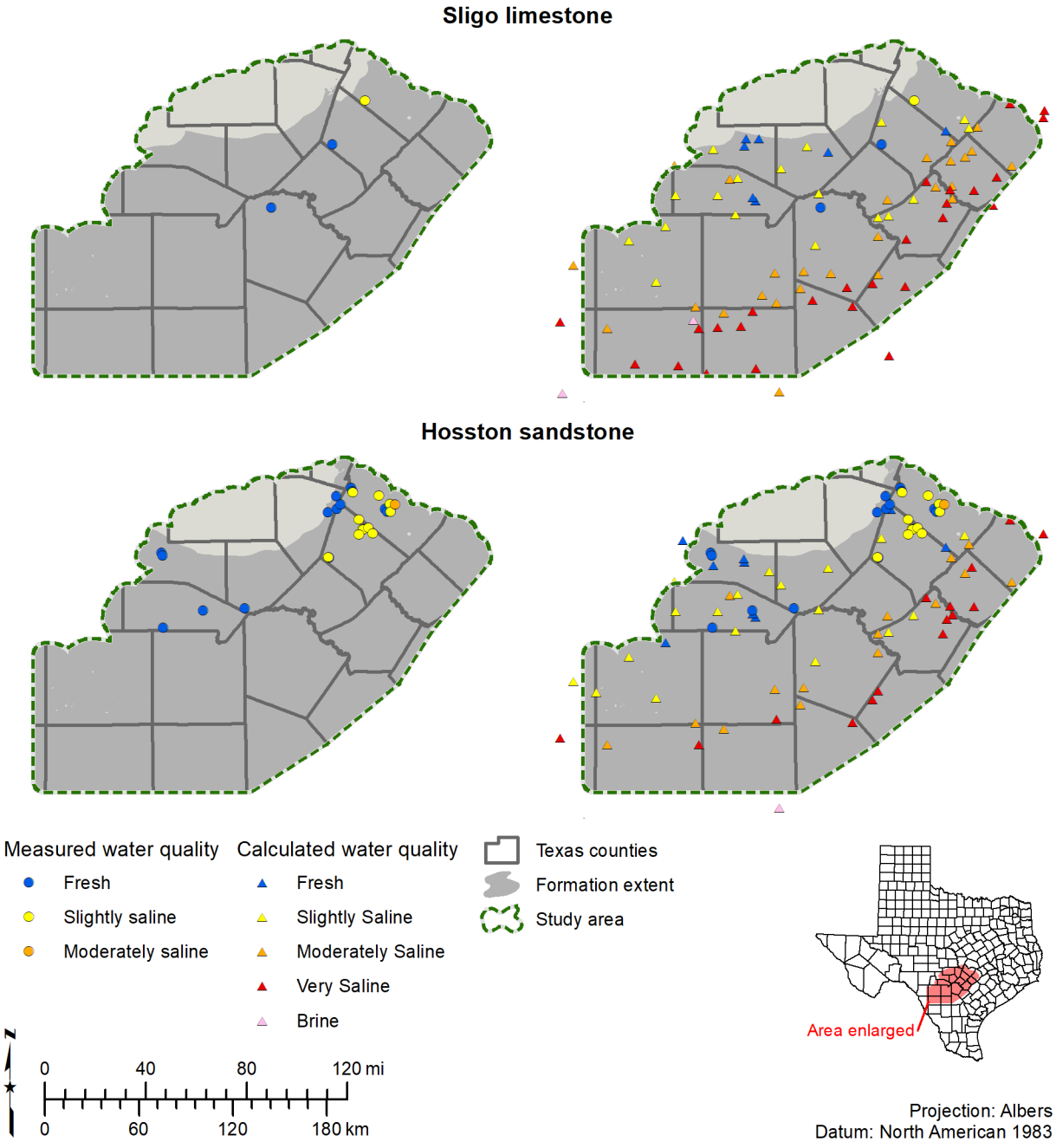

Figure 11-3 **Locations of measured water quality (left) and combined locations of measured water quality and calculated water quality (right) for the Sligo limestone (top) and Hosston sandstone (bottom).**

11.1 Geophysical well log tools

We utilized geophysical well logs to calculate total dissolved solids concentration of groundwater and to define the top and bottom of hydrostratigraphic units. Geophysical well logs are produced from tools that are lowered into a well bore with a wireline and retrieved back to the ground surface at a specific rate to measure various rock, fluid,

borehole, casing, and cement properties. Tools are selected based on many factors including anticipated lithologies, information required from logging, presence of cased or uncased bore holes, and the composition of the well bore fluid (water, air, or drilling mud). Most tools cannot collect meaningful information through surface casing of wells, and because older wells often had shorter segments of surface casing, older logs are often the only logs available for shallower portions of aquifers. Logs in the study area include some as old as the 1940's, and the tool designs and accuracies have greatly improved since then. We could not reliably interpret some of the older logs for total dissolved solids due to tool limitations at the time the older logs were created. We were also limited by the digital image quality of some logs which are illegible.

The resistivity of a formation can be measured from geophysical logging tools that pass electricity into the formation and record voltages between measuring electrodes. The resistivity of dry rock is a good electrical insulator (except for metallic ores), so the only way electricity can pass through a formation is if the rock contains a conducting fluid, such as groundwater. Groundwater is present either in the pores between mineral grains or interstitial clay. Resistivity tools have different depths of investigation and can measure distinct zones of mud filter cake, borehole fluid, the invasion zone where drilling fluid and formation fluid mix, and the uninvaded formation fluid at the deepest depths of investigation.

A normal resistivity log usually consists of multiple tools used to measure the resistivity of rocks and water surrounding the borehole at different depths of investigation. The spacing between the electrodes is directly proportional to the depth of investigation, with larger spacing offering deeper depth of investigation. Resistivity measurements are affected by the borehole, drilling fluids, mud filter cake, borehole fluid invasion zone, formation being investigated, surrounding formations, and formation groundwater. Resistivity tools must be run in an open borehole with a conductive drilling mud (non-oil-based muds). Induction logs are deep investigation tools which use focusing coils to direct the electricity into the formation to minimize the influence of the borehole, drilling fluids, surrounding formations, mud filter cake, and invaded zone (Schlumberger, 1987). Induction tools do not need conductive drilling mud (the tool is compatible with oil-based muds), but still must be run in an open borehole.

The spontaneous potential log is a record of the direct current reading between a fixed electrode at the ground surface and a movable electrode (spontaneous potential tool) in the well bore. The tool must be run in an open borehole with a conductive drilling mud. The electrochemical factors that create the spontaneous potential response are based on the salinity difference between the borehole mud filtrate and the groundwater within permeable beds yielding a positive or negative response (Asquith, 1982). A negative deflection of the spontaneous potential response occurs when the mud filtrate is more resistive than groundwater. A positive deflection occurs when mud filtrate is less resistive than groundwater. When the resistivity of the drilling mud and groundwater are equal there is no deflection of the spontaneous potential response. The spontaneous potential response of shale is relatively constant and is referred to as the shale baseline. We used the spontaneous potential tool to help identify permeable zones for total

dissolved solids calculations, as permeable zones are indicated by positive or negative deflections from the shale baseline.

Gamma ray logs normally reflect the clay content in sedimentary formations (Schlumberger, 1972). Clays such as illite and mica contain the radioactive potassium-40 isotope that produces gamma rays in clay or shale lithologies. Gamma ray tools encountering natural uranium or thorium will record the zone as an elevated measurement much higher than background clay response.

There are several advantages of using gamma ray logs. They are present on most logging runs for newer wells. Gamma ray logs can be recorded in cased holes. Unlike many tools, they generally start near ground surface, which is valuable when you are interested in groundwater. In many situations, their distinct responses to clay content can be used to recognize the boundaries of geologic units and facilitate the interpretation of depositional environments.

There are some challenges when using gamma ray logs. Although they can record useful readings in cased boreholes, there is attenuation of the overall log signature. This attenuation masks the more subtle changes in log response that occur, such as the transition from uncemented to cemented formations. When using gamma ray curves from the cased portion of the hole, there is an inability to evaluate borehole washouts if the caliper logs were not run prior to casing the well. Interpretation of gamma ray logs can also be undermined by the absence of important header information such as tool calibration or complete casing records. Older gamma tool types are especially challenging to use because the documentation of tool parameters is often limited or impossible to acquire. Older gamma ray logs may also have different units of measure compared with the modern standard American Petroleum Institute (API) units. Trying to compare measurements between tools with different units is problematic. Finally, there is an inability to differentiate between clay-free sand, clay-free silt, and clay-free carbonates using just the gamma ray tool.

Other important and useful geophysical well logs are available to measure the sonic, porosity, and density properties of rocks. Newer well logs are even capable of providing direct information on the lithology of the formation rocks. In the study area there were very few of these more modern well logs available, particularly with measurements in the water bearing Trinity Group formations.

11.2 Calculation method literature review

Before selecting a method to calculate salinity from geophysical well logs, we conducted a literature review to ascertain how other authors have calculated salinity in carbonates, and how to select effective parameters for calculations. We also researched the availability of relevant rock properties like lithology and porosity which are required inputs for some of the salinity calculation methods.

Many authors have written about the Hill Country Trinity formations, but two were particularly useful in developing our salinity calculations, Amsbury (1974) and Barker

and Ardis (1996). Although Amsbury (1974) described Trinity Aquifer lithology in a much more limited study area, this text was quite useful in illustrating the variability and complexity of Trinity Aquifer lithology, and therefore porosity. Barker and Ardis (1996) provided a regional view of the Trinity Aquifer, and although regional still highlighted the variable lithology.

Estepp (1998) provided a step-by-step example of calculating the groundwater salinity in the Edwards limestone using the Rwa Minimum method and the Pickett Plot method. The Pickett Plot method involves graphical plotting and is infeasible for a regional aquifer study because we conducted more than 1200 calculations. Given prior BRACS experience with the Rwa minimum method, we considered using it in our study.

Although some regulatory groups in Texas use and prefer to estimate groundwater salinity from geophysical well logs using the SP method (Alger, 1966; Estepp, 1998), we did not consider using it for this study. To effectively use the SP method, sufficiently thick and permeable sandstone strata are required, and the presence of shale will suppress the development of the SP curve (Estepp, 1998). Given the presence of clay beds and structural clay (Inden, 1974) and sometimes thin beds, this method would systemically overestimate salinity. Additionally, Robinson and others (2018) demonstrated that the SP method is inappropriate in well-lithified carbonates as they obtained inconsistent calculation results and could not find any experimental or theoretical support in the literature for using the SP method in similar lithologies.

Because of the 1) heterogeneity of porosity in carbonates, 2) the assumed presence of significant non-interconnected porosity, 3) and insufficient core data, we lacked the information to accurately derive the cementation exponent *m* and the porosity to apply the Rwa minimum method often used in previous studies of clastic aquifers (Meyer and others, 2014; Wise, 2014; Meyer and others, 2020). We do have abundant geophysical well logs with both deep and shallow resistivity measurements and the mud parameters recorded in the log header. We therefore decided to proceed with the Alger-Harrison method for calculating total dissolved solids from geophysical well logs.

11.2.1 Alger-Harrison method

The modified Alger-Harrison method (Alger and Harrison, 1989) was used by Robinson and others (2019) to calculate groundwater salinity estimates in the Northern Trinity Aquifer.

When wells are drilled, mud filtrate typically displaces the native groundwater near the borehole. The modified Alger-Harrison relies on Archie's equation (Archie, 1942) and that the ratio of shallow resistivity and deep resistivity is similar to the ratio of the resistivity of the mud filtrate and the native groundwater (Alger and Harrison, 1989). In a clean, clay-free sand saturated with 100 percent water Alger and Harrison posits that:

$$R_o = R_w \cdot \frac{a}{\phi^m} \qquad \text{(Equation 11-1a)}$$

and $$R_{xo} = R_{mf} \cdot \frac{a}{\phi^m}$$ (Equation 11-1b)

Rearranging the equations yields:

$$\frac{R_o}{R_w} = \frac{a}{\phi^m}$$ (Equation 11-2a)

and $$\frac{R_{xo}}{R_{mf}} = \frac{a}{\phi^m}$$ (Equation 11-2b)

Then

$$\frac{R_o}{R_w} = \frac{R_{xo}}{R_{mf}}$$ (Equation 11-3a)

$$R_w = \frac{R_o \cdot R_{mf}}{R_{xo}}$$ (Equation 11-3b)

Where:

R_w = resistivity of formation water (ohm-meter)
R_{mf} = resistivity of mud filtrate (ohm-meter)
R_{xo} = resistivity of the flushed zone near the wellbore (ohm-meter)
R_o = resistivity of the formation matrix and fluid (ohm-meter)
a = Winsauer factor (unitless)
ϕ = porosity (unitless as a decimal)
m = cementation exponent (unitless)

By using the Alger-Harrison equation, we do not need to know porosity or the cementation exponent from Archie's equation. Without the dedicated rock classification to appropriately select a porosity and cementation exponent, values selected for porosity and *m* would be potentially inaccurate estimates. With the Alger-Harrison method, we only need a geophysical well log with a complete header, a shallow resistivity tool, and a deep resistivity tool, of which there are sufficient available in the study area.

Despite the simplicity of the Alger-Harrison method, there are some drawbacks to consider. Alger-Harrison requires that mud parameters are reported on the log header and that shallow and deep resistivity tools were used to record resistivity in the mud-filtrate in the shallow flushed zone and the native groundwater in the deep zone, respectively. Additionally, inherent to any method utilizing resistivity to calculate total dissolved solids it is important to have sufficient bed thickness from which the resistivity measurement is read. Lowe and Dunlap (1986) assert that mud parameters reported on log headers can be 30 to 40 percent off and say the best mud parameters come from daily measurements, though this sort of data is unavailable to us. We utilized logs spanning seven decades (1950-2019) over which differences in mud resistivity measurement methods and reliability undoubtedly occur. We did not determine a method to ascertain the reliability of the mud parameters reported on the log header. Though corrections can

be made for mud invasion and bed thickness using tool specific corrections (Estepp, 1998; Alger and Harrison, 1989), we did not attempt these corrections since we did not have exhaustive tool-specific corrections.

11.2.2 Data availability

Before calculating groundwater salinity for the study area, we conducted a thorough quality control of the TWDB BRACS Database with these goals in mind:

- Ensure all tool suites on a scanned log are in the TWDB BRACS Database. This was necessary because sometimes more than one geophysical log for a well is combined into a single scanned image, and only the tool suite from the first log gets entered in the database.
- Ensure tools recorded in the BRACS database are accurate. Since the Alger-Harrison method requires a shallow and deep resistivity tool to conduct calculations, we wanted to be more specific about recording resistivity tools in the BRACS database. For example, many were simply recorded as "Resistivity" in the BRACS database when it was maybe a shallow laterolog and deep induction tool. Additionally, we did not want to conduct calculations on lateral logs. Logs with only one kind of resistivity tool also do not meet the criteria to use in calculations. More accurate descriptions of resistivity tools allowed us to look at eligible logs more efficiently.
- Ensure mud parameters are recorded in the database for logs in the study area.

As a result of this database quality control effort, we identified the following tool counts in the study area:

- 1,121 resistivity tools of varying depths of investigation on geophysical well logs
- 225 density porosity tools
- 193 neutron porosity tools
- 82 sonic tools
- 46 PEF tools
- 6 magnetic resonance tools

Unfortunately, only 39 wells with porosity logs and resistivity logs intersected the study area, and only one well logged the Trinity Aquifer. Ultimately, we relied on well logs with resistivity tools to calculate groundwater salinity. Because we did not have many porosity logs to use, we used knowledge of expected lithology to determine where we saw good porosity on a log. Spontaneous potential, resistivity, and when available, gamma ray logs were utilized to identify suitable lithologies for calculations. Spontaneous potential and resistivity tools were then utilized to select depths with good porosity for calculations.

11.3 Application of the Alger-Harrison method

This section discusses the data and process elements involved in applying the Alger-Harrison method and how the proper determination of various input parameters and correction factors affects the accuracy of the calculation. Methodology considerations can also have an impact on the calculated total dissolved solids values. We also discuss how we used "well pairs," or measured groundwater samples paired with available geophysical well logs that have header data, to test how well our calculations can predict actual measurements.

11.3.1 Well pairs

In order to assess how well the Alger-Harrison method performs in our study area, we attempted to identify "well pairs," which are wells that include both 1) a lab-analyzed measured water quality sample, 2) a geophysical well log with shallow and deep resistivity tools logged over the same formation of interest. Additionally, the measured water quality needed both total dissolved solids and specific conductivity analyzed, and the geophysical well logs needed adequate mud parameters reported (R_m, R_{mf}, T_{Rm}, and T_{Rmf}). We only used wells with well construction information that allowed us to assign the sample to a particular hydrostratigraphic unit. We did allow measured water quality samples to span more than one hydrostratigraphic unit if the combination represented only one of the Trinity hydrologic units.

Finding well pairs that met the above criteria was a challenge and we were able to identify only five such well pairs. In order to increase the number of well pairs, we expanded our search so a well pair could consist of a measured water quality sample that occurred within one mile of an adequate geophysical well log. Expanding our search added an additional four well pairs. There were 146 potential well pairs that we reviewed during this process. We did not exhaustively search for well pairs with a measured total dissolved solids of less than 500 milligrams per liter because we were primarily concerned with calculating higher values of total dissolved solids.

Among the reasons that potential well pairs could not be used in our analysis were 1) the logs did not have recorded mud parameters, 2) we could not read the scanned log, 3) the log and measured water quality sample did not overlap in depth, 4) the measured water quality sample anions and cations did not balance within 5 percent, 6) the measured water quality was sourced from multiple formations, 7) the resistivity overrange readings were not plotted on the log, or 8) the resistivity was measured with a lateral type tool.

We established total dissolved solids and specific conductance relationships to convert a calculated water conductivity (C_w) value to a corresponding value of total dissolved solids (Section 10.4). Given the small set of only 9 well pairs (Table 11-1) and limited total dissolved solids range (7 samples with total dissolved solids less than 1000 milligrams per liter and 2 samples with total dissolved solids greater than 1000 milligrams per liter), it is difficult to assess the accuracy of our calculations.

Table 11-1 Well pairs assessed for the study.

BRACS well identifier	State Well Number	Pair type	Measured water quality formation(s) from aquifer determination	Total dissolved solids (full bicarbonate sum, mg/L)	Specific Conductance (measured, *=calculated, microsiemens -centimeter)
16713	6920201	same well	Cow Creek limestone	1,164	1,400
33091	5664601	1-mile	Sligo limestone	820	1,140
33376	5664701	same well	Hosston sandstone	616	828
33996	5663614	same well	Hosston sandstone	552	745
37772	6923803	1-mile	Sligo limestone	715	1,013
52983	6924214	1-mile	Hensell sandstone and Cow Creek limestone	700	1,064
52986	6924202	same well	Hosston sandstone	657	797
60015	-	same well	Lower Glen Rose limestone	4,653	4,265*
87214	5663606	1-mile	Sligo limestone	807	1,341

11.3.2 Mud filtrate resistivity (R_{mf}) parameter

Crucial to the Alger-Harrison method is an accurate mud resistivity (R_{mf}) measurement. Obtaining reliable R_{mf} measurements presented challenges to the study and in this section, we explain how we attempted to constrain these challenges. Geophysical well logs prior to about 1955 do not typically report an R_{mf} value in the header, and it was not common for R_{mf} values to be reported until after 1960 in our study area (Figure 11-4).

In order to validate R_{mf} values, we reviewed data from wells in the study area that were logged through the Trinity aquifer and that had complete geophysical headers. For a header to be considered complete, it needs values for mud resistivity (R_m), temperature of the mud the resistivity was reported at (T_{Rm}), resistivity of the mud filtrate (R_{mf}), and the temperature the mud resistivity was reported at (T_{Rmf}). To standardize comparisons of R_m and R_{mf} for logs from different depths, we converted the R_m and R_{mf} at their

reported temperatures to an R_{m75} and R_{mf75} at 75 degrees Fahrenheit. We used a simple gradient-based equation:

$$R_{m75} = R_m \left(\frac{T_{Rm}}{75}\right) \text{ and } R_{mf75} = R_{mf} \left(\frac{T_{Rmf}}{75}\right) \qquad \text{(Equation 11-4)}$$

Where:

R_m = resistivity of the mud as reported on the log header (ohm-meter)
R_{mf} = resistivity of the mud filtrate as reported on the log header (ohm-meter)
T_{Rm} = temperature of the mud reported for the R_m (degrees Fahrenheit)
T_{Rmf} = temperature of the mud filtrate reported for the R_{mf} (degrees Fahrenheit)
R_{m75} = resistivity of the mud calculated at 75 degrees Fahrenheit (ohm-meter)
R_{mf75} = resistivity of the mud filtrate calculated at 75 degrees Fahrenheit (ohm-meter)

This data was plotted to identify outliers (Figure11-5). One obvious outlier is located at R_{m75} = 23.39 and R_{mf75} = 11.41.

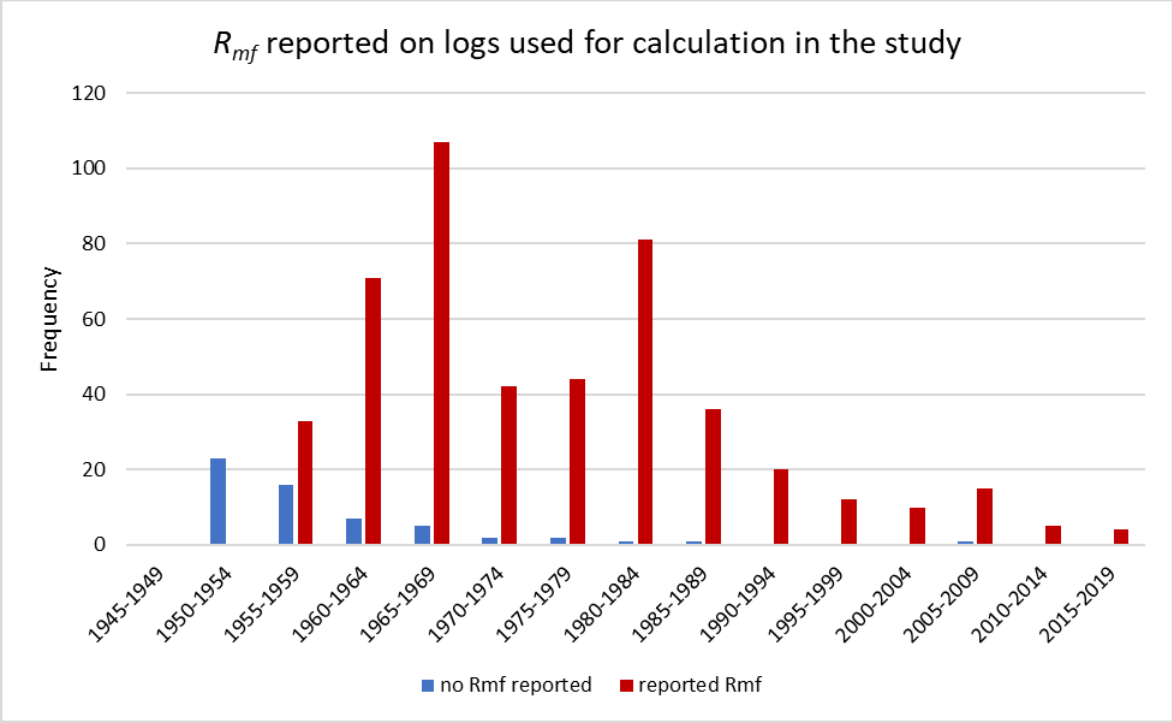

Figure 11-4 Distribution of logs used to calculate estimated groundwater salinity with and without a header reported R_{mf} value by five-year interval from 1945-2019.

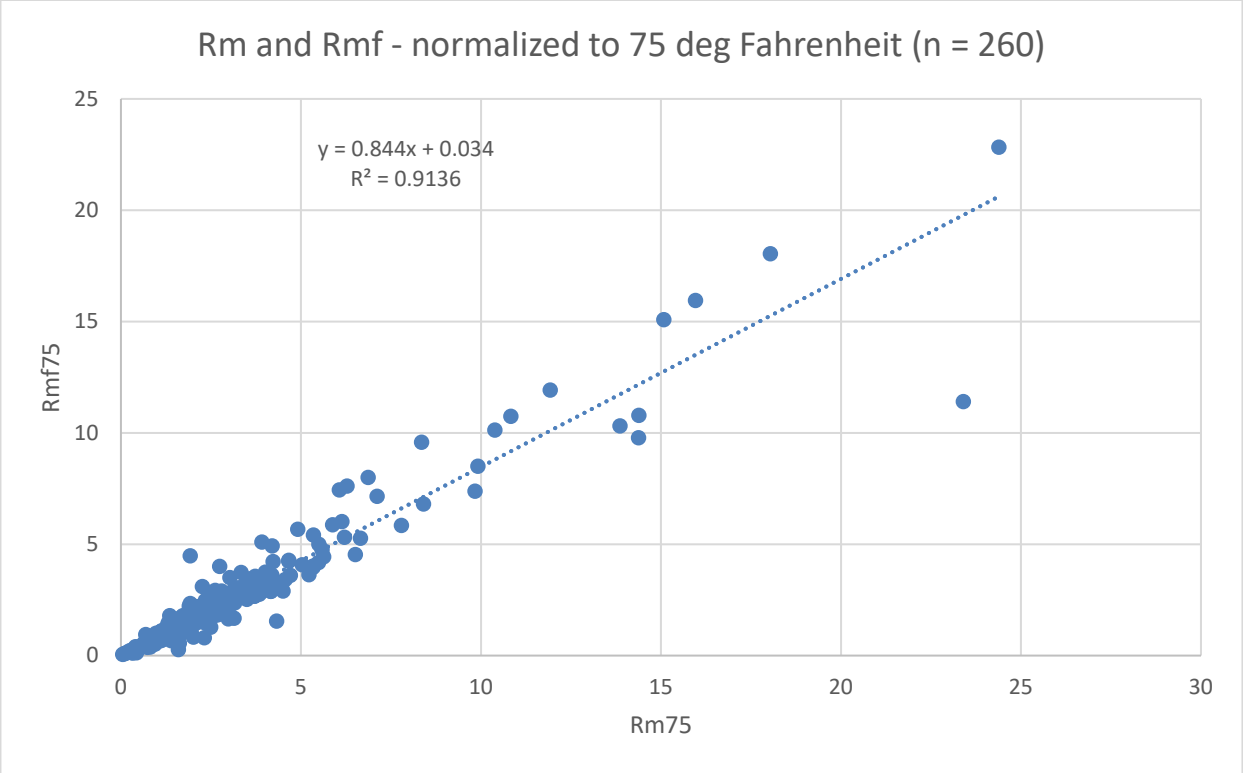

Figure 11-5 ***R_{m75}* and *R_{mf75}* from 260 well logs in the study area.**

Additionally, we calculated summary statistics for the 260 samples (Table 11-2).

Table 11-2 **Minimum, median, mean, maximum, and standard deviation of *R_{m75}*, *R_{mf75}*, and *R_{m75}/R_{mf75}* for study area wells.**

	Minimum	Median	Mean	Maximum	Standard deviation
R_{m75}	0.049	2.016	3.024	24.381	3.292
R_{mf75}	0.049	1.703	2.587	22.827	2.907
R_{m75}/R_{mf75}	0.429	1.226	1.282	5.767	0.449

To test for outliers, we determined for each R_{mf75} value whether it was within a standard deviation using the trend in Figure 11-5:

1. Calculate an R_{mf75} from the equation in Figure 11-5
2. Subtract the reported R_{mf75} from the calculated R_{mf75}
3. Compare the absolute value of the difference between the calculated and reported R_{mf75}. If the difference is greater than the standard deviation of the R_{mf75}, then we considered the data point an outlier.

Only one point of 260 was identified as an outlier (the same point identified as an outlier by visual inspection; R_{m75} = 23.39 and R_{mf75} = 11.41).

We removed the outlier from the dataset and calculated a new linear regression for use in calculating values for R_{mf75} (Figure 11-6). We used the resulting linear regression solution (Equation 11-5) to calculate the R_{mf} for logs where it was not recorded.

(R_{mf75} = 0.9157*R_{m75} - 0.1446) (Equation 11-5)

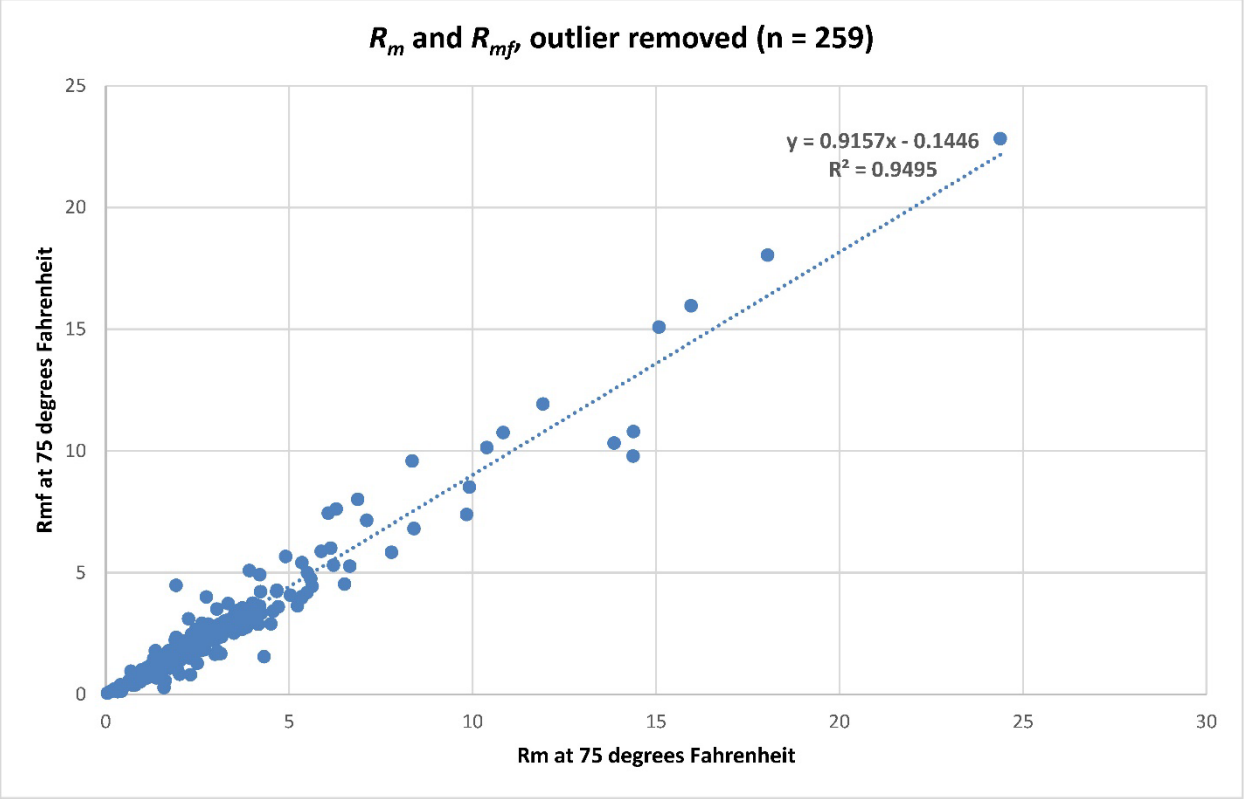

Figure 11-6 R_{m75} and R_{mf75} from 256 well logs in the study area. One outlier was removed.

We used the equation to calculate an R_{mf} for our outlier data point (BRACS ID 82998) and used the calculated R_{mf} in subsequent salinity calculations for that well as it resulted in a more reasonable calculated salinity value. If we compare the log reported R_{mf} and a trend derived R_{mf} in the test calculations, we see significant improvement in the calculated salinity for the identified outlier. Measured water quality is 575 milligrams per liter total dissolved solids. However, when using the log reported R_{mf} and a straight average of 4 calculated depths, we get a total dissolved solids value of 1,186 milligrams per liter. If we use a trend derived R_{mf} value for this well and the same depths and calculation method, we get a calculated total dissolved solids value of 688 milligrams per liter. The calculated R_{mf} significantly improved total dissolved solids calculations for our one outlier data point.

11.3.3 Well log curve input methods

Before selecting a well log curve input method, we conducted a literature review of how previous studies of the Hill Country Trinity aquifer and other carbonate aquifers have estimated total dissolved solids. MacCary (1980) suggests using a "resistivity-feet" approach, which includes the following steps: 1) identify the depth of aquifer you want to analyze, 2) identify beds with porosity, 3) calculate a water conductivity (*Cw)* for one-to-many beds within the overall depth of interest, and 4) average the calculated *Cw* values together using the bed thickness as a weight. Schultz (1992, 1993) uses a similar weighted average approach.

Using our identified well pairs, we compared three well log curve input approaches of varying complexity and methodology for assigning a total dissolved solids to an aquifer unit: 1) single point calculations, 2) averaged calculations, and 3) bed-thickness weight-averaged calculations.

Single point calculation

This method is the simplest, but also the most prone to user-error. For this method you identify the "best" place to perform a single Alger-Harrison calculation to assign a salinity class for the formation. For thin formations, like the Cow Creek limestone, this method may be appropriate, but if the wrong depth interval is selected (such as a non-permeable interval) you can calculate unrealistic salinity values yielding an incorrect salinity class.

The single point calculation performed poorly when compared to a measured water sample. If the classification relies on one calculation, and the depth to perform the calculation at is selected improperly, wildly inappropriate calculated total dissolved solids values may result. For example, we have a geophysical well log and measured water quality sample for BRACS ID 82998. When testing calculations, an inappropriate depth was unintentionally selected for a calculation. The calculated total dissolved solids value is 2,346 milligrams per liter, but the measured total dissolved solids is 575 milligrams per liter. This kind of inaccuracy would have misclassified the water quality for this well. We did not proceed with testing for a single-point calculation.

Averaged calculations

To overcome limitations of the single point calculation method, averaging multiple calculations to derive a salinity classification for a formation may mitigate the effects of selecting inappropriate and/or suboptimal depths for salinity calculations. In this method several points are selected (if available) to perform Alger-Harrison calculations and the resulting salinity calculations are averaged together. The averaged total dissolved solids value is then used to select a salinity classification for the formation. This averaged calculation method was one of the variations tested in the current study.

Bed-thickness weight-averaged calculations

A form of weighted average was suggested by MacCary (1980) and Schultz (1992, 1993) with the idea that some formation beds will contribute more water to a sample than

others. With this method, several points are selected (if available) to perform salinity calculations which are then weighted by bed thickness and averaged together. The weighted average is then used to select a salinity classification for the formation. This weighted average method was one of the variations tested in the current study.

11.3.4 Comparison of tested variations of the Alger-Harrison method

In order to determine the optimum approach to implementing the Alger-Harrison method, we created four scenarios that combined different Alger-Harrison method application components.

- Groundwater type correction as suggested by Estepp (2010) used or not used.
- Mud invasion correction (Estepp, 1998; Estepp, 2010) used or not used.
- Use the partial bicarbonate value (Robinson and others, 2019; Meyer and others, 2020) or use the full bicarbonate value (derived from the analyses in Section 10 of this report).
- Calculate salinity using a sodium chloride equivalent total dissolved solids (Robinson and others, 2019; Meyer and others, 2020).

The scenarios were further evaluated on the type of R_{mf} value used:

- Use only header reported R_{mf} values.
- Use only calculated R_{mf} values.
- Use a mixture of header reported and calculated R_{mf} values.

Since we established a relationship between R_m and R_{mf} for the study area, we were curious as to whether we should use only log-header reported R_{mf} values, only calculated R_{mf} values, or whether a mix of log-header and calculated R_{mf} values was appropriate. For the mixture of header reported and calculated R_{mf} values, we used a calculated R_{mf} value if only an R_m value was reported on the header or if the R_{mf} value was an outlier.

When we tested calculations on the well pairs, using only log-header reported R_{mf} values inflated the calculated total dissolved solids values by as much as approximately 2,000 milligrams per liter total dissolved solids on average (Figure 11-7 and Figure 11-8). Using only calculated R_{mf} values inflated total dissolved solids by as much as 750 milligrams per liter total dissolved solids on average over measured values, and a mixture of header reported and calculated R_{mf} values inflated total dissolved solids by approximately 800 milligrams per liter total dissolved solids on average over measured values. Since the results from using only calculated R_{mf} or a mixture of header reported and calculated R_{mf} values are comparable, we decided to use the mixture of R_{mf} values. So, if a log had an R_{mf} value in the header, and the value was not an outlier value, we used the value as reported. Otherwise, we calculated an R_{mf} value from the R_m.

Groundwater correction

A groundwater type correction factor is suggested by Estepp (2010). To test the groundwater type correction factor, we used the major cations and anions from

individual measured water quality samples to select the most appropriate correction factor from Estepp (2010). This correction appears to originally be introduced by Alger (1966) as a necessary component to calculate groundwater salinity using the SP log, as the SP response is sensitive to the groundwater chemistry composition. We think that if an appropriate relationship between groundwater chemistry specific conductance and total dissolved solids is established for a study area, a groundwater type correction factor is inappropriate in the Alger-Harrison method (Alger and Harrison, 1989). This appears to be corroborated by Alger and Harrison (1989) as they suggest converting a calculated specific conductance to a total dissolved solids value using empirical relationships of specific conductance and total dissolved solids. In addition to the physical basis for not using a groundwater type correction factor, we found that using a groundwater correction factor was inappropriate as it inflated the calculated total dissolved solids values over the measured values of our well pairs the most of any variation and corrections. Given there are sufficient measured water quality samples and sufficient understanding of the expected groundwater chemistry, groundwater type correction factors should not be applied to a method other than the SP method (Alger, 1966).

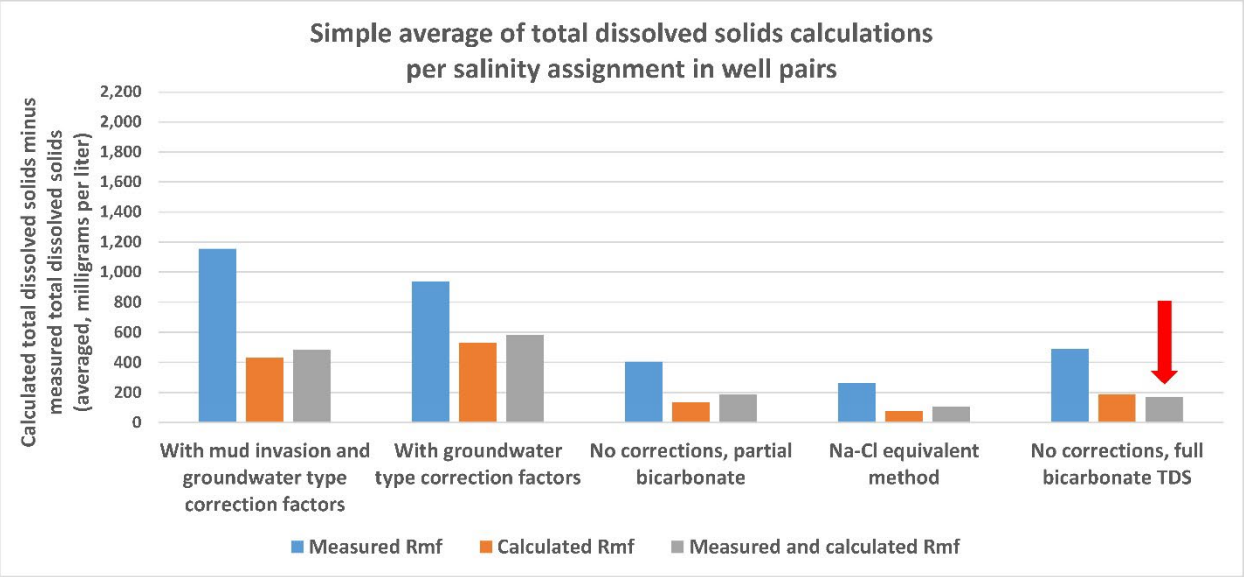

Figure 11-7 Average of the calculated total dissolved solids minus the measured total dissolved solids by calculation variation for the straight-average approach. The red arrows highlight the method selected for the study.

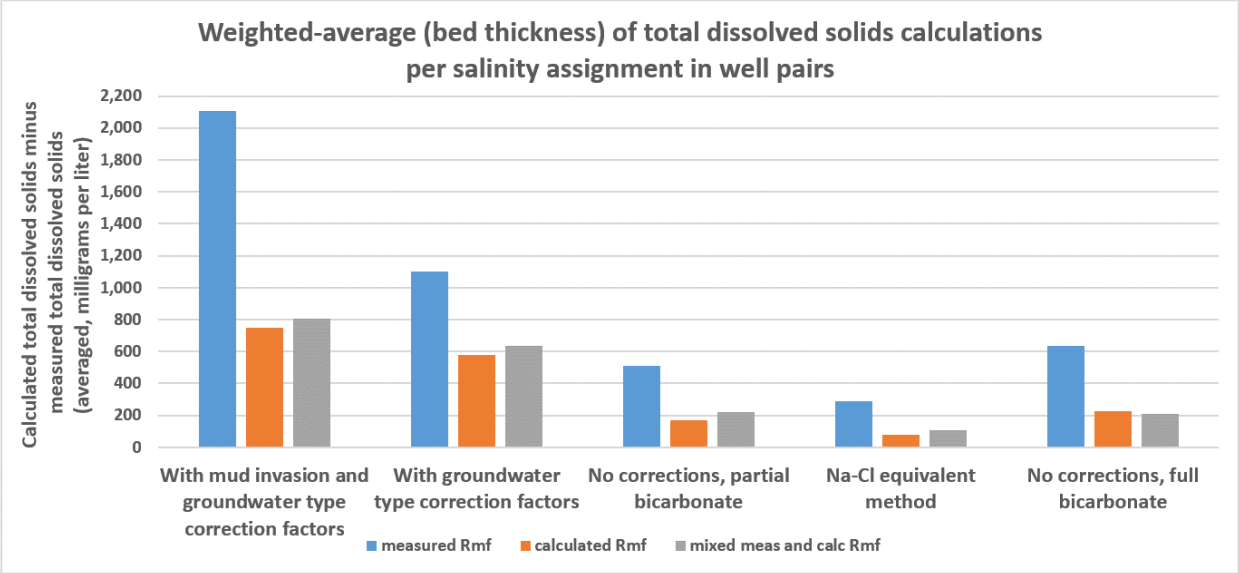

Figure 11-8 **Average of the calculated total dissolved solids minus the measured total dissolved solids by calculation variation for the weighted-average approach. The weighted-average method was not used in the study.**

Mud invasion correction

We used various resistivity tools to calculate salinity. These tools are from various companies from approximately 70 years of logging in the Hill Country Trinity aquifer. We did not have comprehensive mud invasion correction equations for the resistivity tools we used as they are not typically provided on geophysical well logs. When we tested mud invasion corrections, we used the 16- and 64-inch normal resistivity correction listed in Estepp (2010) since these tools are well represented in our dataset. Using somewhat generic mud invasion corrections seemed inappropriate and inflated calculated total dissolved solids values. As such, we did not pursue mud invasion corrections for our calculations.

Partial and full bicarbonate

As explained in Section 10.4 of this report, we decided to use the full bicarbonate value to develop relationships of total dissolved solids versus specific conductance for calculating salinity. On average, the simple average and weighted-average approaches overestimate the calculated total dissolved solids, meaning it calculates saltier water than measured. When we compared using the partial bicarbonate value and the full bicarbonate value, we found that for the simple average, partial bicarbonate values overestimated the calculated total dissolved solids value by 13 milligrams per liter more than using full bicarbonate values. Partial bicarbonate values overestimated calculated total dissolved solids by 15 milligrams per liter more than using full bicarbonate values in the weighted-average approach. From a calculation standpoint, we found either partial bicarbonate or full bicarbonate values acceptable, but as explained in Section 10 of this report, we think using full bicarbonate values to be more technically defensible, so we used full

bicarbonate values in our variation of the Alger-Harrison method (Alger and Harrison, 1989).

Calculate salinity using a sodium chloride equivalent total dissolved solids

The Northern Trinity Aquifer brackish groundwater mapping project (Robinson and others, 2019) selected a total dissolved solids calculation method in which they did the following:

1) Calculated a sodium chloride equivalent total dissolved solids for each measured water quality sample using Schlumberger chart GEN-4 (Schlumberger, 2009).
2) Segregated measured water quality by mapped formation.
3) Plot sodium chloride equivalent total dissolved solids on the x-axis and measured total dissolved solids on the y-axis.
4) Derive a linear relationship relating the measured total dissolved solids to a sodium chloride equivalent total dissolved solids.
5) When performing discreet total dissolved solids calculations, calculate a groundwater equivalent resistivity at 77 degrees Fahrenheit (R_{we77}).
6) Convert the R_{we77} to a sodium chloride equivalent total dissolved solids value using the Bateman and Konen (1977) equation.
7) Convert the sodium chloride equivalent total dissolved solids to a study area total dissolved solids using the relationships derived in step 4.

Although on average the sodium-chloride equivalent method looks appealing as it had the lowest average difference between the calculated and measured total dissolved solids, it had the second highest range of differences of the tested variations (Figure 11-9). This method underestimated total dissolved solids the most, and this is likely due to ion complexing. As explained in Section 10 of this report, there is significant ion complexing in the groundwater of the study area, and since this method calculates a sodium chloride equivalent total dissolved solids, it likely underestimates the amount of complexing in the groundwater. For this reason, we did not pursue this method.

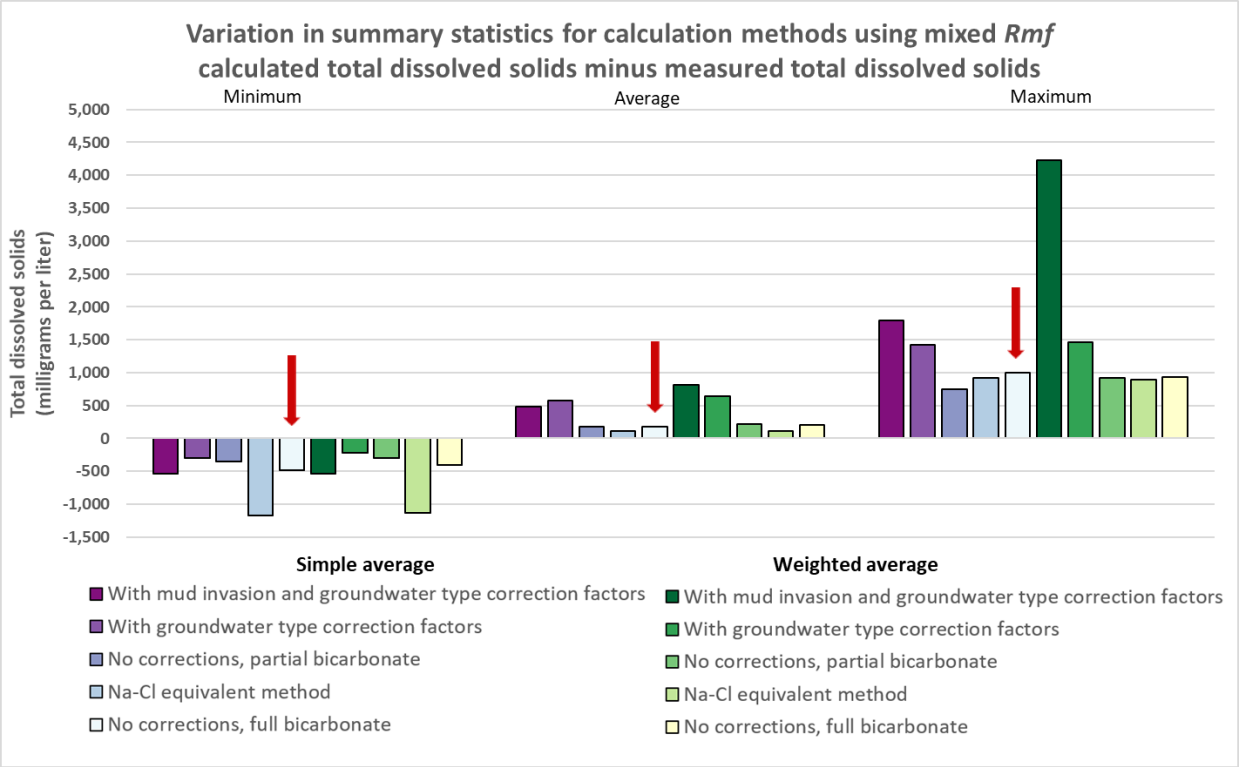

Figure 11-9 **Summary statistics (minimum, average, and maximum) for the various tested salinity calculation methods using mixed log-header and calculated *Rmf* values. Summary statistics were compiled based on the calculated total dissolved solids minus the measured total dissolved solids. The red arrows highlight the method selected for the study.**

11.3.5 Selecting appropriate depths

The optimal depth to calculate salinity is where a geophysical well log indicates that the rock has porosity that will hold fluids. This statement may seem obvious, but in practice it can be challenging to identify appropriate depths in carbonates given the limited data we have available. Selecting depths with good porosity can be done in a few ways: 1) by using porosity type geophysical well logs, like sonic, neutron porosity, or density porosity logs (Carlos Torres-Verdin, unpublished class material, 2019), 2) by understanding the lithology that you will encounter in the subsurface, or 3) by combining knowledge from porosity logs and lithologic analysis. Since we did not have many porosity logs, we primarily used knowledge of expected lithology and SP logs to select depths to calculate total dissolved solids.

For the carbonate dominated lithologies (Upper Glen Rose limestone, Lower Glen Rose limestone, and Sligo limestone) we looked for "resistivity lows" (MacCary, 1980). The logic behind looking for resistivity lows is that in carbonates, tight rock with little porosity should be very resistive, and depths with appreciable groundwater would have porosity. Thus, zones with groundwater, and porosity, should appear less resistive than the competent rock. To distinguish between resistivity lows caused by shale versus resistivity lows caused by porosity within carbonates, we looked for at least two

additional context clues. If a resistivity low was caused by shale, we would not expect much, if any, mud invasion so the deep and shallow resistivities should be similar. Additionally, the SP tool, which is typically present, is useful in identifying shales and typically deflects right for shales. The most useful tool to identify shales is the gamma ray tool. If there was a large spike in the GR tool, there was likely a clay-bearing rock present and we did not select that depth for analysis. Unfortunately, not many logs in the study area had a gamma ray log available so this additional check was not often possible. Figure 11-10, Figure 11-11, and Figure 11-14 are examples of analysis depths selected by looking for resistivity lows.

The Cow Creek limestone proved, at times, more difficult to select appropriate analysis depths. Although the Cow Creek limestone is dominated by carbonates like the Upper Glen Rose limestone, Lower Glen Rose limestone, and the Sligo limestone, the Cow Creek limestone is comparatively thin and can include significant oolites in places (Amsbury, 1974). Due to the nature of oolites and oomoldic porosity (Verwer, 2011), we would expect to see high resistivity in the groundwater bearing beds. Given the expected high resistivity and thin beds, we did not often observe a resistivity low (Figure 11-13). Of the mapped formations, we would expect our calculations to systemically underestimate salinity in the Cow Creek limestone as the deep resistivity curve reading is most likely to be underdeveloped.

For the clastic dominated formations, like the Hensell sandstone and Hosston sandstone, we used a more traditional depth selection approach. We looked for relatively clay-free sand beds using the SP, resistivity, and when available, GR tools. Once we located appropriate beds, we selected the peak of the resistivity curve within the bed for our salinity analysis (Figure 11-12 and Figure 11-15).

Figure 11-12 depicts an interesting phenomenon we occasionally observed in the logs we used for analysis. At 600 feet below measuring point, it appears that the deep resistivity of the formation exceeds the measuring capability of the tool, this typically occurred in carbonates in presumably competent rock. Since we would not want to do calculations in competent carbonate, we simply avoided these intervals. When we observed this in the Hensell sandstone or Hosston sandstone, we avoided these depths when possible. In Figure 11-12, we selected this depth because the Hensell sandstone was one of the formations that we had a difficult time finding appropriate logs. The consequence of selecting this depth is we may have overestimated salinity for this well. However, since the overestimation is in the same salinity classification as a fully developed deep resistivity reading would have calculated (fresh), we kept this depth.

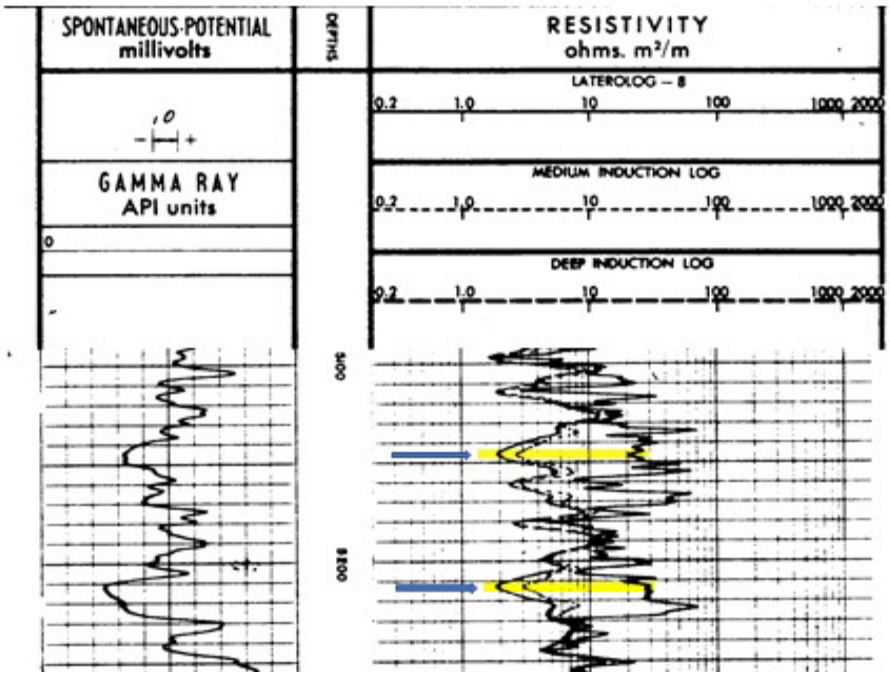

Figure 11-10 **Two examples of depths used in salinity calculations for the Upper Glen Rose limestone highlighted in yellow from BRACS ID 68507. The left-hand side of the log displays the spontaneous potential tool, and the right-hand side displays the deep induction log (bold dashed line), medium induction log (thin dashed line), and shallow laterolog (solid line).**

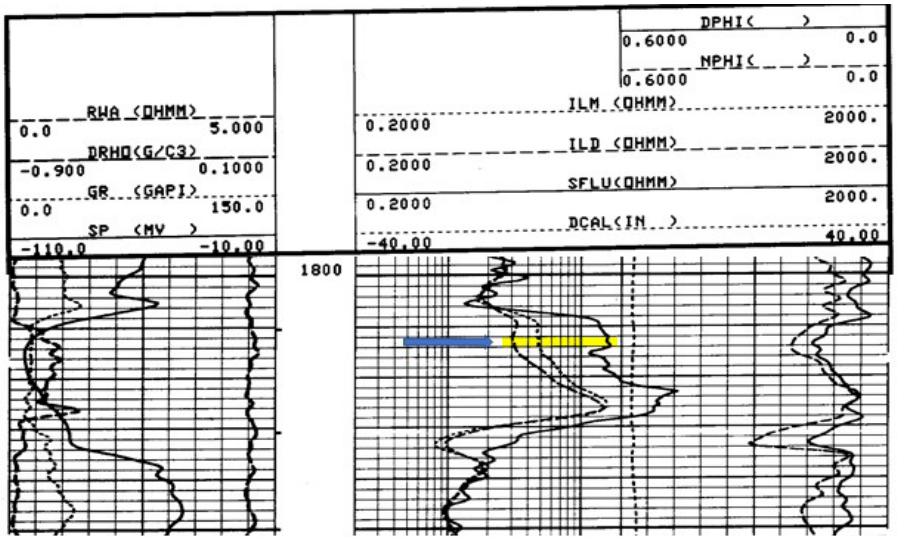

Figure 11-11 **One example of depths used in salinity calculations for the Lower Glen Rose limestone highlighted in yellow from BRACS ID 67791. The left-hand side of the log displays the spontaneous potential log (solid line), gamma ray log (thin dashed line), change in density measurements (long dashed line), and the resistivity of water apparent log (medium dashed line). The right-hand side displays the deep induction log (bold dashed line), medium induction log (left most thin dashed line), shallow focused laterolog (solid line), and the differential caliper log (right most small-dashed line).**

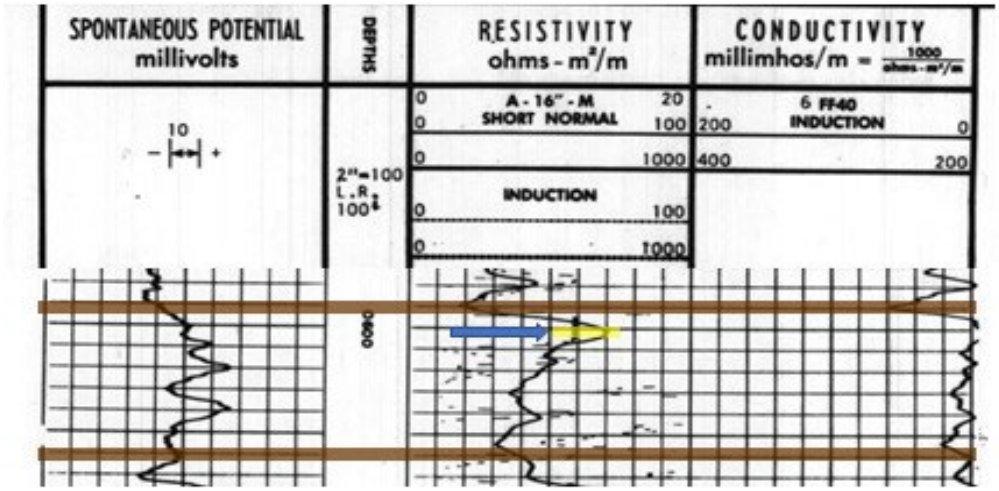

Figure 11-12 **One example of depths used in salinity calculations for the Hensell sandstone highlighted in yellow from BRACS ID 37777. The left-hand side of the log displays the spontaneous potential log, and the right-hand side displays the deep induction log (dashed line) and short normal (solid line). The brown line represents the mapped top of the Hensell sandstone.**

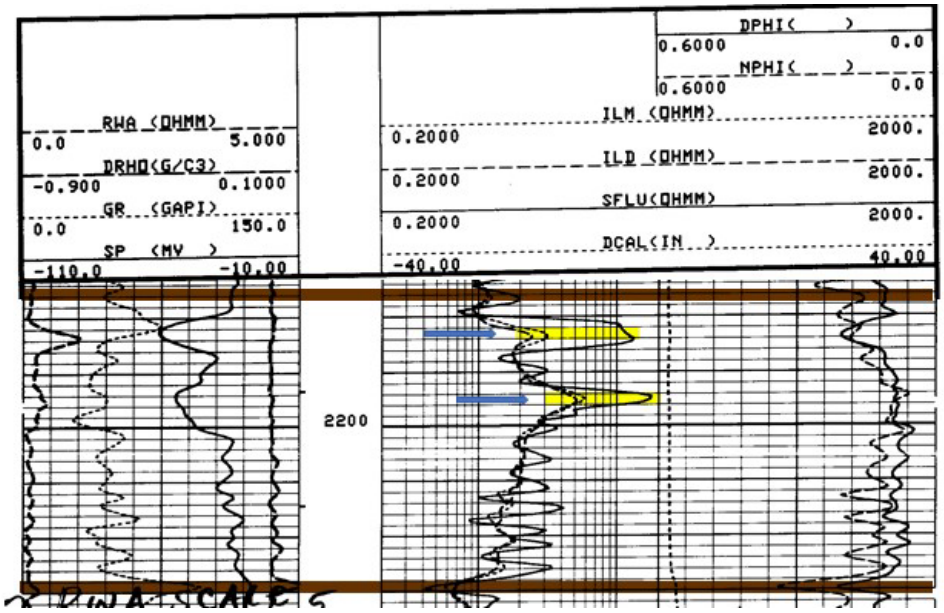

Figure 11-13 **Two examples of depths used in salinity calculations for the Cow Creek limestone highlighted in yellow from BRACS ID 67791. The left-hand side of the log displays the spontaneous potential log (solid line), gamma ray log (thin dashed line), change in density measurements (long dashed line), and the resistivity of water apparent log (medium dashed line). The right-hand side displays the deep induction log (bold dashed line), medium induction log (left most thin dashed line), shallow focused laterolog (solid line), and the differential caliper log (right most small-dashed line). Brown lines represent the mapped top and bottom of the Cow Creek limestone.**

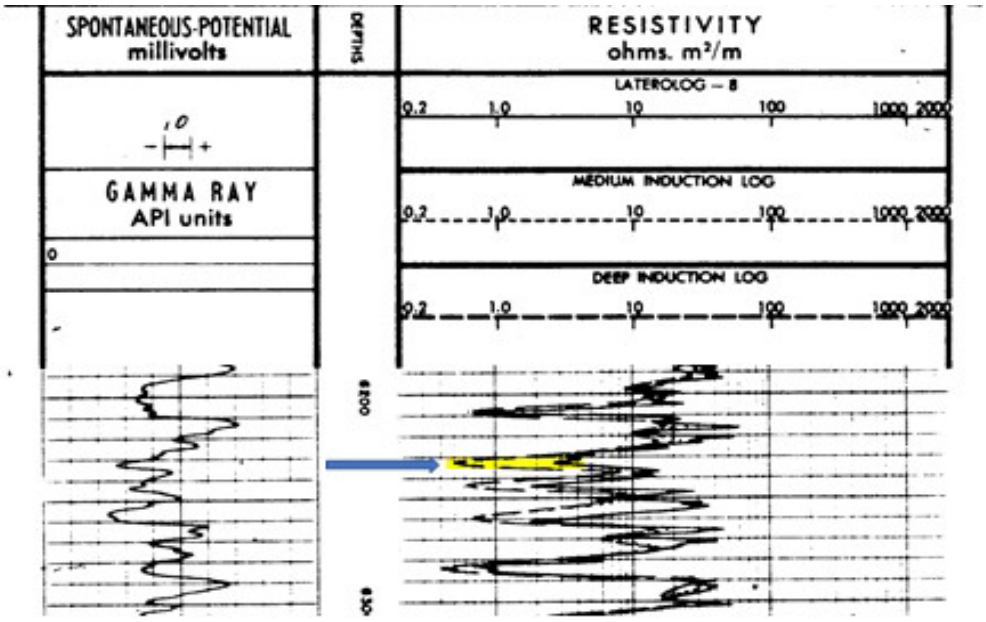

Figure 11-14 **One example of depths used in salinity calculations for the Sligo limestone highlighted in yellow from BRACS ID 68507. The left-hand side of the log displays the spontaneous potential tool, and the right-hand side displays the deep induction log (bold dashed line), medium induction log (thin dashed line), and shallow laterolog (solid line).**

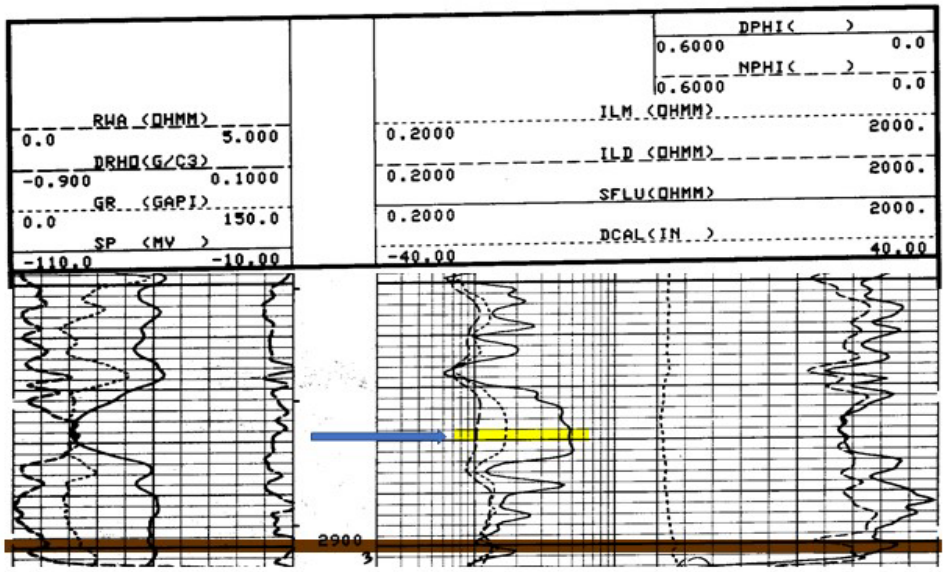

Figure 11-15 **One example of depths used in salinity calculations for the Hosston sandstone highlighted in yellow from BRACS ID 67791. The left-hand side of the log displays the spontaneous potential log (solid line), gamma ray log (thin dashed line), change in density measurements (long dashed line), and the resistivity of water apparent log (medium dashed line). The right-hand side displays the deep induction log (bold dashed line), medium induction log (left most thin dashed line), shallow focused laterolog (solid line), and the differential caliper log (right most small dashed line). The brown line represents the mapped bottom of the Hosston sandstone.**

11.3.6 Alger-Harrison method procedure

Our methodology for calculating groundwater salinity with the Alger-Harrison method is outlined in the steps below:

1. Select a resistivity-type log to analyze which included at a minimum an R_m value in the log header.

2. Calculate a corrected bottom hole temperature (*Tbh)* using the SMU-Harrison equation (Blackwell and others, 2010) with the log reported *Tbh*, total depth of the well (D_t) and a surface temperature from Larkin and Bomar's (1983) 30-year average surface temperature data.

   Depending on the total depth of the well:

   a. $D_t < 3000$

   $$T_{BH\_cor} = T_{BH} \quad \text{(Equation 11-6)}$$

   b. $3000 \leq D_t \leq 12900$

   $$T_{BHC\_cf} = -16.51213476 + 0.01826842109 \cdot D_{tm} - 0.000002344936959(D_{tm})^2 \quad \text{(Equation 11-7a)}$$

   $$T_{BH\_cor} = 1.8\left(T_{BHC} + T_{BHC\_cf}\right) + 32 \quad \text{(Equation 11-7b)}$$

   c. $D_t > 12900$

   $$T_{BH\_cf} = \frac{D_t - 12900}{500} \cdot 0.05 \quad \text{(Equation 11-8a)}$$

   $$T_{BH\_cor} = T_{BH} + 34.3 + T_{BH\_cf} \quad \text{(Equation 11-8b)}$$

3. Select an appropriate depth to perform a calculation (D_f).

4. Determine the formation temperature (T_f) at D_f.

   $$G_g = \frac{T_{BH\_cor} - T_s}{D_t} \quad \text{(Equation 11-9)}$$

   $$T_f = \left(G_g \cdot D_f\right) + T_s \quad \text{(Equation 11-10)}$$

5. If no R_{mf} was provided, or the header reported R_{mf} value was an outlier, calculate an R_{mf} from the empirically determined Hill Country Trinity aquifer relationship of R_m and R_{mf} shown in Equation 11-11.

   If no R_{mf} provided:

   $$R_{mf75} = 0.9157 \cdot R_{m75} - 0.9495 \quad \text{(Equation 11-11)}$$

6. Correct the resistivity of the mud filtrate as reported on the log header to the resistivity for the temperature at D_f, "R_{mf_Tf}".

$$R_{mf\_Tf} = R_{mf} \cdot \frac{T_s}{T_f} \quad \text{(Equation 11-12)}$$

7. Read the shallow resistivity (R_{xo}) and deep resistivity (R_o) from the log.

8. Calculate the resistivity of the groundwater (R_w) at the formation temperature using Alger-Harrison method (Alger and Harrison, 1989).

$$R_{xo\_}R_o = \frac{R_{xo}}{R_o} \quad \text{(Equation 11-13)}$$

$$R_w = \frac{R_{mf}}{R_{xo\_}R_o} \quad \text{(Equation 11-14)}$$

9. Convert the R_w to an R_w at 75 degrees Fahrenheit (R_{w75}).

$$R_{w75} = R_w \cdot \frac{T_f}{75} \quad \text{(Equation 11-15)}$$

10. Convert the R_{w75} to a conductivity of water at 75 degrees Fahrenheit (C_{w75}).

$$C_{w75} = \frac{10000}{R_{w75}} \quad \text{(Equation 11-16)}$$

11. Used the formation specific total dissolved solids and conductivity (C_w) relationship (see Chapter 10 of this report) to convert the C_{w75} into a total dissolved solids value.

Based on formation and C_{w75}:

- Upper Glen Rose limestone or Lower Glen Rose limestone; $C_{w75} \leq 4{,}000$

$$TDS = 9 \cdot 10^{-5} \cdot (C_{w75})^2 + 0.6622C_{w75} + 76.044 \quad \text{(Equation 11-17a)}$$

- Hensell sandstone and Cow Creek limestone; $C_{w75} \leq 4{,}000$

$$TDS = 0.0001(C_{w75})^2 + 0.4215C_{w75} + 222.14 \quad \text{(Equation 11-17b)}$$

- Sligo limestone and Hosston sandstone; $C_{w75} \leq 4{,}900$

$$TDS = 0.7029C_{w75} + 84.748 \quad \text{(Equation 11-17c)}$$

- Upper Glen Rose limestone, Lower Glen Rose limestone, Hensell sandstone, or Cow Creek limestone; $4{,}000 < C_{w75} \leq 15{,}000$

$$TDS = 0.5801C_{w75} + 1826.5 \quad \text{(Equation 11-17d)}$$

- Sligo limestone or Hosston sandstone; $4{,}900 < C_{w75} \leq 10{,}000$

$$TDS = 0.377C_{w75} + 1699.3 \quad \text{(Equation 11-17e)}$$

- Upper Glen Rose limestone, Lower Glen Rose limestone, Hensell sandstone, or Cow Creek limestone; $C_{w75} > 15{,}000$
  $TDS = 0.6644C_{w75} + 442.87$ (Equation 11-17f)

- Sligo limestone or Hosston sandstone; $C_{w75} > 10{,}000$
  $TDS = 0.6388C_{w75} - 951.91$ (Equation 11-17g)

Where:

C_{w75} = conductivity of water at 75 degrees Fahrenheit, (microsiemens-centimeter)

D_t = total depth of the well, (feet)

D_{tm} = total depth of the well, (meters)

G_g = geothermal gradient, (unitless)

R_{m75} = mud resistivity at 75 degrees Fahrenheit, (ohm-meter)

R_{mf75} = mud filtrate resistivity at 75 degrees Fahrenheit, (ohm-meter)

R_{mf_Tf} = the mud filtrate resistivity at the formation temperature, (ohm-meter)

R_{w75} = the water resistivity at 75 degrees Fahrenheit, (ohm-meter)

$R_{xo}\_R_o$ = the ratio of the shallow resistivity measurement to the deep resistivity measurement, (unitless)

T_{BH} = the temperature of the bottom hole, (degrees Fahrenheit)

T_{BH_cf} = the correction factor to the bottom hole temperature, (degrees Fahrenheit)

T_{BH_cor} = the corrected bottom hole temperature, (degrees Fahrenheit)

T_{BHC} = the bottom hole temperature, (degrees Celsius)

T_{BHC_cf} = the correction factor to the bottom hole temperature, (degrees Celsius)

T_f = the temperature of the formation, (degrees Fahrenheit)

T_s = the surface temperature, (degrees Fahrenheit)

TDS = Total dissolved solids estimate, (milligrams per liter)

Note that for our calculations which were executed in the BRACS database, steps 3 and 10 are rounded to an integer, and steps 4 through 9 are rounded to two digits. Additionally, this routine is performed in the BRACS database using custom-coded class modules and forms written in Visual Basic for Applications. These results are saved directly to the BRACS database.

These calculations were conducted for as many depths as seemed appropriate in a formation. After the calculations were completed for a formation, we averaged the values together to assign a salinity classification to the formation. We used these salinity calculations to map formation groundwater salinity classes as detailed in Section 12 of this report.

In Figure 11-16, we have marked an example well log to indicate where we performed calculations to determine the salinity of the formation water. The results of these calculations are detailed in Table 11-3 which summarizes the calculation inputs, relevant mid-points, calculated total dissolved solids values, and the final salinity classification for this example well.

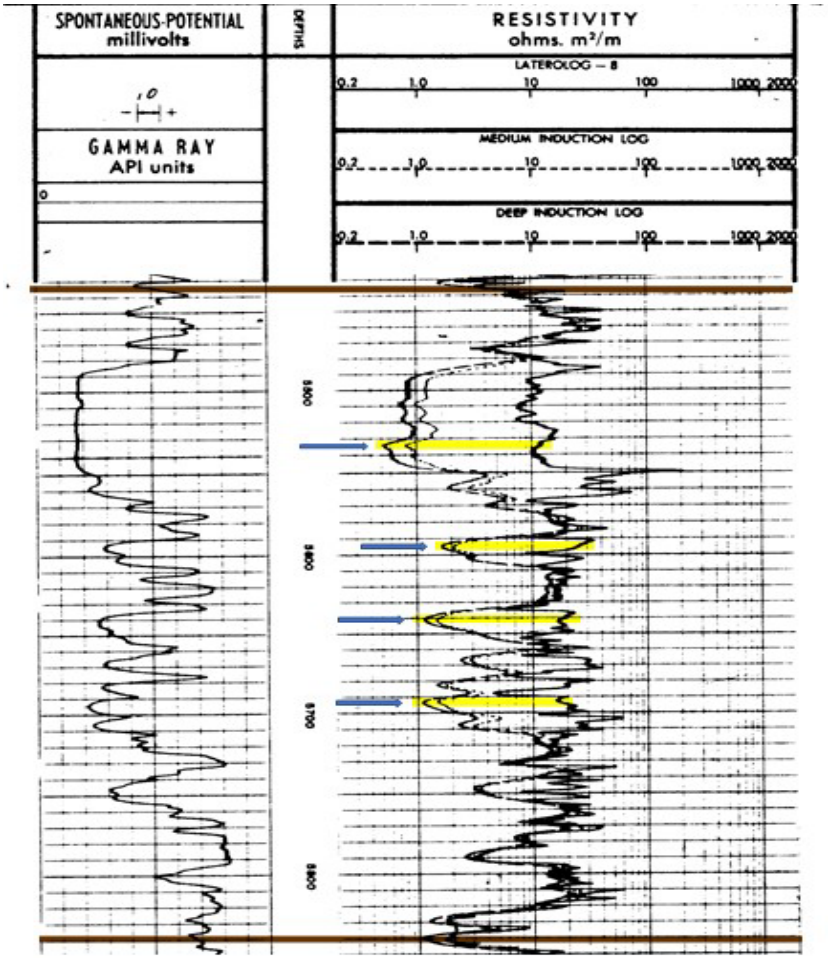

Figure 11-16 **Depths selected (yellow highlights) to assign a salinity classification for the Lower Glen Rose limestone for example BRACS ID 68507. The left-hand side of the log displays the spontaneous potential tool, and the right-hand side displays the deep induction log (bold dashed line), medium induction log (thin dashed line), and shallow laterolog (solid line). Brown lines represent the mapped top and bottom of the formation.**

Table 11-3 Summary of calculation inputs and intermediate values for example BRACS ID 68507 used to derive the salinity classification for the Lower Glen Rose limestone. (Note that an "*" denotes a calculated input parameter.)

Log header information	**Run**	R_m	T_{Rm}	R_{mf}	T_{Rmf}	T_{BH}		
	2	1.73	97	1.9*	75*	145		
Additional calculation input information	T_s			T_{BH_cor}				
	68			162.8				
D_f	T_f	R_{mf_Tf}	R_{xo}	R_o	R_w	R_{w75}	C_{w75}	TDS
5534	151	0.94	11	0.5	0.04	0.08	12,5000	83,493
5594	152	0.94	28	1.7	0.06	0.12	83,333	55,810
5641	153	0.93	18	1.1	0.06	0.12	83,333	55,810
5693	154	0.93	16	1.1	0.06	0.12	83,333	55,810
salinity classification					brine	average TDS		62,731

11.3.7 QA/QC procedures

We utilized a few methods to assess the quality of the calculations we performed. Since the majority of our calculations are performed in regions of the aquifer without measured control, we could not compare the calculations to measurements. Instead, we had team members review calculations and resulting salinity classifications, we utilized mapping to identify unexpected salinity trends, and we also plotted the depth a calculation was performed at and the resulting total dissolved solids for each hydrostratigraphic unit (Figure 11-17 to Figure 11-22). Team review and mapping of calculated values identified some inappropriate calculation depths, which were then corrected. Plotting depth to a formation calculation (D_f) and total dissolved solids did not necessarily reveal inappropriate calculations, but it did identify outlier data and calculated values that are potentially high due to rounding. The outlier data identified from the plots did not affect the salinity mapping because the values calculated as brackish.

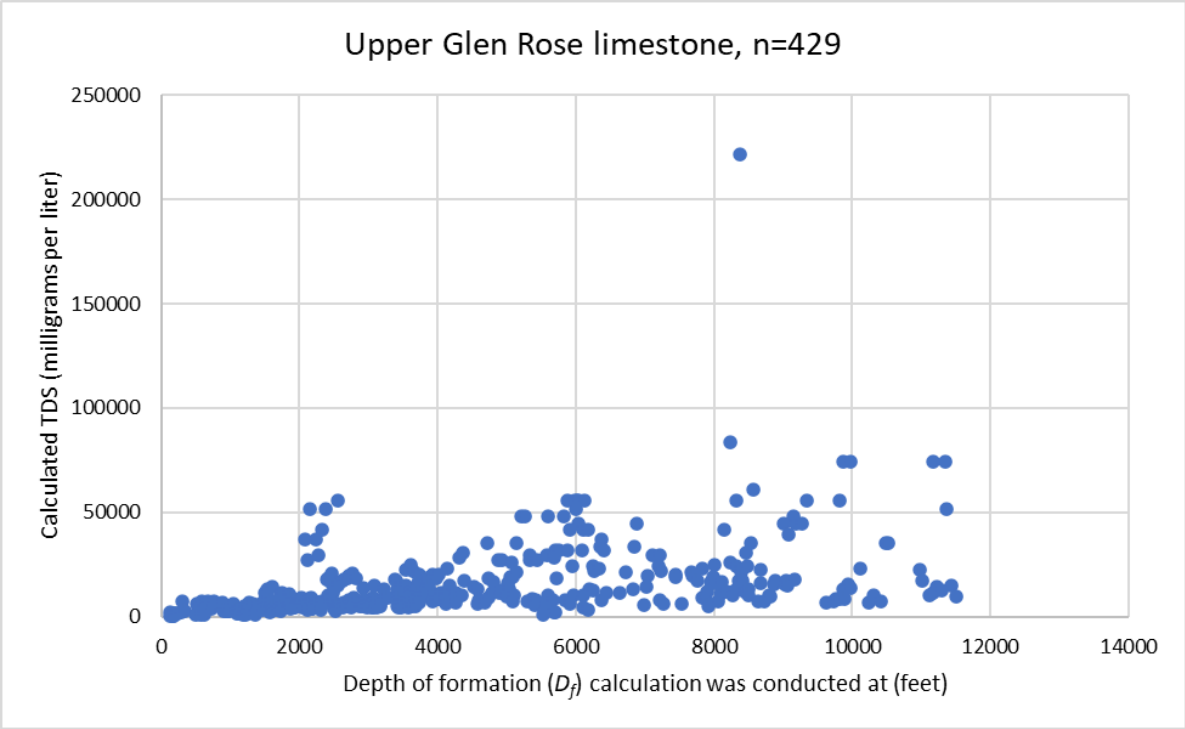

Figure 11-17 Depth of formation (D_f) in feet and the calculated total dissolved solids (TDS) in milligrams per liter for the Upper Glen Rose limestone.

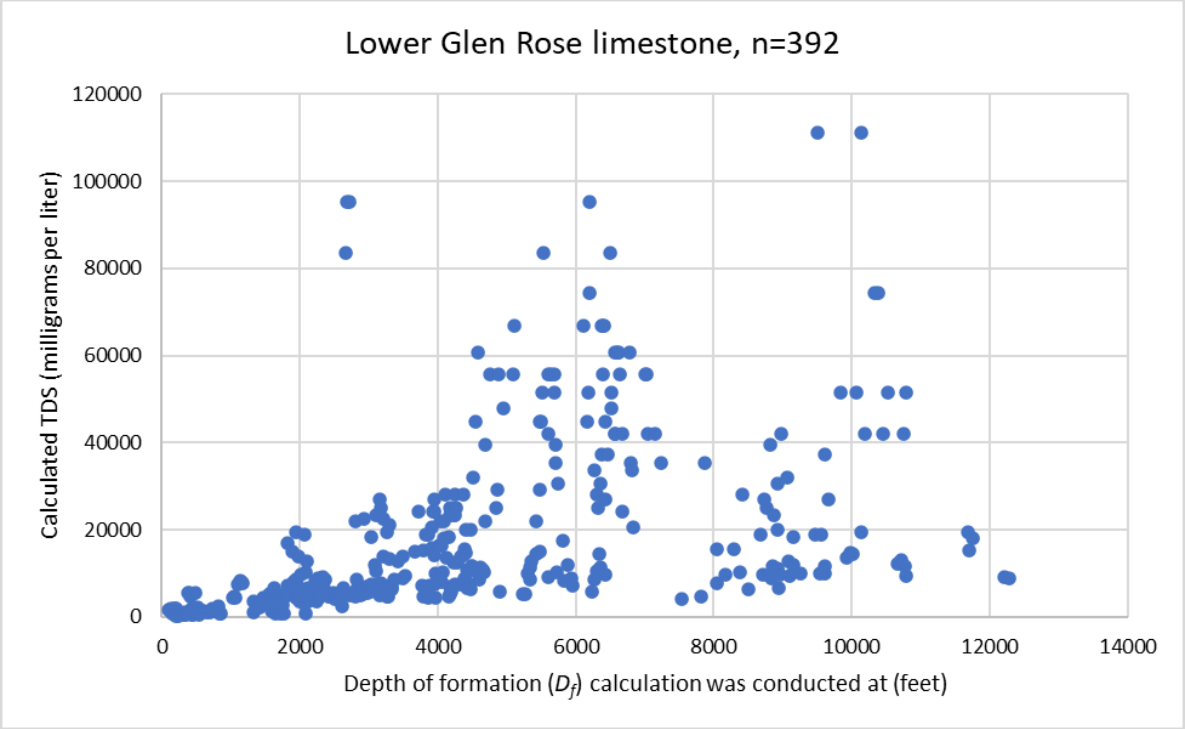

Figure 11-18 Depth of formation (D_f) in feet and the calculated total dissolved solids (TDS) in milligrams per liter for the Lower Glen Rose limestone.

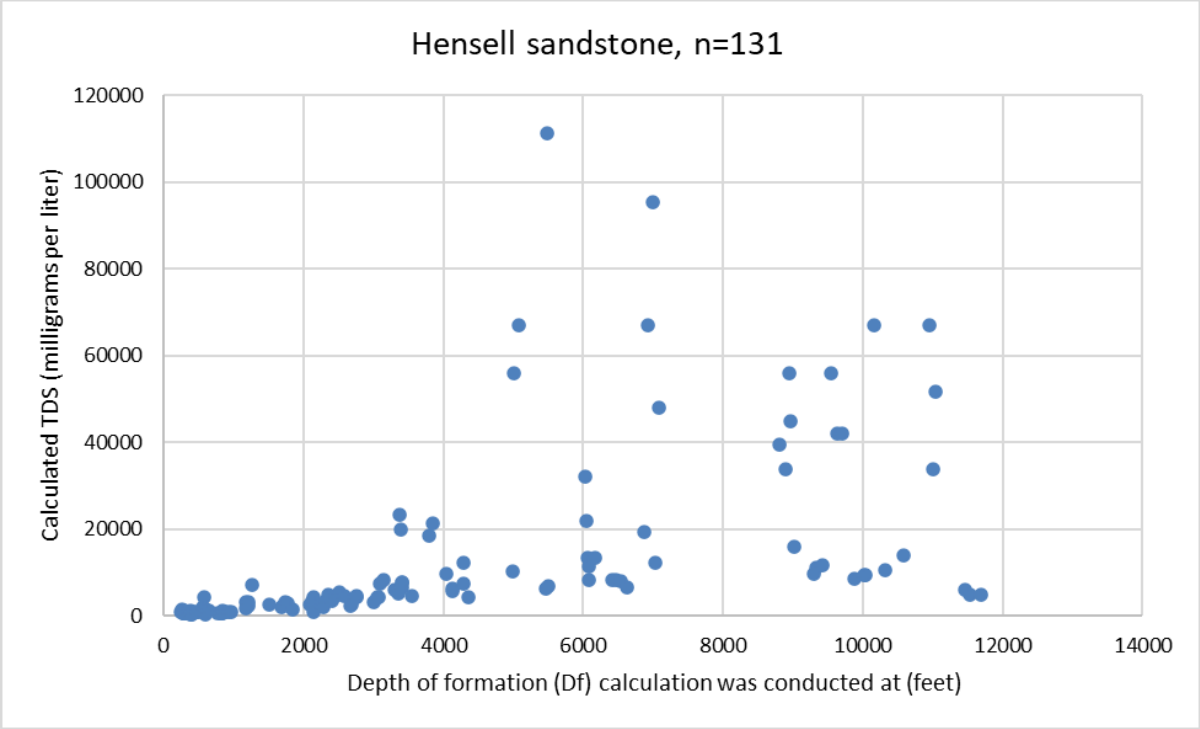

Figure 11-19 Depth of formation (D_f) in feet and the calculated total dissolved solids (TDS) in milligrams per liter for the Hensell sandstone.

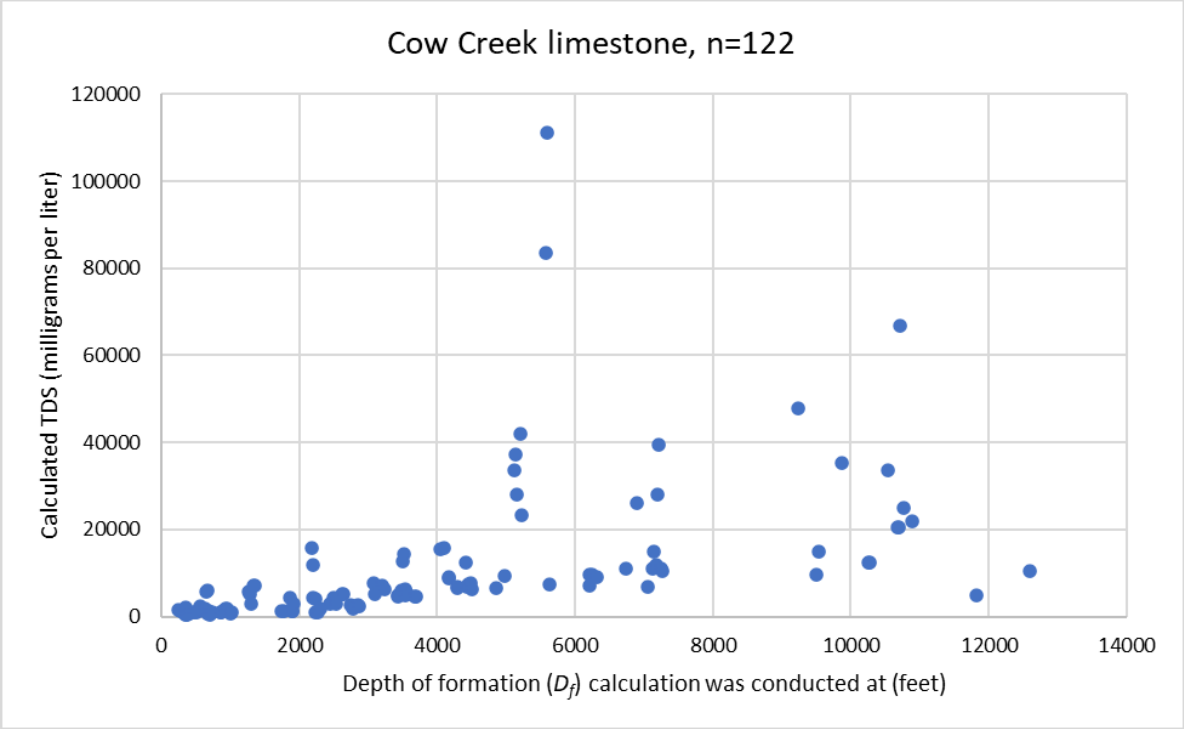

Figure 11-20 Depth of formation (D_f) in feet and the calculated total dissolved solids (TDS) in milligrams per liter for the Cow Creek limestone.

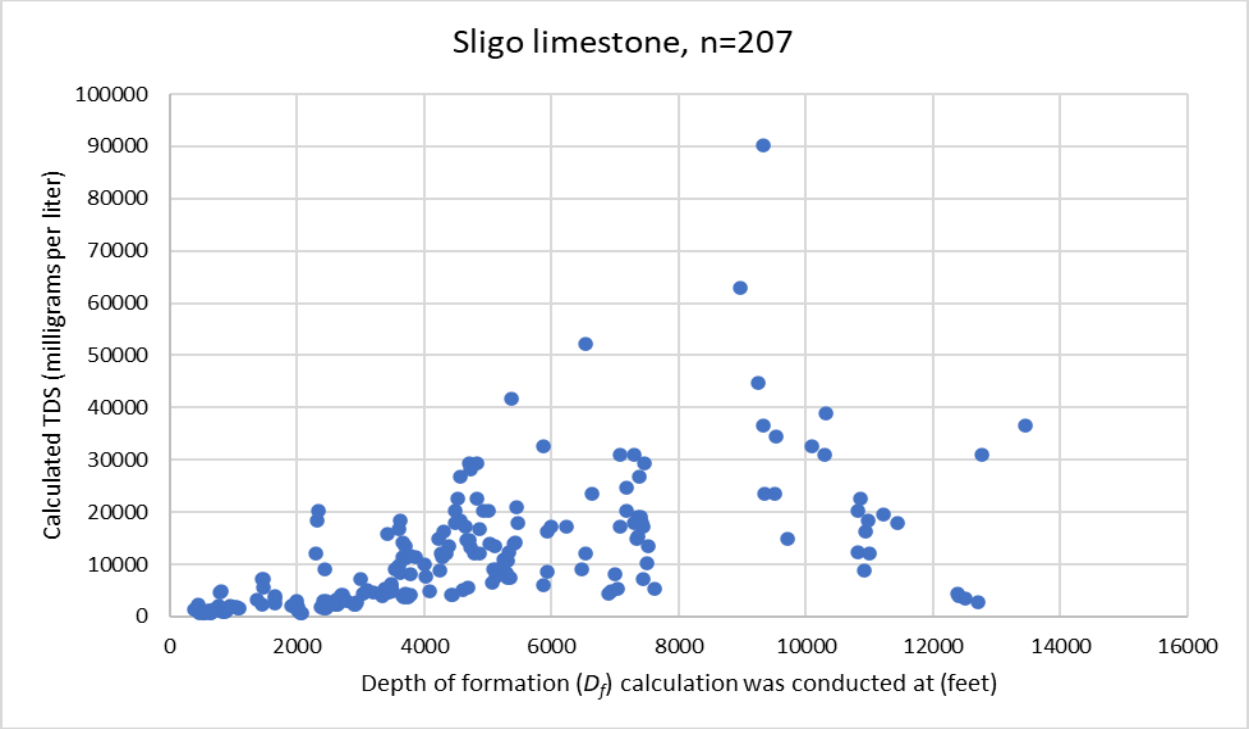

Figure 11-21 Depth of formation (D_f) in feet and the calculated total dissolved solids (TDS) in milligrams per liter for the Sligo limestone.

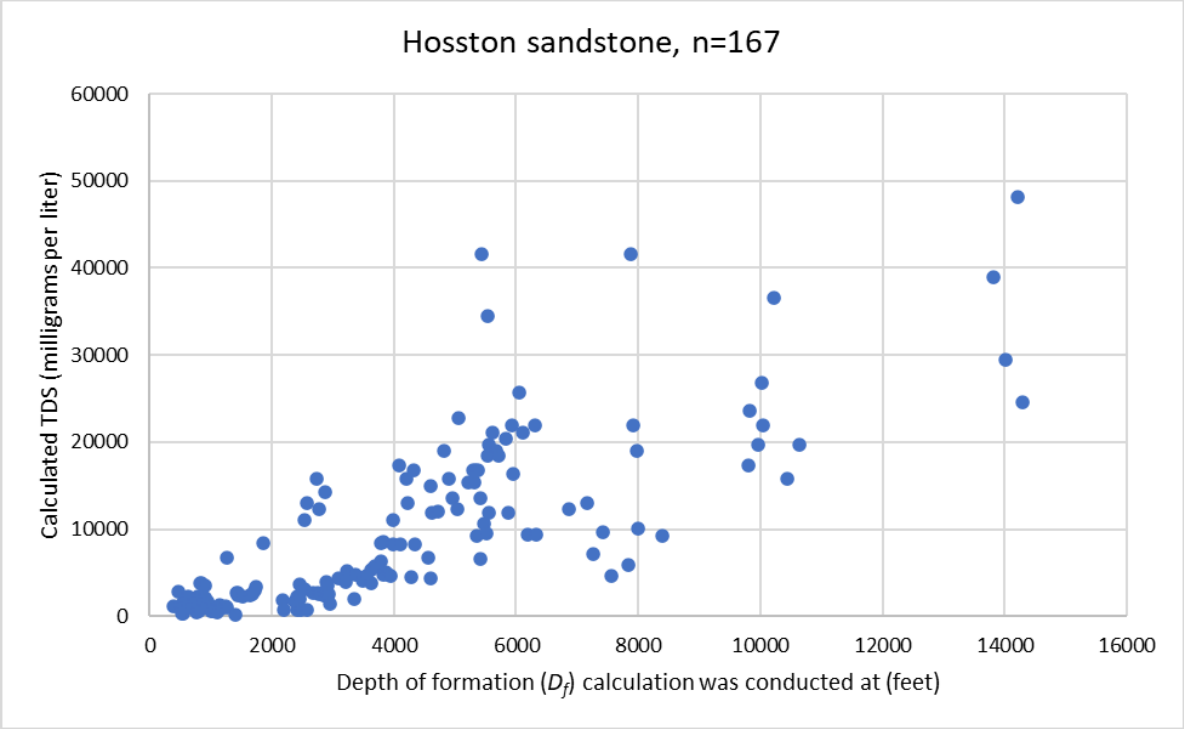

Figure 11-22 Depth of formation (*Df*) in feet and the calculated total dissolved solids (TDS) in milligrams per liter for the Hosston sandstone.

11.4 Salinity calculations discussion

Generally, we see that total dissolved solids increase with depth in all of the mapped hydrostratigraphic units (Figure 11-17 to Figure 11-22). However, the scatter plots exhibit heteroscedasticity (scatter), suggesting that depth is not the only variable correlating to the increase in total dissolved solids. Faulting could certainly complicate this relationship because it could potentially slow the flow of water downdip (Camp and others, 2020). Faulting can also act as an impervious block to groundwater flow further restricting downdip flow of groundwater. Other possible reasons for increased salinity in shallow groundwater could be the presence of mineral deposits such as gypsum or anthropogenic influences.

Additionally, although we did not conduct a rigorous uncertainty analysis for this study, our salinity calculations likely become less reliable beyond 10,000 milligrams per liter total dissolved solids. This reduction in reliability is likely attributable to several reasons. The first, and primary reason, is that we lose measured water quality control beyond about 4,000 milligrams per liter total dissolved solids. Further, as explained in Section 10 of this report, our estimate of what water quality should look like beyond 10,000 milligrams per liter total dissolved solids is in part based upon our best estimate of the expected dominant water chemistry.

The second reason we likely lose reliability is that we utilize well logs from approximately 70 years of logging in the Hill Country Trinity aquifer study area. These tools will have various designs and associated degrees of accuracy. Presumably newer tools will be more accurate than older tools. Depending on the mud parameters, resistivity measurements as low as less than one ohm-meter are used to calculate total dissolved solids, and newer tools would likely be able to measure resistivity more accurately.

A third reason salinity calculations may be less reliable beyond 35,000 milligrams per liter total dissolved solids is related to the rounding we used in our calculations. In brine groundwater (greater than 35,000 milligrams per liter total dissolved solids), we found that the numerical rounding built into the BRACS database could change calculated total dissolved solids by more than 10,000 milligrams per liter. However, we only begin to see this effect with calculated values greater than 60,000 milligrams per liter total dissolved solids. The numerical rounding error observed does not impact the mapped salinity zones classifications because all groundwater with total dissolved solids greater than 35,000 milligrams per liter total dissolved solids would classify as brine.

The specific conductivity – total dissolved solids conversion (*ct*) factor is a way to convert a sodium chloride equivalent total dissolved solids value to a study area representative total dissolved solids value. Previous brackish groundwater mapping studies by the TWDB have utilized a *ct* factor in calculating total dissolved solids from specific conductance (*Cw*) (Wise, 2014, Meyer and others, 2014; Robinson and others, 2018; Meyer and others, 2020). We however did not use a *ct* factor since we established empirical relationships between total dissolved solids and specific conductance.

Additionally, Estepp (2010) describes an R_{mf} correction based on mud type for the Alger-Harrison method. We reviewed the study cited by Estepp that details the SP method for calculating total dissolved solids (Alger, 1966), and could not find support for using a mud type correction with the Alger-Harrison method.

12 Salinity class determination

The combined datasets of total dissolved solids from the measured water quality samples and the calculated water qualities from geophysical well logs were used to map groundwater salinity. We used all samples for which the aquifer determination process was able to uniquely associate a single hydrostratigraphic unit of the Hill Country Trinity aquifer. With this data, we generated salinity class maps for each hydrostratigraphic unit (Figure 12-1 to Figure 12-6).

Measured water quality analyses were assigned an aquifer code from the aquifer determination process discussed in Section 8. Calculated total dissolved solids values were obtained in the salinity estimation process described in Section 11 of this report. If more than one calculation was performed for a formation in a well, we used the average of the calculated values in determining the appropriate salinity class. When defining salinity classes from the total dissolved solids values, we gave preference to measured water quality.

The creation of the salinity classes went through a series of iterations to validate samples or calculations that appeared to be anomalous. We identified a number of groundwater samples that had been assigned to the Upper Glen Rose limestone that were actually water wells producing from the Edwards Aquifer. These samples occurred in areas where there was insufficient data to accurately model the Upper Glen Rose limestone surface in structurally complex areas of the Balcones Fault Zone. We further identified some of the calculated values as anomalous compared to adjacent water quality samples. These data points have been marked with an “x” on some of the maps.

In addition to considering the plotted total dissolved solids values, we considered the location of faults used to develop the stratigraphic rasters when contouring the salinity classes. Because the stratigraphic rasters developed for the study do not include all faulting in the study area, we found that in highly faulted areas some of the measured water quality analyses were assigned to the wrong hydrostratigraphic unit. The data points determined to be improperly assigned are marked with an ‘x’ on the maps.

The salinity zones are considered to exist in three dimensions delimited above and below by the corresponding stratigraphic surfaces. Our analysis treats the salinity of the groundwater to be constant within a salinity zone. This is a significant simplification as the range for very saline groundwater (10,000 to 35,000 milligrams per liter of total dissolved solids) demonstrates. It would also be expected that thick hydrostratigraphic units such as the Hosston sandstone could see groundwater of varying salinity between the top of the unit and the base of the unit at a specific location. Table 12-1 shows the average and maximum depths to the upper bounding surface for each salinity class for the entire study area. These values are presented to provide a numerical comparison and should not be used for specific site location analysis.

Table 12-1 Average and maximum depths of salinity zones.

Hydrostratigraphic unit	Salinty	Average depth (feet)	Maximum depth (feet)
Upper Glen Rose limestone	Fresh	45	1,758
	Slightly saline	297	1,819
	Moderately saline	2,257	7,018
	Very saline	5,732	8,904
Lower Glen Rose limestone	Fresh	288	2,509
	Slightly saline	740	2,853
	Moderately saline	2,728	8,096
	Very saline	5,787	9,879
Hensell sandstone	Fresh	423	3,168
	Slightly saline	1,193	3,057
	Moderately saline	3,935	9,742
	Very saline	6,290	10,153
Cow Creek limestone	Fresh	559	3,409
	Slightly saline	1,238	3,187
	Moderately saline	3,620	7,608
	Very saline	7,260	10,849
Sligo limestone	Fresh	702	2,261
	Slightly saline	1,415	3,554
	Moderately saline	3,645	7,165
	Very saline	7,669	11,328
Hosston sandstone	Fresh	708	3,734
	Slightly saline	1,419	3,970
	Moderately saline	3,897	7,296
	Very saline	7,643	11,953

12.1 Salinity maps discussion

We reviewed the salinity maps for the six hydrostratigraphic units of the Hill Country Trinity aquifer. In general, we found that groundwater that is classified as very brackish or brine exists in the deeper southern and southeastern portions of the study area. We also observed in all of the hydrostratigraphic units that these two most brackish zones can be seen to spatially overlap. This indicates that the transition to groundwater with greater than 10,000 total dissolved solids occurs at increasing depths for each hydrostratigraphic zone. The average depth to the top of very saline groundwater for the Upper Glen Rose limestone is 5,732 feet below ground surface compared to 7,643 feet for the Hosston sandstone (Table 12-1).

Moderately saline groundwater lies updip from the more saline zones in a 10 mile to 25-mile-wide band across the middle of the project area. We did find that the moderately saline groundwater zone in western Zavala County appears to extend much deeper than we would generally expect. We also observed that moderately saline groundwater could

be found in western Bandera County for all hydrostratigraphic zones. Isolated areas of moderately saline groundwater can also be seen in Travis, Blanco, and Kendall counties in water wells that were most likely completed in Upper and Lower Glen Rose limestone intervals that included evaporite deposits.

We found that the slightly saline and fresh groundwater zones are significantly intermingled in all zones across the northern half of the study area. Except for the Hosston sandstone unit, we observed a relatively narrow band of slightly saline groundwater, 5 miles to 8 miles wide, in southern Travis, Hays, and Comal counties. Except for the Upper Glen Rose limestone unit, we observed the slightly saline zone in Bexar, Medina, Bandera, and Uvalde counties to expand broadly.

There are a few common threads between the mapped hydrostratigraphic units:

- In general, salinity increases downdip from north to south and from northwest to southeast in all hydrostratigraphic units.
- We observed relatively more saline groundwater in northwestern Bandera County in all hydrostratigraphic units. While this trend is only driven by a few data points, we did not find the data points to be anomalous during our QA/QC. Additional measured samples would help verify and define this trend.
- Relatively narrow transitions from less saline to more saline groundwater can occur across faults in every hydrostratigraphic unit.
- Slightly saline and moderately saline measured groundwater samples occur in updip and generally freshwater portions of the Upper and Lower Glen Rose limestones and Cow Creek limestone. These were not found to be anomalous during our QA/QC process and may be the result of water well completions that are open to evaporite beds.

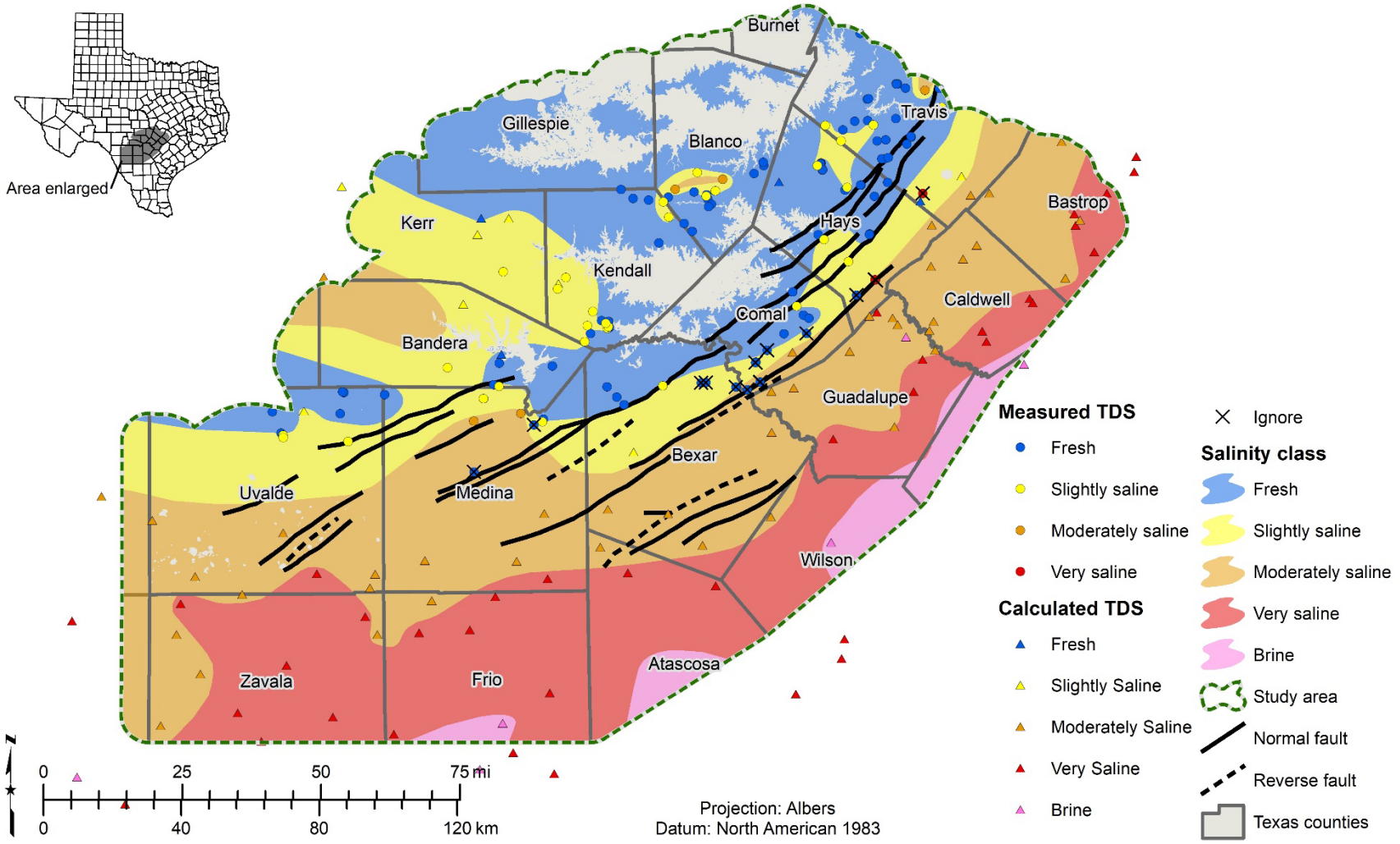

Figure 12-1 Salinity classes and well control in the Upper Glen Rose limestone.

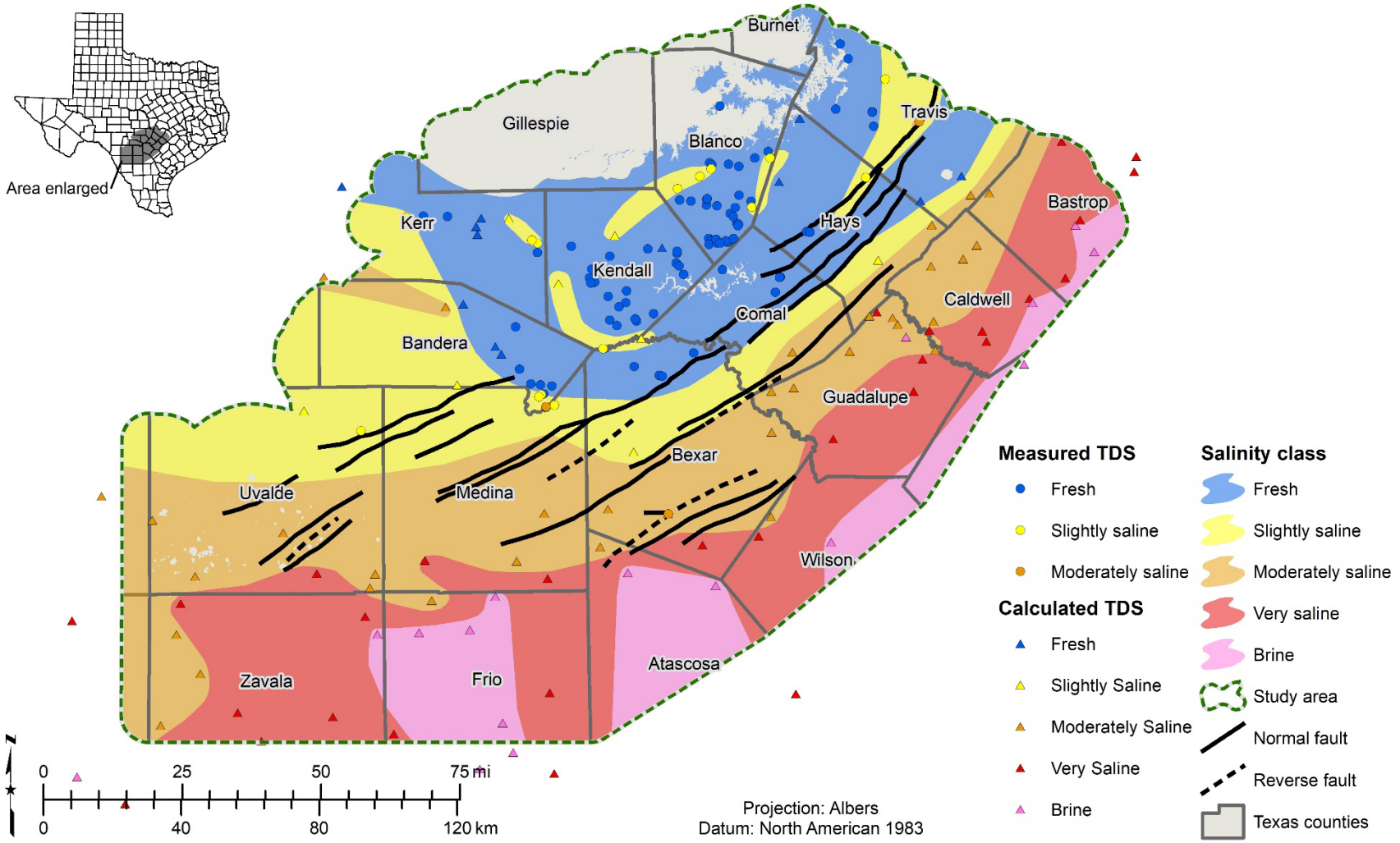

Figure 12-2 Salinity classes and well control in the Lower Glen Rose limestone.

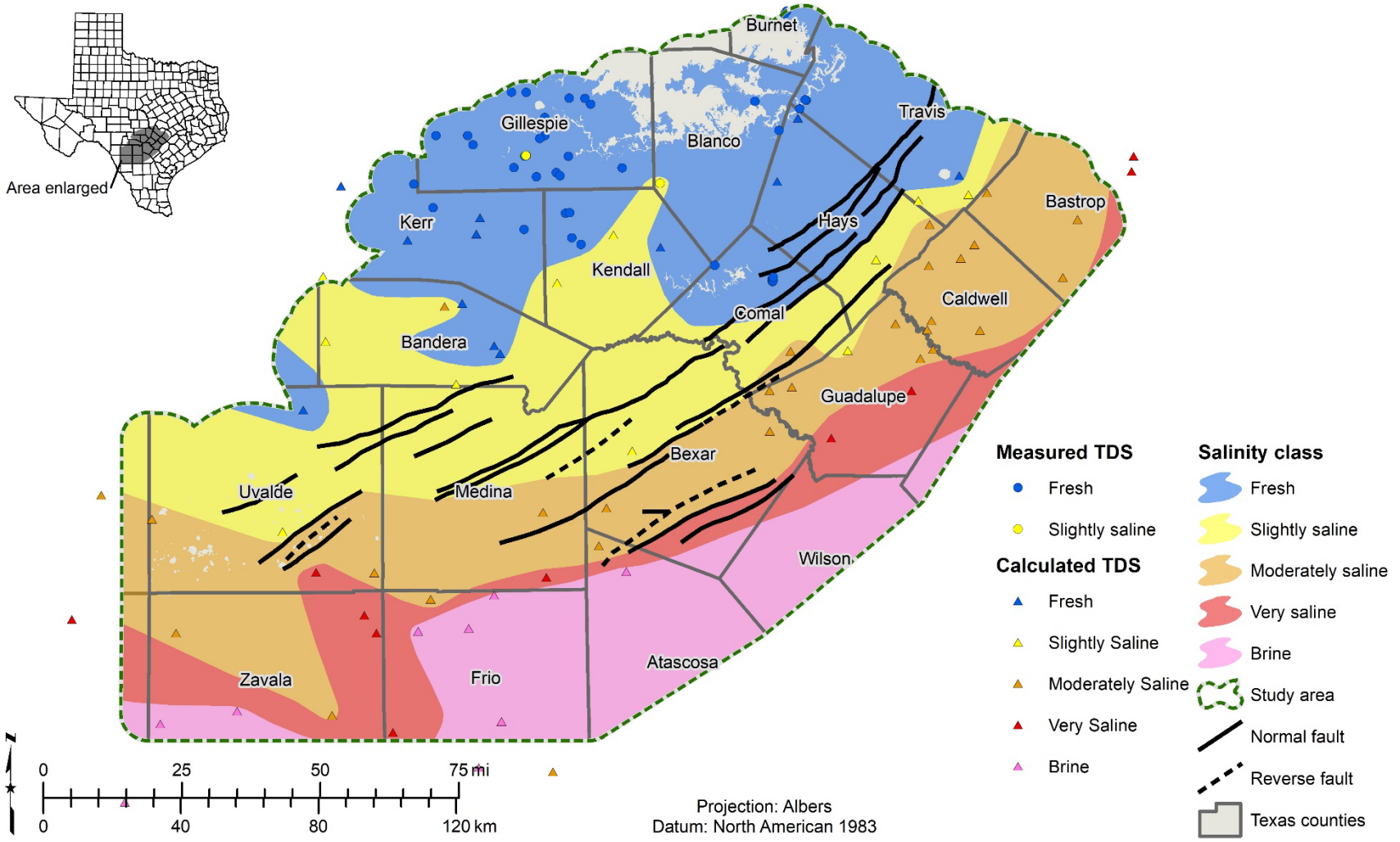

Figure 12-3 Salinity classes and well control in the Hensell sandstone.

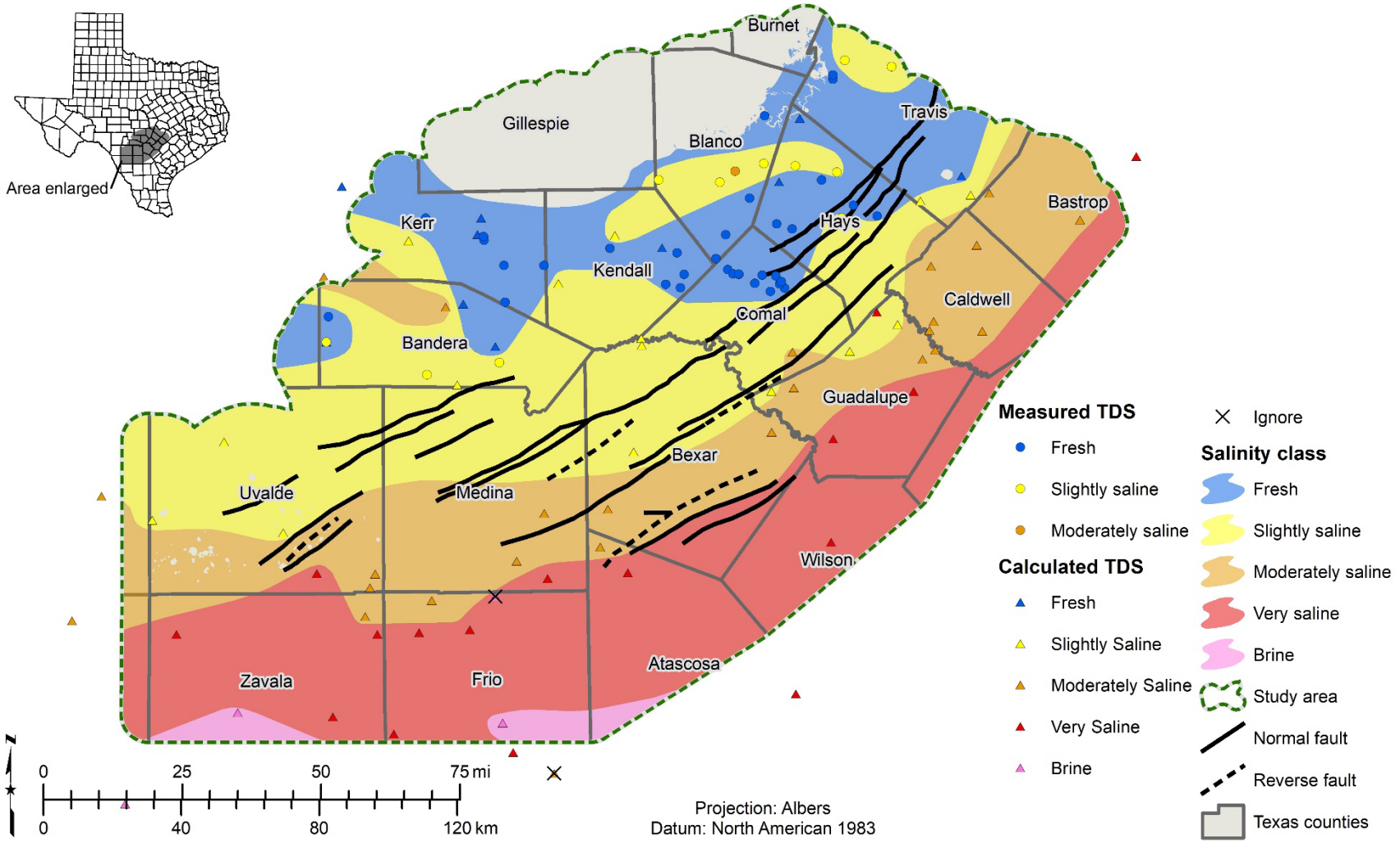

Figure 12-4 Salinity classes and well control in the Cow Creek limestone.

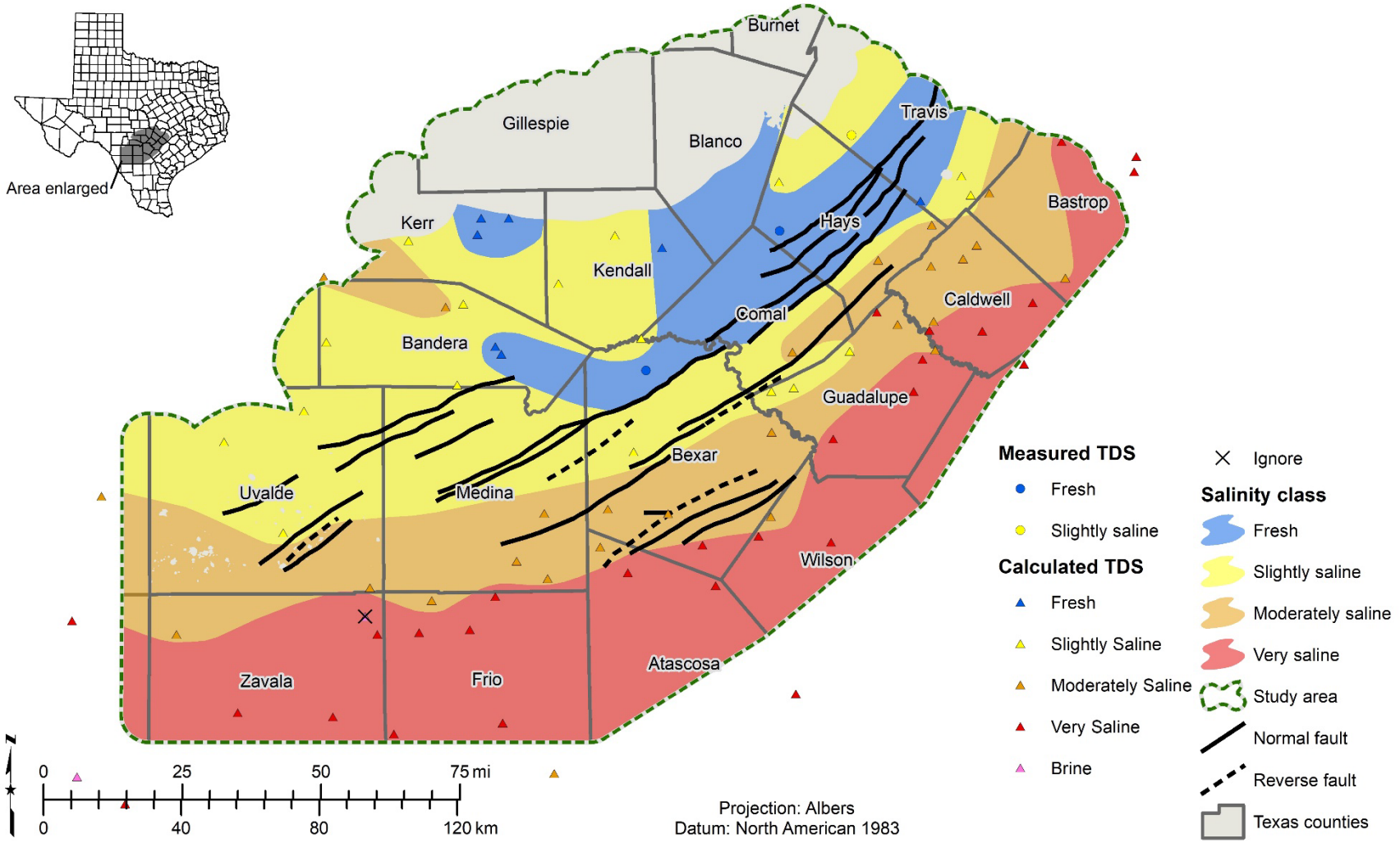

Figure 12-5 Salinity classes and well control in the Sligo limestone.

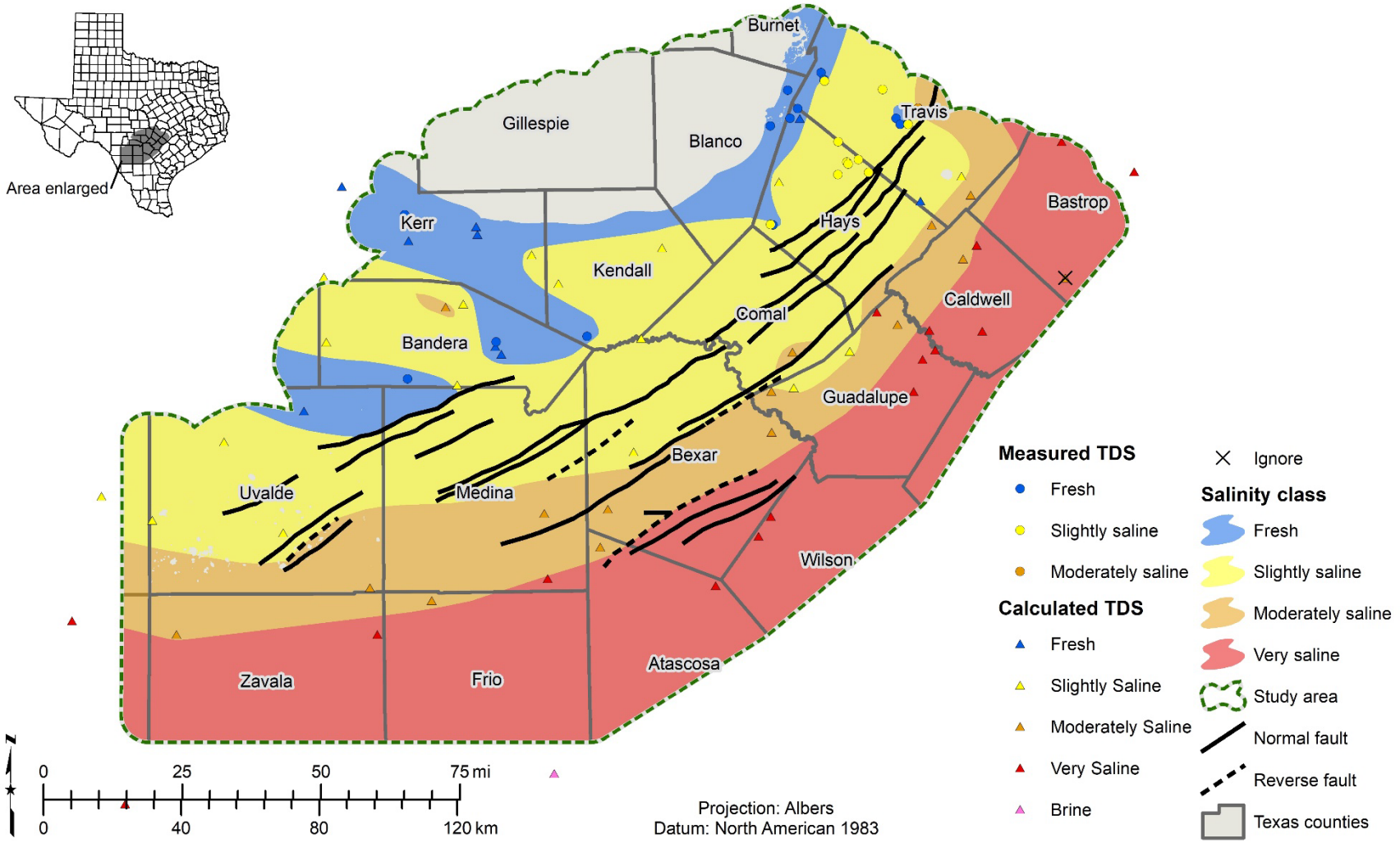

Figure 12-6 Salinity classes and well control in the Hosston sandstone.

13 Groundwater volumes

Total aquifer storage volumes of brackish groundwater were calculated for the six water-bearing hydrostratigraphic units defined for the Hill Country Trinity aquifer. We used the stratigraphic surfaces, salinity zones, aquifer properties, and static water level surfaces composed of both measured and estimated elements to calculate groundwater volumes. Of the approximately 979 million acre-feet of groundwater in the Hill Country Trinity aquifer, about 90 percent (887 million acre-feet) are brackish with salinities of between 1,000 to 35,000 milligrams-per-liter of total dissolved solids. The largest volume contribution is from the Hosston sandstone which contains almost 40 percent (390 million acre-feet) of the volume of which approximately 98 percent (382 million acre-feet) is brackish.

Our primary purpose for calculating these volumes is to provide some form of quantitative volumetric measurement of the brackish groundwater resources of the Hill Country Trinity aquifer study area. These volumes should not be used for formal water planning purposes, nor should they be used in place of site-specific studies when developing a well field.

13.1 Static water levels and saturated thickness

We queried static water level measurements from the TWDB Groundwater Database (64,386 records) and the TWDB BRACS database (16,660 records) for wells within the study area. We restricted our selection to static water level measurements dating from the year 1911 to 2018 and collected them into table ***tblBracs_SWL***, stored in the TWDB BRACS database. To approximate current static water level elevations, we included only the most recent record for each well with a measurement year greater than or equal to 2010 for our mapping.

We assigned a Trinity Group hydrostratigraphic unit to each static water level record by using our aquifer determination method described in Section 8 of this report. We chose to map static water level elevations for the three Trinity hydrologic units (Upper, Middle, and Lower) rather than by the six hydrostratigraphic units for two reasons: 1) we lack sufficient data to adequately interpolate static water levels for individual hydrostratigraphic units (particularly for the Cow Creek limestone and Sligo limestone), and 2) we assume there is hydraulic connectivity between the hydrostratigraphic units within their respective hydrologic units, thus their static water level elevations should be equal.

First, we isolated static water level elevation records representing the upper Trinity (Upper Glen Rose limestone; number of records = 28), middle Trinity (Lower Glen Rose limestone, Hensell sandstone, and Cow Creek limestone; number of records = 155), and lower Trinity (Sligo limestone and Hosston sandstone; number of records = 43). Next, we interpolated static water level elevation surfaces for each Trinity hydrologic unit using the Topo to Raster tool in ArcGIS 10.7.

We found that the static water level measurements were only from wells updip of the Balcones Fault Zone, and because the ground elevation in the study area decreases downdip of the Balcones Fault Zone, our static water level interpolations extended well above the ground surface in the downdip regions of the study area. We also noted that there are no known flowing artesian Trinity Aquifer wells south of the Balcones Fault Zone, and so the static water level is unlikely to be above the ground surface. Therefore, where our interpolations from static water level measurements extend above the ground surface, we decided to set the static water level elevations equal to halfway between the ground surface and top surface of the uppermost hydrostratigraphic unit in each hydrologic unit to approximate what we believe are reasonable static water level elevations. This possibly conservative approach represents a reasonable approximation where no static water level data exists.

Through the above assumptions, our resulting static water level elevations over the study area are equal to interpolation of static water level elevation data where the interpolation is below the ground surface (generally in the updip half of the study area), and where the interpolation of static water level elevation is above the ground surface, we set the static water level elevation equal to halfway between the ground surface and top of the upper hydrostratigraphic unit for each hydrologic unit.

Maps of the final static water elevation surfaces used for our calculations of total aquifer storage volumes of brackish groundwater are shown in Figure 13-1 to Figure 13-3.

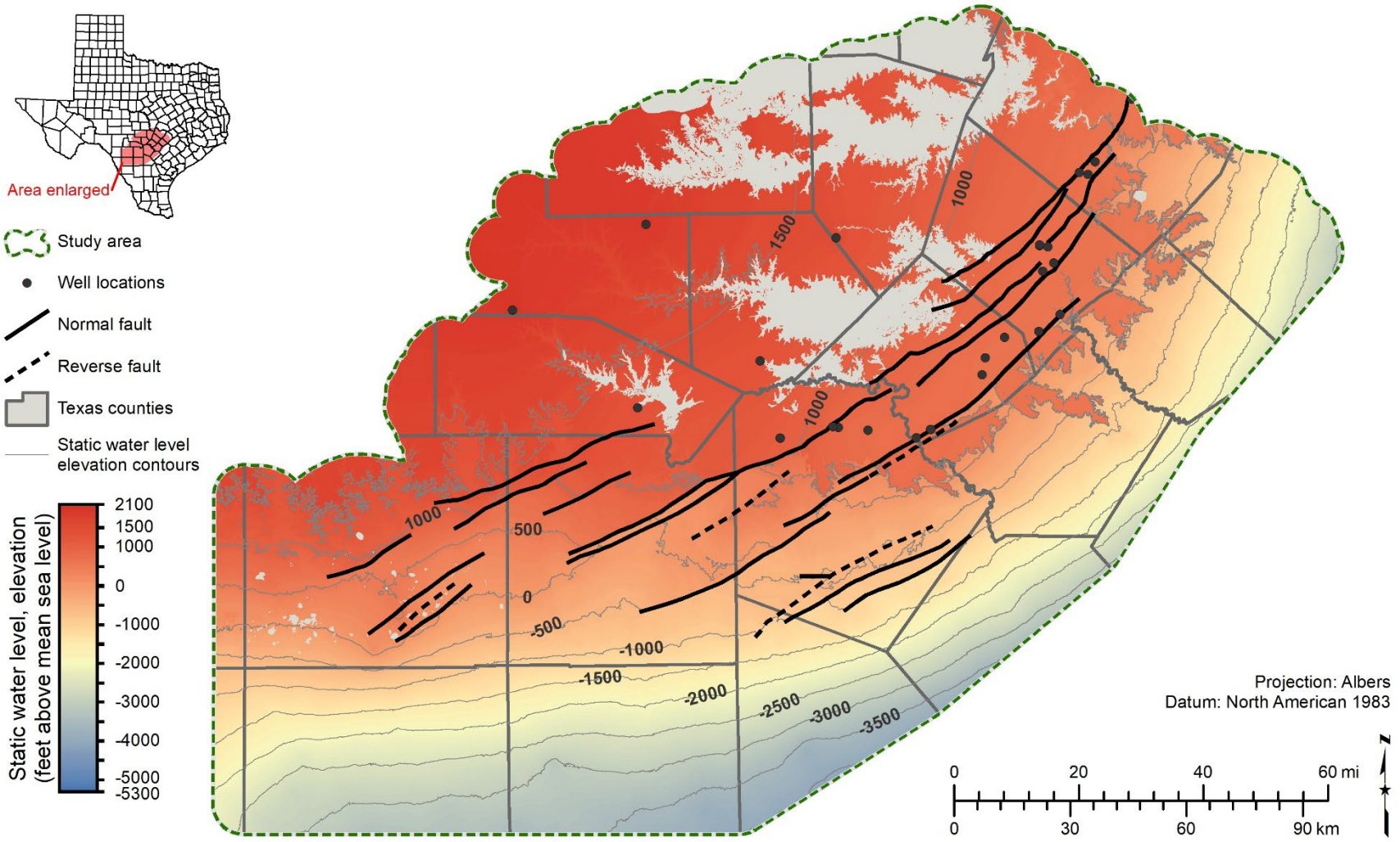

Figure 13-1 Upper Trinity (Upper Glen Rose limestone) static water level elevation (number of wells = 28).

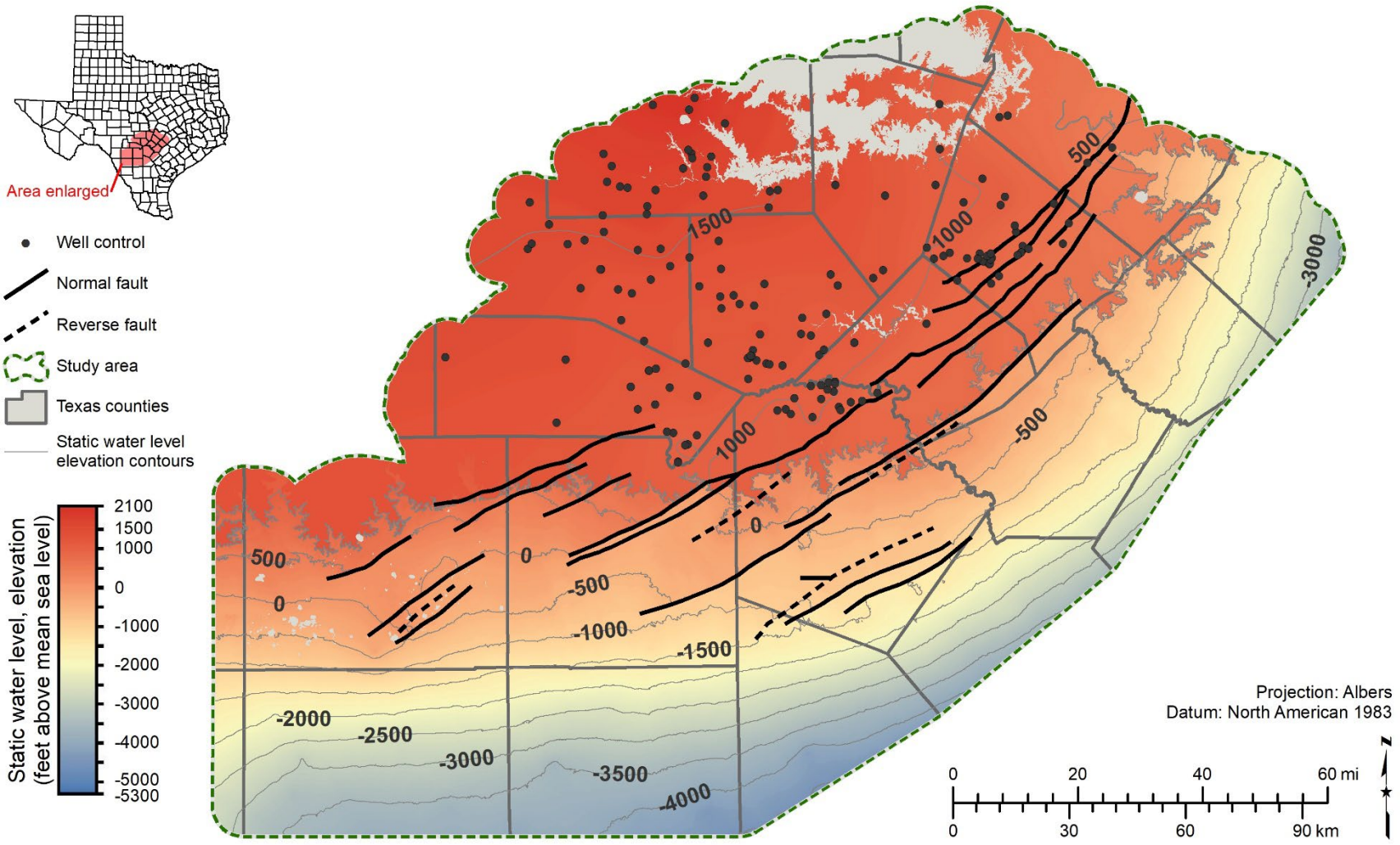

Figure 13-2 **Middle Trinity (Lower Glen Rose limestone, Hensell sandstone, and Cow Creek limestone) static water level elevation (number of wells = 155).**

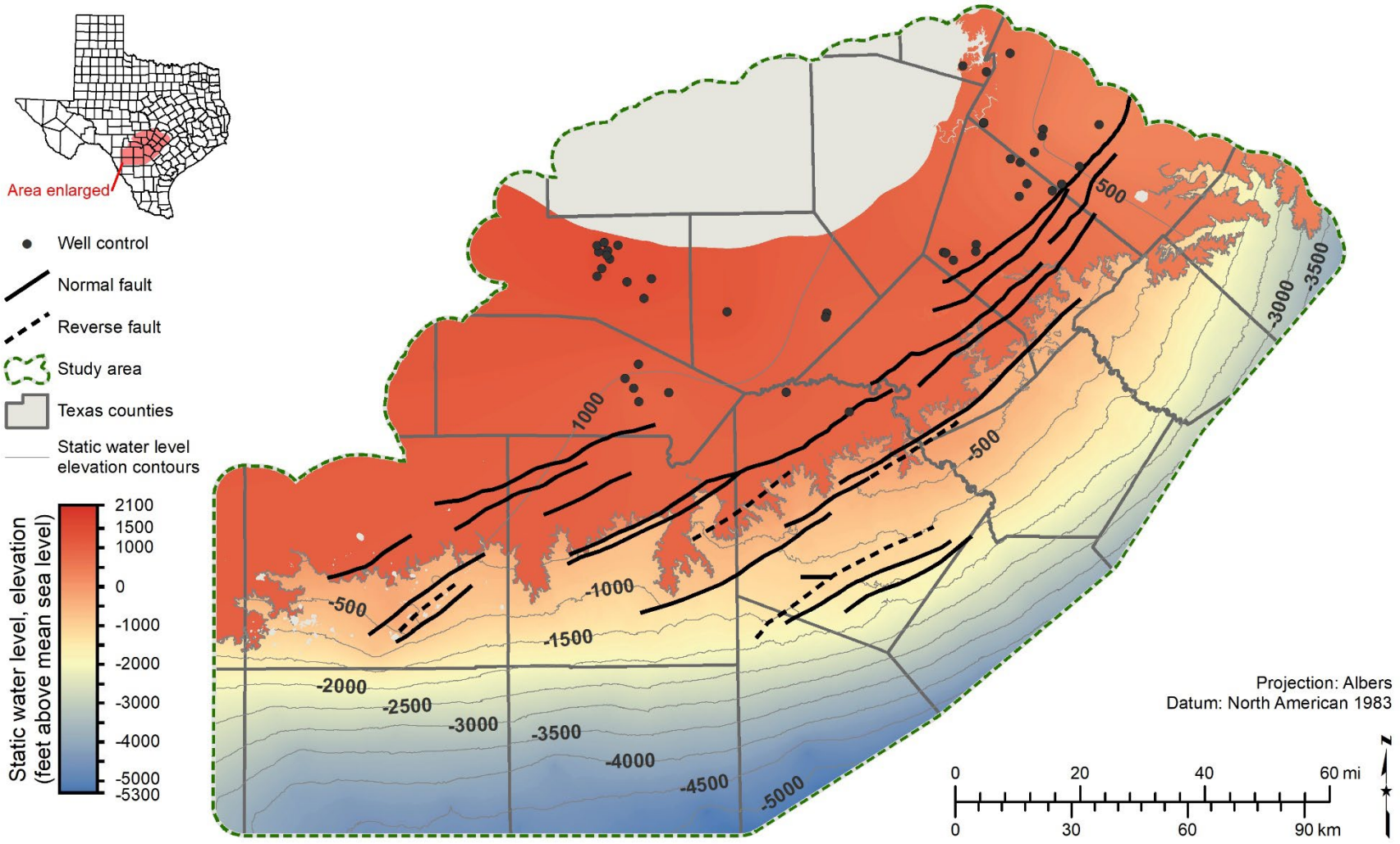

Figure 13-3 Lower Trinity (Sligo limestone and Hosston sandstone) static water level elevation (number of wells = 43).

This page is intentionally blank.

13.2 Groundwater volume calculation

In this section, we discuss how estimates of the total aquifer storage volumes of brackish groundwater were generated for the different salinity classes in the Hill Country Trinity aquifer. These volumes are based upon the groundwater salinity classes defined in Section 12 that were developed using water quality data from samples and through the analysis of geophysical logs as presented in Section 10 and Section 11. The six water-producing intervals defined for the Hill Country Trinity aquifer are the Upper Glen Rose limestone, Lower Glen Rose limestone, Hensell sandstone, Cow Creek limestone, Sligo limestone, and Hosston sandstone hydrostratigraphic units.

13.2.1 Mechanics of calculating groundwater volumes in the Trinity Aquifer

Shi and others (2014) provide a good overview of the calculation of the volume of groundwater stored in an aquifer as part their calculation of total estimated recoverable storage (TERS) for different aquifers in Groundwater Management Area 8. The method used to calculate groundwater volume in both Shi and others (2014) and in this report is dependent on whether or not the aquifer is confined or unconfined. The following section provides a general discussion about confined and unconfined aquifers and how storage is calculated differently in each type of aquifer.

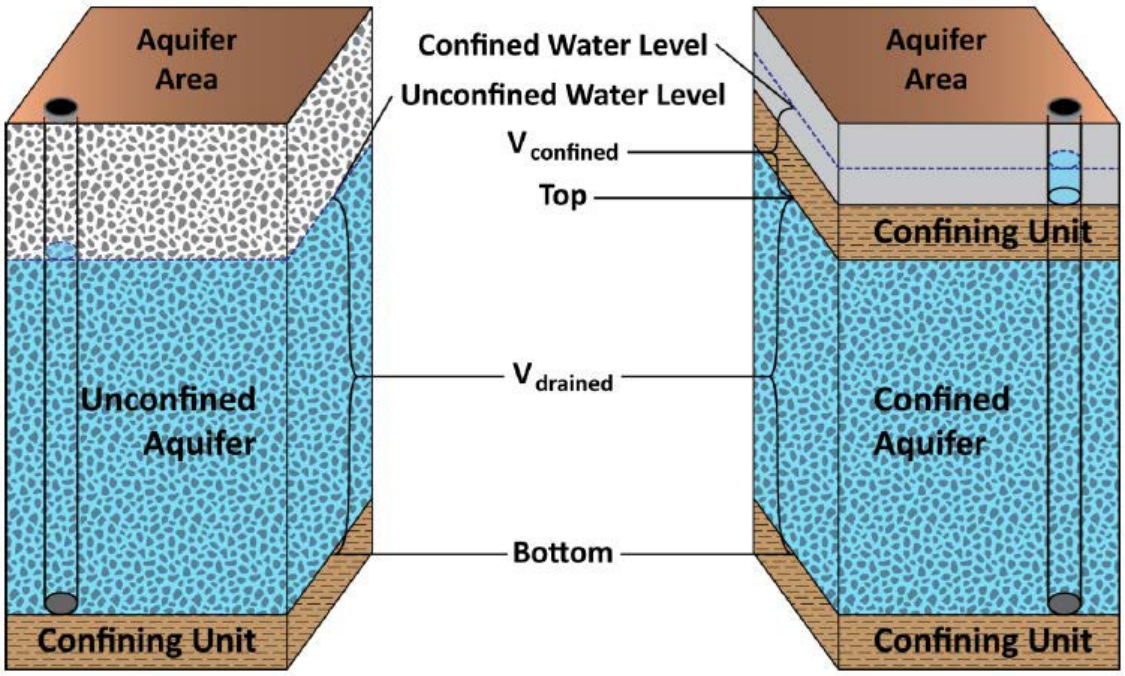

Figure 13-4 Schematic graph showing the difference between unconfined and confined aquifers (from Shi and others, 2014).

13.2.2 Confined and unconfined aquifer

In general, the Hill Country Trinity aquifer is a dipping aquifer that is unconfined updip and confined downdip. Figure 13-4 shows a schematic of idealized groundwater

conditions in this kind of aquifer. The term "unconfined" refers to the portion of the aquifer where the water level occurs below the top of the aquifer. This generally coincides with the outcrop area and area immediately downdip of the outcrop. In the Hill Country Trinity aquifer, the formations generally dip towards the southeast. Therefore, the unconfined portions of the Hill Country Trinity aquifer hydrostratigraphic units fall along their northwestern edge in the outcrop area. The term "confined" refers to the portion of the aquifer where the water level occurs above the top of the aquifer. The Trinity Aquifer hydrostratigraphic units become confined south and east of their outcrops, as the units dip deeper and are overlain by younger units.

As shown in Figure 13-4, storage is conceptualized differently in confined and unconfined aquifers. For an unconfined aquifer, the total storage is equal to the volume of groundwater removed by pumping that makes the water level fall to the aquifer bottom. This portion of aquifer storage is referred to as the unconfined aquifer storage. For a confined aquifer, the total storage is the sum of both confined and unconfined storage. Confined storage is groundwater released from the aquifer when the water level falls from above the top of the aquifer to the top of the aquifer. The reduction of hydraulic head in the aquifer, which can be thought of as pressure, by pumping causes expansion of groundwater and deformation of the aquifer matrix. The aquifer is still fully saturated when water is released from confined storage. Once confined aquifer storage is depleted, water can be released from unconfined storage through actual dewatering of the aquifer as the water level in the aquifer falls below the top of the aquifer and ultimately to the bottom of the aquifer.

Given the same aquifer area and water level decline, the amount of water released from unconfined storage is much greater (orders of magnitude) than that released from confined storage. The difference is because of the physical nature of storage reduction occurring under confined versus unconfined conditions. In confined storage reduction, water is being supplied through groundwater expansion and aquifer volume reduction. In unconfined storage reduction, water is being supplied through dewatering of pore space.

The parameters that quantify these physical differences are storativity of a confined aquifer and specific yield of an unconfined aquifer. Aquifer storativity typically ranges from 10^{-5} to 10^{-3} for most confined aquifers, while specific yield values typically range from 0.01 to 0.3 for most unconfined aquifers. The TWDB makes a distinction between the total volume of groundwater in unconfined aquifer storage versus that portion that is considered drainable. The equations for calculating the total aquifer storage groundwater volume are presented below:

For unconfined aquifers:

$$\text{Total Volume} = V_{drained} = \text{Area} * Sy * (\text{Water Level} - \text{Bottom}) \qquad \text{(Equation 13-1a)}$$

For confined aquifers:

$$\text{Total Volume} = V_{confined} + V_{drained} \qquad \text{(Equation 13-1b)}$$

Volume for confined part

$$V_{confined} = Area * [S *(Water\ level-Top)] \quad \text{(Equation 13-2a)}$$

or

$$V_{confined} = Area * [Ss *(Thickness)*(Water\ level-Top)] \quad \text{(Equation 13-2b)}$$

Volume for drained part

$$V_{drained} = Area * [Sy *(Thickness)] \quad \text{(Equation 13-3)}$$

Where (variables illustrated in Figure 13-4):

$V_{drained}$ = storage volume from water draining from the formation (acre-feet)

$V_{confined}$ = storage volume from the elastic properties of the aquifer and water (acre-feet)

Area = area of aquifer (acre)

Water Level = groundwater elevation (feet above mean sea level)

Top = elevation of aquifer top (feet above mean sea level)

Bottom = elevation of aquifer bottom (feet above mean sea level)

Thickness = thickness of aquifer (feet)

Sy = specific yield (no units)

Ss = specific storage (inverse feet)

S = storativity or storage coefficient (no units)

13.2.3 Specific yield and storativity values used

We used specific yield and storativity values in the volumetric calculations for the Hill Country Trinity aquifer based upon measurements from cores and existing published literature. In the studies reviewed in which storativity was derived from well tests, there was a significant range in the few values available. We found that storativity values could differ by as much as two to three orders of magnitude (Hunt and others, 2010; Toll and others, 2018). We also performed an analysis of 170 well test records from water wells in the study area are shown in Table 9-5, where many of the wells were screened across several aquifer units leading us to categorize according to the more general hydrologic units of upper, middle, and lower Trinity.

The widely varying lithologies of the Trinity Group means that no single number used will accurately represent the aquifer storage properties throughout the study area. It was therefore necessary for us to use a possibly conservative set of values that reflect the storage properties of the upper, middle, and lower Trinity hydrologic units within the study area. The values for specific yield and storativity shown in Table 13-1 were used in this study to calculate the total aquifer storage volume of brackish groundwater. The

storativity numbers are the median values from Table 9-5 of this report. The specific yield numbers are from Standen and others (2021). We took the effective porosity values from 81 nuclear magnetic resonance (NMR) laboratory core analyses and assigned them to the appropriate hydrologic intervals. The core samples analyzed were representative of several lithologies and come from an average depth of 4,016 feet below ground surface. To be conservative, we decided to use the numerical averages of the effective porosities for the unconfined specific yield values and for the confined specific yield values we used 50 percent of the unconfined values.

Table 13-1 Specific yield and storativity values used for volume calculations

Hydrogeologic unit	Specific yield unconfined (unitless)	Specific yield confined (unitless)	Storativity (unitless)
Upper Trinity	0.054	0.027	1.7x10-4
Middle Trinity	0.108	0.054	1.5x10-4
Lower Trinity	0.120	0.060	3.2x10-4

13.2.4 Process for calculating groundwater volumes

Our brackish groundwater volume calculations for total aquifer storage were implemented on a 250-foot grid. We calculated both confined storage and unconfined drained storage for each of the six hydrostratigraphic units of the Hill Country Trinity aquifer: Upper Glen Rose limestone, Lower Glen Rose limestone, Hensell sandstone, Cow Creek limestone, Sligo limestone, and Hosston sandstone. We calculated the unconfined drained groundwater storage using Equation 13-1a and we calculated the confined groundwater storage using Equation 13-2a. The variable "Top" is the top elevation of the hydrostratigraphic unit in question while the variable "Bottom" is the bottom elevation of that unit. Three water level surfaces were used, 1) upper Trinity for the Upper Glen Rose limestone hydrostratigraphic unit (Figure 13-1), 2) middle Trinity for the Lower Glen Rose limestone, Hensell sandstone, and Cow Creek limestone hydrostratigraphic units (Figure 13-2), and 3) lower Trinity for the Sligo limestone and Hosston sandstone hydrostratigraphic units (Figure 13-3). We performed the calculations using a Python script. The complete detailed algorithm and equations implemented are listed in Appendix 19.1.5 of this report.

13.3 Calculated groundwater volumes

Table 13-2 contains the total aquifer storage volume of brackish groundwater for the six hydrostratigraphic units within the study area. The volumes are subdivided into fresh, slightly saline, moderately saline, and very saline classifications. The volume of groundwater in the brine classification was not tabulated as this is considered too saline to be considered a brackish groundwater resource. Table 13-3 to Table 13-6 contain the groundwater volumes per salinity class and hydrostratigraphic unit detailed by county,

regional water planning area, groundwater management area, and groundwater conservation district, respectively.

These volumes do not consider the effects of land surface subsidence, degradation of water quality, or any changes to surface water-groundwater interaction that may result from extracting groundwater from the aquifer. These volumes should not be used for joint groundwater planning or evaluation of achieving adopted desired future conditions in the same way TERS and modeled available groundwater are used according to the joint planning process described in Texas Water Code § 36.108. Volumes calculated for brackish aquifer studies in the BRACS program differ from TERS volumes determined by the TWDB Groundwater Availability Modeling (GAM) Program (Wade and Bradley, 2013; Wade and Shi, 2014) because of differences in the area, saturated thickness, and storage parameters used in the calculations.

Differences in the area used to calculate brackish groundwater volumes arise due to: (1) differences in the areal extent of the GAM models, as brackish groundwater often extends beyond the official TWDB boundaries for major and minor aquifers used to develop TERS, and (2) differences in the grid cell size and orientation of the GAM models used to estimate area.

Differences in the saturated thickness used to calculate brackish groundwater volumes arise due to: (1) differences in aquifer top and bottom elevations and static water levels of the GAM models due to differences in interpretations and data availability during subsurface mapping and (2) whether bulk aquifer thickness (static water level or aquifer top minus aquifer bottom) or net sand, or percent sand, was used to estimate feet of saturated aquifer thickness.

Differences in the storage component used to calculate brackish groundwater volumes include: (1) the value of specific yield (the ratio of drainable water in an aquifer, which is less than porosity), (2) whether volumes calculated from specific yield are further reduced to "recoverable volumes," and (3) whether confined storage is included, though this is generally a negligible volume.

Additionally, TERS does not take water quality into account and therefore cannot be directly compared to BRACS volumes which are divided by salinity class categories.

Table 13-2 The volumes of fresh, slightly saline, moderately saline, very saline, and total groundwater volumes in the Hill Country Trinity aquifer.

Hydrostratigraphic unit	Total aquifer storage volume (acre-feet)				
	Fresh	Slightly saline	Moderately saline	Very saline	Total
Upper Glen Rose limestone	9,530,362	22,344,252	53,212,654	49,388,081	134,475,350
Lower Glen Rose limestone	34,573,100	35,608,649	61,689,916	67,289,482	199,161,147
Hensell sandstone	9,300,826	12,906,665	23,325,590	15,825,480	61,358,561
Cow Creek limestone	24,131,596	12,907,039	10,275,586	18,581,271	65,895,492
Sligo limestone	4,859,227	30,809,060	16,976,735	74,641,576	127,286,598
Hosston sandstone	8,769,583	86,970,453	77,588,464	217,030,438	390,358,937
Total	91,164,693	201,546,118	243,068,946	442,756,328	978,536,086

Table 13-3 The volumes of fresh, slightly saline, moderately saline, very saline, and total groundwater volumes in the Hill Country Trinity aquifer by county.

County and hydrostratigraphic unit	Total aquifer storage volume (acre-feet)				
	Fresh	Slightly saline	Moderately saline	Very saline	Total
Atascosa County					
Upper Glen Rose limestone	0	0	591,092	7,534,067	8,125,159
Lower Glen Rose limestone	0	0	465,446	4,400,987	4,866,433
Hensell sandstone	0	0	183,465	178,972	362,437
Cow Creek limestone	0	0	80,390	3,316,598	3,396,988
Sligo limestone	0	0	352,812	11,593,992	11,946,805
Hosston sandstone	0	0	856,680	31,648,759	32,505,439
Total	0	0	2,529,885	58,673,376	61,203,261
Bandera County					
Upper Glen Rose limestone	596,598	2,018,647	1,550,864	0	4,166,109
Lower Glen Rose limestone	3,153,646	6,080,147	644,460	0	9,878,252
Hensell sandstone	694,446	1,682,416	0	0	2,376,862
Cow Creek limestone	426,105	1,496,918	300,054	0	2,223,077
Sligo limestone	669,411	1,994,501	232,003	0	2,895,914
Hosston sandstone	1,856,173	3,865,597	79,847	0	5,801,616
Total	7,396,377	17,138,226	2,807,227	0	27,341,830

County and hydrostratigraphic unit	Total aquifer storage volume (acre-feet)				
	Fresh	Slightly saline	Moderately saline	Very saline	Total
Bastrop County					
Upper Glen Rose limestone	0	0	4,233,002	2,428,766	6,661,768
Lower Glen Rose limestone	0	0	1,391,555	4,160,900	5,552,456
Hensell sandstone	0	0	1,844,852	266,231	2,111,083
Cow Creek limestone	0	0	902,448	345,860	1,248,309
Sligo limestone	0	20,349	3,526,777	3,150,830	6,697,957
Hosston sandstone	0	0	841,352	16,386,730	17,228,082
Total	0	20,349	12,739,987	26,739,318	39,499,654
Bexar County					
Upper Glen Rose limestone	593,359	2,519,510	7,497,394	404,989	11,015,252
Lower Glen Rose limestone	2,719,635	3,452,353	9,763,724	2,157,003	18,092,715
Hensell sandstone	0	1,753,480	2,451,879	627,605	4,832,964
Cow Creek limestone	0	1,726,342	1,209,972	456,623	3,392,937
Sligo limestone	655,961	1,855,136	5,233,700	1,136,297	8,881,095
Hosston sandstone	0	8,760,964	10,942,419	10,655,473	30,358,856
Total	3,968,955	20,067,786	37,099,088	15,437,989	76,573,819
Blanco County					
Upper Glen Rose limestone	6,925	3,332	8	0	10,265
Lower Glen Rose limestone	2,813,027	104,949	0	0	2,917,976
Hensell sandstone	736,737	14,220	0	0	750,957
Cow Creek limestone	3,428,572	328,386	0	0	3,756,958
Sligo limestone	99,875	3,826	0	0	103,700
Hosston sandstone	560,132	446,271	0	0	1,006,402
Total	7,645,267	900,984	8	0	8,546,259
Burnet County					
Upper Glen Rose limestone	15,286	0	0	0	15,286
Lower Glen Rose limestone	8,687	0	0	0	8,687
Hensell sandstone	87,597	0	0	0	87,597
Cow Creek limestone	489,943	0	0	0	489,943
Sligo limestone	0	0	0	0	0

County and hydrostratigraphic unit	Total aquifer storage volume (acre-feet)				
	Fresh	Slightly saline	Moderately saline	Very saline	Total
Hosston sandstone	25,625	0	0	0	25,625
Total	627,138	0	0	0	627,138
Caldwell County					
Upper Glen Rose limestone	0	0	3,586,295	1,943,663	5,529,958
Lower Glen Rose limestone	0	0	3,209,454	3,189,596	6,399,049
Hensell sandstone	0	2,886	2,012,450	295,774	2,311,110
Cow Creek limestone	0	25,530	852,765	245,003	1,123,299
Sligo limestone	0	13,020	3,240,244	4,197,097	7,450,362
Hosston sandstone	0	0	3,306,068	10,788,023	14,094,091
Total	0	41,437	16,207,275	20,659,156	36,907,869
Comal County					
Upper Glen Rose limestone	806,464	764,675	860,818	0	2,431,958
Lower Glen Rose limestone	2,069,020	1,868,421	1,265,906	0	5,203,347
Hensell sandstone	549,888	912,806	235,800	0	1,698,495
Cow Creek limestone	686,625	1,090,464	53,446	0	1,830,535
Sligo limestone	1,033,193	777,905	461,656	0	2,272,755
Hosston sandstone	0	7,698,404	239,295	0	7,937,698
Total	5,145,191	13,112,676	3,116,922	0	21,374,788
Frio County					
Upper Glen Rose limestone	0	0	1,085,580	13,936,686	15,022,266
Lower Glen Rose limestone	0	0	577,034	10,434,479	11,011,514
Hensell sandstone	0	0	212,446	3,082,315	3,294,761
Cow Creek limestone	0	0	500,030	5,196,769	5,696,799
Sligo limestone	0	0	500,723	19,419,560	19,920,283
Hosston sandstone	0	0	2,746,104	54,484,891	57,230,995
Total	0	0	5,621,918	106,554,701	112,176,619
Gillespie County					
Upper Glen Rose limestone	909,436	0	0	0	909,436
Lower Glen Rose limestone	12,878,927	8,811	0	0	12,887,737
Hensell sandstone	2,174,610	5,034	0	0	2,179,644
Cow Creek limestone	14,928,920	9,165	0	0	14,938,086

County and hydrostratigraphic unit	Total aquifer storage volume (acre-feet)				
	Fresh	Slightly saline	Moderately saline	Very saline	Total
Sligo limestone	0	0	0	0	0
Hosston sandstone	521	0	0	0	521
Total	30,892,414	23,010	0	0	30,915,423
Gonzales County					
Upper Glen Rose limestone	0	0	0	23,754	23,754
Lower Glen Rose limestone	0	0	0	366,570	366,570
Hensell sandstone	0	0	0	399,252	399,252
Cow Creek limestone	0	0	0	301,624	301,624
Sligo limestone	0	0	0	2,695,460	2,695,460
Hosston sandstone	0	0	0	4,391,502	4,391,502
Total	0	0	0	8,178,162	8,178,162
Guadalupe County					
Upper Glen Rose limestone	0	0	3,999,535	2,800,372	6,799,906
Lower Glen Rose limestone	0	59	3,378,066	6,967,295	10,345,419
Hensell sandstone	0	78,078	1,509,061	1,622,392	3,209,530
Cow Creek limestone	0	160,069	511,204	642,140	1,313,414
Sligo limestone	0	542,308	2,820,676	6,283,338	9,646,322
Hosston sandstone	0	740,095	4,676,022	10,975,794	16,391,911
Total	0	1,520,609	16,894,563	29,291,330	47,706,503
Hays County					
Upper Glen Rose limestone	675,361	1,405,633	751,487	0	2,832,481
Lower Glen Rose limestone	3,784,584	1,663,933	1,124,717	0	6,573,235
Hensell sandstone	677,837	396,644	116,783	0	1,191,264
Cow Creek limestone	901,058	768,557	60,526	0	1,730,140
Sligo limestone	1,163,825	464,651	948,252	0	2,576,728
Hosston sandstone	323,824	7,882,367	1,032,958	0	9,239,149
Total	7,526,489	12,581,785	4,034,724	0	24,142,998
Kendall County					
Upper Glen Rose limestone	391,674	262,864	0	0	654,538
Lower Glen Rose limestone	1,041,982	353,194	0	0	1,395,177
Hensell sandstone	761,189	919,178	0	0	1,680,366

County and hydrostratigraphic unit	Total aquifer storage volume (acre-feet)				
	Fresh	Slightly saline	Moderately saline	Very saline	Total
Cow Creek limestone	734,061	867,419	0	0	1,601,481
Sligo limestone	46,215	736,233	0	0	782,448
Hosston sandstone	561,516	2,984,157	0	0	3,545,674
Total	3,536,637	6,123,046	0	0	9,659,683
Kerr County					
Upper Glen Rose limestone	867,022	3,048,145	152,734	0	4,067,901
Lower Glen Rose limestone	2,331,800	1,000,651	84,928	0	3,417,379
Hensell sandstone	2,157,867	67,156	0	0	2,225,023
Cow Creek limestone	1,152,788	342,834	46,274	0	1,541,897
Sligo limestone	120,142	399,817	84,275	0	604,233
Hosston sandstone	2,096,988	321,534	0	0	2,418,522
Total	8,726,607	5,180,137	368,211	0	14,274,955
Kinney County					
Upper Glen Rose limestone	37,884	844,139	1,236,684	0	2,118,707
Lower Glen Rose limestone	0	1,003,494	2,366,130	0	3,369,624
Hensell sandstone	0	307,442	651,626	0	959,068
Cow Creek limestone	0	341,063	262,035	0	603,098
Sligo limestone	0	267,528	605,277	0	872,805
Hosston sandstone	0	2,831,766	1,924,885	0	4,756,651
Total	37,884	5,595,431	7,046,638	0	12,679,953
Maverick County					
Upper Glen Rose limestone	0	0	2,285,332	0	2,285,332
Lower Glen Rose limestone	0	0	4,197,958	0	4,197,958
Hensell sandstone	0	0	351,288	784,147	1,135,436
Cow Creek limestone	0	0	126,035	573,888	699,923
Sligo limestone	0	0	294,869	978,038	1,272,907
Hosston sandstone	0	0	1,661,300	5,951,298	7,612,598
Total	0	0	8,916,781	8,287,372	17,204,153
Medina County					
Upper Glen Rose limestone	539,223	2,781,439	10,338,285	734,939	14,393,886
Lower Glen Rose limestone	251,508	5,652,630	11,994,872	2,338,662	20,237,673

County and hydrostratigraphic unit	Total aquifer storage volume (acre-feet)				
	Fresh	Slightly saline	Moderately saline	Very saline	Total
Hensell sandstone	0	2,065,509	3,598,133	359,850	6,023,491
Cow Creek limestone	0	2,029,153	3,113,056	275,214	5,417,422
Sligo limestone	117,056	3,917,598	5,424,435	415,916	9,875,004
Hosston sandstone	570,489	11,527,542	23,753,640	2,027,317	37,878,988
Total	1,478,276	27,973,871	58,222,421	6,151,896	93,826,464
Real County					
Upper Glen Rose limestone	384,581	286,682	182,777	0	854,041
Lower Glen Rose limestone	0	1,462,369	3,796	0	1,466,165
Hensell sandstone	142,075	237,983	0	0	380,058
Cow Creek limestone	202,537	99,987	487	0	303,011
Sligo limestone	0	291,958	0	0	291,958
Hosston sandstone	462,055	390,832	0	0	852,887
Total	1,191,248	2,769,812	187,060	0	4,148,120
Travis County					
Upper Glen Rose limestone	1,688,182	1,108,018	1,201,751	0	3,997,951
Lower Glen Rose limestone	3,520,232	2,925,542	707,293	0	7,153,067
Hensell sandstone	1,076,729	282,471	129,923	0	1,489,123
Cow Creek limestone	1,180,980	617,091	102,948	0	1,901,019
Sligo limestone	953,549	1,169,822	428,332	0	2,551,703
Hosston sandstone	411,298	5,657,091	4,012,638	476,403	10,557,430
Total	8,830,971	11,760,035	6,582,885	476,403	27,650,294
Uvalde County					
Upper Glen Rose limestone	2,018,368	7,301,167	8,781,094	657,304	18,757,933
Lower Glen Rose limestone	51	10,032,095	13,995,799	1,669,062	25,697,006
Hensell sandstone	241,852	4,181,362	3,998,160	454,360	8,875,734
Cow Creek limestone	8	3,004,059	1,793,364	204,575	5,002,006
Sligo limestone	0	4,522,084	4,151,027	24,856	8,697,968
Hosston sandstone	1,900,961	24,481,844	17,172,392	0	43,555,198
Total	4,161,240	53,522,612	49,891,836	3,010,157	110,585,845
Wilson County					
Upper Glen Rose limestone	0	0	266,308	3,666,677	3,932,984

County and hydrostratigraphic unit	Total aquifer storage volume (acre-feet)				
	Fresh	Slightly saline	Moderately saline	Very saline	Total
Lower Glen Rose limestone	0	0	274,693	7,480,274	7,754,967
Hensell sandstone	0	0	0	285,779	285,779
Cow Creek limestone	0	0	0	1,320,224	1,320,224
Sligo limestone	0	0	723,356	9,597,945	10,321,300
Hosston sandstone	0	0	0	19,763,577	19,763,577
Total	0	0	1,264,356	42,114,476	43,378,832
Zavala County					
Upper Glen Rose limestone	0	0	4,611,614	15,256,864	19,868,479
Lower Glen Rose limestone	0	0	6,244,085	24,124,656	30,368,741
Hensell sandstone	0	0	6,029,725	7,468,802	13,498,526
Cow Creek limestone	0	0	360,551	5,702,752	6,063,303
Sligo limestone	0	0	1,780,646	15,148,245	16,928,891
Hosston sandstone	0	0	13,724,853	49,480,672	63,205,525
Total	0	0	32,751,473	117,181,992	149,933,465

Table 13-4 The volumes of fresh, slightly saline, moderately saline, very saline, and total groundwater volumes in the Hill Country Trinity aquifer by regional water planning area.

RWPA and hydrostratigraphic unit	Total aquifer storage volume (acre-feet)				
	Fresh	Slightly saline	Moderately saline	Very saline	Total
Plateau Water Planning Region (J)					
Upper Glen Rose limestone	1,885,063	6,189,747	3,121,038	0	11,195,848
Lower Glen Rose limestone	5,485,265	9,536,998	3,093,175	0	18,115,439
Hensell sandstone	2,994,525	2,291,618	651,120	0	5,937,263
Cow Creek limestone	1,781,372	2,277,802	608,850	0	4,668,024
Sligo limestone	789,632	2,950,875	920,884	0	4,661,391
Hosston sandstone	4,414,663	7,392,395	2,004,732	0	13,811,791
Total	17,350,521	30,639,435	10,399,799	0	58,389,755
Lower Colorado Regional Water Planning Group (K)					
Upper Glen Rose limestone	3,120,420	1,218,312	5,436,320	2,428,639	12,203,692

RWPA and hydrostratigraphic unit	Total aquifer storage volume (acre-feet)				
	Fresh	**Slightly saline**	**Moderately saline**	**Very saline**	**Total**
Lower Glen Rose limestone	21,308,005	3,701,426	2,100,419	4,161,333	31,271,183
Hensell sandstone	4,471,991	324,945	1,975,294	266,189	7,038,419
Cow Creek limestone	20,596,078	1,143,499	1,005,722	345,854	23,091,153
Sligo limestone	1,591,777	1,340,397	3,956,678	3,150,779	10,039,631
Hosston sandstone	1,165,759	9,128,867	4,855,456	16,865,167	32,015,249
Total	52,254,030	16,857,446	19,329,888	27,217,962	115,659,327
South Central Texas Regional Water Planning Group (L)					
Upper Glen Rose limestone	4,524,878	14,936,193	42,374,613	46,959,442	108,795,127
Lower Glen Rose limestone	7,779,829	22,370,225	52,306,809	63,128,149	145,585,011
Hensell sandstone	1,834,310	10,290,103	20,349,014	14,776,438	47,249,865
Cow Creek limestone	1,754,146	9,485,738	8,535,353	17,662,557	37,437,795
Sligo limestone	2,477,818	12,685,463	25,637,568	70,514,499	111,315,348
Hosston sandstone	3,189,161	61,067,202	78,454,109	194,224,072	336,934,544
Total	21,560,142	130,834,924	227,657,466	407,265,157	787,317,689
Rio Grande Regional Water Planning Group (M)					
Upper Glen Rose limestone	0	0	2,280,683	0	2,280,683
Lower Glen Rose limestone	0	0	4,189,514	0	4,189,514
Hensell sandstone	0	0	350,162	782,853	1,133,014
Cow Creek limestone	0	0	125,661	572,859	698,520
Sligo limestone	0	0	293,931	976,298	1,270,229
Hosston sandstone	0	0	82,036	5,941,198	6,023,234
Total	0	0	7,321,986	8,273,209	15,595,195

Table 13-5 The volumes of fresh, slightly saline, moderately saline, very saline, and total groundwater volumes in the Hill Country Trinity aquifer by groundwater management area.

groundwater management area and hydrostratigraphic unit	Total aquifer storage volume (acre-feet)				
	Fresh	Slightly saline	Moderately saline	Very saline	Total
Groundwater Management Area 7					
Upper Glen Rose limestone	3,349,603	1,856,815	182,777	0	5,389,196
Lower Glen Rose limestone	12,878,927	7,714,412	3,796	0	20,597,134
Hensell sandstone	2,558,517	1,050,318	0	0	3,608,835
Cow Creek limestone	15,131,457	1,047,480	487	0	16,179,424
Sligo limestone	0	1,379,633	0	0	1,379,633
Hosston sandstone	2,360,575	2,632,565	0	0	4,993,140
Total	36,279,079	15,681,222	187,060	0	52,147,361
Groundwater Management Area 8					
Upper Glen Rose limestone	801,774	387,826	586,083	0	1,775,684
Lower Glen Rose limestone	1,170,763	1,360,392	217,062	0	2,748,216
Hensell sandstone	599,086	86,547	61,899	0	747,531
Cow Creek limestone	846,973	400,015	48,113	0	1,295,101
Sligo limestone	270,072	346,573	242,221	0	858,866
Hosston sandstone	183,891	1,179,099	2,221,366	476,257	4,060,613
Total	3,872,559	3,760,451	3,376,744	476,257	11,486,011
Groundwater Management Area 9					
Upper Glen Rose limestone	3,730,017	7,144,399	1,737,090	0	12,611,506
Lower Glen Rose limestone	18,246,822	12,940,657	784,087	0	31,971,566
Hensell sandstone	5,755,859	4,199,547	36	0	9,955,443
Cow Creek limestone	7,719,341	5,189,862	346,328	0	13,255,530
Sligo limestone	3,618,340	4,550,762	316,278	0	8,485,379
Hosston sandstone	6,201,051	22,969,261	104,753	0	29,275,065
Total	45,271,431	56,994,487	3,288,571	0	105,554,489
Groundwater Management Area 10					
Upper Glen Rose limestone	1,648,968	12,955,211	26,038,285	74,025	40,716,488
Lower Glen Rose limestone	2,276,588	13,593,189	36,309,340	482,247	52,661,363
Hensell sandstone	387,364	7,570,254	9,415,023	54,565	17,427,206

groundwater management area and hydrostratigraphic unit	Total aquifer storage volume (acre-feet)				
	Fresh	Slightly saline	Moderately saline	Very saline	Total
Cow Creek limestone	433,825	6,269,683	5,058,114	24,715	11,786,337
Sligo limestone	970,815	10,679,419	13,140,301	12,179	24,802,714
Hosston sandstone	24,066	50,807,539	41,154,343	388,313	92,374,260
Total	5,741,625	101,875,295	131,115,406	1,036,043	239,768,369
Groundwater Management Area 12					
Upper Glen Rose limestone	0	0	4,233,096	2,428,766	6,661,862
Lower Glen Rose limestone	0	0	1,391,660	4,160,900	5,552,560
Hensell sandstone	0	0	1,844,881	266,231	2,111,112
Cow Creek limestone	0	0	902,469	345,860	1,248,330
Sligo limestone	0	20,349	3,526,865	3,150,830	6,698,045
Hosston sandstone	0	0	841,352	16,386,993	17,228,345
Total	0	20,349	12,740,324	26,739,581	39,500,254
Groundwater Management Area 13					
Upper Glen Rose limestone	0	0	20,435,323	46,885,291	67,320,614
Lower Glen Rose limestone	0	0	22,983,972	62,646,335	85,630,308
Hensell sandstone	0	0	12,003,751	15,504,683	27,508,434
Cow Creek limestone	0	0	3,920,074	18,210,696	22,130,770
Sligo limestone	0	0	13,583,395	71,478,567	85,061,961
Hosston sandstone	0	0	42,648,640	199,778,875	242,427,514
Total	0	0	115,575,155	414,504,446	530,079,601

Table 13-6 **The volumes of fresh, slightly saline, moderately saline, very saline, and total groundwater volumes in the Hill Country Trinity aquifer by groundwater conservation district. Note: GCD = groundwater conservation district, UWCD = underground water conservation district.**

GCD and hydrostratigraphic unit	Total aquifer storage volume (acre-feet)				
	Fresh	Slightly Saline	Moderately Saline	Very Saline	Total
Bandera County River Authority and Groundwater Conservation District					
Upper Glen Rose limestone	596,602	2,018,681	1,550,808	0	4,166,091
Lower Glen Rose limestone	3,153,646	6,080,191	644,420	0	9,878,257
Hensell sandstone	694,428	1,682,422	0	0	2,376,850
Cow Creek limestone	426,105	1,496,933	300,037	0	2,223,075
Sligo limestone	669,411	1,994,511	231,994	0	2,895,916
Hosston sandstone	1,856,173	3,865,598	79,847	0	5,801,617
Total	7,396,363	17,138,337	2,807,106	0	27,341,806
Barton Springs/Edwards Aquifer Conservation District					
Upper Glen Rose limestone	1,043,812	1,479,329	1,063,694	0	3,586,835
Lower Glen Rose limestone	1,657,505	1,373,713	1,442,072	0	4,473,290
Hensell sandstone	293,397	471,483	201,772	0	966,652
Cow Creek limestone	334,907	584,873	109,700	0	1,029,481
Sligo limestone	798,286	592,143	1,084,583	0	2,475,013
Hosston sandstone	0	6,083,763	1,839,146	0	7,922,909
Total	4,127,908	10,585,305	5,740,968	0	20,454,181
Blanco-Pedernales Groundwater Conservation District					
Upper Glen Rose limestone	6,925	3,332	8	0	10,265
Lower Glen Rose limestone	2,813,025	104,956	0	0	2,917,982
Hensell sandstone	736,705	14,220	0	0	750,924
Cow Creek limestone	3,428,517	328,390	0	0	3,756,907
Sligo limestone	99,851	3,828	0	0	103,679
Hosston sandstone	560,130	446,101	0	0	1,006,231
Total	7,645,154	900,827	8	0	8,545,989
Central Texas Groundwater Conservation District					
Upper Glen Rose limestone	15,286	0	0	0	15,286
Lower Glen Rose limestone	8,687	0	0	0	8,687
Hensell sandstone	87,589	0	0	0	87,589

GCD and hydrostratigraphic unit	Total aquifer storage volume (acre-feet)				
	Fresh	Slightly Saline	Moderately Saline	Very Saline	Total
Cow Creek limestone	489,943	0	0	0	489,943
Sligo limestone	0	0	0	0	0
Hosston sandstone	2,089	0	0	0	2,089
Total	603,594	0	0	0	603,594
Comal Trinity Groundwater Conservation District					
Upper Glen Rose limestone	806,475	764,666	860,344	0	2,431,486
Lower Glen Rose limestone	2,068,073	1,864,015	1,265,412	0	5,197,499
Hensell sandstone	549,989	908,148	235,604	0	1,693,741
Cow Creek limestone	686,976	1,084,242	53,400	0	1,824,619
Sligo limestone	1,033,083	771,706	461,655	0	2,266,444
Hosston sandstone	0	7,679,904	239,295	0	7,919,198
Total	5,144,595	13,072,682	3,115,710	0	21,332,987
Cow Creek Groundwater Conservation District					
Upper Glen Rose limestone	391,674	262,854	0	0	654,528
Lower Glen Rose limestone	1,039,671	351,108	0	0	1,390,780
Hensell sandstone	761,145	912,451	0	0	1,673,597
Cow Creek limestone	733,995	857,875	0	0	1,591,870
Sligo limestone	46,178	727,210	0	0	773,388
Hosston sandstone	561,519	2,955,561		0	3,517,080
Total	3,534,183	6,067,060	0	0	9,601,242
Edwards Aquifer Authority (The EAA has authority over the Edwards Aquifer, these numbers are provided for informational purposes.)					
Upper Glen Rose limestone	3,846,947	14,198,873	33,188,639	2,392,023	53,626,482
Lower Glen Rose limestone	3,608,350	21,531,854	43,287,758	8,132,102	76,560,064
Hensell sandstone	347,850	9,078,547	12,595,266	1,655,495	23,677,157
Cow Creek limestone	8,166	7,903,661	7,095,398	1,004,540	16,011,765
Sligo limestone	1,009,140	11,776,949	20,314,643	3,274,078	36,374,810
Hosston sandstone	2,471,526	51,503,032	59,949,761	16,793,691	130,718,010
Total	11,291,978	115,992,916	176,431,464	33,251,930	336,968,288

GCD and hydrostratigraphic unit	Total aquifer storage volume (acre-feet)				
	Fresh	Slightly Saline	Moderately Saline	Very Saline	Total
Evergreen Underground Water Conservation District					
Upper Glen Rose limestone	0	0	1,942,954	25,137,327	27,080,281
Lower Glen Rose limestone	0	0	1,317,174	22,315,584	23,632,758
Hensell sandstone	0	0	395,911	3,546,986	3,942,897
Cow Creek limestone	0	0	580,420	9,833,556	10,413,976
Sligo limestone	0	0	1,576,891	40,611,369	42,188,260
Hosston sandstone	0	0	3,602,784	105,896,844	109,499,628
Total	0	0	9,416,135	207,341,667	216,757,801
Gonzales County Underground Water Conservation District					
Upper Glen Rose limestone	0	0	279,174	846,767	1,125,942
Lower Glen Rose limestone	0	0	0	979,162	979,162
Hensell sandstone	0	0	338,074	565,030	903,103
Cow Creek limestone	0	0	43,618	470,397	514,015
Sligo limestone	0	0	267,698	4,159,661	4,427,358
Hosston sandstone	0	0	0	7,530,748	7,530,748
Total	0	0	928,564	14,551,764	15,480,328
Guadalupe County Groundwater Conservation District					
Upper Glen Rose limestone	0	0	1,246,680	2,800,396	4,047,076
Lower Glen Rose limestone	0	0	321,240	6,754,104	7,075,344
Hensell sandstone	0	0	338,513	1,622,392	1,960,905
Cow Creek limestone	0	0	152,335	642,031	794,366
Sligo limestone	0	0	589,794	6,280,345	6,870,139
Hosston sandstone	0	0	547,077	10,911,232	11,458,309
Total	0	0	3,195,640	29,010,499	32,206,139
Hays Trinity Groundwater Conservation District					
Upper Glen Rose limestone	127,810	146,227	0	0	274,037
Lower Glen Rose limestone	2,768,350	586,232	0	0	3,354,582
Hensell sandstone	500,521	0	0	0	500,521
Cow Creek limestone	759,048	256,776	0	0	1,015,824
Sligo limestone	691,630	146,227	0	0	837,857
Hosston sandstone	323,183	3,328,051	0	0	3,651,234

GCD and hydrostratigraphic unit	Total aquifer storage volume (acre-feet)				
	Fresh	Slightly Saline	Moderately Saline	Very Saline	Total
Total	5,170,542	4,463,513	0	0	9,634,055
Headwaters Groundwater Conservation District					
Upper Glen Rose limestone	867,034	3,048,133	152,789	0	4,067,956
Lower Glen Rose limestone	2,331,808	1,000,631	84,968	0	3,417,407
Hensell sandstone	2,157,915	67,162	0	0	2,225,077
Cow Creek limestone	1,152,808	342,828	46,291	0	1,541,927
Sligo limestone	120,142	399,823	84,283	0	604,248
Hosston sandstone	2,096,986	321,589	0	0	2,418,575
Total	8,726,693	5,180,165	368,331	0	14,275,190
Hill Country Underground Water Conservation District					
Upper Glen Rose limestone	909,424	0	0	0	909,424
Lower Glen Rose limestone	12,878,928	8,811	0	0	12,887,739
Hensell sandstone	2,174,585	5,034	0	0	2,179,619
Cow Creek limestone	14,928,910	9,165	0	0	14,938,076
Sligo limestone	0	0	0	0	0
Hosston sandstone	520	0	0	0	520
Total	30,892,367	23,010	0	0	30,915,377
Kinney County Groundwater Conservation District					
Upper Glen Rose limestone	37,884	844,139	1,236,684	0	2,118,707
Lower Glen Rose limestone	0	1,003,494	2,366,130	0	3,369,624
Hensell sandstone	0	307,442	651,626	0	959,068
Cow Creek limestone	0	341,063	262,035	0	603,098
Sligo limestone	0	267,528	605,277	0	872,805
Hosston sandstone	0	2,831,766	841,150	0	3,672,915
Total	37,884	5,595,431	5,962,902	0	11,596,217
Lost Pines Groundwater Conservation District					
Upper Glen Rose limestone	0	0	4,232,946	2,428,766	6,661,712
Lower Glen Rose limestone	0	0	1,391,498	4,160,837	5,552,335
Hensell sandstone	0	0	1,844,820	266,231	2,111,051
Cow Creek limestone	0	0	902,431	275,214	1,177,645
Sligo limestone	0	20,264	3,526,748	3,150,830	6,697,843

GCD and hydrostratigraphic unit	Total aquifer storage volume (acre-feet)				
	Fresh	Slightly Saline	Moderately Saline	Very Saline	Total
Hosston sandstone	0	0	841,150	16,386,758	17,227,908
Total	0	20,264	12,739,593	26,668,637	39,428,495
Medina County Groundwater Conservation District					
Upper Glen Rose limestone	539,212	2,781,427	10,338,285	734,939	14,393,862
Lower Glen Rose limestone	251,508	5,652,585	11,994,872	2,338,662	20,237,628
Hensell sandstone	0	2,065,496	3,598,133	359,850	6,023,478
Cow Creek limestone	0	2,029,137	3,113,056	275,214	5,417,407
Sligo limestone	117,056	5,424,435	5,424,435	415,916	11,381,842
Hosston sandstone	570,466	11,527,519	23,753,640	2,027,317	37,878,942
Total	1,478,242	29,480,599	58,222,421	6,151,896	95,333,158
Plum Creek Conservation District					
Upper Glen Rose limestone	0	236,029	2,208,158	919,625	3,363,813
Lower Glen Rose limestone	12,674	301,157	2,104,591	1,897,652	4,316,075
Hensell sandstone	0	66,778	1,191,487	87,232	1,345,497
Cow Creek limestone	0	95,854	563,738	65,485	725,076
Sligo limestone	11,692	114,567	2,052,015	1,971,774	4,150,047
Hosston sandstone	0	663,936	2,497,968	5,259,140	8,421,044
Total	24,366	1,478,321	10,617,958	10,200,908	22,321,552
Real-Edwards Conservation and Reclamation District					
Upper Glen Rose limestone	384,479	286,682	182,777	0	853,939
Lower Glen Rose limestone	0	1,462,166	3,796	0	1,465,962
Hensell sandstone	142,055	237,983	0	0	380,039
Cow Creek limestone	202,537	99,968	487	0	302,992
Sligo limestone	0	291,936	0	0	291,936
Hosston sandstone	461,980	390,832	0	0	852,812
Total	1,191,052	2,769,568	187,060	0	4,147,680
Southwestern Travis County Groundwater Conservation District					
Upper Glen Rose limestone	346,642	36,751	0	0	383,393
Lower Glen Rose limestone	1,131,398	915,019	51,391	0	2,097,807
Hensell sandstone	307,823	0	0	0	307,823
Cow Creek limestone	464,863	19,615	0	0	484,478

GCD and hydrostratigraphic unit	Total aquifer storage volume (acre-feet)				
	Fresh	Slightly Saline	Moderately Saline	Very Saline	Total
Sligo limestone	185,441	112,137	0	0	297,577
Hosston sandstone	224,520	1,762,553	20,724	0	2,007,796
Total	2,660,686	2,846,075	72,114	0	5,578,876
Trinity Glen Rose Groundwater Conservation District					
Upper Glen Rose limestone	593,252	751,975	29,381	0	1,374,609
Lower Glen Rose limestone	2,721,575	993,304	0	0	3,714,879
Hensell sandstone	0	920,205	36	0	920,242
Cow Creek limestone	0	968,289	0	0	968,289
Sligo limestone	655,945	588,639	0	0	1,244,584
Hosston sandstone	0	4,567,853	0	0	4,567,853
Total	3,970,772	8,790,265	29,418	0	12,790,455
Uvalde County Underground Water Conservation District					
Upper Glen Rose limestone	2,018,477	7,301,167	8,781,055	657,272	18,757,971
Lower Glen Rose limestone	51	10,032,319	13,995,799	1,668,964	25,697,132
Hensell sandstone	241,871	4,181,369	3,998,139	454,339	8,875,718
Cow Creek limestone	8	3,004,085	1,793,354	204,565	5,002,011
Sligo limestone	0	4,522,115	4,150,981	24,856	8,697,952
Hosston sandstone	1,901,059	24,481,844	17,172,166	0	43,555,070
Total	4,161,467	53,522,899	49,891,494	3,009,994	110,585,854
Wintergarden Groundwater Conservation District					
Upper Glen Rose limestone	0	0	4,611,653	15,256,977	19,868,630
Lower Glen Rose limestone	0	0	6,244,085	24,124,820	30,368,904
Hensell sandstone	0	0	6,029,746	7,468,894	13,498,640
Cow Creek limestone	0	0	360,561	5,702,794	6,063,354
Sligo limestone	0	0	1,780,692	15,148,351	16,929,043
Hosston sandstone	0	0	13,725,079	49,480,948	63,206,027
Total	0	0	32,751,815	117,182,783	149,934,598

14 Desalination concentrate disposal

Future development of brackish groundwater may require desalination depending on use. An important consideration of desalination is the disposal of concentrate as disposal can be costly and impede a project from moving forward. There is currently one existing brackish groundwater desalination plant in the study area (San Antonio Water System, H2Oaks Center) that uses Class I injection wells to dispose the concentrate from the reverse osmosis process. San Antonio Water System is the first municipal water utility to permit a Class I injection well under the Texas Commission on Environmental Quality's Class I General Permit. The General Permit only applies to wells disposing of nonhazardous desalination concentrate or nonhazardous drinking water treatment residuals. The injection zone is within the Edwards Aquifer with native groundwater quality greater than 90,000 milligrams per liter total dissolved solids concentration.

Class II injection wells inject produced water, obtained from oil and gas wells, into subsurface zones where groundwater is greater than 10,000 milligrams per liter total dissolved solids (except in very specific circumstances). Class II injection wells can be used for disposal of nonhazardous desalination concentrate or nonhazardous drinking water treatment residuals if the following well types and conditions apply (CDM Smith, 2014):

Class II Type 1: *Disposal injection well into a nonproductive oil and gas zone or interval. The well can be dually permitted as a Class I injection well under the Texas Commission of Environmental Quality General Permit. The well must meet all applicable construction standards of a Class I well, 30 Texas Administrative Code Section 331.62.*

The Railroad Commission of Texas also refers to this as a (Railroad Commission of Texas Form) W-14 well. These wells are permitted under the Railroad Commission of Texas Statewide Rule 9.

Class II Type 2: *Disposal injection well into a productive oil and gas zone or interval. The well can be dually permitted as a Class I injection well under the Texas Commission of Environmental Quality General Permit. The well must meet all applicable construction standards of a Class I well, 30 Texas Administrative Code Section 331.62.*

The Railroad Commission of Texas also refers to this as an (Railroad Commission of Texas Form) H-1 well. These wells are permitted under the Railroad Commission of Texas Statewide Rule 46.

Class II Type 3: *Enhanced recovery injection well into a productive oil and gas zone or interval. This type of well can receive a permit amendment from the Railroad Commission of Texas.*

> *The Railroad Commission of Texas also refers to this as an (Railroad Commission of Texas Form) H-1 well. These wells are permitted under the Railroad Commission of Texas Statewide Rule 46.*

If a Class II injection well is considered as a potential option for concentrate disposal, a considerable amount of research must be undertaken to ensure that the well meets construction requirements, appropriate permits are obtained, and a contract with the owner of the injection well can be obtained for the lifetime of the project (Mace and others, 2006; CDM Smith, 2014).

There are other concentrate disposal options that are currently being used by desalination plants in Texas: (1) disposal to surface water bodies, (2) disposal to wastewater treatment plants, (3) evaporation ponds, and (4) zero liquid discharge (partial stream of concentrate being evaluated at the Kay Bailey Desalination Plant in El Paso). These methods are specific to a site and require permits from the Texas Commission on Environmental Quality.

15 Future improvements

There are several things that can be done to improve groundwater salinity estimates for the Hill Country Trinity aquifer. Most importantly, we would like to acquire more lab-analyzed water quality samples between 1,000 and 35,000 milligrams per liter total dissolved solids from wells to help us build a more robust relationship between total dissolved solids and specific conductivity. Additional higher salinity measured samples would also provide feedback as to whether salinity estimates from geophysical well log calculations are reasonable. Aside from obtaining water quality samples from an expanded salinity range, obtaining samples that are more spatially representative would be quite useful, as many of the samples available to us are from wells completed in the outcrop or shallow subsurface portions of the Hill Country Trinity aquifer.

Additionally, although we used the Alger-Harrison method (Alger and Harrison, 1989) to calculate salinity from geophysical well logs, with sufficient data the Rwa minimum method may be more appropriate. The Rwa minimum method does not require mud parameters, thus avoiding the potential systemic error introduced by relying on log header mud parameters (Lowe and Dunlap, 1986), and therefore could potentially produce more reliable groundwater salinity estimates. Specific recommendations are:

- Acquire more well logs that provide insight into porosity and interconnected porosity, including neutron porosity logs, density porosity logs, sonic logs, and nuclear magnetic resonance logs.
- Conduct a thorough rock property classification analysis for the study area. The goal of this would be to map the study area into regions that could be more accurately represented by a key well (a well with multiple log types including resistivity, spontaneous potential, and porosity).
- Obtain and analyze core for each identified rock property region to pin down reliable *m* values, as well as accurate porosity and permeability. The core data collected in a recently contracted study resulted in a ten-fold increase in aquifer storage properties.
- Conduct Rwa minimum method calculations using the core and log-derived *m*, porosity, and resistivity logs.

Collection of static water level measurements in the more brackish portions of the aquifers would improve storage volume estimates. Although the volume from confined storage is significantly smaller than the volume from unconfined storage, better data would provide better estimates of the confined storage volume.

Lastly, additional stratigraphic interpretations of the overlying Edwards Group would provide greater control for the structural complexities of the Trinity Group formations. This would be particularly useful in those portions of the study area where complex faulting may play a significant role in the movement of groundwater.

16 Conclusions

This study is intended to provide a researched technical evaluation of the brackish groundwater resource of the Hill Country Trinity aquifer. We collected and analyzed available well information to accurately map the structure of the Trinity Group hydrostratigraphic units. Salinity measurements from water samples from wells were used in conjunction with calculated water quality from geophysical well logs to create salinity class maps for the Hill Country Trinity aquifer. We evaluated well test results to determine the storage properties of the Trinity Aquifer hydrologic units and used all the above study elements to calculate total aquifer storage volumes of brackish groundwater within the study area.

We estimate there is a total aquifer storage volume for slightly and moderately saline groundwater of approximately 445 million acre-feet. Divided by salinity class, we estimate there are 202 million acre-feet of slightly saline (1,000 to 3,000 milligrams-per-liter of total dissolved solids) groundwater, 243 million acre-feet of moderately saline (3,000 to 10,000 milligrams-per-liter of total dissolved solids) groundwater, and 442 million acre-feet of very saline (10,000 to 35,000 milligrams-per-liter of total dissolved solids) groundwater.

We realize that not all brackish groundwater can be produced or economically developed. However, these estimates and detailed mapping provide users a beneficial tool to evaluate potential sites for brackish groundwater well fields. These volumes do not consider the effects of land surface subsidence, degradation of water quality, or any changes to surface water-groundwater interaction that may result from extracting groundwater from the aquifer. These volumes should not be used for joint groundwater planning or evaluation of achieving adopted desired future conditions in the same way total estimated recoverable storage (TERS) and modeled available groundwater are used according to the joint planning process described in Texas Water Code § 36.108.

Publicly available study deliverables include 1) this report, 2) geographic information system (GIS) map files, 3) BRACS Database and Data Dictionary, 4) and water well and geophysical well log files.

Finally, information contained in this report is not intended to serve as a substitute for site-specific studies that are required to evaluate local aquifer characteristics and groundwater conditions for a desalination plant. Well-field-scale data collection using test and monitor wells is strongly recommended to evaluate the brackish groundwater resource at a particular site. Collection and evaluation of additional well control in a prospective site area is essential in understanding potential target zones for groundwater development.

17 Acknowledgements

This study could not have been performed without the inspiration of John Meyer whose vision and talents have been fundamental in the study of brackish groundwater in Texas. Thank you, John, for being a bright light for those of us who follow. Special thanks to Andrea Croskrey who freely shared her time and talents.

We would also like to acknowledge Paul Bertetti who provided insight into certain problematic specific conductance values in the TWDB Groundwater Database. We thank Emma Peterman who, during an internship with the TWDB in the summer of 2020, utilized her expertise of the United States Geological Survey PHREEQC software to perform the specific conductance calculations.

Finally, this work could not have been undertaken or completed without the support and encouragement of Erika Mancha (director of the Conservation and Innovative Water Technologies Division), and John Dupnik (deputy executive administrator of the Office of Water Science and Conservation).

18 References

AECOM Technical Services, Inc., James Kowis Consulting, LLC, and Trungate Engineering & Science, 2020, 2021 Region K Water Plan for the Lower Colorado Regional Water Planning Group, vol. 2, 887 p.

Alger, R.P., 1966, Interpretation of electric logs in freshwater wells in unconsolidated sediments: Society of Professional Well Log Analysts, Tulsa, Oklahoma, 7th Annual Logging Symposium Transaction, 25 p.

Alger, R.P., and Harrison, C.W., 1989, Improved freshwater assessment in sand aquifers utilizing geophysical well logs: The Log Analyst, v. 30, no. 1, p. 31-44.

Amsbury, D.L., 1974, Stratigraphic petrology of lower and middle Trinity rocks on the San Marcos Platform, south-central Texas, *in* Perkins, B.F., ed., Aspects of trinity division geology – a symposium: Louisiana State University, Geoscience and man, v.8, p. 1-35.

Andrews, A.G., and Croskrey, A., 2019, Brackish groundwater production zone recommendations for the Blossom Aquifer, Texas: Texas Water Development Board Open File Report 19-01, 17 p.

Archie, G.E., 1942, The electrical resistivity logs as an aid in determining some reservoir characteristics: Petroleum Technology, v. 5, p. 54-62.

Asquith, G.B., 1982, Basic well log analysis for geologists: American Association of Petroleum Geologists Methods in Exploration Series, 216 p.

Asquith, G.B., 1985, Handbook of log evaluation techniques for carbonate reservoirs: American Association of Petroleum Geologists Methods in Exploration Series, v. 5, 47 p.

Ashworth, J.B., 1983, Ground-water availability of the Lower Cretaceous formations in the Hill Country of South-Central Texas: Texas Department of Water Resources, Report 273, 65p.

Barker, R.A., and Ardis, A.F., 1996, Hydrogeologic framework of the Edwards-Trinity Aquifer system, west-central Texas: United States Geological Survey, Professional Paper 1421-B, 61 p. and 8 plates.

Barnes, V.E., project director, 1965-1994, Geologic Atlas of Texas: The University of Texas at Austin, Bureau of Economic Geology, 38 sheets, scale 1:250,000.

Bateman, R.M., and Konen, C.E., 1977, Wellsite log analysis and the programmable pocket calculator: Society of Professional Well Log Analysts Annual Logging Symposium, 18th, Houston, Texas, p. B1-B35.

Bay, T.A., Jr., 1977, Lower Cretaceous stratigraphic models from Texas and Mexico, in Bebout, D.G., and Loucks, R.G., eds., Cretaceous Carbonates of Texas and Mexico: University of Texas Bureau of Economic Geology, Report of Investigations no. 89, p. 12–23.

Bebout, D.G., 1977, Sligo and Hosston depositional patterns, subsurface of South Texas, in Bebout, D.G., and Loucks, R.G., eds., Cretaceous Carbonates of Texas and Mexico: University of Texas Bureau of Economic Geology, Report of Investigations no. 89, p. 79-96.

Bebout, D.G. and Loucks, R.G., 1977, Cretaceous carbonates of Texas and Mexico: University of Texas Bureau of Economic Geology, Report of Investigations, no. 89, 332 p.

Bense, V.F., Gleeson, T., Loveless, S.E., Bour, O., and Scibek, J., 2013, Fault zone hydrogeology: Earth-Science Reviews 127, p. 171-192.

Bhattacharya, J. and Walker, R.G, 1991, Allostratigraphic subdivision of the Upper Cretaceous Dunvegan, Shaftesbury, and Kaskapau formations in the subsurface of northwestern Alberta: Bulletin of Canadian Petroleum Geology, v. 39., p. 145-164.

Black&Veath, Daniel B. Stephens&Associates, Inc., SWCA Environmental Consultants, and Ximenes&Associates, Inc., 2020, 2021 South Central Texas Regional Water Plan, volume 2, 868 p.

Blackwell, D., Richards, M., and Stepp, P., 2010, Texas geothermal assessment for the I35 Corridor East for Texas State Energy Conservation Office contract CM709: SMU Geothermal Laboratory Contract Report, 78 p. with appendices

Blondes, M.S., Gans, K.D., Rowan, E.L., Thordsen, J.J., Reidy, M.E., Engle, M.A., Kharaka, Y.K., and Thomas, B., 2016, United States Geological Survey national produced waters geochemical database v2.2 (Provisional): United States Geological Survey, 28 p. and database files.

Brune, G. and Duffin, G., 1983, Occurrence, Availability, and Quality of Ground Water in Travis County, Texas: Texas Department of Water Resources, Report 276, 219 p.

Caine, J.S., Evans, J.P., and Forster, C.B., 1996, Fault zone architecture and permeability structure: Geology, v. 24, no.11, p. 1015-1028.

Camp, J., Hunt, B.B., Smith, B.A., 2020, Evaluating the potential groundwater availability within a Lower Trinity Aquifer well field, Balcones Fault Zone, Hays County, Central Texas: Barton Springs/Edwards Aquifer Conservation District Technical Memo 2020-0630, 70 p.

CDM Smith, 2014, Guidance manual for permitting Class I and Class II wells for the injection and disposal of desalination concentrate: CDM Smith, contract report to the Texas Water Development Board, variously paginated.

Christian, B. and Wuerch, D., 2012, Compilation of Results of Aquifer Tests in Texas: Texas Water Development Board Report no. 381, 106 p.

Clark, A.K., Golab, J.A., and Morris, R.R., 2016, Geologic framework and hydrostratigraphy of the Edwards and Trinity aquifers within northern Bexar and Comal Counties, Texas: United States Geological Survey Scientific Investigations Map 1366, 1 sheet, scale 1:24,000, pamphlet, 28 p.

Clark, A.K. and Morris, R.R., 2015. Geologic and hydrostratigraphic map of the Anhalt, Fischer, and Spring Branch 7.5-Minute Quadrangles, Blanco, Comal, and Kendall Counties, Texas: United States Geological Survey, Scientific Investigations Map 3333.

Clark, A.K., Pedraza, D.E., and Morris, R.R., 2018, Geologic framework and hydrostratigraphy of the Edwards and Trinity aquifers within Hays County, Texas: United States Geological Survey Scientific Investigations Map 3418, 1 sheet.

Clark, A.K., Blome, C.D., and Faith, J.R., 2009, Map showing the geology and hydrostratigraphy of the Edwards aquifer catchment area, northern Bexar County, south-central Texas: United States Geological Survey Open-File Report 2009–1008, 24 p.

Collier, H.A., 1993, Borehole Geophysical Techniques for Determining the Water Quality and Reservoir Parameters of Fresh and Saline Water Aquifers in Texas – Volume I of II: Texas Water Development Board, Report 343, 343 p.

Collins, E.W. and Hovorka, S.D., 1997, Structure map of the San Antonio segment of the Edwards Aquifer and Balcones Fault Zone, South-Central Texas: Structural framework of a major limestone aquifer: Kinney, Uvalde, Medina, Bexar, Comal, and Hays counties: The University of Texas at Austin, Bureau of Economic Geology, Miscellaneous Map no. 38, 38 p.

Cooper, H.H., Jr., and Jacob, C.E., 1946, A generalized graphical method for evaluating formation constants and summarizing well field history: American Geophysical Union Transactions, v. 27, p. 526-534.

Core Laboratories, 1972, A survey of the subsurface saline water of Texas: Texas Water Development Board Report 157, 8 volumes, variously paginated.

Croskrey, A.D., Suydam, A.K., Robinson, M.C, and Meyer, J.E., 2019, Brackish groundwater production zone recommendations for the Nacatoch Aquifer, Texas: Texas Water Development Board Open File Report 19-02, 22p.

Culotta, R., Latham, T., Sydow, M., Oliver, J., Brown, L. and Kaufman, S., 1992, Deep structure of the Texas Gulf passive margin and its Ouachita-Precambrian basement: Results of the COCORP San Marcos Arch survey, American Association of Petroleum Geologists, v. 76, no. 2, p. 270-283.

Daniel B. Stephens and Associates, 2006, Aquifer tests from county availability studies: Daniel B. Stephens and Associates, contract report to Texas Water Development Board, variously paginated, TWDB Contract 2005483554.

Dutton, S.P., and Loucks, R.G., 2014, Reservoir quality and porosity-permeability trends in onshore Wilcox sandstone, Texas and Louisiana Gulf Coast: Application to deep Wilcox plays, offshore Gulf of Mexico: Gulf Coast Association of Geological Societies Volume 3, p. 33-40.

Estepp. J.D., 1998, Evaluation of ground-water quality using geophysical logs: Texas Natural Resource Conservation Commission, unpublished report, 516 p.

Estepp, J.D., 2010, Determining groundwater quality using geophysical logs: Texas Commission on Environmental Quality, unpublished report, 85 p.

Ferrill, D.A. and Morris, A.P., 2008, Fault zone deformation controlled by carbonate mechanical stratigraphy, Balcones fault system, Texas: AAPG Bulletin, v. 92, no. 3, p. 359-380.

Ferrill, D.A., Sims, D.W., Morris, A.P., Waiting, D.J., and Franklin, N., 2003, Structural Controls on the Edwards Aquifer/Trinity Aquifer Interface in the Camp Bullis Quadrangle, Texas: final report prepared by Southwest Research Institute, for the Edwards Aquifer Authority and the US Army Corps of Engineers, variously paginated.

Ferrill, D.A., Sims, D.W., Franklin, N., Morris, A.P., and Waiting, D.J., 2005, Structural Controls on the Edward Aquifer/Trinity Aquifer Interface in the Helotes Quadrangle, Texas: final report prepared by Southwest Research Institute and The University of Texas at Austin, for the Edwards Aquifer Authority and the US Army Corps of Engineers, variously paginated.

Finch, S.T., Standen, A.R., and Blandford, T.N., 2016, Brackish groundwater in the Blaine Aquifer System, North-Central Texas: contract report by Daniel B. Stephens and Associates, Inc., to the Texas Water Development Board, 73 p.

Flawn, P.T., Goldstein, A., King, P. B, and Weaver, C. E., 1961, The Ouachita System: Texas Bureau of Economic Geology Publication 6120, Austin, 401 p.

Forgotson, J.M. Jr., 1963, Depositional history and paleotectonic framework of Comanchean Cretaceous Trinity Stage, Gulf Coast area: American Association of Petroleum Geologists Bulletin, vol. 47, no. 1, pp. 69-103.

Forgotson, J.M. Jr., 1957, Stratigraphy of Comanchean Cretaceous Trinity Group: AAPG Bulletin, v. 41, no. 10, p. 2328-2363.

George, W.O. and Hastings, W.W., 1947, Geology and ground-water resources of Comal County, Texas: Texas Board of Water Engineers, 142 p.

Gradstein, F.M., Ogg, J.G., Schmitz, M.D., and Ogg, G.M., editors, 2012, The geological time scale 2012: Amsterdam, Elsevier, 2 volumes, 1144 p.

Grimshaw, T.W., and C.M. Woodruff, Jr., 1986, Structural style in an en echelon fault system, Balcones Fault Zone, Central Texas: Geomorphologic and hydrologic implications, *in* P. L. Abbott and C. M. Woodruff, Jr., eds., The Balcones Escarpment: Geology, hydrology, ecology and social development in Central Texas: Geological Society of America, Boulder, Colorado, p. 71–76.

HDR, 2011, Texas water system map: The compilation of a statewide geodataset and digital maps of water service area boundaries: HDR, contract report to the Texas Water Development Board, 35 p. and digital datasets.

Hem, J.D., 1985, Study and interpretation of the chemical characteristics of natural water: United States Geological Survey Water-Supply Paper 2254, 263 p. and 4 plates.

Hill, R.T., 1901, Geography and geology of the Black and Grand Prairies, Texas: United States Geological Survey 21st Annual Report, Part 7, 666 p.

Hill, R.T., and Vaughan, T.W., 1889, Geology of the Edwards Plateau and Rio Grande Plain adjacent to Austin and San Antonio, Texas: United States Geological Survey 18th Annual Report, Part 2, p. 193-321.

Hunt, B.B., Cockrell, L.P., Gary, R.H., Vay, J.M., Kennedy, V., Smith, B.A., and Camp, J.P., 2020, Hydrogeologic Atlas of Southwest Travis County, Central Texas: Barton Springs/Edwards Aquifer Conservation District, Report of Investigations 2020-0429, April 2020, 80 p. + digital datasets.

Hunt, B.B., Smith, B.A., Andrews, A., Wierman, D.A., Broun, A.S., and Gary, M.O., 2015, Relay ramp structures and their influence on groundwater flow in the Edwards and Trinity Aquifers, Hays and Travis Counties, Central Texas, in Doctor D.H., Land L., and Stephenson J.B., Proceedings of the 14th Multidisciplinary Conference on Sinkholes and the Engineering and Environmental Impacts of Karst; 2015 Oct. 5–10, 2015, Rochester, MN: National Cave and Karst Research Institute. p. 189–199.

Hunt, B.B., Smith, B.A., Gary, R., and Camp, J., 2019, March 2018 potentiometric map of the Middle Trinity Aquifer, Central, Texas: Barton Springs/Edwards Aquifer Conservation District, Report of Investigations 2019-0109, 28 p.

Hunt, B.B., Smith, B.A., Kromann, J., Wierman, D.A., and Mikels, J.K., 2010, Compilation of pumping tests in Travis and Hays counties, central Texas: Barton Springs/Edwards Aquifer Conservation District Data Series Report 2010-0701. 86 p.

Imlay, R.W., 1945, Subsurface Lower Cretaceous formations of South Texas: American Association of Petroleum Geologists Bulletin, vol. 29, no. 10, pp. 1416-1469.

Inden, R.F., 1974, Lithofacies and depositional model for a Trinity Cretaceous sequence, central Texas, in Perkins, B. F, ed., Aspects of Trinity Geology: Geoscience and Man, v. 8, p. 37–52.

INTERA, 2014, Updated groundwater availability model of the Northern Trinity and Woodbine Aquifers: contract report by INTERA, Inc., to the Texas Water Development Board, variously paginated.

Jones, I.C., Anaya, R., and Wade, S.C., 2011, Groundwater Availability Model, Hill Country Portion of the Trinity Aquifer of Texas: Texas Water Development Board Report 377, 165 p.

Jones, I.C., and Bradley, R., 2013, GAM Task 13-032: Total Estimated Recoverable Storage for Aquifers in Groundwater Management Area 9. October 2013.

Jones, I.C., Shi, J., and Bradley, R., 2013, GAM Task 13-033: Total Estimated Recoverable Storage for Aquifers in Groundwater Management Area 10. August 2013.

Lang, J.W., 1954, Ground-water resources of the San Antonio Area, Texas: Texas Board of Water Engineers, Bulletin 5412, 30 p.

Larkin, T.J., and Bomar, G.W., 1983, Climatic atlas of Texas: Texas Department of Water Resources Report LP 192, 151 p.

LBG-Guyton Associates, 2003, Brackish groundwater manual for Texas regional water planning groups: contract report by LBG-Guyton Associates, to the Texas Water Development Board, 188 p.

Lowe, T.A., and Dunlap, H.F., 1986, Estimation of mud filtrate resistivity in fresh water drilling muds: The Log Analyst, v. 27, no. 2, March-April, p.77-84.

Lower Colorado Regional Water Planning group, AECOM Technical Services, Inc., James Kowis Consulting, LLC, Laura Raun Public Relations and Trungale Engineering and Science, 2015, Adopted 2016 Region K Water Plan for the Lower Colorado Regional Water Planning Group, volume II, 1490 p.

Lupton, D., Kelley, V., Powers, D., Torres-Verdín, C., editors, Harding, J.J., Martínez, G., Oliver, W., Godbout, L., Bennis, M., and Sutherland, J., contributors, 2016, Identification of potential brackish groundwater production areas – Rustler Aquifer: Texas Water Development Board Contract Number 1600011949, 358 p.

MacCary, L.M., 1978, Interpretation of well logs in a carbonate aquifer: U.S. Geological Survey, Water-Resources Investigations 78-88, 30 p.

MacCary, L.M., 1980, Use of geophysical logs to estimate water-quality trends in carbonate aquifers: U.S. Geological Survey, Water-Resources Investigations 80-57, 23 p.

Mace, R. E., 1997, Determination of transmissivity from specific capacity data in a karst aquifer: Ground Water, v. 35 no. 5, p. 738-742.

Mace, R.E., Chowdhury, A.H., Anaya, R., and Way, S.C., 2000, Groundwater availability of the Trinity Aquifer, Hill County area, Texas—Numerical simulations through 2050: Texas Water Development Board Report 353, 117 p.

Mace, R. E., Smyth, R.C., Xu, L. and Liang, J., 2000, Transmissivity, Hydraulic Conductivity and Storativity of the Carrizo-Wilcox Aquifer in Texas: Texas Water Development Board Technical Report, Contract no. 99-483-279, 76 p.

Mace, R.E., Nicot, J.P., Chowdhury, A.H., Dutton, A.R., and Kalaswad, S., 2006, Please pass the salt: using oil fields for the disposal of concentrate from desalination plants: Texas Water Development Board Report 366, 214 p.

Martin, N.M., Green, R.T., Nicholaides, K.D., Fratesi, S.B., Nunu, R.R., and Flores, M.E. 2019. Blanco River aquifer assessment tool: A tool to assess how the Blanco River interacts with its aquifer, creating the conceptual model: Technical Report prepared for the Meadows Center for Water and the Environment. Texas State University at San Marcos, Texas. 136 p.

McWhorter, D.B., and Sunada, D.K., 2010, Ground-water hydrology and hydraulics (reprint ed.), Fort Collins, CO, Water Resources Publications, 304 p.

Meyer, J.E., 2012, Geologic characterization of and data collection in the Corpus Christi Aquifer Storage and Recovery Conservation District and surrounding counties: Texas Water Development Board Open File Report 12-01, 42 p.

Meyer, J.E., Wise, M.R., and Kalaswad, S., 2012, Pecos Valley Aquifer, West Texas, Structure and brackish groundwater: Texas Water Development Board Report 382, 86 p.

Meyer, J.E., Croskrey, A.D., Wise, M.R., and Kalaswad, S., 2014, Brackish groundwater in the Gulf Coast Aquifer, lower Rio Grande Valley, Texas: Texas Water Development Board Report 383, 169 p.

Meyer, J.E., Croskrey, A.D., Suydam, A.K., and Van Oort, N., 2020, Brackish groundwater in aquifers of the Upper Coastal Plains, Central Texas: Texas Water Development Board Report 385, 278p.

Miller, R.L., Bradford, W.L., and Peters, N.E., 1988, Specific Conductance: Theoretical Considerations and Application to Analytical Quality Control: U.S. Geological Survey Water-Supply Paper 2311, 16 p.

Myers, B.N., 1969, Compilation of Results of Aquifer Tests in Texas: Texas water Development Board Report no. 98, 533 p.

Perkins, B.F., 1974, Aspects of Trinity Division Geology: Louisiana State University, Geoscience and Man, vol. VIII, 228 p.

Preston, R.D., Pavilcek, D.J., Bluntzer, R.L., and Derton, J., 1996, The Paleozoic and related aquifers of Central Texas: Texas Water Development Board Report 346, 95 p.

Ramamoorthy, R., Ramakrishnan, T.S., Dasgupta, S., and Raina, I., Towards a petrophysically consistent implementation of Archie's equation for heterogeneous carbonate rocks, in Society of Petrophysicists and Well Log Analysts: The Woodlands, Texas, 60th Annual Logging Symposium Transaction, 22 p.

Robinson, M.C., Webb, M.L., Perez, J.B., and Andrews, A.G., 2018, Brackish groundwater in the Lipan Aquifer area, Texas: Texas Water Development Board Report 384, 230 p.

Robinson, M.C., Deeds, N.E., Lupton, D.M., 2019, Identification of potential brackish groundwater production areas – Northern Trinity Aquifer: Texas Water Development Board Technical Note 19-1, 132 p.

Rose, P.R., 1972, Edwards Group, Surface and Subsurface, Central Texas: The University of Texas at Austin, Bureau of Economic Geology Report of Investigations No. 74, 198 p. 35 figs, 19 plates.

Rose, P.R., 2016, Late Cretaceous and Tertiary burial history, Central Texas: GCAGS Journal, v. 5, p. 141-179.

Rossum, J.R., 1949, Conductance method for checking accuracy of water analyses: Anal. Chem., Vol. 21, p. 631.

Schlumberger, 1972, Log Interpretation, Volume 1 – Principles: Schlumberger Ltd., 113 p.

Schlumberger, 1987, Log interpretation principles/applications: Schlumberger Educational Services, 198 p.

Schlumberger, 2009, Log interpretation charts: Schlumberger, Houston, Texas.

Schultz, A.L., 1992, Using geophysical logs in the Edwards Aquifer to estimate water quality along the freshwater/saline-water interface, Uvalde, Texas to San Antonio, Texas: Edwards Underground Water District Report 92-03, 47 p. and 5 plates.

Schultz, A.L., 1993, Defining the Edwards Aquifer freshwater/saline-water interface with geophysical logs and measured data (San Antonio to Kyle, Texas): Edwards Underground Water District Report 93-06, 81 p. and 4 plates.

Senger, R.K., and Kreitler, C.W., 1984, Hydrogeology of the Edwards Aquifer, Austin Area, Central Texas: Bureau of Economic Geology, Report of Investigations, No. 141, 35 p.

Shi, J., Bradley, R. G., Wade, S., Jones, I., Anaya, R. and Seiter-Weatherford, C., 2014, GAM TASK 13-031: Total Estimated Recoverable Storage for Aquifers in Groundwater Management Area 8: Texas Water Development Board report, variously paginated.

Smith, B.A., and Hunt, B.B., 2009, Potential hydraulic connections between the Edwards and Trinity Aquifers in the Balcones Fault Zone of central Texas: Bulletin of the South Texas Geological Society, L, 2, p. 15 – 34.

Smith, B.A., Hunt, B.B., Wierman, D.A., and Gary, M.O., 2018, Groundwater Flow Systems of Multiple Karst Aquifers of Central Texas, *in* Sasowsky, I.D., Byle, M.J., and Land, L., eds., Proceedings of the 15th Multidisciplinary Conf. on Sinkholes and the Engineering and Environmental Impacts of Karst and the 3rd Appalachian Karst Symp.: National Cave and Karst Research Inst. (NCKRI) Symp. 7, p 17-29.

Standen, A.R., and Murphy, S.C., 2021, Core testing for the Hill Country Trinity Aquifer: Texas Water Development Board Contract Number 2000012440, 31 p.

Stricklin, F.L., Jr., and D.L. Amsbury, 1974, Depositional environments on a low-relief carbonate shelf, middle Glen Rose Limestone, central Texas, in B. F. Perkins, ed., Geoscience and Man, v. VIII: Louisiana State University Press, Baton Rouge, p. 53-66.

Stricklin, F.L., Jr., Smith, C.I., and Lozo, F.E., 1971, Stratigraphy of Lower Cretaceous Trinity deposits of Central Texas: University of Texas Bureau of Economic Geology, Report of Investigations 71, 63 p.

TCEQ (Texas Commission on Environmental Quality), 2015, Subchapter F: Drinking water standards governing water quality and reporting requirements for public water systems: 30 Texas Administrative Code Chapter 290, §§ 290.101 – 290.122.

Theis, C.V., 1935. The relation between the lowering of the piezometric surface and the rate and duration of discharge of a well using groundwater storage: Am. Geophys. Union Trans., vol. 16, pp. 519-524.

Thoms, E., 2005, Creating and managing digital cross section within ArcGIS: U.S. Geological Survey Open-file Report 2005-1428, p. 247-251.

Tian, L., Smith, B.A., Hunt, B.B., Doster, J.D., and Gao, Y., 2020, Geochemical evaluation of hydrogeologic interaction between the Edwards and Trinity Aquifers based on BSEACD multiport well results: National Cave and Karst Research Institute, Symposium 8, Proceedings of the 16th Multidisciplinary Conference on Sinkholes and the Engineering and Environmental Impacts of Karst, First Edition, p. 269-277.

Toll, N.J., Green R.T., McGinnis, R.N., Stepchinski, L.M., Nunu, R.R., Walter, G.R., Harding, J., Deeds, N.E., Flores, M.E., and Gulliver, K.D.H., 2018, Conceptual Model Report for the Hill Country Trinity Aquifer Groundwater Availability Model: Texas Water Development Board, 2018, 266 p.

Torres-Verdín, C., 2017, Integrated geological-petrophysical interpretation of well logs: Department of Petroleum and Geosystems Engineering, The University of Texas at Austin, unpublished class notes, variously paginated.

Tucker, D.R., 1962, Subsurface Lower Cretaceous stratigraphy, Central Texas, *in* Stapp, W. L., ed., Contributions to geology of South Texas: South Texas Geological Society, p. 177-216.

TWDB (Texas Water Development Board), 2021a, Brackish resources aquifer characterization system database data dictionary: Texas Water Development Board Open File Report 12-02, Sixth Edition, 195 p.

TWDB (Texas Water Development Board), 2021b, BRACS Database.

Verwer, K., Eberli, G.P., Weger, R.J., 2011, Effect of pore structure on electrical resistivity in carbonates: American Association of Petroleum Geologists Bulletin, v. 95, no. 2, p. 175-190.

Wade, S.C., and Bradley, R., 2013, GAM Task 13-036 (revised): Total estimated recoverable storage for aquifers in Groundwater Management Area 13: Texas Water Development Board Technical Note, 30 p.

Wade, S.C., and Shi, J., 2014, GAM Task 13-035 version 2: Total estimated recoverable storage for aquifers in Groundwater Management Area 12: Texas Water Development Board Technical Note, 43 p.

Wierman, D.A., Broun, A.S., and Hunt, B.B. 2010, Hydrogeologic Atlas of the Hill Country Trinity Aquifer Blanco, Hays, and Travis Counties, Central Texas: Hay-Trinity Groundwater Conservation District, 17 p.

Winslow, A.G., and Kister, L.R., 1956, Saline-water resources of Texas: U.S. Geological Survey Water-Supply Paper 1365, 105 p.

Wise, M.R., 2014, Queen City and Sparta Aquifers, Atascosa and McMullen Counties, Texas: Structure and brackish groundwater: Texas Water Development Board Technical Note 14-01, 67 p.

Wong, C.I., Kromann, J.S., Hunt, B.B., Smith, B.A., and Banner, J.L., 2014, Investigating Groundwater Flow Between Edwards and Trinity Aquifers in Central Texas: Groundwater, vol. 52, no 4. P. 624-639.

WSP, and Carollo Engineers, 2021 Plateau Region Water Plan, 460 p.

Young, S.C., Jigmond, M., Deeds, N., Blainey, J., Ewing, T.E., Banerji, D., editors, Piemonti, D., Jones, T., Griffith, C., Lupton, D., Martínez, G., Hudson, C., Hamlin, S., and Sutherland, J., contributors, 2016, Identification of potential brackish groundwater production areas – Gulf Coast Aquifer system: Texas Water Development Board Contract Number 1600011947, 636 p.

Zappitello, S.J., Johns, D.A., and Hunt, B.B., 2019, Summary of groundwater tracing in the Barton Springs Edwards Aquifer from 1996 to 2017: City of Austin Watershed Protection Department Report DR-19-04, 30 p.

19 Appendices

19.1 Python scripts

We developed and used a total of five python scripts during this project. Four of these scripts were used to create the surfaces of the hydrostratigraphic units. One python script was developed to compute the volumes used to populate the tables in Section 13-3 of this report. The file listings included here are meant to provide an opportunity for a Python knowledgeable reader to review the logic and algorithms used in our calculations. The scripts were created for the sole purpose of processing data by us for this report and were not intended to be used for any other application or purpose.

19.1.1 Convert spreadsheet data to shapefiles in GAM projection

```
# -*- coding: utf-8 -*-
# ---------------------------------------------------------------------------
# test2.py
# Created on: 2019-08-14 10:00:11.00000
#   (generated by ArcGIS/ModelBuilder)
#
# Description:
# ---------------------------------------------------------------------------
import arcpy
import os

# Script arguments
FILE_LIST =
['00_BUD_TOP','01_UGR_TOP','02_LGR_TOP','03_HEN_TOP','04_CCK_TOP','05_HAM_TOP','06_SLG_TOP','07_
HSN_TOP','08_BOK_TOP']

X_Field = "longitude"
Y_Field = "latitude"

def XY2GAM(XYT, X_Field, Y_Field):
  XY_Table = "User file path/" + XYT + ".xls/" + XYT

  Shapefile_in_GAM_Albers_Projection = " User file path \\" + XYT + ".shp"

  arcpy.Delete_management(Shapefile_in_GAM_Albers_Projection)

  # set workspace gdb
  arcpy.env.workspace = r" User file path \HCT_GeoDB1.gdb"

  # Local variables:
  Spatial_Reference =
"GEOGCS['GCS_North_American_1983',DATUM['D_North_American_1983',SPHEROID['GRS_1980',6378137.
0,298.257222101]],PRIMEM['Greenwich',0.0],UNIT['Degree',0.0174532925199433]];-400 -400
1000000000;-100000 10000;-100000 10000;8.98315284119521E-09;0.001;0.001;IsHighPrecision"

  Event = "BRACS_GIS1"
```

```
 Output_Coordinate_System =
"GEOGCS['GCS_North_American_1983',DATUM['D_North_American_1983',SPHEROID['GRS_1980',6378137.
0,298.257222101]],PRIMEM['Greenwich',0.0],UNIT['Degree',0.0174532925199433]]"

 Shapefile_in_GCS_NAD83 = "User file path \\XY Table.shp"

 TWDB_GAM_Projection_prj =
"PROJCS['GAM',GEOGCS['GCS_North_American_1983',DATUM['D_North_American_1983',SPHEROID['GRS_
1980',6378137.0,298.257222101]],PRIMEM['Greenwich',0.0],UNIT['Degree',0.0174532925199433]],PROJ
ECTION['Albers'],PARAMETER['False_Easting',4921250.0],PARAMETER['False_Northing',19685000.0],PA
RAMETER['Central_Meridian',-
100.0],PARAMETER['Standard_Parallel_1',27.5],PARAMETER['Standard_Parallel_2',35.0],PARAMETER['Lat
itude_Of_Origin',31.25],UNIT['Foot_US',0.3048006096012192]]"

 Input_Coordinate_System = ""

 # Process: Make XY Event Layer
 arcpy.MakeXYEventLayer_management(XY_Table, X_Field, Y_Field, Event, Spatial_Reference, "")

 # Process: Copy Features
 tempEnvironment0 = arcpy.env.outputCoordinateSystem
 #52
 arcpy.env.outputCoordinateSystem =
"GEOGCS['GCS_North_American_1983',DATUM['D_North_American_1983',SPHEROID['GRS_1980',6378137.
0,298.257222101]],PRIMEM['Greenwich',0.0],UNIT['Degree',0.0174532925199433]]"

 arcpy.CopyFeatures_management(Event, Shapefile_in_GCS_NAD83, "", "0", "0", "0")

 arcpy.env.outputCoordinateSystem =
"GEOGCS['GCS_North_American_1983',DATUM['D_North_American_1983',SPHEROID['GRS_1980',6378137.
0,298.257222101]],PRIMEM['Greenwich',0.0],UNIT['Degree',0.0174532925199433]]"

 # Process: Project
 arcpy.Project_management(Shapefile_in_GCS_NAD83, Shapefile_in_GAM_Albers_Projection,
TWDB_GAM_Projection_prj, "", Input_Coordinate_System, "NO_PRESERVE_SHAPE", "", "NO_VERTICAL")

for XYT in FILE_LIST:
 XY2GAM(XYT, "longitude", "latitude")
```

19.1.2 Use TopoToRaster to interpolate surfaces

```
#
try:
   arcpy.Delete_management("User file path /00BUD_TTR1.tif")
except Exception as e:
   print e.message

   # If using this code within a script tool, AddError can be used to return messages
   #   back to a script tool.  If not, AddError will have no effect.
   arcpy.AddError(e.message)

arcpy.gp.TopoToRaster_sa("User file path /X_BUD_DEM.shp RASTERVALU PointElevation;User file
path/00_BUD_TOP.shp BUD_SS PointElevation;User file path/HCT_FLTN00.shp # Cliff;User file
path/HCT_FLTN01.shp # Cliff;User file path/HCT_FLTN02.shp # Cliff;User file path/HCT_FLTN03.shp #
Cliff;User file path/HCT_FLTN04.shp # Cliff;User file path/HCT_FLTN05.shp # Cliff;User file
```

path/HCT_FLTN06.shp # Cliff;***User file path***/HCT_FLTN07.shp # Cliff;***User file path***/HCT_FLTN08.shp # Cliff;***User file path***/HCT_FLTN09.shp # Cliff;***User file path***/HCT_FLTN10.shp # Cliff;***User file path***/HCT_FLTN11.shp # Cliff;***User file path***/HCT_FLTN12.shp # Cliff;***User file path***/HCT_FLTN13.shp # Cliff;***User file path***/HCT_FLTN14.shp # Cliff;***User file path***/HCT_FLTN15.shp # Cliff;***User file path***/HCT_FLTN16.shp # Cliff;***User file path***/HCT_FLTN17.shp # Cliff;***User file path***/HCT_FLTR1.shp # Cliff;***User file path***/HCT_FLTR2.shp # Cliff;***User file path***/HCT_FLTR3.shp # Cliff;***User file path***/HCT_FLTR4.shp # Cliff", "***User file path***/00BUD_TTR1.tif", "250", "4811000 18691000 5860000 19490000", "5", "", "", "NO_ENFORCE", "SPOT", "20", "", "1", "0", "0", "200", "", "", "", "", "", "", "", "")

```
try:
  arcpy.Delete_management("User file path/01UGR_TTR1.tif")
except Exception as e:
  print e.message

  # If using this code within a script tool, AddError can be used to return messages
  #   back to a script tool.  If not, AddError will have no effect.
  arcpy.AddError(e.message)
```

arcpy.gp.TopoToRaster_sa("***User file path***/X_GRU_DEM.shp RASTERVALU PointElevation;***User file path***/01_UGR_TOP.shp UGR_SS PointElevation;***User file path***/HCT_FLTN00.shp # Cliff;***User file path***/HCT_FLTN01.shp # Cliff;***User file path***/HCT_FLTN02.shp # Cliff;***User file path***/HCT_FLTN03.shp # Cliff;***User file path***/HCT_FLTN04.shp # Cliff;***User file path***/HCT_FLTN05.shp # Cliff;***User file path***/HCT_FLTN06.shp # Cliff;***User file path***/HCT_FLTN07.shp # Cliff;***User file path***/HCT_FLTN08.shp # Cliff;***User file path***/HCT_FLTN09.shp # Cliff;***User file path***/HCT_FLTN10.shp # Cliff;***User file path***/HCT_FLTN11.shp # Cliff;***User file path***/HCT_FLTN12.shp # Cliff;***User file path***/HCT_FLTN13.shp # Cliff;***User file path***/HCT_FLTN14.shp # Cliff;***User file path***/HCT_FLTN15.shp # Cliff;***User file path***/HCT_FLTN16.shp # Cliff;***User file path***/HCT_FLTN17.shp # Cliff;***User file path***/HCT_FLTR1.shp # Cliff;***User file path***/HCT_FLTR2.shp # Cliff;***User file path***/HCT_FLTR3.shp # Cliff;***User file path***/HCT_FLTR4.shp # Cliff", "***User file path***/01UGR_TTR1.tif", "250", "4811000 18691000 5860000 19490000", "5", "", "", "NO_ENFORCE", "SPOT", "20", "", "1", "0", "0", "200", "", "", "", "", "", "", "", "")

```
try:
  arcpy.Delete_management("User file path/02LGR_TTR1.tif")
except Exception as e:
  print e.message

  # If using this code within a script tool, AddError can be used to return messages
  #   back to a script tool.  If not, AddError will have no effect.
  arcpy.AddError(e.message)
```

arcpy.gp.TopoToRaster_sa("***User file path***/X_GRL_DEM.shp RASTERVALU PointElevation;***User file path***/02_LGR_TOP.shp LGR_SS PointElevation;***User file path***/HCT_FLTN00.shp # Cliff;***User file path***/HCT_FLTN01.shp # Cliff;***User file path***/HCT_FLTN02.shp # Cliff;***User file path***/HCT_FLTN03.shp # Cliff;***User file path***/HCT_FLTN04.shp # Cliff;***User file path***/HCT_FLTN05.shp # Cliff;***User file path***/HCT_FLTN06.shp # Cliff;***User file path***/HCT_FLTN07.shp # Cliff;***User file path***/HCT_FLTN08.shp # Cliff;***User file path***/HCT_FLTN09.shp # Cliff;***User file path***/HCT_FLTN10.shp # Cliff;***User file path***/HCT_FLTN11.shp # Cliff;***User file path***/HCT_FLTN12.shp # Cliff;***User file path***/HCT_FLTN13.shp # Cliff;***User file path***/HCT_FLTN14.shp # Cliff;***User file path***/HCT_FLTN15.shp # Cliff;***User file path***/HCT_FLTN16.shp # Cliff;***User file path***/HCT_FLTN17.shp # Cliff;***User file path***/HCT_FLTR1.shp # Cliff;***User file path***/HCT_FLTR2.shp # Cliff;***User file path***/HCT_FLTR3.shp # Cliff;***User file path***/HCT_FLTR4.shp # Cliff", "***User file path***/02LGR_TTR1.tif", "250", "4811000 18691000 5860000 19490000", "5", "", "", "NO_ENFORCE", "SPOT", "20", "", "1", "0", "0", "200", "", "", "", "", "", "", "", "")

```
try:
  arcpy.Delete_management("User file path/03HEN_TTR1.tif")
```

```
except Exception as e:
   print e.message

   # If using this code within a script tool, AddError can be used to return messages
   #   back to a script tool.  If not, AddError will have no effect.
   arcpy.AddError(e.message)

arcpy.gp.TopoToRaster_sa("User file path/X_HEN_DEM.shp RASTERVALU PointElevation;User file
path/03_HEN_TOP.shp HEN_SS PointElevation;User file path/HCT_FLTN00.shp # Cliff;User file
path/HCT_FLTN01.shp # Cliff;User file path/HCT_FLTN02.shp # Cliff;User file path/HCT_FLTN03.shp #
Cliff;User file path/HCT_FLTN04.shp # Cliff;User file path/HCT_FLTN05.shp # Cliff;User file
path/HCT_FLTN06.shp # Cliff;User file path/HCT_FLTN07.shp # Cliff;User file path/HCT_FLTN08.shp #
Cliff;User file path/HCT_FLTN09.shp # Cliff;User file path/HCT_FLTN10.shp # Cliff;User file
path/HCT_FLTN11.shp # Cliff;User file path/HCT_FLTN12.shp # Cliff;User file path/HCT_FLTN13.shp #
Cliff;User file path/HCT_FLTN14.shp # Cliff;User file path/HCT_FLTN15.shp # Cliff;User file
path/HCT_FLTN16.shp # Cliff;User file path/HCT_FLTN17.shp # Cliff;User file path/HCT_FLTR1.shp #
Cliff;User file path/HCT_FLTR2.shp # Cliff;User file path/HCT_FLTR3.shp # Cliff;User file
path/HCT_FLTR4.shp # Cliff", "User file path/03HEN_TTR1.tif", "250", "4811000 18691000 5860000
19490000", "5", "", "", "NO_ENFORCE", "SPOT", "20", "", "1", "0", "0", "200", "", "", "", "", "", "", "", "")

try:
   arcpy.Delete_management("User file path/04CCK_TTR1.tif")
except Exception as e:
   print e.message

   # If using this code within a script tool, AddError can be used to return messages
   #   back to a script tool.  If not, AddError will have no effect.
   arcpy.AddError(e.message)

arcpy.gp.TopoToRaster_sa("User file path/X_CCK_DEM.shp RASTERVALU PointElevation;User file
path/04_CCK_TOP.shp CCK_SS PointElevation;User file path/HCT_FLTN00.shp # Cliff;User file
path/HCT_FLTN01.shp # Cliff;User file path/HCT_FLTN02.shp # Cliff;User file path/HCT_FLTN03.shp #
Cliff;User file path/HCT_FLTN04.shp # Cliff;User file path/HCT_FLTN05.shp # Cliff;User file
path/HCT_FLTN06.shp # Cliff;User file path/HCT_FLTN07.shp # Cliff;User file path/HCT_FLTN08.shp #
Cliff;User file path/HCT_FLTN09.shp # Cliff;User file path/HCT_FLTN10.shp # Cliff;User file
path/HCT_FLTN11.shp # Cliff;User file path/HCT_FLTN12.shp # Cliff;User file path/HCT_FLTN13.shp #
Cliff;User file path/HCT_FLTN14.shp # Cliff;User file path/HCT_FLTN15.shp # Cliff;User file
path/HCT_FLTN16.shp # Cliff;User file path/HCT_FLTN17.shp # Cliff;User file path/HCT_FLTR1.shp #
Cliff;User file path/HCT_FLTR2.shp # Cliff;User file path/HCT_FLTR3.shp # Cliff;User file
path/HCT_FLTR4.shp # Cliff", "User file path/04CCK_TTR1.tif", "250", "4811000 18691000 5860000
19490000", "5", "", "", "NO_ENFORCE", "SPOT", "20", "", "1", "0", "0", "200", "", "", "", "", "", "", "", "")

try:
   arcpy.Delete_management("User file path/05HAM_TTR1.tif")
except Exception as e:
   print e.message

   # If using this code within a script tool, AddError can be used to return messages
   #   back to a script tool.  If not, AddError will have no effect.
   arcpy.AddError(e.message)

arcpy.gp.TopoToRaster_sa("User file path/X_HAM_DEM.shp RASTERVALU PointElevation;User file
path/05_HAM_TOP.shp HAM_SS PointElevation;User file path/HCT_FLTN00.shp # Cliff;User file
path/HCT_FLTN01.shp # Cliff;User file path/HCT_FLTN02.shp # Cliff;User file path/HCT_FLTN03.shp #
Cliff;User file path/HCT_FLTN04.shp # Cliff;User file path/HCT_FLTN05.shp # Cliff;User file
```

path/HCT_FLTN06.shp # Cliff;***User file path***/HCT_FLTN07.shp # Cliff;***User file path***/HCT_FLTN08.shp # Cliff;***User file path***/HCT_FLTN09.shp # Cliff;***User file path***/HCT_FLTN10.shp # Cliff;***User file path***/HCT_FLTN11.shp # Cliff;***User file path***/HCT_FLTN12.shp # Cliff;***User file path***/HCT_FLTN13.shp # Cliff;***User file path***/HCT_FLTN14.shp # Cliff;***User file path***/HCT_FLTN15.shp # Cliff;***User file path***/HCT_FLTN16.shp # Cliff;***User file path***/HCT_FLTN17.shp # Cliff;***User file path***/HCT_FLTR1.shp # Cliff;***User file path***/HCT_FLTR2.shp # Cliff;***User file path***/HCT_FLTR3.shp # Cliff;***User file path***/HCT_FLTR4.shp # Cliff", "***User file path***/05HAM_TTR1.tif", "250", "4811000 18691000 5860000 19490000", "5", "", "", "NO_ENFORCE", "SPOT", "20", "", "1", "0", "0", "200", "", "", "", "", "", "", "", "")

```
try:
  arcpy.Delete_management("User file path/06SLG_TTR1.tif")
except Exception as e:
  print e.message

  # If using this code within a script tool, AddError can be used to return messages
  #   back to a script tool.  If not, AddError will have no effect.
  arcpy.AddError(e.message)
```

arcpy.gp.TopoToRaster_sa("***User file path***/06_SLG_TOP.shp SLG_SS PointElevation;***User file path***/HCT_FLTN00.shp # Cliff;***User file path***/HCT_FLTN01.shp # Cliff;***User file path***/HCT_FLTN02.shp # Cliff;***User file path***/HCT_FLTN03.shp # Cliff;***User file path***/HCT_FLTN04.shp # Cliff;***User file path***/HCT_FLTN05.shp # Cliff;***User file path***/HCT_FLTN06.shp # Cliff;***User file path***/HCT_FLTN07.shp # Cliff;***User file path***/HCT_FLTN08.shp # Cliff;***User file path***/HCT_FLTN09.shp # Cliff;***User file path***/HCT_FLTN10.shp # Cliff;***User file path***/HCT_FLTN11.shp # Cliff;***User file path***/HCT_FLTN12.shp # Cliff;***User file path***/HCT_FLTN13.shp # Cliff;***User file path***/HCT_FLTN14.shp # Cliff;***User file path***/HCT_FLTN15.shp # Cliff;***User file path***/HCT_FLTN16.shp # Cliff;***User file path***/HCT_FLTN17.shp # Cliff;***User file path***/HCT_FLTR1.shp # Cliff;***User file path***/HCT_FLTR2.shp # Cliff;***User file path***/HCT_FLTR3.shp # Cliff;***User file path***/HCT_FLTR4.shp # Cliff", "***User file path***/06SLG_TTR1.tif", "250", "4811000 18691000 5860000 19490000", "5", "", "", "NO_ENFORCE", "SPOT", "20", "", "1", "0", "0", "200", "", "", "", "", "", "", "", "", "")

```
try:
  arcpy.Delete_management("User file path/07HSN_TTR1.tif")
except Exception as e:
  print e.message

  # If using this code within a script tool, AddError can be used to return messages
  #   back to a script tool.  If not, AddError will have no effect.
  arcpy.AddError(e.message)
```

arcpy.gp.TopoToRaster_sa("***User file path***/X_HSN_DEM.shp RASTERVALU PointElevation;***User file path***/07_HSN_TOP.shp HSN_SS PointElevation;***User file path***/HCT_FLTN00.shp # Cliff;***User file path***/HCT_FLTN01.shp # Cliff;***User file path***/HCT_FLTN02.shp # Cliff;***User file path***/HCT_FLTN03.shp # Cliff;***User file path***/HCT_FLTN04.shp # Cliff;***User file path***/HCT_FLTN05.shp # Cliff;***User file path***/HCT_FLTN06.shp # Cliff;***User file path***/HCT_FLTN07.shp # Cliff;***User file path***/HCT_FLTN08.shp # Cliff;***User file path***/HCT_FLTN09.shp # Cliff;***User file path***/HCT_FLTN10.shp # Cliff;***User file path***/HCT_FLTN11.shp # Cliff;***User file path***/HCT_FLTN12.shp # Cliff;***User file path***/HCT_FLTN13.shp # Cliff;***User file path***/HCT_FLTN14.shp # Cliff;***User file path***/HCT_FLTN15.shp # Cliff;***User file path***/HCT_FLTN16.shp # Cliff;***User file path***/HCT_FLTN17.shp # Cliff;***User file path***/HCT_FLTR1.shp # Cliff;***User file path***/HCT_FLTR2.shp # Cliff;***User file path***/HCT_FLTR3.shp # Cliff;***User file path***/HCT_FLTR4.shp # Cliff", "***User file path***/07HSN_TTR1.tif", "250", "4811000 18691000 5860000 19490000", "5", "", "", "NO_ENFORCE", "SPOT", "20", "", "1", "0", "0", "200", "", "", "", "", "", "", "", "")

```
try:
  arcpy.Delete_management("User file path/08BOK_TTR1.tif")
```

```
except Exception as e:
   print e.message

   # If using this code within a script tool, AddError can be used to return messages
   #   back to a script tool.  If not, AddError will have no effect.
   arcpy.AddError(e.message)

arcpy.gp.TopoToRaster_sa("User file path/X_BOK_DEM2.shp RASTERVALU PointElevation;User file
path/08_BOK_TOP.shp BOK_SS PointElevation;User file path/HCT_FLTN00.shp # Cliff;User file
path/HCT_FLTN01.shp # Cliff;User file path/HCT_FLTN02.shp # Cliff;User file path/HCT_FLTN03.shp #
Cliff;User file path/HCT_FLTN04.shp # Cliff;User file path/HCT_FLTN05.shp # Cliff;User file
path/HCT_FLTN06.shp # Cliff;User file path/HCT_FLTN07.shp # Cliff;User file path/HCT_FLTN08.shp #
Cliff;User file path/HCT_FLTN09.shp # Cliff;User file path/HCT_FLTN10.shp # Cliff;User file
path/HCT_FLTN11.shp # Cliff;User file path/HCT_FLTN12.shp # Cliff;User file path/HCT_FLTN13.shp #
Cliff;User file path/HCT_FLTN14.shp # Cliff;User file path/HCT_FLTN15.shp # Cliff;User file
path/HCT_FLTN16.shp # Cliff;User file path/HCT_FLTN17.shp # Cliff;User file path/HCT_FLTR1.shp #
Cliff;User file path/HCT_FLTR2.shp # Cliff;User file path/HCT_FLTR3.shp # Cliff;User file
path/HCT_FLTR4.shp # Cliff", "User file path/08BOK_TTR1.tif", "250", "4811000 18691000 5860000
19490000", "5", "", "", "NO_ENFORCE", "SPOT", "20", "", "1", "0", "0", "200", "", "", "", "", "", "", "", "")
```

19.1.3 Clip surfaces at onlaps and ground surface

```
##load HCT_Con_Calc.py
import sys
import os
import traceback
import arcpy
from arcpy import env
from arcpy.sa import *

# import arcpy module

# set workspace gdb
env.workspace = r" User file path \HCT_GeoDB1.gdb"

#Hosston:

arcpy.gp.RasterCalculator_sa("""Con(IsNull("User file path/HSN_DEM_D2.tif")==0, "User file
path/HSN_DEM_D2.tif", "User file path/07HSN_TTR1.tif")""", "User file path/Con_HSN_DEM_X5.tif")

#Sligo:

#Hammet:

arcpy.gp.RasterCalculator_sa("""Con(IsNull("User file path/HAM_DEM_X1.tif")==0, "User file
path/HAM_DEM_X1.tif", "User file path/05HAM_TTR1.tif")""", "User file path/Con_HAM_DEM_X5.tif")

#Cow Creek:

arcpy.gp.RasterCalculator_sa("""Con(IsNull("User file path/CCK_DEM_X1.tif")==0, "User file
path/CCK_DEM_X1.tif", "User file path/04CCK_TTR1.tif")""", "User file path/Con_CCK_DEM_X5.tif")

#Hensill:
```

```
arcpy.gp.RasterCalculator_sa("""Con(IsNull("User file path/HEN_DEM_X1.tif")==0, "User file path/HEN_DEM_X1.tif", "User file path/03HEN_TTR1.tif")""", "User file path/Con_HEN_DEM_X5.tif")

#Lower Glen Rose:

arcpy.gp.RasterCalculator_sa("""Con(IsNull("User file path/GRL_DEM_X1.tif")==0, "User file path/GRL_DEM_X1.tif", "User file path/02LGR_TTR1.tif")""", "User file path/Con_LGR_DEM_X5.tif")

#Upper Glen Rose:

arcpy.gp.RasterCalculator_sa("""Con(IsNull("User file path/UGR_DEM_X1.tif")==0, "User file path/UGR_DEM_X1.tif", "User file path/01UGR_TTR1.tif")""", "User file path/Con_UGR_DEM_X5.tif")

#Buda Lime:

arcpy.gp.RasterCalculator_sa("""Con(IsNull("User file path/BUD_DEM_X1.tif")==0, "User file path/BUD_DEM_X1.tif", "User file path/00BUD_TTR1.tif")""", "User file path/Con_BUD_DEM_X5.tif")

##load HCT_BOK_clip1.py

# root Base of Cretaceous file name
try:
  arcpy.Delete_management("User file path/BOK_CLIP1.tif")
except Exception as e:
  print e.message

  # If using this code within a script tool, AddError can be used to return messages
  #   back to a script tool.  If not, AddError will have no effect.
  arcpy.AddError(e.message)

surfnam_ina = arcpy.Raster("User file path/08BOK_TTR1.tif")

TF1a = Con((surfnam_ina-"tex30m_HCT1.tif")>0,"tex30m_HCT1.tif",surfnam_ina)

TF2a = Con((IsNull("User file path/HSN_DEM_D2.tif") == 0) & ((TF1a-"tex30m_HCT1.tif") == 0),(TF1a-10),TF1a)

TF3a = Con((IsNull("User file path/HAM_DEM_X1.tif") == 0) & ((TF2a-"tex30m_HCT1.tif") == 0),(TF2a-10),TF2a)

TF4a = Con((IsNull("User file path/CCK_DEM_X1.tif") == 0) & ((TF3a-"tex30m_HCT1.tif") == 0),(TF3a-10),TF3a)

TF5a = Con((IsNull("User file path/HEN_DEM_X1.tif") == 0) & ((TF4a-"tex30m_HCT1.tif") == 0),(TF4a-10),TF4a)

TF6a = Con((IsNull("User file path/GRL_DEM_X1.tif") == 0) & ((TF5a-"tex30m_HCT1.tif") == 0),(TF5a-10),TF5a)

TF7a = Con((IsNull("User file path/UGR_DEM_X1.tif") == 0) & ((TF6a-"tex30m_HCT1.tif") == 0),(TF6a-10),TF6a)

TFOUT1a = Con((IsNull("User file path/BOK_DEM_D2.tif") == 0), "tex30m_HCT1.tif", TF7a)

TFOUT1a.save("User file path/BOK_CLIP1.tif")
```

```
print "Base of Cretaceous complete!!"

##load HCT_HSN_clip1.py
## root Hosston file name
try:
   arcpy.Delete_management("User file path/HSN_CLIP1.tif")
except Exception as e:
   print e.message
   arcpy.AddError(e.message)

surfnam_inb = arcpy.Raster("User file path/Con_HSN_DEM_X5.tif")

TF1b = Con((surfnam_inb-"tex30m_HCT1.tif")>0,"tex30m_HCT1.tif",surfnam_inb)

TF2b = Con((IsNull("User file path/HAM_DEM_X1.tif") == 0) & ((TF1b-"tex30m_HCT1.tif") == 0),(TF1b-
10),TF1b)

TF3b = Con((IsNull("User file path/CCK_DEM_X1.tif") == 0) & ((TF2b-"tex30m_HCT1.tif") == 0),(TF2b-
10),TF2b)

TF4b = Con((IsNull("User file path/HEN_DEM_X1.tif") == 0) & ((TF3b-"tex30m_HCT1.tif") == 0),(TF3b-
10),TF3b)

TF5b = Con((IsNull("User file path/GRL_DEM_X1.tif") == 0) & ((TF4b-"tex30m_HCT1.tif") == 0),(TF4b-
10),TF4b)

TF6b = Con((IsNull("User file path/UGR_DEM_X1.tif") == 0) & ((TF5b-"tex30m_HCT1.tif") == 0),(TF5b-
10),TF5b)

TF7b = Con((TF6b - "User file path/BOK_Clip1.tif")<=0,0,9999)

TF8b = SetNull(TF7b,TF6b,"VALUE = 0")

TF9b = Con(IsNull("User file path/RP250_IG_D.tif")==1,TF8b,9999)

TF10b = SetNull(TF9b,TF8b,"VALUE = 9999")

TFOUT1b = Con((IsNull("User file path/HSN_DEM_D2.tif") == 0), "tex30m_HCT1.tif", TF10b)

TFOUT1b.save("User file path/HSN_CLIP1.tif")

print "Hosston complete!!"

##load HCT_SLG_clip1.py
## root Sligo file name
try:
   arcpy.Delete_management("User file path/SLG_CLIP1.tif")
except Exception as e:
   print e.message
   arcpy.AddError(e.message)

#
surfnam_inc = arcpy.Raster("User file path/06SLG_TTR1.tif")
```

```
TF1c = Con((surfnam_inc-"tex30m_HCT1.tif")>0,"tex30m_HCT1.tif",surfnam_inc)

TF2c = Con((IsNull("User file path/HAM_DEM_X1.tif") == 0) & ((TF1c-"tex30m_HCT1.tif") == 0),(TF1c-
10),TF1c)

TF3c = Con((IsNull("User file path/CCK_DEM_X1.tif") == 0) & ((TF2c-"tex30m_HCT1.tif") == 0),(TF2c-
10),TF2c)

TF4c = Con((IsNull("User file path/HEN_DEM_X1.tif") == 0) & ((TF3c-"tex30m_HCT1.tif") == 0),(TF3c-
10),TF3c)

TF5c = Con((IsNull("User file path/GRL_DEM_X1.tif") == 0) & ((TF4c-"tex30m_HCT1.tif") == 0),(TF4c-
10),TF4c)

TF6c = Con((IsNull("User file path/UGR_DEM_X1.tif") == 0) & ((TF5c-"tex30m_HCT1.tif") == 0),(TF5c-
10),TF5c)

TF7c = Con((TF6c - "User file path/BOK_Clip1.tif")<=0,0,9999)

TF8c = Con((TF6c - "User file path/Con_HSN_DEM_X5.tif")<=0,0,TF7c)

TF9c = SetNull(TF8c,TF6c,"VALUE = 0")

TF10c = Con(IsNull("User file path/RP250_IG_D.tif")==1,TF9c,9999)

TFOUT1c = SetNull(TF10c,TF9c,"VALUE = 9999")

TFOUT1c.save("User file path/SLG_CLIP1.tif")

print "Sligo complete!!"

##load HCT_HAM_clip1.py
## root Hammett file name
try:
   arcpy.Delete_management("User file path/HAM_CLIP1.tif")
except Exception as e:
   print e.message
   arcpy.AddError(e.message)

surfnam_ind = arcpy.Raster("User file path/Con_HAM_DEM_X5.tif")

TF1d = Con((surfnam_ind-"tex30m_HCT1.tif")>0,"tex30m_HCT1.tif",surfnam_ind)

TF2d = Con((IsNull("User file path/CCK_DEM_X1.tif") == 0) & ((TF1d-"tex30m_HCT1.tif") == 0),(TF1d-
10),TF1d)

TF3d = Con((IsNull("User file path/HEN_DEM_X1.tif") == 0) & ((TF2d-"tex30m_HCT1.tif") == 0),(TF2d-
10),TF2d)

TF4d = Con((IsNull("User file path/GRL_DEM_X1.tif") == 0) & ((TF3d-"tex30m_HCT1.tif") == 0),(TF3d-
10),TF3d)

TF5d = Con((IsNull("User file path/UGR_DEM_X1.tif") == 0) & ((TF4d-"tex30m_HCT1.tif") == 0),(TF4d-
10),TF4d)
```

```
TF6d = Con((TF5d - "User file path/BOK_Clip1.tif")<=0,0,9999)

TF7d = Con((TF5d - "User file path/Con_HSN_DEM_X5.tif")<=0,0,TF6d)

TF8d = Con((TF5d - "User file path/06SLG_TTR1.tif")<=0,0,TF7d)

TF9d = SetNull(TF8d,TF5d,"VALUE = 0")

TF10d = Con(IsNull("User file path/RP250_IG_D.tif")==1,TF9d,9999)

TF11d = SetNull(TF10d,TF9d,"VALUE = 9999")

TFOUT1d = Con((IsNull("User file path/HAM_DEM_X1.tif") == 0), "tex30m_HCT1.tif", TF11d)

TFOUT1d.save("User file path/HAM_CLIP1.tif")

print "Hammett complete!!"

##load HCT_CCK_clip1.py
## root Cow Creek file name
try:
   arcpy.Delete_management("User file path/CCK_CLIP1.tif")
except Exception as e:
   print e.message
   arcpy.AddError(e.message)

surfnam_ine = arcpy.Raster("User file path/Con_CCK_DEM_X5.tif")

TF1e = Con((surfnam_ine-"tex30m_HCT1.tif")>0,"tex30m_HCT1.tif",surfnam_ine)

TF2e = Con((IsNull("User file path/HEN_DEM_X1.tif") == 0) & ((TF1e-"tex30m_HCT1.tif") == 0),(TF1e-
10),TF1e)

TF3e = Con((IsNull("User file path/GRL_DEM_X1.tif") == 0) & ((TF2e-"tex30m_HCT1.tif") == 0),(TF2e-
10),TF2e)

TF4e = Con((IsNull("User file path/UGR_DEM_X1.tif") == 0) & ((TF3e-"tex30m_HCT1.tif") == 0),(TF3e-
10),TF3e)

TF5e = Con((TF4e - "User file path/BOK_Clip1.tif")<=0,0,9999)

TF6e = Con((TF4e - "User file path/Con_HSN_DEM_X5.tif")<=0,0,TF5e)

TF7e = Con((TF4e - "User file path/06SLG_TTR1.tif")<=0,0,TF6e)

TF8e = Con((TF4e - "User file path/Con_HAM_DEM_X5.tif")<=0,0,TF7e)

TF9e = SetNull(TF8e,TF4e,"VALUE = 0")

TF10e = Con(IsNull("User file path/RP250_IG_D.tif")==1,TF9e,9999)

TF11e = SetNull(TF10e,TF9e,"VALUE = 9999")

TFOUT1e = Con((IsNull("User file path/CCK_DEM_X1.tif") == 0), "tex30m_HCT1.tif", TF11e)
```

```
TFOUT1e.save("User file path/CCK_CLIP1.tif")

print "Cow Creek complete!!"

##load HCT_HEN_clip1.py
## root Hensell file name
try:
   arcpy.Delete_management("User file path/HEN_CLIP1.tif")
except Exception as e:
   print e.message
   arcpy.AddError(e.message)

surfnam_inf = arcpy.Raster("User file path/Con_HEN_DEM_X5.tif")

TF1f = Con((surfnam_inf-"tex30m_HCT1.tif")>0,"tex30m_HCT1.tif",surfnam_inf)

TF2f = Con((IsNull("User file path/GRL_DEM_X1.tif") == 0) & ((TF1f-"tex30m_HCT1.tif") == 0),(TF1f-
10),TF1f)

TF3f = Con((IsNull("User file path/UGR_DEM_X1.tif") == 0) & ((TF2f-"tex30m_HCT1.tif") == 0),(TF2f-
10),TF2f)

TF4f = Con((TF3f - "User file path/BOK_Clip1.tif")<=0,0,9999)

TF5f = Con((TF3f - "User file path/Con_HSN_DEM_X5.tif")<=0,0,TF4f)

TF6f = Con((TF3f - "User file path/06SLG_TTR1.tif")<=0,0,TF5f)

TF7f = Con((TF3f - "User file path/Con_HAM_DEM_X5.tif")<=0,0,TF6f)

TF8f = Con((TF3f - "User file path/Con_CCK_DEM_X5.tif")<=0,0,TF7f)

TF9f = SetNull(TF8f,TF3f,"VALUE = 0")

TF10f = Con(IsNull("User file path/RP250_IG_D.tif")==1,TF9f,9999)

TF11f = SetNull(TF10f,TF9f,"VALUE = 9999")

TFOUT1f = Con((IsNull("User file path/HEN_DEM_X1.tif") == 0), "tex30m_HCT1.tif", TF11f)

TFOUT1f.save("User file path/HEN_CLIP1.tif")

print "Hensell complete!!"

##load HCT_LGR_clip1.py
## root Lower Glen Rose file name
try:
   arcpy.Delete_management("User file path/LGR_CLIP1.tif")
except Exception as e:
   print e.message
   arcpy.AddError(e.message)

surfnam_ing = arcpy.Raster("User file path/Con_LGR_DEM_X5.tif")

TF1g = Con((surfnam_ing-"tex30m_HCT1.tif")>0,"tex30m_HCT1.tif",surfnam_ing)
```

```
TF2g = Con((IsNull("User file path/UGR_DEM_X1.tif") == 0) & ((TF1g-"tex30m_HCT1.tif") == 0),(TF1g-
10),TF1g)

TF3g = Con((TF2g - "User file path/BOK_Clip1.tif")<=0,0,9999)

TF4g = Con((TF2g - "User file path/Con_HSN_DEM_X5.tif")<=0,0,TF3g)

TF5g = Con((TF2g - "User file path/06SLG_TTR1.tif")<=0,0,TF4g)

TF6g = Con((TF2g - "User file path/Con_HAM_DEM_X5.tif")<=0,0,TF5g)

TF7g = Con((TF2g - "User file path/Con_CCK_DEM_X5.tif")<=0,0,TF6g)

TF8g = Con((TF2g - "User file path/Con_HEN_DEM_X5.tif")<=0,0,TF7g)

TF9g = SetNull(TF8g,TF2g,"VALUE = 0")

TF10g = Con(IsNull("User file path/RP250_IG_D.tif")==1,TF9g,9999)

TF11g = SetNull(TF10g,TF9g,"VALUE = 9999")

TFOUT1g = Con((IsNull("User file path/GRL_DEM_X1.tif") == 0), "tex30m_HCT1.tif", TF11g)

TFOUT1g.save("User file path/LGR_CLIP1.tif")

print "Lower Glen Rose complete!!"

##load HCT_UGR_clip1.py
## root Upper Glen Rose file name
try:
   arcpy.Delete_management("User file path/UGR_CLIP1.tif")
except Exception as e:
   print e.message
   arcpy.AddError(e.message)

surfnam_inh = arcpy.Raster("User file path/Con_UGR_DEM_X5.tif")

TF1h = Con((surfnam_inh-"tex30m_HCT1.tif")>0,"tex30m_HCT1.tif",surfnam_inh)

TF2h = Con((TF1h - "User file path/BOK_Clip1.tif")<=0,0,9999)

TF3h = Con((TF1h - "User file path/Con_HSN_DEM_X5.tif")<=0,0,TF2h)

TF4h = Con((TF1h - "User file path/06SLG_TTR1.tif")<=0,0,TF3h)

TF5h = Con((TF1h - "User file path/Con_HAM_DEM_X5.tif")<=0,0,TF4h)

TF6h = Con((TF1h - "User file path/Con_CCK_DEM_X5.tif")<=0,0,TF5h)

TF7h = Con((TF1h - "User file path/Con_HEN_DEM_X5.tif")<=0,0,TF6h)

TF8h = Con((TF1h - "User file path/Con_LGR_DEM_X5.tif")<=0,0,TF7h)

TF9h = SetNull(TF8h,TF1h,"VALUE = 0")
```

```
TF10h = Con(IsNull("User file path/RP250_IG_D.tif")==1,TF9h,9999)

TF11h = SetNull(TF10h,TF9h,"VALUE = 9999")

TFOUT1h = Con((IsNull("User file path/UGR_DEM_X1.tif") == 0), "tex30m_HCT1.tif", TF11h)

TFOUT1h.save("User file path/UGR_CLIP1.tif")

print "Upper Glen Rose complete!!"

##load HCT_BUD_clip1.py
## root Buda Lime file name
try:
  arcpy.Delete_management("User file path/BUD_CLIP1.tif")
except Exception as e:
  print e.message
  arcpy.AddError(e.message)

surfnam_ini = arcpy.Raster("User file path/Con_BUD_DEM_X5.tif")

TF1i = Con((surfnam_ini-"tex30m_HCT1.tif")>0,"tex30m_HCT1.tif",surfnam_ini)

TF2i = Con((TF1i - "User file path/BOK_Clip1.tif")<=0,0,999)

TF3i = Con((TF1i - "User file path/Con_HSN_DEM_X5.tif")<=0,0,TF2i)

TF4i = Con((TF1i - "User file path/06SLG_TTR1.tif")<=0,0,TF3i)

TF5i = Con((TF1i - "User file path/Con_HAM_DEM_X5.tif")<=0,0,TF4i)

TF6i = Con((TF1i - "User file path/Con_CCK_DEM_X5.tif")<=0,0,TF5i)

TF7i = Con((TF1i - "User file path/Con_HEN_DEM_X5.tif")<=0,0,TF6i)

TF8i = Con((TF1i - "User file path/Con_LGR_DEM_X5.tif")<=0,0,TF7i)

TF9i = Con((TF1i - "User file path/Con_UGR_DEM_X5.tif")<=0,0,TF8i)

TF10i = SetNull(TF9i,TF1i,"VALUE = 0")

TF11i = Con((IsNull("User file path/EDW_DEM_X1.tif") == 0), 9, TF10i)

TF12i = SetNull(TF11i,TF1i,"VALUE = 9")

TF13i = Con(IsNull("User file path/RP250_IG_D.tif")==1,TF12i,9999)

TF14i = SetNull(TF13i,TF12i,"VALUE = 9999")

TFOUT1i = Con((IsNull("User file path/BUD_DEM_X1.tif") == 0), "tex30m_HCT1.tif", TF14i)

TFOUT1i.save("User file path/BUD_CLIP1.tif")

print "Buda Lime complete!!"
```

```
arcpy.gp.ExtractByMask_sa("User file path/BOK_CLIP1.tif", "User file path/HCT_STUDY1_Bx2_Poly.shp",
"User file path/BOK_CLIP1x.tif")
arcpy.gp.ExtractByMask_sa("User file path/HSN_CLIP1.tif", "User file path/HCT_STUDY1_Bx2_Poly.shp",
"User file path/HSN_CLIP1x.tif")
arcpy.gp.ExtractByMask_sa("User file path/SLG_CLIP1.tif", "User file path/HCT_STUDY1_Bx2_Poly.shp",
"User file path/SLG_CLIP1x.tif")
arcpy.gp.ExtractByMask_sa("User file path/HAM_CLIP1.tif", "User file path/HCT_STUDY1_Bx2_Poly.shp",
"User file path/HAM_CLIP1x.tif")
arcpy.gp.ExtractByMask_sa("User file path/CCK_CLIP1.tif", "User file path/HCT_STUDY1_Bx2_Poly.shp",
"User file path/CCK_CLIP1x.tif")
arcpy.gp.ExtractByMask_sa("User file path/HEN_CLIP1.tif", "User file path/HCT_STUDY1_Bx2_Poly.shp",
"User file path/HEN_CLIP1x.tif")
arcpy.gp.ExtractByMask_sa("User file path/LGR_CLIP1.tif", "User file path/HCT_STUDY1_Bx2_Poly.shp",
"User file path/LGR_CLIP1x.tif")
arcpy.gp.ExtractByMask_sa("User file path/UGR_CLIP1.tif", "User file path/HCT_STUDY1_Bx2_Poly.shp",
"User file path/UGR_CLIP1x.tif")
arcpy.gp.ExtractByMask_sa("User file path/BUD_CLIP1.tif", "User file path/HCT_STUDY1_Bx2_Poly.shp",
"User file path/BUD_CLIP1x.tif")
```

19.1.4 Make isopach maps for each hydrostratigraphic unit

```
import sys
import os
import traceback
import arcpy
from arcpy import env
from arcpy.sa import *

# set workspace gdb
env.workspace = r" User file path \HCT_GeoDB1.gdb"

#Hosston:

## root Hosston file name
try:
   arcpy.Delete_management("User file path/HSN_ISO1.tif")
except Exception as e:
   print e.message
   arcpy.AddError(e.message)

arcpy.gp.Minus_sa("User file path/HSN_CLIP1x.tif", "User file path/BOK_CLIP1x.tif", "User file
path/HSN_ISO1.tif")

print "Hosston complete!!"

## root Sligo file name
try:
   arcpy.Delete_management("User file path/SLG_ISO1.tif")
except Exception as e:
   print e.message
   arcpy.AddError(e.message)
try:
   arcpy.Delete_management("User file path/TF1c.tif")
except Exception as e:
```

```
   print e.message
   arcpy.AddError(e.message)
try:
   arcpy.Delete_management("User file path/TF2c.tif")
except Exception as e:
   print e.message
   arcpy.AddError(e.message)
try:
   arcpy.Delete_management("User file path/TF3c.tif")
except Exception as e:
   print e.message
   arcpy.AddError(e.message)

#surfnam_inc = arcpy.Raster("User file path/SLG_CLIP1x.tif")
arcpy.gp.Minus_sa("User file path/SLG_CLIP1x.tif", "User file path/BOK_CLIP1x.tif", "User file
path/TF1c.tif")
arcpy.gp.Minus_sa("User file path/SLG_CLIP1x.tif", "User file path/HSN_CLIP1x.tif", "User file
path/TF2c.tif")

TF3c = Con((IsNull("User file path/SLG_CLIP1x.tif") == 0) & (IsNull("User file path/HSN_CLIP1x.tif") ==
0),"User file path/TF2c.tif","User file path/TF1c.tif")

TF3c.save("User file path/SLG_ISO1.tif")

print "Sligo complete!!"

## root Hammett file name
try:
   arcpy.Delete_management("User file path/HAM_ISO1.tif")
except Exception as e:
   print e.message
   arcpy.AddError(e.message)
try:
   arcpy.Delete_management("User file path/TF1d.tif")
except Exception as e:
   print e.message
   arcpy.AddError(e.message)
try:
   arcpy.Delete_management("User file path/TF2d.tif")
except Exception as e:
   print e.message
   arcpy.AddError(e.message)
try:
   arcpy.Delete_management("User file path/TF3d.tif")
except Exception as e:
   print e.message
   arcpy.AddError(e.message)

#
#surfnam_inc = arcpy.Raster("User file path/HAM_CLIP1x.tif")
arcpy.gp.Minus_sa("User file path/HAM_CLIP1x.tif", "User file path/BOK_CLIP1x.tif", "User file
path/TF1d.tif")
arcpy.gp.Minus_sa("User file path/HAM_CLIP1x.tif", "User file path/HSN_CLIP1x.tif", "User file
path/TF2d.tif")
```

```
arcpy.gp.Minus_sa("User file path/HAM_CLIP1x.tif", "User file path/SLG_CLIP1x.tif", "User file
path/TF3d.tif")

TF4d = Con((IsNull("User file path/HAM_CLIP1x.tif") == 0) & (IsNull("User file path/HSN_CLIP1x.tif") ==
0),"User file path/TF2d.tif","User file path/TF1d.tif")

TF5d = Con((IsNull("User file path/HAM_CLIP1x.tif") == 0) & (IsNull("User file path/SLG_CLIP1x.tif") ==
0),"User file path/TF3d.tif",TF4d)

TF5d.save("User file path/HAM_ISO1.tif")

print "Hammett complete!!"

## root Cow Creek file name
try:
   arcpy.Delete_management("User file path/CCK_ISO1.tif")
except Exception as e:
   print e.message
   arcpy.AddError(e.message)
try:
   arcpy.Delete_management("User file path/TF1e.tif")
except Exception as e:
   print e.message
   arcpy.AddError(e.message)
try:
   arcpy.Delete_management("User file path/TF2e.tif")
except Exception as e:
   print e.message
   arcpy.AddError(e.message)
try:
   arcpy.Delete_management("User file path/TF3e.tif")
except Exception as e:
   print e.message
   arcpy.AddError(e.message)
try:
   arcpy.Delete_management("User file path/TF4e.tif")
except Exception as e:
   print e.message
   arcpy.AddError(e.message)

#surfnam_inc = arcpy.Raster("User file path/CCK_CLIP1x.tif")
arcpy.gp.Minus_sa("User file path/CCK_CLIP1x.tif", "User file path/BOK_CLIP1x.tif", "User file
path/TF1e.tif")
arcpy.gp.Minus_sa("User file path/CCK_CLIP1x.tif", "User file path/HSN_CLIP1x.tif", "User file
path/TF2e.tif")
arcpy.gp.Minus_sa("User file path/CCK_CLIP1x.tif", "User file path/SLG_CLIP1x.tif", "User file
path/TF3e.tif")
arcpy.gp.Minus_sa("User file path/CCK_CLIP1x.tif", "User file path/HAM_CLIP1x.tif", "User file
path/TF4e.tif")

TF5e = Con((IsNull("User file path/CCK_CLIP1x.tif") == 0) & (IsNull("User file path/HSN_CLIP1x.tif") ==
0),"User file path/TF2e.tif","User file path/TF1e.tif")

TF6e = Con((IsNull("User file path/CCK_CLIP1x.tif") == 0) & (IsNull("User file path/SLG_CLIP1x.tif") ==
0),"User file path/TF3e.tif",TF5e)
```

```
TF7e = Con((IsNull("User file path/CCK_CLIP1x.tif") == 0) & (IsNull("User file path/HAM_CLIP1x.tif") ==
0),"User file path/TF4e.tif",TF6e)

TF7e.save("User file path/CCK_ISO1.tif")

print "Cow Creek complete!!"

## root Hensell file name
try:
   arcpy.Delete_management("User file path/HEN_ISO1.tif")
except Exception as e:
   print e.message
   arcpy.AddError(e.message)
try:
   arcpy.Delete_management("User file path/TF1f.tif")
except Exception as e:
   print e.message
   arcpy.AddError(e.message)
try:
   arcpy.Delete_management("User file path/TF2f.tif")
except Exception as e:
   print e.message
   arcpy.AddError(e.message)
try:
   arcpy.Delete_management("User file path/TF3f.tif")
except Exception as e:
   print e.message
   arcpy.AddError(e.message)
try:
   arcpy.Delete_management("User file path/TF4f.tif")
except Exception as e:
   print e.message
   arcpy.AddError(e.message)
try:
   arcpy.Delete_management("User file path/TF5f.tif")
except Exception as e:
   print e.message
   arcpy.AddError(e.message)

#surfnam_inc = arcpy.Raster("User file path/HEN_CLIP1x.tif")
arcpy.gp.Minus_sa("User file path/HEN_CLIP1x.tif", "User file path/BOK_CLIP1x.tif", "User file
path/TF1f.tif")
arcpy.gp.Minus_sa("User file path/HEN_CLIP1x.tif", "User file path/HSN_CLIP1x.tif", "User file
path/TF2f.tif")
arcpy.gp.Minus_sa("User file path/HEN_CLIP1x.tif", "User file path/SLG_CLIP1x.tif", "User file
path/TF3f.tif")
arcpy.gp.Minus_sa("User file path/HEN_CLIP1x.tif", "User file path/HAM_CLIP1x.tif", "User file
path/TF4f.tif")
arcpy.gp.Minus_sa("User file path/HEN_CLIP1x.tif", "User file path/CCK_CLIP1x.tif", "User file
path/TF5f.tif")

TF6f = Con((IsNull("User file path/HEN_CLIP1x.tif") == 0) & (IsNull("User file path/HSN_CLIP1x.tif") ==
0),"User file path/TF2f.tif","User file path/TF1f.tif")
```

```
TF7f = Con((IsNull("User file path/HEN_CLIP1x.tif") == 0) & (IsNull("User file path/SLG_CLIP1x.tif") ==
0),"User file path/TF3f.tif",TF6f)

TF8f = Con((IsNull("User file path/HEN_CLIP1x.tif") == 0) & (IsNull("User file path/HAM_CLIP1x.tif") ==
0),"User file path/TF4f.tif",TF7f)

TF9f = Con((IsNull("User file path/HEN_CLIP1x.tif") == 0) & (IsNull("User file path/CCK_CLIP1x.tif") ==
0),"User file path/TF5f.tif",TF8f)

TF9f.save("User file path/HEN_ISO1.tif")

print "Hensell complete!!"

## root Lower Glen Rose file name
try:
   arcpy.Delete_management("User file path/LGR_ISO1.tif")
except Exception as e:
   print e.message
   arcpy.AddError(e.message)
try:
   arcpy.Delete_management("User file path/TF1g.tif")
except Exception as e:
   print e.message
   arcpy.AddError(e.message)
try:
   arcpy.Delete_management("User file path/TF2g.tif")
except Exception as e:
   print e.message
   arcpy.AddError(e.message)
try:
   arcpy.Delete_management("User file path/TF3g.tif")
except Exception as e:
   print e.message
   arcpy.AddError(e.message)
try:
   arcpy.Delete_management("User file path/TF4g.tif")
except Exception as e:
   print e.message
   arcpy.AddError(e.message)
try:
   arcpy.Delete_management("User file path/TF5g.tif")
except Exception as e:
   print e.message
   arcpy.AddError(e.message)
try:
   arcpy.Delete_management("User file path/TF6g.tif")
except Exception as e:
   print e.message
   arcpy.AddError(e.message)

#
#surfnam_inc = arcpy.Raster("User file path/LGR_CLIP1x.tif")
arcpy.gp.Minus_sa("User file path/LGR_CLIP1x.tif", "User file path/BOK_CLIP1x.tif", "User file
path/TF1g.tif")
```

```
arcpy.gp.Minus_sa("User file path/LGR_CLIP1x.tif", "User file path/HSN_CLIP1x.tif", "User file path/TF2g.tif")
arcpy.gp.Minus_sa("User file path/LGR_CLIP1x.tif", "User file path/SLG_CLIP1x.tif", "User file path/TF3g.tif")
arcpy.gp.Minus_sa("User file path/LGR_CLIP1x.tif", "User file path/HAM_CLIP1x.tif", "User file path/TF4g.tif")
arcpy.gp.Minus_sa("User file path/LGR_CLIP1x.tif", "User file path/CCK_CLIP1x.tif", "User file path/TF5g.tif")
arcpy.gp.Minus_sa("User file path/LGR_CLIP1x.tif", "User file path/HEN_CLIP1x.tif", "User file path/TF6g.tif")

TF7g = Con((IsNull("User file path/LGR_CLIP1x.tif") == 0) & (IsNull("User file path/HSN_CLIP1x.tif") == 0),"User file path/TF2g.tif","User file path/TF1g.tif")

TF8g = Con((IsNull("User file path/LGR_CLIP1x.tif") == 0) & (IsNull("User file path/SLG_CLIP1x.tif") == 0),"User file path/TF3g.tif",TF7g)

TF9g = Con((IsNull("User file path/LGR_CLIP1x.tif") == 0) & (IsNull("User file path/HAM_CLIP1x.tif") == 0),"User file path/TF4g.tif",TF8g)

TF10g = Con((IsNull("User file path/LGR_CLIP1x.tif") == 0) & (IsNull("User file path/CCK_CLIP1x.tif") == 0),"User file path/TF5g.tif",TF9g)

TF11g = Con((IsNull("User file path/LGR_CLIP1x.tif") == 0) & (IsNull("User file path/HEN_CLIP1x.tif") == 0),"User file path/TF6g.tif",TF10g)

TF11g.save("User file path/LGR_ISO1.tif")

print "Lower Glen Rose complete!!"

## root Upper Glen Rose file name
try:
   arcpy.Delete_management("User file path/UGR_ISO1.tif")
except Exception as e:
   print e.message
   arcpy.AddError(e.message)
try:
   arcpy.Delete_management("User file path/TF1h.tif")
except Exception as e:
   print e.message
   arcpy.AddError(e.message)
try:
   arcpy.Delete_management("User file path/TF2h.tif")
except Exception as e:
   print e.message
   arcpy.AddError(e.message)
try:
   arcpy.Delete_management("User file path/TF3h.tif")
except Exception as e:
   print e.message
   arcpy.AddError(e.message)
try:
   arcpy.Delete_management("User file path/TF4h.tif")
except Exception as e:
   print e.message
```

```
   arcpy.AddError(e.message)
try:
   arcpy.Delete_management("User file path/TF5h.tif")
except Exception as e:
   print e.message
   arcpy.AddError(e.message)
try:
   arcpy.Delete_management("User file path/TF6h.tif")
except Exception as e:
   print e.message
   arcpy.AddError(e.message)
try:
   arcpy.Delete_management("User file path/TF7h.tif")
except Exception as e:
   print e.message
   arcpy.AddError(e.message)

#surfnam_inc = arcpy.Raster("User file path/UGR_CLIP1x.tif")
arcpy.gp.Minus_sa("User file path/UGR_CLIP1x.tif", "User file path/BOK_CLIP1x.tif", "User file
path/TF1h.tif")
arcpy.gp.Minus_sa("User file path/UGR_CLIP1x.tif", "User file path/HSN_CLIP1x.tif", "User file
path/TF2h.tif")
arcpy.gp.Minus_sa("User file path/UGR_CLIP1x.tif", "User file path/SLG_CLIP1x.tif", "User file
path/TF3h.tif")
arcpy.gp.Minus_sa("User file path/UGR_CLIP1x.tif", "User file path/HAM_CLIP1x.tif", "User file
path/TF4h.tif")
arcpy.gp.Minus_sa("User file path/UGR_CLIP1x.tif", "User file path/CCK_CLIP1x.tif", "User file
path/TF5h.tif")
arcpy.gp.Minus_sa("User file path/UGR_CLIP1x.tif", "User file path/HEN_CLIP1x.tif", "User file
path/TF6h.tif")
arcpy.gp.Minus_sa("User file path/UGR_CLIP1x.tif", "User file path/LGR_CLIP1x.tif", "User file
path/TF7h.tif")

TF8h = Con((IsNull("User file path/UGR_CLIP1x.tif") == 0) & (IsNull("User file path/HSN_CLIP1x.tif") ==
0),"User file path/TF2h.tif","User file path/TF1h.tif")

TF9h = Con((IsNull("User file path/UGR_CLIP1x.tif") == 0) & (IsNull("User file path/SLG_CLIP1x.tif") ==
0),"User file path/TF3h.tif",TF8h)

TF10h = Con((IsNull("User file path/UGR_CLIP1x.tif") == 0) & (IsNull("User file path/HAM_CLIP1x.tif")
== 0),"User file path/TF4h.tif",TF9h)

TF11h = Con((IsNull("User file path/UGR_CLIP1x.tif") == 0) & (IsNull("User file path/CCK_CLIP1x.tif") ==
0),"User file path/TF5h.tif",TF10h)

TF12h = Con((IsNull("User file path/UGR_CLIP1x.tif") == 0) & (IsNull("User file path/HEN_CLIP1x.tif") ==
0),"User file path/TF6h.tif",TF11h)

TF13h = Con((IsNull("User file path/UGR_CLIP1x.tif") == 0) & (IsNull("User file path/LGR_CLIP1x.tif") ==
0),"User file path/TF7h.tif",TF12h)

TF13h.save("User file path/UGR_ISO1.tif")

print "Upper Glen Rose complete!!"
```

```
arcpy.gp.ExtractByMask_sa("User file path/HSN_ISO1.tif", "User file path/HCT_STUDY1_Bx2_Poly.shp",
"User file path/HSN_ISO1x.tif")

arcpy.gp.ExtractByMask_sa("User file path/SLG_ISO1.tif", "User file path/HCT_STUDY1_Bx2_Poly.shp",
"User file path/SLG_ISO1x.tif")

arcpy.gp.ExtractByMask_sa("User file path/HAM_ISO1.tif", "User file path/HCT_STUDY1_Bx2_Poly.shp",
"User file path/HAM_ISO1x.tif")

arcpy.gp.ExtractByMask_sa("User file path/CCK_ISO1.tif", "User file path/HCT_STUDY1_Bx2_Poly.shp",
"User file path/CCK_ISO1x.tif")

arcpy.gp.ExtractByMask_sa("User file path/HEN_ISO1.tif", "User file path/HCT_STUDY1_Bx2_Poly.shp",
"User file path/HEN_ISO1x.tif")

arcpy.gp.ExtractByMask_sa("User file path/LGR_ISO1.tif", "User file path/HCT_STUDY1_Bx2_Poly.shp",
"User file path/LGR_ISO1x.tif")

arcpy.gp.ExtractByMask_sa("User file path/UGR_ISO1.tif", "User file path/HCT_STUDY1_Bx2_Poly.shp",
"User file path/UGR_ISO1x.tif")
```

19.1.5 Volume calculations

```
# Import arcpy module
import arcpy, os, sys
import numpy as np
import time
import csv

#Allow for overwriting of outputs
arcpy.env.overwriteOutput = True

## start code Timer
t0 = time.time()

# Set the input grid location & ouput directory location
#TrinityGrid =  "User file path\\HCT_UGg3.shp" # Specify path for Trinity Grid Input
#TrinityGrid =  "User file path\\HCT_LGg3.shp" # Specify path for Trinity Grid Input
#TrinityGrid =  "User file path\\HCT_HEg3.shp" # Specify path for Trinity Grid Input
#TrinityGrid =  "User file path\\HCT_CCg3.shp" # Specify path for Trinity Grid Input
#TrinityGrid =  "User file path\\HCT_SLg3.shp" # Specify path for Trinity Grid Input
TrinityGrid =  "User file path\\HCT_HOg3.shp" # Specify path for Trinity Grid Input
OutputDir   = "User file path\\Volume"  # Specify path for Output directory

#filename = "User file path\\Volume\\UGvol.txt"
#filename = "User file path\\Volume\\LGvol.txt"
#filename = "User file path\\Volume\\HEvol.txt"
#filename = "User file path\\Volume\\CCvol.txt"
#filename = "User file path\\Volume\\SLvol.txt"
filename = "User file path\\Volume\\HOvol.txt"
myfile = open(filename,'w')

if not os.path.exists(OutputDir):
   os.makedirs(OutputDir)
```

```
print "test1"
arcpy.AddMessage('Output Directory:' + OutputDir)
arcpy.env.scratchWorkspace = os.path.dirname(OutputDir)  #GM
arcpy.AddMessage("Starting processing") #GM

arcpy.MakeFeatureLayer_management(TrinityGrid, "Grid_lyr")
#arcpy.CopyFeatures_management ("Grid_lyr", AOI)
#arcpy.MakeFeatureLayer_management(AOI, "AOI_lyr")

aq_Names = ['Paluxy','GlenRose', 'Hensell', 'Pearsall', 'Hosston']
sc_Acronyms = ['FR', 'SS', 'MS', 'VS', 'BR']

# Step #1d Process: Calculate Volumes
x = 0
area_cell = 62500 ### area of cell in sq ft
#Storativity
#S = .00017 ### Trinity 1 Storativity
#S = .00015 ### Trinity 2 Storativity
S = .00032 ### Trinity 3 Storativity

# Core values
#Syc = 0.027  ### Upper Trinity confined
#Syc = 0.054  ### Middle Trinity confined
Syc = 0.060  ### Lower Trinity confined

#Syu = 0.054  ### Upper Trinity unconfined
#Syu = 0.108  ### Middle Trinity unconfined
Syu = 0.120  ### Lower Trinity unconfined

Ss = .00002 ### Trinity Specific storage

    #  0    1    2    3     4       5     6       7      8      9     10    11    12     13     14    15
#fields = ['FID',
'Shape','ID','ORIG_FID','CountyName','GCD_Name','GCD2_Name','GCD3_Name','GMA_Name','RWPG','Sal_Cla
ss','OC', 'HCT_UGTE','HCT_UGTK', 'swle_ug','tex30m_DEM']
#fields = ['FID',
'Shape','ID','ORIG_FID','CountyName','GCD_Name','GCD2_Name','GCD3_Name','GMA_Name','RWPG','Sal_Cla
ss','OC', 'HCT_LGTE','HCT_LGTK', 'swle_t2','tex30m_DEM']
#fields = ['FID',
'Shape','ID','ORIG_FID','CountyName','GCD_Name','GCD2_Name','GCD3_Name','GMA_Name','RWPG','Sal_Cla
ss','OC', 'HCT_HETE','HCT_HETK', 'swle_t2','tex30m_DEM']
#fields = ['FID',
'Shape','ID','ORIG_FID','CountyName','GCD_Name','GCD2_Name','GCD3_Name','GMA_Name','RWPG','Sal_Cla
ss','OC', 'HCT_CCTE','HCT_CCTK', 'swle_t2','tex30m_DEM']
#fields = ['FID',
'Shape','ID','ORIG_FID','CountyName','GCD_Name','GCD2_Name','GCD3_Name','GMA_Name','RWPG','Sal_Cla
ss','OC', 'HCT_SLTE','HCT_SLTK', 'swle_slho','tex30m_DEM']
fields = ['FID',
'Shape','ID','ORIG_FID','CountyName','GCD_Name','GCD2_Name','GCD3_Name','GMA_Name','RWPG','Sal_Cla
ss','OC', 'HCT_HOTE','HCT_HOTK', 'swle_slho','tex30m_DEM']
whereQ = '"GCD3_Name" = \'{}\''.format('EAA')
print "Starting processing"
with arcpy.da.SearchCursor(TrinityGrid, fields) as cursor: # For each row, evaluate the top and bottom
surfaces for each formation and calculate & update thickness field
```

```
  for row in cursor:
    # Calculate thickness by layer
    Thickness = row[13]
    ##95
    ##96
    # Start Volume calculation

    #V_Aq_unconfined  = np.nan; V_Aq_confined  = np.nan #Set inital volumes as null.
    outcrop = row[11] # field "VALUE" indicates whether it's pass-thru (outcrop) for that aquifer or not
    ##101
    salinity = row[10]
    tope = row[12]
    thk = row[13]
    WL = row[14]  #head_ini or water level
    Stor = Ss*thk # mod_Ss or specific storage
    AvailDD_conf = WL - row[12] ###  head - top of Aq
    AvailDD_unconf = WL - (row[12] - row[13]) ### head - bott of Aq
    #print "FID="+ str(row[0])
    if salinity <> ' ' and outcrop == 'OC':
      V_Aq_unconfined = AvailDD_unconf*area_cell*Syu
      V_Aq_confined   = 0
      #print "volume=" + str(V_Aq_unconfined) + "FID=" + str(row[0])
    elif salinity <> ' ' and outcrop <> 'OC':
      if WL > tope :
        V_Aq_unconfined = thk*area_cell*Syc
      else:
        V_Aq_unconfined = AvailDD_unconf*area_cell*Syc

      V_Aq_confined   = AvailDD_conf*area_cell*S
      #print "volume conf=" + str(V_Aq_unconfined+V_Aq_confined) + "FID=" + str(row[0])
    else:
      V_Aq_unconfined = 0
      V_Aq_confined   = 0
    if V_Aq_confined < 0 :
      V_Aq_confined   = 0
    x = V_Aq_confined + V_Aq_unconfined
    if salinity <> '' and x > 0 :
      myfile.write(str(row[0]) + "|" + row[4] + "|" + row[5] + "|" + row[6] + "|" + row[7] + "|" + row[8] + "|"
+ row[9] + "|" + row[10] + "|"+ row[11] + "|" + str(x) + "|" + str(V_Aq_unconfined) + "|" +
str(V_Aq_confined) + "|" + str(Stor) +'\n')
    #arcpy.AddMessage("Starting processing=" + str(x)) #GM

myfile.close()
```

19.2 Modeled ion concentrations

Upper Glen Rose limestone, Lower Glen Rose limestone, Hensell sandstone, and Cow Creek limestone

SiO2	Ca	Mg	Na	K	Sr	CO3	HCO3	SO4	Cl	Fl	NO3	pH	TDS sum	total alkalinity	SC measured	SC calc	StateWellNumber	SampleDate
9.5	**540**	**434**	**61**	**0**	**0**	**0**	**251**	**2900**	**27**	**0**	**4**	**6.7**	**4227**	**206**	**4080**	4037	6931901	11/6/1950
9.3	574	433	233	11	0	0	271	2884	419	4	4	6.5	4834	222	n/a	5157		
9.3	574	433	234	11	0	0	271	2884	422	4	4	6.5	4846	222	n/a	5165		
9.3	575	433	240	11	0	0	272	2883	436	4	4	6.5	4853	223	n/a	5202		
9.3	576	433	249	11	0	0	272	2883	452	4	4	6.5	4872	223	n/a	5251		
9.3	579	433	262	12	0	0	274	2881	485	4	4	6.5	4944	225	n/a	5340		
9.2	585	433	290	14	0	0	277	2878	550	4	4	6.5	5045	227	n/a	5524		
9.2	591	433	319	16	0	0	281	2876	615	4	4	6.5	5147	230	n/a	5706		
9.2	596	433	348	18	0	0	284	2873	681	4	4	6.5	5249	233	n/a	5889		
9.1	602	433	376	19	0	0	287	2870	746	4	4	6.5	5351	235	n/a	6070		
9.1	607	433	405	21	0	0	291	2868	812	4	4	6.5	5445	238	n/a	6252		
8.9	641	432	577	32	0	0	310	2851	1204	4	4	6.6	6056	254	n/a	7332		
8.7	675	432	749	42	0	0	330	2835	1596	4	4	6.6	6667	271	n/a	8399		
8.5	709	431	921	53	0	0	350	2819	1989	4	4	6.6	7279	287	n/a	9455		
8.3	742	430	1092	63	0	0	370	2803	2381	4	4	6.6	7890	303	n/a	10500		
8.1	776	430	1264	74	0	0	390	2787	2773	4	4	6.6	8501	319	n/a	11537		
7.9	810	429	1436	84	0	0	409	2770	3165	4	4	6.7	9112	336	n/a	12564		
7.7	843	429	1608	95	0	0	429	2754	3558	4	4	6.7	9723	352	n/a	13583		
7.5	**877**	**428**	**1780**	**105**	**0**	**0**	**449**	**2738**	**3950**	**4**	**0**	**6.5**	**10339**	**368**	**14800**	14581	6701830	3/31/1995
5.9	1147	423	3155	189	0	0	608	2608	7088	4	0	6.5	15228	498	n/a	22457		
4.3	1416	418	4530	273	0	0	766	2479	10227	4	0	6.5	20118	628	n/a	29606		
2.7	1686	414	5906	357	0	0	925	2349	13365	4	0	6.5	25008	758	n/a	37331		
1.1	1955	409	7281	441	0	0	1083	2220	16504	4	0	6.5	29897	887	n/a	44432		
0.0	2225	404	8656	525	0	0	1241	2090	19642	4	0	6.5	34787	1017	n/a	51345		

Sligo limestone and Hosston sandstone

SiO2	Ca	Mg	Na	K	Sr	CO3	HCO3	SO4	Cl	Fl	NO3	pH	TDS sum	total alkalinity	SC measured	SC calc	StateWellNumber	SampleDate
10	**185**	**126**	**710**	**45**	**0**	**0**	**271**	**1580**	**496**	**4.2**	**0.4**	**7.9**	**3428**	**222**	**n/a**	4570	5834802	5/1/1972
7.5	154	118	958	34	0	0	289	1218	1047	3.2	0.3	7.825	3827	237	n/a	5653		
5	123	109	1205	23	0	0	307	856	1598	2.1	0.2	7.75	4227	251	n/a	6718		
2.5	91	101	1453	11	0	0	324	494	2149	1.1	0.1	7.675	4626	266	n/a	7773		
0	**60**	**92**	**1700**	**0**	**0**	**0**	**342**	**132**	**2700**	**0**	**0**	**7.6**	**5026**	**280**	**n/a**	8810	5834401	9/12/1953
0	0	75	2195	0	0	0	342	0	3380	0	0	**7.1**	5992	280	n/a	10595		
0	0	58	2690	0	0	0	342	0	4143	0	0	**7.1**	7233	280	n/a	12701		
0	0	41	3185	0	0	0	342	0	4905	0	0	**7.1**	8473	280	n/a	14780		
0	0	24	3680	0	0	0	342	0	5667	0	0	**7.1**	9713	280	n/a	16833		
0	0	7	4175	0	0	0	342	0	6430	0	0	**7.1**	10954	280	n/a	18863		
0	0	0	4670	0	0	0	342	0	7192	0	0	**7.1**	12204	280	n/a	20894		
0	0	0	6155	0	0	0	342	0	9479	0	0	**7.1**	15976	280	n/a	26909		
0	0	0	7640	0	0	0	342	0	11766	0	0	**7.1**	19748	280	n/a	32766		
0	0	0	9125	0	0	0	342	0	14053	0	0	**7.1**	23520	280	n/a	38485		
0	0	0	10610	0	0	0	342	0	16339	0	0	**7.1**	27292	280	n/a	44081		
0	0	0	12095	0	0	0	342	0	18626	0	0	**7.1**	31063	280	n/a	49566		

Blue rows are from measured water quality. Concentrations in milligrams per liter. TDS = total dissolved solids. SC = specific conductance, units of micromhos/centimeter

This page is intentionally blank

19.3 BRACS Database

All water well and geophysical well log information and supporting databases for the Hill Country Trinity aquifer study are managed in the BRACS Database using Microsoft® Access® 2010. When spatial analysis is required, copies of information are exported into ArcGIS®. Information developed in ArcGIS® is then exported back into Microsoft® Access® and the tables are updated accordingly. Although this approach may be cumbersome, it takes advantage of the strengths of the software. The project also relied on other software for specific tasks, including Microsoft® Excel® IHS-Markit Kingdom® geological application.

For the study, we assembled information from external agencies and updated these databases frequently. All of these databases are maintained in Microsoft® Access® and GIS files were developed for spatial analysis and well selection. Many of the database objects were built from scratch or were redesigned to meet project objectives. Data from external agencies or projects were available in many different data designs, so establishing a common design structure proved beneficial in leveraging information compiled by other groups.

The BRACS and supporting databases are fully relational. Data fields common to multiple datasets have been standardized in data type and name with lookup tables shared between all databases. Database object names use a self-documenting style that follows the Hungarian naming convention (Novalis, 1999). The volume of project information required us to develop comprehensive data entry and analysis procedures (coded as tools) that were embedded on forms used to display information. Visual Basic for Applications® is the programming language used in Microsoft® Access®, and all code was written at the Microsoft® ActiveX® Data Objects level with full code annotation. The code for geophysical well log resistivity analysis was specifically written with class objects to support a rapid analysis of information with the benefit of only having data appended when the user approved the results.

The BRACS Database is described in the BRACS Database (TWDB, 2021b) and Data Dictionary (TWDB, 2021a), which both are available from the TWDB website (**www.twdb.texas.gov/groundwater/bracs/database.asp**). We develop custom tables for each study and incorporate these into the BRACS Database and add a study appendix describing these tables to the data dictionary after each study is completed.

19.3.1 Table relationships

The BRACS Database contains 18 primary tables of information (Figure 19-1), 32 lookup tables, tables designed for GIS export, and many supporting tables for analysis purposes. A brief description of each of the primary tables is provided in this section. Lookup tables provide control on data entry codes or values for specific data fields (for example, a county lookup table with all 254 county names in Texas). The tables for GIS export are copies of information obtained from one or more tables and in some cases are reformatted to meet GIS analysis needs. These tables can be custom tailored to meet study needs and will not be discussed further.

A fully relational database design has information organized into tables based on a common theme. Information must be segregated into separate tables for each one-to-many data relationship. For example, one well may have many well screens with unique top and bottom depth values; each well screen constitutes one record. Tables are linked by key fields. The well id field is the primary key field for every table in the BRACS Database. For each one-to-many relationship at least one additional key field is required.

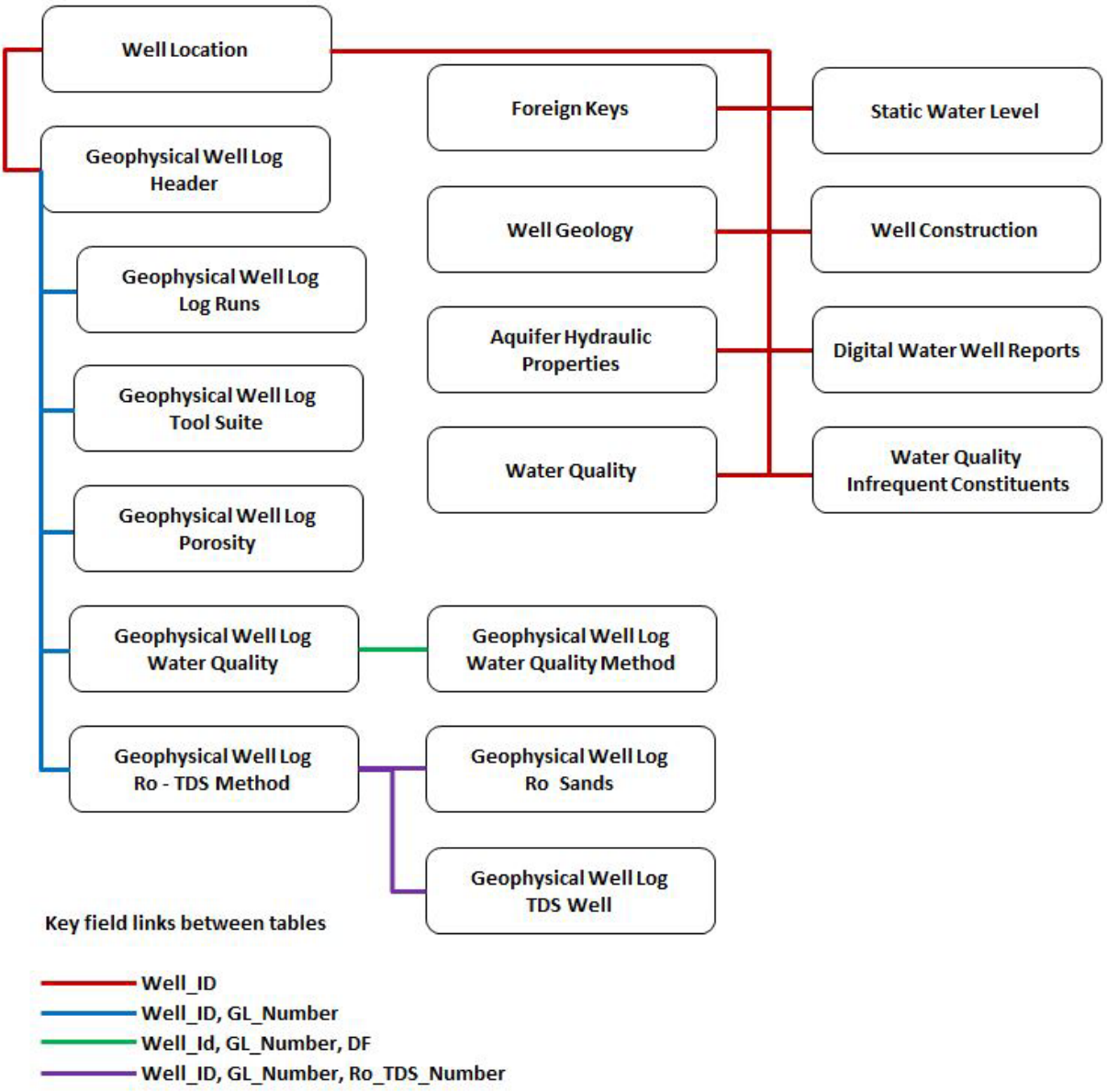

Figure 19-1 **Table relationships in the BRACS Database. Each rectangle represents a primary data table. The lines connecting the tables represent key fields: red represents the primary key *Well_ID*, blue represents the second key, green represents the third key, and purple represents the fourth key. New well records must be appended to the well location table to set the unique *Well_ID*. The tables, fields, and key fields are described in more detail in TWDB (2021a).**

Well locations

The table called **tblWell_Location** contains one record for each well record in the BRACS Database and is assigned a unique *Well_ID* as the key field. The *Well_ID* field links all the tables together. This table contains information such as well owner, well depth(s), location attributes (such as latitude, longitude, and elevation), source of well information, county name, and date drilled.

Foreign keys

The table called **tblBracs_ForeignKey** has zero to many unique well identification names or numbers assigned to it (for example, state well number and American Petroleum Institute number). These identifiers, also known as foreign keys, permit database linkage to the supporting databases developed from external agencies and other TWDB project databases with geophysical well logs and stratigraphic pick information.

Digital well reports

The table called **tblBracsWaterWellReports** contains zero to many records for digital copies of water well reports and miscellaneous records including oil and gas well scout tickets. The purpose of this table is to track the digital file names, file types, and hyperlinks to the documents.

Geophysical well logs

Information on the digital geophysical well logs is recorded in the table called **tblGeophysicalLog_Header**. This includes the type of digital file, digital file name, data hyperlink to the log image, and well log parameters such as depth. The well log parameters are only recorded if the well log is to be used for resistivity analysis for interpreted total dissolved solids.

Each geophysical well log may have one or more tools used to record subsurface parameters. This information is recorded in the table **tblGeophysicalLog_Suite**. Each tool name and its start and bottom depth values in units of feet below ground surface are recorded in this table.

A geophysical well log may be collected during different drilling stages (runs) within specific depth intervals. Each log run will usually have different drilling mud and temperature parameters. These parameters are recorded in the table called **tblGeophysicalLog_Header_LogRuns**.

The results from resistivity analysis for interpreted total dissolved solids are recorded in several tables. Evaluating more than one depth interval per well necessitated designing the table **tblGeophysicalLog_WQ** to hold the depth of formation, temperature, and resistivity of the mud filtrate values for that interval. Evaluating more than one resistivity technique per depth interval dictated designing one table, **tblGeophysicalLog_WQ_Method**, to hold the analysis results including interpreted total dissolved solids, log correction values, method used, geophysical well log used, and a multitude of intermediate values.

One log analysis technique, the "Ro-TDS Method", involves the comparison of log resistivity versus total dissolved solids concentration. This information is placed in the following tables: **tblBRACS_GL_Analysis_Ro_TDS_Main**, **tblBRACS_GL_Analysis_Ro_Sands**, and **tblBRACS_GL_Analysis_TDS_Well**. These tables record the final data pairs, the sands and their respective resistivity values, and the total dissolved solids concentration sample results for all wells used in the analysis. Geophysical well log analysis is used to determine the porosity of specific geologic intervals. This information is recorded in the table called **tblGeophysicalLog_Porosity**.

Well geology

The descriptions of rock types reported on drillers' well logs, simplified lithologic descriptions, stratigraphic picks, and hydrochemical zones are all contained in the table called **tblWell_Geology**. Each record contains a top and bottom depth, thickness of the unit, top and bottom elevations, source of data, and a value for type of geologic pick (for example, lithologic, stratigraphic, or hydrogeologic). The latter field permits the storage of all this information in one table and the ability to view the information in one form.

Well construction

Well casing and screen information is contained in the table called **tblBracs_Casing**. This table design is similar to the well-casing table in the TWDB Groundwater Database and contains top and bottom depths for casing and screen.

Water quality

Two tables contain the results of water quality analyses recorded for wells that are not in the TWDB Groundwater Database: **tblBracsWaterQuality** and **tblBracsInfrequentConstituents**. The table designs are similar to those in the TWDB Groundwater Database.

All water quality records used to develop the maps and tables in Section 11 of the report were appended to the table called **tblBRACS_HCT_MasterWaterQuality**. This table includes records obtained from the TWDB Groundwater Database and records obtained from research for wells in the BRACS Database.

Static water level

Static water level information is contained in the table called **tblBRACS_SWL**. The table is similar to its equivalent in the TWDB Groundwater Database. Information on dates, water levels, and source of measurement are recorded in the table. Static water levels for all wells in the study area were compiled into a custom table called **tblBRACS_HCT_SWL**.

Aquifer hydraulic properties

Information from existing aquifer tests conducted for all BRACS studies is contained in the table called **tblBRACS_AquiferTestInformation**. The table contains fields for hydraulic conductivity, transmissivity, specific yield, storage coefficient, drawdown, pumping rate, specific capacity, the types of units for each measurement, date of analysis, source of information, and remarks. If an analysis included the top and bottom depths of the screen, well depth, and static water level, it was captured in this table in case the

values differed from what is presented in the casing table (test may have been performed before total depth of the well was reached). The length of aquifer tests, values for drawdown versus recovery, pumping and static water levels, and two analysis remarks fields complete the table design. We created two custom tables to store aquifer test data for this study area; 1) **tblBRACS_HCT_AT** to store 170 well test summaries and 2) **tblBRACS_HCT_FieldData** to record the 12 public supply wells with drawdown details.

Aquifer determination

The results of the aquifer determination for well records described in Section 8 are presented in the table called **tblBRACS_HCT_AquiferDetermination**. This table includes fields for the new aquifer decision, TWDB Groundwater Database aquifer code assigned to the well (if any), well and screen depths, whether the well has multiple screens, well owner, and latitude/longitude coordinates. Fields for geological formation top and bottom depths derived from GIS geological formation datasets are listed.

19.4 Geographic information system datasets

Many GIS datasets were created during the course of this study. The GIS techniques used to build the files are explained in the following sections and noted in the GIS file metadata. ArcGIS® 10.7 and the Spatial Analyst® extension software by Environmental Systems Research Institute, Inc. (ESRI) were used to create the GIS files. Each of the GIS files prepared for this BRACS study is available for download from the TWDB website (**www.twdb.texas.gov/groundwater/bracs/studies.asp**).

Each point file is in the ArcGIS® shape file format. Point files of well control used for general purposes have a geographic projection and the North American Datum 1983 as the horizontal datum. Point files used for GIS surface (raster) creation have an Albers projection and the North American Datum 1983 as the horizontal datum.

All surface files are in the ArcGIS® raster integer grid file format with an Albers projection and the North American Datum 1983 as the horizontal datum. All raster files are snapped to the project snap grid raster with a cell size of 250 by 250 feet.

Polygon and polyline files are in the ArcGIS® shape file format with an Albers projection and the North American Datum 1983 as the horizontal datum.

All well records are managed in Microsoft® Access® databases. Well records are queried from the database and imported into ArcGIS® for spatial analysis. When new attributes are added to a well using ArcGIS®, the information is imported into Microsoft® Access®, and the well records updated.

Every well record in each database used for this study contains latitude and longitude coordinates in the format of decimal degrees with a North American Datum of 1983. All of these well records were imported into ArcGIS® and georeferenced in a geographic coordinate system, North America, North American Datum 1983 projection. A point shapefile was then saved in a working directory. Every well record then had an elevation assigned from the U.S. Geological Survey seamless 30-meter digital elevation model using

the ArcGIS® ArcToolbox (Spatial Analyst® Tools, Extraction, and Extract Values to Points). The dbase file from each shapefile was then imported into Microsoft® Access® and the elevation data updated to each well record, along with date, method, vertical datum, and agency attributes. Each well record also recorded the kelly bushing height when available.

In many cases, new wells were plotted in ArcGIS® and the latitude, longitude, and elevation were determined and appended to the database tables manually. The Original Texas Land Survey obtained from the Railroad Commission of Texas was the principal base map used to plot well locations; county highway maps and topographic maps were used on occasion.

GIS file name codes

ArcGIS® raster files are limited to 12 characters, necessitating the development of a file naming scheme for all GIS files created for BRACS studies. The full list of naming codes can be found in the BRACS Database in the table called **tblGisFile_NamingConventions**, and a shortened list of codes is presented in Table 19-1.

Each code is separated from the next code with an underscore character. For example, the code CC_T_D refers to the Cow Creek limestone hydrostratigraphic unit top depth.

Table 19-1 GIS file naming codes applied to the Hill Country Trinity Aquifer study area.

Code	Code type	Code position	Code description
HCT	BRACS Project	1	Hill Country Trinity aquifer project
UG	Stratigraphic	2	Upper Glen Rose limestone
LG	Stratigraphic	2	Lower Glen Rose limestone
HE	Stratigraphic	2	Hensell sandstone
CC	Stratigraphic	2	Cow Creek limestone
HM	Stratigraphic	2	Hammett shale
SL	Stratigraphic	2	Sligo limestone
HO	Stratigraphic	2	Hosston sandstone
BK	Stratigraphic	2	Base of Cretaceous
SC	Salinity zones	2	All classes
T	Surface position	3	Top
B	Surface position	3	Bottom
swl	Value	3	Static water level
E	Value	4	Elevation above mean sea level (units: feet)
D	Value	4	Depth below ground surface (units: feet)
TK	Value	3	Thickness (units: feet)
10ft	Contour interval	5	Contour interval of 25 feet (units: feet)
20ft	Contour interval	5	Contour interval of 50 feet (units: feet)
100ft	Contour interval	5	Contour interval of 100 feet (units: feet)
500ft	Contour interval	5	Contour interval of 250 feet (units: feet)
con	Data type	6	Contour
ext	Data type	6	Extent
pt	Data type	6	Point
pl	Data type	6	Polyline
pg	Data type	6	Polygon

Project support GIS files

Unique GIS datasets representing administrative, geologic, and well control features were developed for the project. The filenames associated with these datasets are presented in Table 19-2.

Table 19-2 Project support GIS files.

File purpose	File name	File type
Project snap grid	HCT_snap250	Raster
Project elevation	HCT_texas30m	Raster
Project boundary	HCT_studyarea_pg	Polygon
Project well control	BRACS_GL_HCT_20200327_pt	Point
Aquifer determination	HCT_AQD5_pt	Point
Surface geology	hct_ug_ext_pg hct_lg_ext_pg hct_he_ext_pg hct_cc_ext_pg hct_hm_ext_pg hct_ho_ext_pg	Polygon
Master water quality	HCT_MWQ_all_Trinity_pt	Point
Public water supply boundary	HCT_PWS_clip1_pg	Polygon
Texas counties	Texas_counties_pg	Polygon
Texas cities	Urban_Areas_GAM_pg	Polygon
Texas groundwater conservation districts	TWDB_GCDs_JULY2019_pg	Polygon
Texas groundwater management areas	HCT_GMA_GAM_pg	Polygon
Texas regional water planning areas	TWDB_RWPAs_2014_GAM_pg	Polygon
Geologic cross section	HCT_xs_a_pl HCT_xs_b_pl HCT_xs_c_pl HCT_xs_d_pl	Line
Figure feathering	HCT_FeatherEdge_pg	Polygon
Aquifer test data	HCT_AT_GAM_pt	Point

Geologic formation GIS files

Raster GIS datasets representing the mapped geologic structural features in the study area are presented in Table 19-3.

Table 19-3 Geological formation GIS files.

Unit name	Raster surface file name
Upper Glen Rose limestone	HCT_UG_T_D
	HCT_UG_T_E
	HCT_UG_TK
Lower Glen Rose limestone	HCT_LG_T_D
	HCT_LG_T_E
	HCT_LG_TK
Hensell sandstone	HCT_HE_T_D
	HCT_HE_T_E
	HCT_HE_TK
Cow Creek limestone	HCT_CC_T_D
	HCT_CC_T_E
	HCT_CC_TK
Hammett shale	HCT_HM_T_D
	HCT_HM_T_E
	HCT_HM_TK
Sligo limestone	HCT_SL_T_D
	HCT_SL_T_E
	HCT_SL_TK
Hosston sandstone	HCT_HO_T_D
	HCT_HO_T_E
	HCT_HO_TK
Base of Cretaceous	HCT_BK_T_D
	HCT_BK_T_E

Salinity class polygon files

GIS polygon datasets representing the mapped salinity classes in the study area are presented in Table 19-4.

Table 19-4 Salinity class polygon files.

Hydrostratigraphic unit	Polygon file name
Upper Glen Rose limestone	HCT_UG_TDS_SC_PG
Lower Glen Rose limestone	HCT_LG_TDS_SC_PG
Hensell sandstone	HCT_HE_TDS_SC_PG
Cow Creek limestone	HCT_CC_TDS_SC_PG
Sligo limestone	HCT_SL_TDS_SC_PG
Hosston sandstone	HCT_HO_TDS_SC_PG